

https://dspace.org/

# Method development for the extraction of nitroaromatic compounds and polycyclic aromatic hydrocarbons from aqueous solutions by application of natural and synthetic sorbents

**Tavengwa, Nikita Tawanda**

**2016**

http://hdl.handle.net/10539/21693

Tavengwa, Nikita Tawanda (2016) Method development for the extraction of nitroaromatic compounds and polycyclic aromatic hydrocarbons from aqueous solutions by application of natural and synthetic sorbents, University of Witwatersrand, Johannesburg, <http://wiredspace.wits.ac.za/handle/10539/21693>

Downloaded from a DSpace repository. https://dspace.org/

# Method development for the extraction of nitroaromatic compounds and polycyclic aromatic hydrocarbons from aqueous solutions by application of natural and synthetic sorbents




By

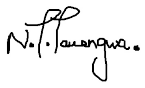
Nikita Tawanda Tavengwa

A thesis submitted to the Faculty of Science, University of the Witwatersrand in fulfilment of the requirements for the degree of Doctor of Philosophy

WITS University, Johannesburg, 2016

**Declaration**

I declare that this research is my own, unaided work. It is being submitted for the Degree of Doctor of Philosophy at the University of the Witwatersrand, Johannesburg. It has not been submitted before for any degree or examination at any other University.



Nikita Tawanda Tavengwa

This 4th day of October 2016 in Johannesburg

**List of publications**

***This thesis is based on the following papers:***

I. **Application of raw and biochared *Moringa oleifera* seeds for the removal of nitrobenzene from aqueous solutions**
   Nikita Tawanda Tavengwa, Ewa Cukrowska and Luke Chimuka
   *Desalination and Water Treatment* (DOI: 10.1080/19443994.2016.1151381)

II. **Application of polymer-composites for the solid phase extraction of selected nitroaromatic compounds from contaminated aqueous environments**
   Nikita Tawanda Tavengwa, Ewa Cukrowska and Luke Chimuka
   *Separation Science and Technology* (Submitted)

III. **Extraction of explosive compounds from aqueous solutions by solid phase extraction using β-cyclodextrin functionalized carbon nanofibers as sorbents**
   Nikita Tawanda Tavengwa, Nomso Hintsho, Shane Durbach, Isabel Weiersbye, Ewa Cukrowska and Luke Chimuka
   *Journal Environmental Chemical Engineering*, 4(2) (2016) 2450-2457

IV. **Determination of polycyclic aromatic hydrocarbons from sewage wastewater by application of molecularly imprinted polymers - membrane assisted solvent extraction combination**
   Nikita Tawanda Tavengwa, Ewa Cukrowska and Luke Chimuka
   *(Manuscript in preparation)*

V. **Miniaturized pipette tip-based electrospun polycrylonitrile for micro–solid–phase extraction of nitro based explosive compounds**
   Nikita Tawanda Tavengwa, Pardon Nyamukamba, Ewa Cukrowska and Luke Chimuka
   *Journal of Separation Science* (Submitted)

**Other publications not included:**

VI. **Equilibrium and kinetic studies on the adsorption of humic acid unto cellulose and activated carbon sorbents**

Nikita Tawanda Tavengwa, Luke Chimuka and Lilian Tichagwa

*Desalination and Water Treatment*, 57(36) (2016) 16843-16854

VII. **QuEChERS Method development for bio-monitoring of low molecular weight polycyclic aromatic hydrocarbons in South African carp fish using HPLC-Fluorescence: An initial assessment**

Afolake Olufunmilola Oduntan, Nikita Tawanda Tavengwa, Sabelo Dalton Mhlanga and Luke Chimuka

*South African Journal of Chemistry*, 69 (2016) 98-104

**Contribution of the authors**

**Paper I.** Principal author, involved in planning, performed the sorbent preparation and characterization, sorption experiments, evaluation of the results and writing of the article. Co-authors revised the draft manuscript and made suggestions for improvement.

**Paper II.** Principal author, involved in planning, performed the sorbent preparation and characterization, sorption experiments, evaluation of the results and writing of the article. Co-authors revised the draft manuscript and made suggestions for improvement.

**Paper III.** Principal author, involved in planning, performed the carbon nanofibers functionalization and characterization, sorption experiments, evaluation of the results and writing of the article. Co-authors synthesized the carbon nanofibers from waste fly ash, revised the draft manuscript and made suggestions for improvement.

**Paper IV.** Principal author, involved in planning, performed the sorbent preparation and characterization, sorption experiments, evaluation of the results and writing of the article. Co-authors revised the draft manuscript and made suggestions for improvement.

**Paper V.** Principal author, involved in planning, performed characterization, sorption experiments, and evaluation of the results and writing of the article. Co-authors synthesized the polyacrylonitrile nanofibers, revised the draft manuscript and made suggestions for improvement.

**Paper VI.** Principal author, involved in planning, performed the sorbent preparation and characterization, sorption experiments, evaluation of the results and writing of the article. Co-authors revised the draft manuscript and made suggestions for improvement.

**Paper VII.** Co-author, involved in drafting of the manuscript, synthesized the molecular imprinted polymers, assisted in the interpretation of some data. Other authors revised the draft manuscript and made suggestions for improvement.

*All papers are reproduced with kind permission from the respective copyright holders.*

**Abstract**

In this work, natural and synthetic sorbents were investigated for the extraction and removal of different organic compounds (nitroaromatic compounds and polycyclic aromatic hydrocarbons) from aqueous samples.

Natural sorbents like the raw *Moringa oleifera* seed powder and the physically modified biochared powder were investigated for their potential in the extraction of nitrobenzene (NB) (**paper I**). For the raw and biochared *Moringa oleifera* seed powder, the carbon content as determined by energy dispersive X-ray spectroscopy (EDS) was 80% and 70%, respectively. Though the surface area of the biochared was double that of the raw (12.6 $m^2 g^{-1}$ and 6.3 $m^2 g^{-1}$, respectively), the uptake of nitrobenzene by the later was higher in all optimizations and applications investigated. This implied that the interaction type between the *Moringa oleifera* seed powder and nitrobenzene was more chemisorption than physiosorption. The presence and absence of the proteneous compounds (bearers of the functional groups) infuenced the performance of the *Moringa oleifera* seed powder as a sorbent. For the raw and biochared *Moringa oleifera* seed powder sorbent, the kinetic data was best modelled by the pseudo-second-order and the adsorption capacities were found to be 0.084 and 0.071 mg $g^{-1}$, respectively. As determination by HPLC-UV method, the LOD and LOQ for NB were found to be 11.5 and 38.5 µg $L^{-1}$, respectively.

In **paper II**, 2,4-dinitrotoluene was used as an imprint in the synthesis of magnetic molecularly imprinted polymers (MMIPs). These synthetic sorbents were used for the extraction of nitroaromatic compounds (2,4-dinitrotoluene, 2-nitotoluene and nitrobenzene). In all the optimization parameters investigated, the MMIP had a great extraction of 2,4-dinitrotoluene showing the effect of imprinting. For 2,4-dinitrotoluene, nitrobenzene and 2-nitrotoluene HPLC-UV analysis, detection limits of 13.6, 7.7 and 27.2 µg $L^{-1}$, respectively and good correlations of determination ($R^2$ > 0.993) of all the analytes were obtained. Recoveries of 82.7%, 88.1% and 82.0% were obtained for 2,4-dinitrotoluene,

nitrobenzene and 2-nitrotoluene from spiked real water samples, respectively, with %RSD values ranging from 1.4%-11.9%.

In **paper III,** another synthetic sorbent, β-cyclodextrin covalently functionalized to carbon nanofibers (β-CD@CNFs) was prepared and fully characterized. This material was loaded in solid phase extraction catridges, which were then applied for the extraction and pre-concentration of six nitroaromatic compounds. High correlations of determination ($R^2$ > 0.997) for 3-nitrotoluene (3-NT), 1,3-dinitrobenzene (1,3-DNB), 2,6-dinitrotoluene (2,6-DNT), 4-nitrotoluene (4-NT), nitrobenzene (NB) and 2-nitrotoluene (2-NT) were obtained. Low limits of detection of 3.3, 7.1, 8.6, 9.7, 23.1 and 13.0 μg $L^{-1}$ were found for the respective compounds. The applicability of the developed method using β-CD@CNF as a sorbent was investigated using spiked real water samples collected within the vicinity of an operational gold mine and recoveries of 36.6%-102.2% were obtained.

**Paper IV** dealt with a novel combination of molecularly imprinted polymers (MIPs) dispersed in an organic solvent in membrane assisted solvent extraction (MASE) bags for the extraction of polycyclic aromatic hydrocarbons (PAHs) from sewage wastewater samples from Goudkoppies wastewater treatment plant in Johannesburg, South Africa. Before application to real wastewater, optimization was carried out and toloune was found to be the best acceptor phase, and 80 mg of the MIPs gave optimum extraction of PAHs. 25% N,N-dimethylformamide in aqueous solution as an organic modifier was found to be the best donor composition. An extraction time of 90 min at a stirring rate of 1000 rpm gave the optimum pre-concentration of the PAHs. The optimized parameters where then applied to the sewage wastewater were the effluent was found to be cleaner than the influent.

In **paper V**, nano-sized fibers were synthesized by electrospinning polyacrylonitrile (PAN). Due to the combination of functional groups along the fiber and the increased surface area due to nano-sizing, there was a great extraction of four nitrotoluenes. The approach was loading a small amount of the

electrospun polyacrylonitrile nano-fibres in pipette tips in a miniaturized pipette tip solid phase extraction (SPE). The linear dynamic range was 150 - 1000 µg $L^{-1}$ with coefficients of determination of $R^2$ > 0.99 for all the nitroaromatic compounds. Optimum recoveries were recorded at pH 6, 15 mg of the PAN sorbent. Twenty aspirating/dispensing cycles (at the loadind stage) and 1 mL acetonitrile gave maximum recoveries. Application of the PAN-PT-SPE to real wastewater samples gave recoveries ranging from 70% to 115%. The low values of the relative standard deviations (RSD < 12%) meant the method was suitable for application to real wastewater samples.

**Dedications**

*This work is dedicated to my wife Shamiso and my daughters Tanatswa and Tadiwanashe for being there for me throughout of my doctoral studies.*

*A special thank you goes to my father Orleans and mother Beauty for being very supportive during the course of my postgraduate studies.*

*To my sisters Alleta and Nancy together with my brother Tanaka you urged me to strive on when I was weak and that have seen me successfully completing my PhD.*

How can I repay the LORD for all his acts of kindness to me? (Psalms 116:12)

**Acknowledgements**

- The LORD has always being wonderful to me.
- To my supervisor, Prof Luke Chimuka, I say thank you very much for believing in me. You were actually more than a supervisor to me. You guided me well in this research and adviced me in so many aspects of my life.
- I also value the mentorship of my co-supervisor, Prof Ewa Cukrowska.
- Many thanks also go to Prof Hlanganani Tutu whose constructive comments added value to my work.
- I would like to thank the National Research Foundation (NRF) of South Africa for funding my research. Part of the research funding came from AngloGold Ashanti Ltd S.A. region and the NRF / Department of Trade and Industry (DTI) "THRIP" (TP13080525596) awards to I. Weiersbye and E.T.F. Witkowski. My PhD tuition fees were paid by Postgraduate Merit Award, University of Witwatersrand which I appreciate very much.
- My collegues in the Environmental Analytical Chemistry (EACH) Research group were a pleasure to work with in the lab, especially: Dr Juliene Lusilao, Dr Elysee Bakatula, Dr Bronwyn Grover, Mr Tuthuka Mabaso, Mr Somandla Ncube and Mr Pfano Nekhunguni.
- Outside the EACH group, the following were very supportive of my work: Prof Lilian Tichagwa, Prof Shane Durbach, Dr Nomso Hintsho and Dr Vusumzi Pakade
- The following people helped me with instrumental analysis and characterization of my samples: Prof Alexander Ziegler for TEM, SEM and EDS, Prof Neil Coville for BET and TGA, Ms Joyce Gama for FTIR and UV-Vis and, Prof Lisa Du Toit for zeta potential and size distribution measurements.

**Conference presentations**

1. Nikita Tawanda Tavengwa, Ewa Cukrowska and Luke Chimuka, Application of magnetic molecularly imprinted polymers in selective extraction of 2,4-DNT explosive from aqueous solutions, SACI 2015 Conference, 27 November - 1 December 2015, Durban, South Africa, *Oral presentation*.
2. Nikita Tawanda Tavengwa, Ewa Cukrowska and Luke Chimuka, Selective extraction of 2,4-DNT from a mixture of related explosive compounds, Affinity 2015 Conference, 27 September - 1 October 2015, Puerto Vallarta, Mexico, *Oral presentation*.
3. Nikita Tawanda Tavengwa, Ewa Cukrowska and Luke Chimuka, Preparation, characterization and application of $NaHCO_3$ leached bulk U(VI) imprinted polymers endowed with γ-MPS coated magnetite in contaminated water, Analitika 2014 Conference, 7-11 September 2014, Parys, South Africa, *Oral presentation*.
4. Nikita Tawanda Tavengwa, Ewa Cukrowska and Luke Chimuka, Development of magnetic molecularly imprinted polymers for the removal of explosives from polluted mining water, Chromatography Postgraduate Student ChromSA Workshop, 17 September 2013, University of Pretoria, Pretoria, South Africa, *Oral presentation*.
5. Nikita Tawanda Tavengwa, Ewa Cukrowska and Luke Chimuka, Synthesis, adsorption and selectivity studies of N-propyl quaternized magnetic poly(4-vinylpyridine) for hexavalent chromium, University of Witwatersrand 5$^{th}$ Cross Faculty Postgraduate Symposium, 1-2 August 2013, University of the Witwatersrand, Johannesburg, South Africa, *Oral presentation*.
6. Nikita Tawanda Tavengwa, Ewa Cukrowska and Luke Chimuka, Spectroscopic determination of uranyl ions by arsenazo III complexation, 9$^{th}$ IWA International Conference on Water Reuse, 27-31 October 2013, Windhoek, Namibia, *Poster presentation*.

**Table of contents**

Declaration ..... i
List of publications ..... ii
Contribution of the authors ..... iv
Abstract ..... vi
Dedications ..... ix
Acknowledgements ..... x
Conference presentations ..... xi
Table of contents ..... xii
List of figures ..... xiv
Chapter 1 ..... xvi
1 Introduction and background ..... xvi
1.1 Background of the study ..... 2
1.2 Problem statement ..... 3
1.3 Outline of the thesis ..... 4
Chapter 2 ..... 5
2 Literature review ..... 5
2.1 Explosive compounds ..... 8
2.1.1 Background on explosive compounds ..... 8
2.1.2 Uses and sources of explosive contaminants ..... 9
2.1.3 Effects of explosive compounds ..... 10
2.1.4 Fate of explosive compounds ..... 10
2.1.5 Regulation of dangerous explosive compounds ..... 12
2.1.6 Pollution assessment and monitoring/removal ..... 13
2.2 Polyaromatic hydrocarbon (PAHs) ..... 14
2.2.1 Background on PAHs ..... 14
2.2.2 Physico-chemical properties of PAHs ..... 15
2.2.3 Effects of PAHs ..... 20
2.3 Extraction techniques of organic compounds from liquid samples ..... 20
2.3.1 Solid phase extraction ..... 21
2.3.2 Liquid-liquid extraction ..... 22

2.3.3 Solid phase microextraction ..... 22
2.3.4 Liquid-phase microextraction ..... 22
2.4 Extraction techniques of organic compounds from solid samples ..... 25
2.4.1 Soxhlet extraction ..... 25
2.4.2 Supercritical fluid extraction ..... 25
2.4.3 Microwave assisted extraction ..... 26
2.4.4 Pressurized liquid extraction ..... 26
2.5 Performance comparison of different extraction analytical methods ..... 26
2.6 New sorbent materials ..... 29
2.6.1 Molecularly imprinted polymers ..... 29
2.6.2 Carbon nanomaterials ..... 30
2.6.3 Electrospun fibers ..... 32
2.6.4 Moringa oleifera ..... 33
2.7 Performance comparison of different extraction analytical methods ..... 35
Chapter 3 ..... 38
3 Research objectives ..... 38
3.1 General objectives ..... 39
3.2 Specific objectives ..... 39
3.3 Research questions ..... 39
3.4 General approach ..... 40
Chapter 4 ..... 42
4 List of publications ..... 42
Paper I ..... 43
Paper II ..... 54
Paper III ..... 86
Paper IV ..... 95
Paper V ..... 123
5 General conclusions and future work ..... 153
5.1 Conclusions ..... 154
5.2 Future work ..... 155
References ..... 156
Appendix ..... 174

Paper VI ..... 175
Paper VII ..... 188

## List of figures

Fig. 1. Chemical structures of some selected explosive compounds ..... 9
Fig. 2 Scheme for the possible fate of energetic compounds in the environment (Kalderis *et al*., 2011; Juhasz and Naidu, 2007; Townsend and Myers, 1996) .... 12
Fig. 3. Synthesis scheme of PAHs (Ravindra *et al*., 2008) ..... 14
Fig. 4. Selected PAH structures showing bay regions. ..... 20
Fig. 5. Stages in solid phase extraction. ..... 21
Fig. 6. Schematic diagram for the synthesis of MIPs (Haupt *et al*., 2010) ..... 30
Fig. 7. Structure of carbon nanotubes ..... 31
Fig. 8. Schematic setup for electrospinning ..... 33
Fig. 9. *Moringa oleifera* tree and seed kernels ..... 34

## List of tables

Table 1 Physical properties of some selected explosives compounds ..... 11
Table 2 Allowable limits of different NACs in USA ..... 13
Table 3 Priority listed PAHs with selected physical properties (Lee, 2010). ..... 17
Table 4 Comparison of different methods for the extraction of PAHs and NACs 27
Table 5 Comparison of different methods for the removal of PAHs and NACs .. 36

**List of abbreviations and acronyms**

| | |
|---|---|
| **1,3-NB** | 1,3-Nitrobenzene |
| **2,4-DNT** | 2,4-Dinitrotoluene |
| **2,6-DNT** | 2,6-Dinitrotoluene |
| **2-NT** | 2-Nitrotoluene |
| **3-NT** | 3-Nitrotoluene |
| **AC** | Activated carbon |
| **CNFs** | Carbon nanofibers |
| **CNTs** | Carbon nanotubes |
| **DLLME** | Dispersive liquid-liquid microextraction |
| **HPLC** | High Perfomance Liquid Chromatography |
| **HV** | High voltage |
| **LLE** | Liquid liquid extraction |
| **LPME** | Liquid-phase microextraction |
| **MIP** | Molecularly imprinted polymer |
| **NACs** | Nitroaromatic compounds |
| **NB** | Nitrobenzene |
| **PAHs** | Polycyclic aromatic hydrocarbons |
| **QuEChERS** | Quick, Easy, Cheap, Effective, Rugged and Safe |
| **SDME** | Single drop microextraction |
| **SFE** | Supercritical fluid extraction |
| **SME** | Solvent microextraction |
| **SPE** | Solid phase extraction |
| **Tetryl** | 2,4,6-Trinitrophenylmethylnitramine |
| **TNT** | Trinitrotoluene |
| **USEPA** | United States Environmental Protection Agency |

# Chapter 1

# 1 Introduction and background

This chapter gives the background to the study. The problem statement which gives motivation as to why the research was carried out is also given. It concludes by giving the outline on how the work is presented in this thesis.

## 1.1 Background of the study

Continuous contamination of water bodies from both natural and anthropogenic sources is of great concern to everybody. Since the industrial activities have intensified, environmental pollution and deterioration of ecosystems is on the rise due to the presence of contaminants in effluents (Lenardão *et al*., 2003). Many of these pollutants are known to adversely affect human health as well as the environment. It is therefore of paramount importance to regularly monitor contaminants in the aquatic environment to make sure that the maximum allowable concentrations are not exceeded.

A number of organic compounds can be classified as priority pollutants, and their periodic quantification in aqueous systems is important to make sure that the water quality is not compromised. Organic pollution emanates mainly from urban run-off, industrial effluents, sewage treatment plants and industry which include food processing, pulp and paper making, agriculture and aquaculture wastewater (Rashed, 2013).

There is a lot of literature detailing the extraction of organic compounds from liquid samples. These include liquid-liquid extraction (LLE) (Cortada *et al*., 2011; Darrach *et al*., 2011), dispersive liquid-liquid microextraction (DLLME) (Larki *et al*., 2015; Tobiszewski *et al*., 2014), supercritical fluid extraction (SFE) (Librando *et al*., 2004; Rai *et al*., 2016; Hsueh *et al*., 2013; Batlle *et al*., 2005; Jowkarderis and Raofie 2012), solid-phase extraction (SPE) (Shi *et al*., 2016; Kouzayha *et al*., 2011), solvent microextraction (SME) (Casari and Andrews, 2001; Khajeh *et al*., 2006), liquid-phase microextraction (LPME) (Rezaee *et al*., 2006; Larki *et al*., 2015; Tobiszewski *et al*., 2014) and single drop microextraction (SDME) (Xu *et al*., 2007; Jeannot and Cantwell, 1996; Wang *et al*., 2013; Timofeeva *et al*., 2016; García-Vázquez *et al*., 2016). These methods are reviewed in more detail in Chapter two. Since there is often involvement of high capital and operational costs in some of these extraction techniques, efforts are being made to develop improved and innovative methods of wastewater sample preparation techniques. Adsorption has been identified as one of the most effective technique for the

removal of pollutants because of the low costs involved and the capacity for the sorbents to be regenerated for re-use. Adsorption relies on the high interfacial surface area of the adsorbents. This method was used in this work for the extraction of nitroaromatic compounds (NACs) and polycyclic aromatic hydrocarbons (PAHs) from aqueous samples (**paper I**, **paper II**, **paper III**, **paper IV** and **paper V**).

## 1.2 Problem statement

The presence of organic and inorganic compounds presents a health hazard in drinking water. Various water regulating bodies in many countries have set maximum allowable limits to safe guard the health of their citizens. Beyond these limits, action has to be taken to reduce the amount of the pollutants. These stringent measures are even applied to industries whose effluents are monitored before discharge in different water bodies.

Some of the pollutants occur in trace amounts which make monitoring of these analytes a challenge (Tobiszewski *et al*., 2014). At times, a large amount of water is needed to be sampled for analysis where pollutants are normally present at very small amounts. However, the use of sorbents has been proven to pre-concentrate these pollutants where the approach can either be batch or column. The later method can be through loading of the sorbent in solid phase extraction (SPE) cartridges (e.g., **paper III**). In the case of small sorbents (small mg levels) being used, miniaturized SPE can be carried out (e.g. **paper V**).

In aquatic samples, there is nearly always a lot of interefing matrix which can be pre-concentrated together with the analytes of interest (Cappiello *et al*., 2010; Sarafraz-Yazdi and Amiri, 2010). In this case, application of selective sorbents is necessary, and there is a lot of research going on in the molecularly imprinted polymers (MIPs) development (Jing *et al*., 2014; Luo *et al*., 2011). These polymeric sorbents are used as “artificial receptors”. These receptors (MIPs) show high selectivity towards the targert molecules and were used in **paper II** and **paper IV**.

In rural areas, affordability of commercial sorbents has always been a big challenge. An example of this is where 1 ton of commercial activated carbon from coconut shell costs between $950 and $1400 (Ahmedna *et al*., 2000). There is therefore need to come up with equally effective sorbents to sequestrate potential hazardous pollutants from drinking water. Use can be made of a large volume of agricultural and agroforestry waste which are readily available (Gholz, 1987). More so, most of this biomass is already found in rural areas of developing countries where most of the world's population resides (Hall and Moss, 1983). **Paper I** tested the feasibility of using a waste biosorbent from *Moringa oleifera* seeds for the extraction of nitroaromatic compounds.

Bulk materials are known to have inferior surface area and in adsorption studies, they ultimately have poor adsorption capacities. Reduction of the size of materials was the focus in **paper V**. Polyacrylonitrile was electrospun into nanofibers and was used for the extraction of nitrotoluenes from aqueous solutions.

### 1.3 Outline of the thesis

The outline of the thesis (comprising of five chapters) is presented as follows:

**Chapter 1:** A general introduction and background to water pollution due to organic pollutants is given. This chapter also spells out the problem statement which brings out the motivation of carrying out the research.

**Chapter II:** A consise review of the two model pollutants: nitroaromatic compounds and polycyclic aromatic hydrocarbons is given. Thereafter, the natural and synthetic sorbents used in **paper I-V** for the extraction of the model pollutants were reviewed.

**Chapter III:** The research objectives are provided in this section.

**Chapter IV:** This chapter lists manuscripts (**paper I-V**) presented for my PhD examination. The work carried out, results and discussion are presented in each paper.

**Chapter V:** General conclusions and future work based on experimental findings are discussed in this section.

**References:** The references arising from the introduction and literature review (Chapter 1 and 2) are listed at the end of the thesis.

**Appendix:** This section lists four other papers (**paper VI-VII**) that were prepared and published during my PhD studies.

# Chapter 2

# 2 Literature review

Two groups of organic compounds, nitroaromatic compounds (NACs) and polycyclic aromatic hydrocarbons (PAHs) were investigated as model pollutants. Each group is reviewed in detail in this chapter. Selected modern sample preparation techniques are reviewed. Also discussed are low cost natural abundant sorbents in the form of Moringa seed powder and carbon nanofibers from waste fly ash. The basic principles of electrospinning are also reviewed. Also discussed are molecularly imprinted polymers (MIPs) which were used as selective sorbents.

## 2.1 Explosive compounds

### 2.1.1 Background on explosive compounds

Explosive compounds are chemicals that decompose when exposed to external stimuli. This decomposition is always very rapid with a concomitant production of energy in the form of flame, heat and light (Juhasz and Naidu, 2007). In addition, gaseous products like $N_2$, $CO_2$ and $H_2O$ are produced resulting in the expansion of volume and generation of high pressures. An explosion is therefore defined as a rapid spontaneous expansion of matter into a much greater volume. This expansion results in energy being transformed into mass motion, and this is always accompanied by a loud noise and a generation of a great deal of heat. Explosive devices may be mechanical, chemical or atomic (Oxley, 1993).

Sensitive materials that can be initiated by a relatively small amount of heat or pressure are called primary explosives. Organic secondary explosives can be classified into different groups; nitroaromatics, nitramines and nitrate esters. Nitroaromatic compounds, which include trinitrotoluene, 2,4,6-trinitrophenylmethylnitramine, 1,3,5-trinitrobenzene, hexanitrostilbene and ammonium picrate, have $NO_2$ groups directly bonded to carbon atom(s) on the aromatic ring. On the other hand, nitramines contain $NO_2$ groups bonded to nitrogen(s) present within an alicyclic ring, examples include, cyclotrimethylenetrinitramine and cyclotetramethylene-tetranitramine. Nitrate esters contain $NO_2$ groups bonded to an oxygen atom attached to an aliphatic carbon (Pichtel, 2012). This group includes nitroglycerin and pentaerythritol tetranitrate. Figure 1 shows some common explosive compounds and it is noticeable that all of them have a nitro group and hence are classified under nitro-based explosives.

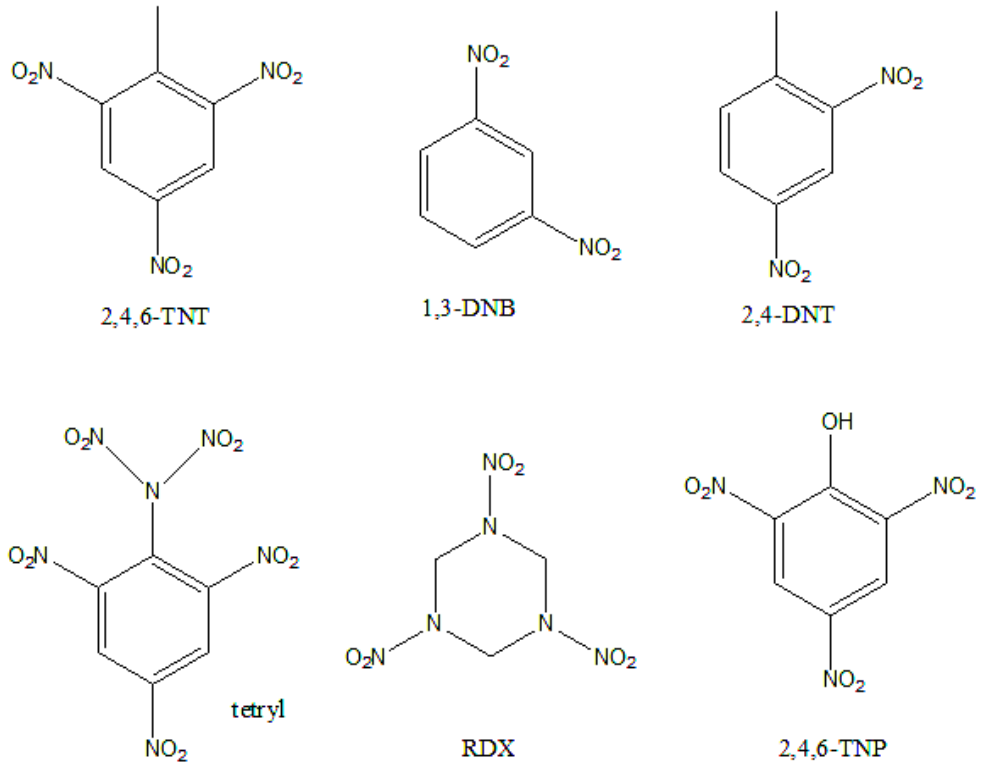



**Fig. 1.** Chemical structures of some selected explosive compounds

### 2.1.2 Uses and sources of explosive contaminants

Explosives are widely used in construction, mining, agriculture and military applications. In most cases, it has become a norm to use TNT for measuring explosive force, even for nuclear weapons (American Chemical Society, 2012). In many situations, when these compounds are prepared and transported, some amounts end up in water bodies (Wynn *et al*., 2008) which is one of the greatest reserviour of NACs because of their hydrophilic nature. Secondary explosives may also enter the environment during manufacturing, assembly, or when packed. During these activities, soil sediment and water may become contaminated with these compounds with potential negative impact on the environment and human health (Juhasz and Naidu, 2007).

Environmental contaminations by explosive compounds and their degradation products have been detected at and around military sites (Pennington and Brannon, 2002; Clark and Boopathy, 2007, Boparai *et al*., 2008). The disposal of military waste has recently become a problem from a health and environmental

point of view (Letzel *et al*., 2003). If management and disposal of explosive compounds at these sites are not handled properly, they and their by-products end up being discharged into the environment. At high accumulated concentrations, humans, animals and aquatic creatures will be affected (Pichtel, 2012).

### 2.1.3 Effects of explosive compounds

Monitoring and detection of explosives in the environment is of importance because of its acute and chronic toxicity to humans, and the possibility of ecological damage (Thurman and Ferrer, 2012). For example, acute toxicity has been shown for TNT in the adult bullfrog (Paden *et al*., 2008). Some explosive compounds such as 2,4,6-trinitrotoluene (TNT) and cyclotrimethylenetrinitramine (RDX) are also known to be toxic and carcinogenic chemicals. These compounds are hazardous to human health and its well-being upon exposure (Richter-Torres, 1995; Smith-Simon and Goldhaber, 1995). Dinitrotoluenes can be absorbed by the skin, the respiratory tract, and the gastrointestinal tract. Furthermore, explosive residues leach from soils at military sites to underlying groundwater (Spiegel *et al*., 2005) and can exceed tolerable quantities. In previous studies by Angerer and Weismantel (1998) on the urine of occupationally exposed workers, there was detectation of 2,4-dinitrobenzoic acid as the main metabolite of 2,4-DNT.

### 2.1.4 Fate of explosive compounds

Because of the health and environmental threat of the explosive compounds as outlined in the previous section, their fate in the environment is of great interest. Removal of pollutants and risk management of contaminated sites require understanding of the fate and transport of explosives and their transformation products in the environment (Pennington and Brannon, 2002). After being discharged into aquatic systems, both abiotic and biotic processes determine the fate of explosive compounds (Juhasz and Naidu, 2007; Brannon and Pennington, 2002). The rate and extent of transport and transformation of energetic compounds are influenced by their physicochemical properties (e.g., solubility, vapour pressure and the Henry's law constant), environmental factors (e.g.,

weather conditions, soil properties, pH and redox status), and biological factors (e.g., population of energetic degrading microorganisms). Some physicochemical properties of NACs are listed in Table 1.

**Table 1** Physical properties of some selected explosives compounds

| Compound | $\lambda_{max}$ (nm) | $\varepsilon_{max}$ ($M^{-1}$ $cm^{-1}$) | p$K_a$ | Log$K_{ow}$ | $K_d$ ($K^+$-mont.) (L $Kg^{-1}$) |
|---|---|---|---|---|---|
| 2,4-DNT | 252 | 14000 | _ | 1.98 | 7400 |
| 2,6-DNT | 241 | 10000 | _ | 2.02 | 125 |
| 2-NT | 265 | 5800 | _ | 2.3 | 4.6 |
| 3-NT | 273 | 7200 | _ | 2.42 | 21 |
| NB | 267 | 7600 | _ | 1.84 | 7.2 |
| 1,3-NB | 242 | >10000 | _ | 1.49 | 45000 |
| TETRYL | 227 | 23000 | nd | 1.65 | 5.8 |

Notes $\lambda_{max}$ Wavelength of maximum absorption
$\varepsilon_{max}$ Molar extinction coefficients
p$K_a$ Acidity constants
Log$K_{ow}$ Octanol/water partition coefficient
$K_d$ ($K^+$-mont.) Adsorption constant for $K^+$-montmorillonite

Processes that affect the environmental fate of explosive compounds can be from influences that affect movement which include dissolution, volatilization and adsorption. Factors such as photolysis, hydrolysis, reduction and biological degradation can influence transformation of explosive compounds (Kalderis *et al.*, 2011). Figure 2 illustrates the major fate and transport pathways for energetic materials.

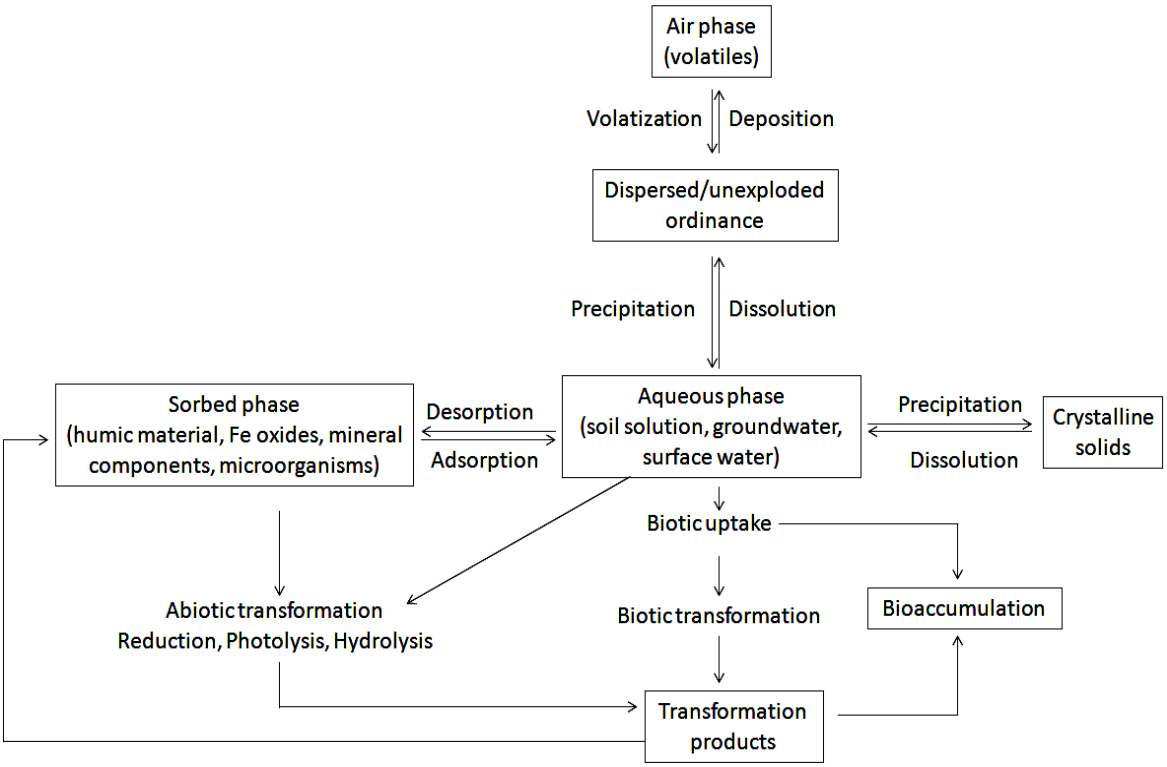



**Fig. 2** Scheme for the possible fate of energetic compounds in the environment (Kalderis *et al*., 2011; Juhasz and Naidu, 2007; Townsend and Myers, 1996)

### 2.1.5 Regulation of dangerous explosive compounds

Water quality impacts due to the introduction of nitrates into the system can be a significant problem for a mining operation. The major sources for the nitrates are known to be explosives used in the mining processes. Nitrates can be introduced into the water in the mine or at rock disposal site. They come from spillage during explosive transportation or charging, leaching of the explosives in wet blastholes or undetonated explosive in the brokec rock after the blast.

Regulatory agencies in Canada and the United States are placing a significant emphasis on compliance with effluent nitrate concentration. Typical limitations are established at 10 mg $L^{-1}$ as N, based on the maximum contaminant level for portable use (USEPA, 1986). Due to the toxicity of the NACs to humans, some water regulating bodies like USEPA have set some allowable limits. A few examples are shown in Table 2. In South Africa, according to the NEMA act

number 59 of 3008, the regulatory requirements for the discharge of 2,4-DNT is 65 µg $L^{-1}$, the lowest value of the standard for human health effects listed for drinking water.

**Table 2** Allowable limits of different NACs in USA

| NAC | Maximun allowable limits (µg $L^{-1}$) | Reference |
|---|---|---|
| TNT | 2 | ATSDR, 1995 |
| 2,4-DNT | 0.1700 | Hajjar *et al*., 1991 |
| 2,6-DNT | 0.0068 | Hajjar *et al*., 1991 |

### 2.1.6 Pollution assessment and monitoring/removal

There has been a long-standing need for fast, simple, accurate ways to detect nitroaromatic compounds in salt water, fresh water and other liquids (American Chemical Society, 2012). Thus, reliable pollution assessment and monitoring of soil and water contaminated with these explosives is of major importance, e.g., in order to prepare and support efficient de-contamination and remediation activities (Pennington and Brannon, 2002; Clarke and Boopathy, 2007; Boparai *et al*., 2008). Many techniques have been used to detect explosives, including gas chromatography, Raman spectroscopy and fluorescence spectroscopy (Mills, 2012). Chemical and other sensor types can provide an excellent solution to many such on-site chemical detection needs both in gas and liquid phase (Yinon, 2003; Singh, 2007). Fluorescence spectroscopy is considered the most useful because of its simplicity, high sensitivity and low cost. With this technique, fluorescent dyes are incorporated into a solid matrix on which they interact with the explosive molecules, causing them to fluoresce. Plants tolerate explosives in soil and water up to a certain extent. Beyond this concentration, plants may be affected. However, they have been used in phytoremediation of explosives (Pennington and Brannon, 2002).

## 2.2 Polyaromatic hydrocarbon (PAHs)

### 2.2.1 Background on PAHs

Polycyclic or polynuclear aromatic hydrocarbons (PAHs) are compounds which include carbon and hydrogen, and always have at least two fused rings in their structures which are normally benzene. It is however common to also have rings that are not six-sided (Ravindra *et al*., 2008).

One way of synthesizing PAHs is through pyrosynthesis and pyrolysis by using saturated hydrocarbons as precursors under oxygen-free environments. When exposed to temperatures exceeding 500$^{o}$C, the C-C and C-C bonds are broken and there is formation of free radicals. These radicals combine with acetylene which then condenses to form aromatic ring structures, which are resistant to degradation at elevated temperatures (Ravindra *et al*., 2008). The general synthetic scheme for PAHs is shown in Fig. 3.

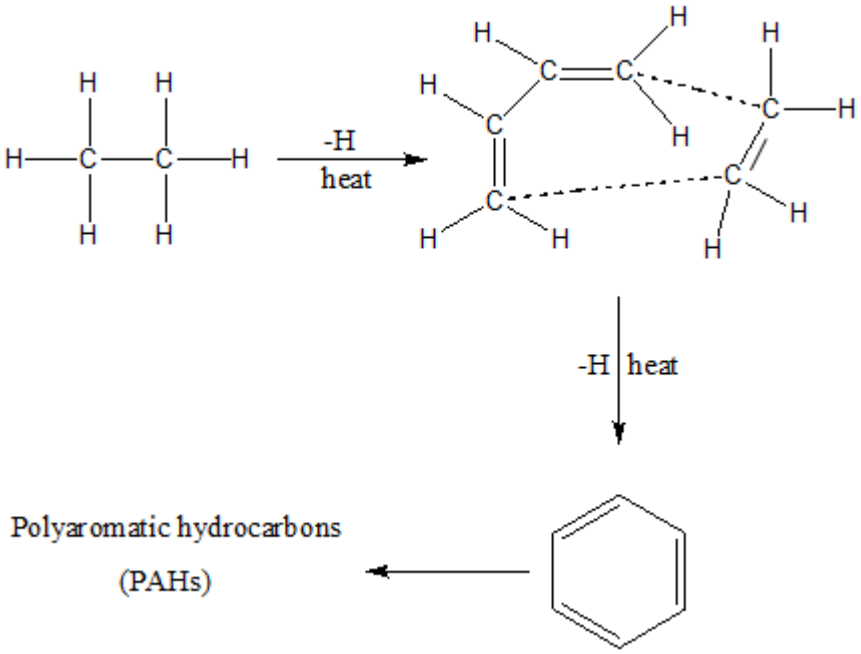



**Fig. 3.** Synthesis scheme of PAHs (Ravindra *et al*., 2008)

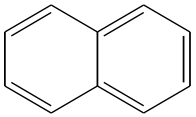
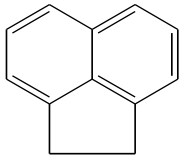
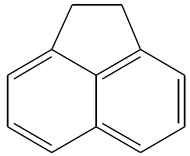
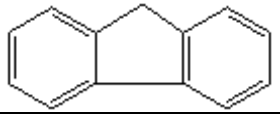
The formation of PAHs is mostly due to the incomplete combustion and pyrolysis of fossil fuels or wood, and from the release of petroleum products (Manahan, 1994). The emission of PAHs by various anthropogenic combustion sources have been briefly discussed by Marchand *et al.* (2004). Forest fires are known to be the single most emmiters of PAHs into the atmoshere. Other pyrogenic non-anthropogenic sources of PAHs include volcanic eruptions and degradation of biological materials (Ravindra *et al*., 2008).

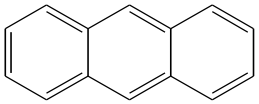
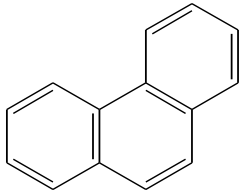
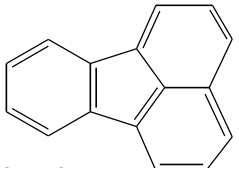
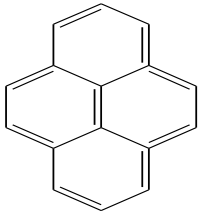
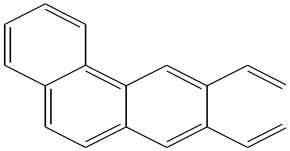
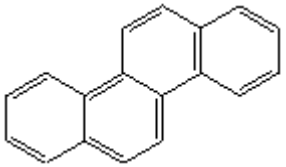
### 2.2.2 Physico-chemical properties of PAHs

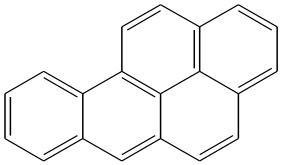
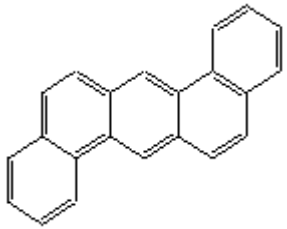
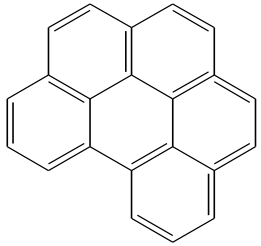
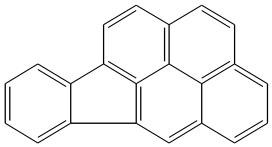
With no functional groups in their structures, PAHs are lipophilic compounds with very low water solubility which implies that their concentration in water is very low (Nasr *et al*., 2010; Qiu *et al*., 2009; Nikolaou *et al*., 2009; Rengarajan *et al*., 2015) in the range of ng $L^{-1}$ to pg $L^{-1}$. The water-soluble fraction is therefore reduced greatly. This low concentration in the aqueous fraction makes the analysis of PAHs difficult. The actual concentration of PAHs in the real water samples is very wide, depending on the closness of the polluted area to where they are produced, industrialization of the area and the type(s) of available PAHs transport (Kanaly and Harayama, 2000). In the atmosphere, 80% of PAHs with greater than 5 rings can be found associated with suspended atmospheric particles with very small aerodynamic diameters (> 2.5 μm) (EU working group on PAHs, 2001). As a consequence of their hydrophobic nature, PAHs in aquatic environments also tend to be associated to the particulate matter and finely dispersed soil colloids ending in sediments. Therefore, PAHs tend to accumulate and concentrate in sediments which represent the most important reservoir in aquatic systems (Kafilzadeh *et al*., 2011). Thus, concentrations of PAHs in water are usually very low as compared to the concentrations in the bottom sediments (Moore and Ramamoorthy, 1984). The United States Agency for Toxic Substances and Disease Registry has listed 17 priority PAHs based on their toxicological profile (ATSDR, 1995). The physical and chemical properties of PAHs strongly influence its transport pathways and how it is distributed in the environment. PAHs represents a wide spread group of environmental chemical pollutants and are ubiquitous contaminants in marine environments (Kafilzadeh *et al*., 2011). As

the molecular weight of PAHs` increase, their solubility in water decreases. At the same time, the corresponding boiling and melting point increase (Nikolaou *et al*., 2009). Table 3 shows some of the physical properties of PAHs which include water solubility, vapour pressure, Henry`s law constant and octanol-water partition coefficient ($K_{ow}$).

**Table 3** Priority listed PAHs with selected physical properties (Lee, 2010).

| Name | Chemical formula | Chemical structure | Molecular weight (g $mol^{-1}$) | Melting point ($^oC$) | Boiling point ($^oC$) | Vapour pressure (mmHg) | Log $K_{ow}$ | Log $K_{oc}$ |
|---|---|---|---|---|---|---|---|---|
| Naphthalene | $C_{10}H_8$ |  | 128.17 | 80.26 | 218 | $8.7 \times 10^{-2}$ | 3.29 | 2.97 |
| Acenaphthene | $C_{12}H_{10}$ |  | 154.21 | 95 | 96 | $4.5 \times 10^{-3}$ | 3.98 | 3.66 |
| Acenaphthylene | $C_{12}H_8$ |  | 152.20 | 92-93 | 265-275 | $2.9 \times 10^{-2}$ | 4.07 | 1.40 |
| Fluorene | $C_{13}H_{10}$ |  | 166.20 | 116-117 | 295 | $3.2 \times 10^{-3}$ | 4.18 | 3.86 |

| | | | | | | | | |
|---|---|---|---|---|---|---|---|---|
| Anthracene | $C_{14}H_{10}$ |  | 178.20 | 218 | 340-342 | $1.8 \times 10^{-6}$ | 4.45 | 4.15 |
| Phenanthrene | $C_{14}H_{10}$ |  | 178.2 | 100 | 340 | $6.8 \times 10^{-4}$ | 4.45 | 4.15 |
| Fluoranthene | $C_{16}H_{10}$ |  | 202.26 | 110.8 | 375 | $5.0 \times 10^{-6}$ | 4.90 | 4.58 |
| Pyrene | $C_{16}H_{10}$ |  | 202.3 | 156 | 393-404 | $2.5 \times 10^{-6}$ | 4.88 | 4.58 |
| Benzo(a)anthracene | $C_{20}H_{12}$ |  | 228.29 | 158 | 438 | $2.5 \times 10^{-6}$ | 5.16 | 5.30 |
| Chrysene | $C_{18}H_{12}$ |  | 228.28 | 254 | 448 | $6.4 \times 10^{-9}$ | 5.90 | - |

| | | | | | | | | |
|---|---|---|---|---|---|---|---|---|
| Benzo(a)pyrene | $C_{20}H_{12}$ |  | 252.3 | 179-179.3 | 495 | $5.6 \times 10^{-9}$ | 6.06 | 6.74 |
| Dibenzo(a,h)anthracene | $C_{22}H_{14}$ |  | 278.35 | 262 | - | $1.0 \times 10^{-10}$ | 6.84 | 6.52 |
| Benzo(g,h,i)perylene | $C_{22}H_{12}$ |  | 276.34 | 273 | 550 | $1.0 \times 10^{-10}$ | 6.50 | 6.20 |
| Ideno(1,2,3-c,d)pyrene | $C_{22}H_{12}$ |  | 276.3 | 163.6 | 530 | $10^{-10}$ - $10^{-16}$ | 6.58 | 6.20 |

**Notes:** Log$K_{ow}$ is the octanol/water partition coefficient
Log$K_{oc}$ is organic carbon-water partitioning coefficient
- No data was supplied

### 2.2.3 Effects of PAHs

Most PAHs are known to be toxic with the following properties; hydrophobic, low water solubility, and lipophilic. They therefore tend to bio-accumulate in the fatty tissue of living organisms and enter the food chain. Some PAHs are in the attention of scientists because they represent one of the largest classes of environmental carcinogens. However, even if some PAHs molecules are not carcinogenic, it was proved that their metabolites are (Tudoran and Putz, 2012). The toxicity of most PAHs has been traced back to the existence of K- and bay-regions which are formed metabolically. The presence of these regions makes the PAHs to be very reactive both chemically and biologically. Some examples of PAHs with bay regions are shown in Fig. 4.

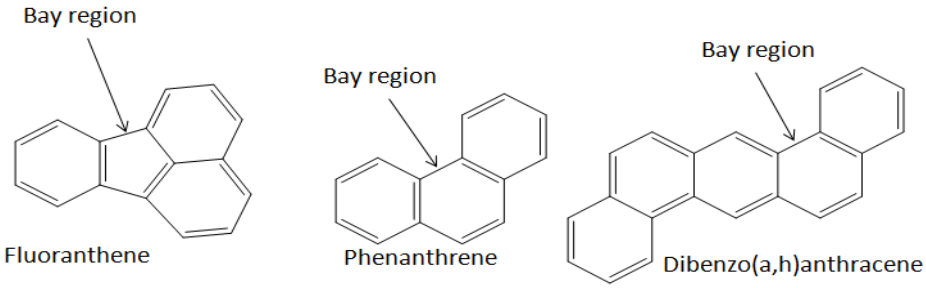



**Fig. 4.** Selected PAH structures showing bay regions.

## 2.3 Extraction techniques of organic compounds from liquid samples

Identification and quantification of PAHs in real environmental samples is associated with many challenges. For example, the specificity of the matrix type (the presence of contaminants, low levels of analytes, and their diverse chemical structure), may not allow for their direct analysis (Tobiszewski *et al.*, 2014). Many sample preparation techniquess have been used before instrumental analysis. These include, as listed in chapter one, liquid-liquid extraction, solid phase extraction, solid-phase micro extraction, gel permeation chromatography, Quick, Easy, Cheap, Effective, Rugged, and Safe (QuEChERS), and matrix solid-phase dispersion. Following this importance of selecting an appropriate extraction technique, Oluseyi *et al.* (2011) devoted their time in the investigation of four

extraction techniques in the determination of PAHs in contaminated soil samples; ultrasonication extraction, Soxhlet extraction, mechanical shaking and solid-phase extraction.

### 2.3.1 Solid phase extraction

Solid-phase extraction (SPE) is by far the mostly used sample preparation method for aqueous samples (Hennion, 1999). A wide variety of distinct SPE-sorbents materials have been used, including polymers (Yang *et al*., 2009), modified silica gel (Wang *et al*., 2004), chemically immobilized with dithizone(I) for the removal of mercury (Mahmoud *et al*., 2000) and multiwalled carbon nanotubes (Liang *et al*., 2004). A typical solid phase extraction involves four basic steps (Fig. 5). However, another additional stage of concentrating the eluted analytes by reducing the volume may be needed (Xu *et al*., 2007). First, the cartridge is equilibrated with a buffer of the same composition as the sample. The sample is then loaded to the cartridge, and it passes through the stationary SPE sorbent where the desired analytes interact and retain. The washing will then remove the impurities and finally, the analytes are eluted with appropriate buffer, before an optional pre-concentration.

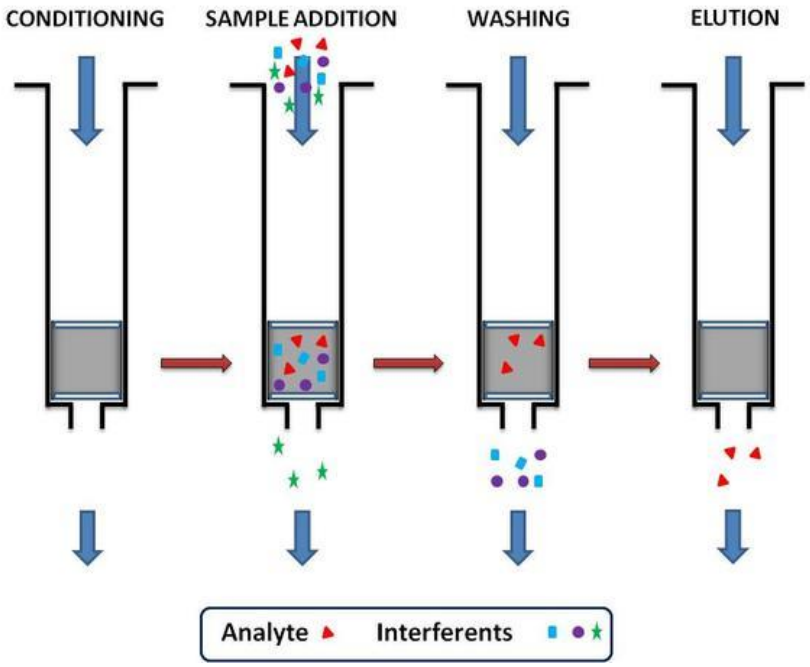



**Fig. 5.** Stages in solid phase extraction.

### 2.3.2 Liquid-liquid extraction

In liquid-liquid extraction (LLE), two or more immiscible liquids that are not in equilibrium are brought in contact. The analytes will then move from one phase to the other across the interfacial area due to the concentration gradient established between the phases (López-Montilla *et al*., 2005). One disadvantage of this method is that large volumes of organic solvents are used. In most cases, these solvents are toxic, and the set-up and operation is difficult to automate (Cortada *et al*., 2011). Just like in SPE, the solvent with the analytes of interest is often evaporated in order to pre-concentrate the samples. During this evaporation step, there is always a possibility of the loss and/or degradation of the desired target analyte (Darrach *et al*., 2011).

### 2.3.3 Solid phase microextraction

Solid phase microextraction (SPME) was introduced by Arthur and Pawliszyn (1990). This method is a solvent-free extraction technique that combines sample pretreatment, concentration and sample introduction all in one step (Saleh *et al*., 2009). In SPME, a polymer-coated fiber, on which the investigated compound adsorbs, is placed in the sample or its headspace. After some time, the polymer-coated fiber will then be inserted into the heated injection port of the GC system where the adsorbed analytes are thermally desorbed (Psillakis and Kalogerakis, 2001).

### 2.3.4 Liquid-phase microextraction

Liquid-phase microextraction (LPME) is also another technique that uses a small amount of a receiver solvent for concentrating analytes from aqueous samples (Rasmussen and Pederson-Bjergaard, 2004). This is fast becoming a method of choice since it is a solvent-minimization technique. This implies that it is a green technique as it uses minute volumes of toxic oganic solvents which are used in the traditional LLE. Wu *et al*. (2016) used LPME for the determination of six steroidal and phenolic endocrine disrupting chemicals in chicken, fish and water samples. Recently, Dolatto *et al*. (2016) used LPME method to extract the highly polar phenolic compounds.

#### 2.3.4.1 Liquid-liquid microextraction

Liquid-liquid microextraction (LLME) was first introduced by Belardi and Pawliszyn (1989). In LLME, the analytes are pre-concentrated into a very small volume implying that there are high enrichment factor achieved (Cortada *et al*., 2011). This method is a single-step extraction with high sample-to-solvent ratios. In order to achieve separation by centrifuge after the extraction, the organic phase must be denser than water. It also has to be in water to achieve high enrichment factor (Zheng *et al*., 2015). Wu and Yu (2012) used *n*-hexane and dimethylformamide for the extraction of PAHs in four different edible oils from China.

#### 2.3.4.2 Dispersive liquid-liquid microextraction

The basic principle of dispersive liquid-liquid microextraction (DLLME) is the dispersion of extraction solvent assisted with a disperser solvent within an aqueous solution that generates a very high contact area between the aqueous phase and the extraction solvent (Larki *et al*., 2015). DLLME is considered a convenient and efficient microextraction technique that was first developed by Rezaee *et al*. (2006). This method was recently used by Larki *et al*. (2015) for the determination of trinitrotoluene and used trioctylmethylammonium chloride as a dispersing agent. In another study, Tobiszewski *et al*. (2014) used DLLME for the extraction of 43 parents and methylated PAHs from water samples with perchloroethylene extractant and methanol as a dispersant.

#### 2.3.4.3 Single-drop microextraction

Single-drop microextraction (SDME) is a technique that is now widely because it is not expensive, its operation is simple and it a green method as it is nearly solvent-free (Xu *et al*., 2007). This technique was developed in quest for solvent-reduction in sample preparation procedure. It uses minute volumes (single drop) of the solvent, and therefore there is minimum usage of toxic organic solvents (Bahmaei *et al*., 2015). SDME was introduced by Jeannot and Cantwell (1996). The procedure for this technique involves suspending a small drop of of an acceptor solvent at the tip of a micro-syringe which will then be exposed to the

sample. This technique reduces the pre-concentration of interfering matrix as only the investigated volatile or semivolatile analytes are saturated into headspace thereby extracted to a hanging drop (Wang, 2013). Recently, Timofeeva *et al*. (2016) used SDME in combination with solvent exchange for the quantification of caffeine in saliva. García-Vázquez *et al*. (2016) coupled SDME with capillary electrophoresis for the determination of nonsteroidal anti-inflammatory drugs in urine samples. A headspace single drop microextraction was used by Wu et al. (2008) using aqueous solution of β-cyclodextrin as extraction solvent for the determination of PAHs in environmental samples.

#### 2.3.4.4 Hollow fiber liquid-phase microextraction (HF-LPME)

Hollow fiber liquid-phase microextraction (HF-LPME) was introduced in 1999 by Pedersen-Bjergaard *et al*. (1999). In this technique, a short hollow fiber is sealed at one end and with the help of a syringe a few microliters are introduced as an acceptor phase into the tube on the other end. The fiber will then be immersed into a solution with the analytes of interest. Due to the concentration gradient, the analytes are found to move into and saturates the acceptor phase across the membrane. Since the HF-LPME uses small amounts of fiber cheap environmentally friendly materials, it implies that they can easily be disposed of without incurring appreciable costs (Payán *et al*., 2010). Another advantage of the HF-LPME is that its pores are very small and cannot allow the traversing of large molecules and this brings about its selectivity as the matrix remains in the bulky donor solution after the pre-concentration process (Xiao *et al*., 2010). This technique has successfully been applied for the pre-concentration of PAHs (Hyder, *et al*., 1999; Liu, 2015).

## 2.4 Extraction techniques of organic compounds from solid samples

### 2.4.1 Soxhlet extraction

Soxhlet extraction is probably the most used method for the extactions of analytes from solid matrices. It is a method with which other extaction methods and techniques are normally benchmarked (Parera *et al*., 2004). In the soxhlet extraction, the solid sample which can be a soil or sediment is placed in a thimble above the extracting solvent in a round bottomed flask in a closed system. The solvent is heated to boiling and the vapour produced passes through a by-pass arm into the condenser where it is condensed back into a liquid above the thimble containing the sample. The solvent penetrates and soaks the sample, thereby extracting the analytes of interest. The solvent loaded with the analytes overflows back into the round bottomed flask where the analytes remain (having a higher boiling point than the solvent). This cycle is repeated as the extracting solvent is heated again. Marvin *et al.* (1992) compared Soxhlet and ultrasonic extraction for PAHs extraction. The ultrasonic extraction was better than the soxhlet extraction in terms of the yield of PAHs extracted from sediments and air particulates (Marvin *et al.* 1992). Oluseyi *et al.* (2011) investigated ultrasonication extraction, mechanical shaking and solid-phase extraction techniques in the determination of PAHs in contaminated soil samples. As is usually the norm, the Soxhlet extraction was included for comparison purposes.

### 2.4.2 Supercritical fluid extraction

Supercritical fluid extraction (SFE) with supercritical carbon dioxide as a solvent is widely used for the extaction organic compounds from solid samples. Its use results in a great reduction in extraction times. Librando *et al*. (2004) extracted PAHs from marine sediments and soil samples. Rai *et al*. (2016) did supercritical extraction of oil from sunflower seeds. Hsueh *et al.* (2013) used supercritical water at 673 K and 240 bars for the extraction of PAHs hindered in fly ashes. Recently, there has been interest in combining SFE with other extraction techniques, e.g., Jowkarderis and Raofie (2012) coupled SFE with LLME as an efficient sample preparation method for the analysis of isomers of nitrotoluene in

a complex matrix. The use of SFE has also been used by Batlle *et al.* (2005) coupled to various analyte collection strategies for the extraction of nitroaromatic compounds and their degradation products from soil samples.

### 2.4.3 Microwave assisted extraction

The principle of this technique is heating the solid sample mixed and homogenized in the extracting solvent by microwaves. This increases the mass tranfer of the analytes from the sample into the bulk solution of the extracting solvent. This technique has an advantage of having short extraction times as compared to other traditional methods. Microwave assisted extraction was also used by many researchers to extract compounds like PAHs (Sibiya *et al*., 2013). Kjellström *et al*. (2008) investigated the extraction of TNT from soil samples.

### 2.4.4 Pressurized liquid extraction

Pressurized liquid extraction is a relatively new technique for the extraction of analytes from solid samples. This method uses common solvents at high pressures and temperatures. Pressurized liquid extraction is a very fast technique and it uses less solvent than conventional techniques (Santos *et al*., 2012; Richter *et al*., 1996). According to the study by Itoh *et al*. (2008), when Soxhlet extraction, microwave-assisted extraction and pressurized liquid extraction where compared for their capabilities of extracting PAHs, and it was found that the later was more efficient.

## 2.5 Performance comparison of different extraction analytical methods

Comparison of selected analytical methods for the extraction and determination of PAHs and NACs is presented in Table 4. From the table, it can be seen that the most common separation-detection method for both PAHs and NACs is the GC-MS.

**Table 4** Comparison of different methods for the extraction of PAHs and NACs

| PAH/NAC | Matrix | Pre-concentration method | Separation-detection method | Reference |
|---|---|---|---|---|
| 16 priority | soil | Acetone-SPE | HPLC-Flu | Kootstra *et al*., 1995 |
| 16 priority | soil | Ultrasonication-SPE | HPLC-UV | Sun *et al*., 1998 |
| PAHs | water | SPE | HPLC | Moja and Mtunzi, 2013 |
| 16 priority | plant | ultrasound | GC-MS | Guatemala-Morales *et al*., 2016 |
| 16 priority | water | LLME | GC-MS | Zheng *et al*., 2016 |
| 16 priority | edible oils | LLME | GC-MS | Wu and Yu, 2012 |
| parent and methylated PAHs | water | DLLME | GC-TOF-MS | Tobiszewski *et al*., 2014 |
| PAHs | wastewater | SDME | GC-FID | Sun *et al*., 2014 |
| TNT | Water and soil | DLLME | UV-Vis | Larki *et al*., 2015 |
| Mono-NTs | Water | DLLME | GC-FID | Sobhi *et al*., 2010 |
| Nitroaromatic | Water | SPME | GC-MS | Psillakis and Kalogerakis, 2001 |

| | | | | |
|---|---|---|---|---|
| explosives | | | | |
| Nitroaromatic explosives | Water | SDME | GC-MS | Psillakis and Kalogerakis, 2001 |
| 16 PAHs | Water | SPME | GC-MS | King *et al*., 2004 |
| Nitroaromatic compounds | water | SPME | GC-MS | Jönsson *et al*., 2007 |
| Nitrobenzenes | Water | SDME | GC-MS | Zhao *et al*., 2004 |
| PAHs | Water | SDME | HPLC-UV | Hou and Lee, 2002 |
| MNTs | Water | DLLE | GC-FID | Sobhi *et al*., 2010 |
| 2,4-DNT | Water | DLLME | GC-FID | Ebrahimzadeh *et al*., 2009 |

## 2.6 New sorbent materials

### 2.6.1 Molecularly imprinted polymers

Research for selective identification and quantification of explosive compounds has attracted the attention of public security specialists and environmental scientists. Recent developments in the area of molecularly imprinted polymers (MIPs) have seen the preparation of specific and selective materials that can adsorb organic compounds from aqueous samples (Jenkins *et al*., 2012). MIPs are synthetic sorbents that work as artificial receptors due to their good selectivity. The synthesis approach involves the co-polymerization of functional and cross-linking monomers in the presence of template molecules. Subsequent extraction of template creates specific molecular recognition sites in solid polymers, which are complementary to the shape, size, and functional group(s) of the template (Yunhe *et al*., 2009). MIPs have been used in solid phase extraction as selective sorbents to concentrate target analytes and at the same time clean-up samples prior to analysis (Ebrahimzadeh and Behbahani, 2013). The biggest benefit of using MIPs is in the selective sorption of the target analyte(s) which always occur alongside complex matrix if real samples are analyzed. Due to a betterfit in shape and surface chemistry, these cavities will later on preferentially adsorb the template molecules over closely related analogues (Wackerlig and Schirhagl, 2016). The affinity and selectivity of MIPs basically depend on the parameters which are determined by the strength and type of intermolecular interactions (Riah *et al*., 2010). Figure 8 shows the general synthetic diagram for the preparation of MIPs.

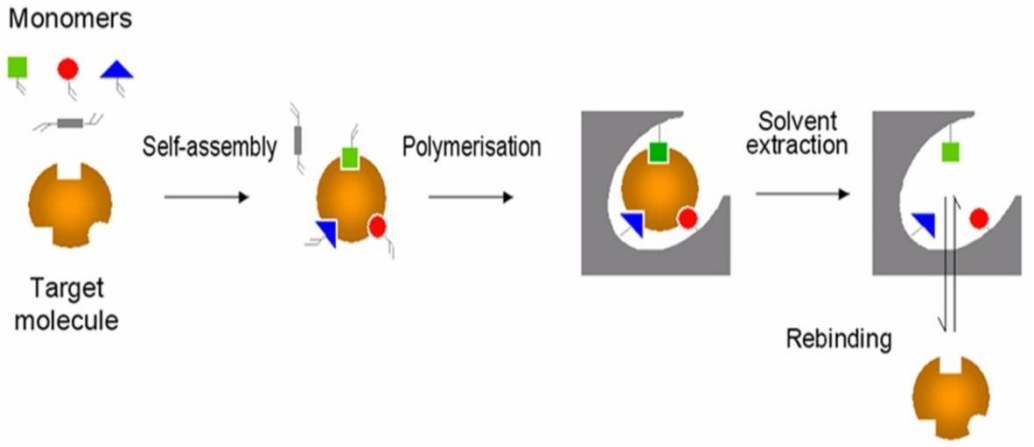



**Fig. 6.** Schematic diagram for the synthesis of MIPs (Haupt *et al*., 2010)

In pharmaceutical field, there is increasing demand for optically pure drugs, and this has resulted in an interest in developing sorbents and methods for efficient chiral separation. Balamurugan *et al*. (2011) synthesized a MIP with either (+) or (-)-Ephedrine ((R∗,S∗)-2-(methylamino)-1-phenylpropan-1-ol) as chiral drug templates and used the material as stationary phases in chromatographic colums. The MIPs were effective for the resolution of Ephedrine enantiomers. In their quest to separate diastereoisomers of mandelic acid, R- and S- hydroxy-1-phenyl-acetic acid, Hung *et al*. (2005) packed MIPs into the HPLC columns. In HPLC sorbents, the size of the packing materials in columns is very crucial. The mechanical processing (grinding of bulk polymers) normally leads to non-homogeneous particles with respect to shape and size resulting in the production of irreproducible quality data. This disadvantage of bulk polymerization is the reason why other imprinting formats have been investigsated. For example, monolithic MIPs columns have been recently prepared directly inside stainless steel columns (Matsui *et al*., 1993; Yin *et al*., 2005).

### 2.6.2 Carbon nanomaterials

Carbon nanofibers (CNFs) are carbonaceous fibrous materials conformed by stacked graphene layers (Serp *et al*., 2003). They are hydrophobic and almost without functional groups. There are two main methods for the synthesis of CNFs which are catalytic thermal chemical vapor deposition growth and electrospinning followed by heat treatment. These two approaches were reviewed by Feng *et al*.

(2014). In the former, CNFs are synthesized from the decomposition of a hydrogen and carbon source (and/or carbon monoxide), and the catalys used are normally the metals or metal oxides. The reaction is normally carried out at high temperatures ranging between 400 and 700°C (Rodriguez, 1993). Since their first synthesis, the carbonaceous fibrous materials (CNFs and carbon nanotubes (CNTs)) have been on the spotlight amongst researchers owing to their potential applications in catalyst support and environmental analysis as sorbents. Raw CNTs are mainly used for the removal and extraction of hydrophobic organic compounds owing to their high adsorption capacity (Xia *et al*., 2013).

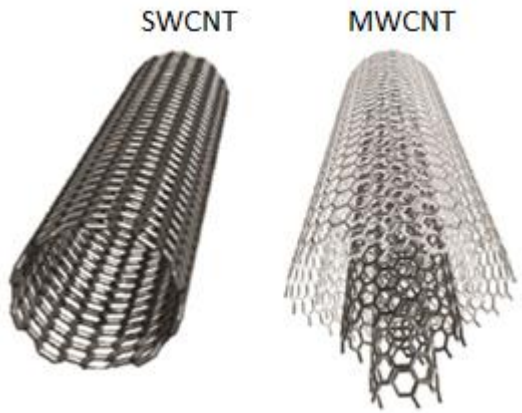



**Fig. 7.** Structure of carbon nanotubes

It is necessary to convert the CNFs into hydrophilic material if the subsequent use is to extract polar compounds. This is normally carried out by modifying or adding functional groups normally carrying heteroatons like O, N and S. With these groups, the surface of the carbonaceous materials is able to extract extract polar organic compounds. There is a lot of literature which reported the modification of CNFs with different surfactants specifically chosen for particular organic analyte, e.g., Norzilah *et al.* (2011) used 4 M of $HNO_3$ to modify CNTs for the sorption of methylene blue and phenol. The effect of the chemical activation, using $HNO_3$, of commercial CNFs on its surface chemistry and adsorption properties was investigated by Cuervo *et al.* (2008).

### 2.6.3 Electrospun fibers

Electrospinning is a method that is used to produce fibers that are characterized by small diameters. In the synthesis of these fibers, there is utilization of a potential difference beteen the collector and the solution being electrospun (Sheikh *et al*., 2013). Electrospinning is an old technique, and cellulose acetate is one of earliest materials to be electrospun and there is a patent regarding this (Formhals, 1938). Key properties for a polymer (natural and synthetic) to be electrospun are that it should be sufficiently soluble, of high molecular weight, and that the dissolved solution should be viscoelastic and conducting electricity (Rutledge and Fridrikh, 2007; Bhattacharjee and Rutledge, 2011). Cellulose and chitosan have been electrospun a lot because these materials are cheap owing to their natural origin and availability in large quantities (Ward, 1943). However, some materials have been investigated, e.g., polyacrylonitrile (PAN) nanofiber membranes coated with calix[8]arenes were electrospun from different composition mixtures of PAN solutions and calixarenes (Chen *et al*., 2013). Deng *et al*. (2009) demonstrated that 1D fluorescent nanofibers prepared from a conjugated polymer, poly(triphenylamine-alt-biphenylene vinylene), with excellent sensory performance which could be a good candidate sensor for detection of TNT. Close to this work, Tao *et al.* (2007) demonstrated the use of porphyrin doped electrospun nanofibers for the detection trace amounts of of TNT in vapours. Electrospun fibers have demonstrated applications in filtration and biosensors (Wang *et al*., 2004). Figure 8 shows the simple horizontal electrospinning set-up.

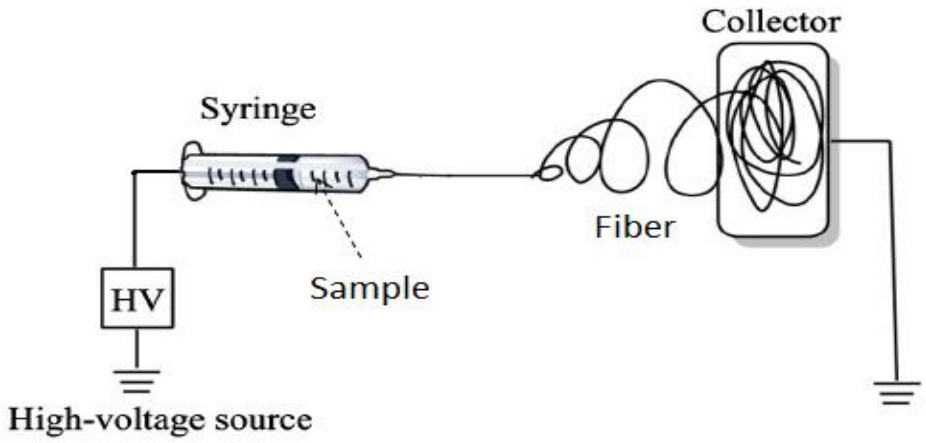



**Fig. 8.** Schematic setup for electrospinning

### 2.6.4 Moringa oleifera

*Moringa oleifera* is one of the fourteen species of trees that fall under genus *Moringaceae*. This plant naturally grows in countries/regions like India, Sri-Lanka, Mexico, Middle East and south-western Africa. It has been a subject of research due to its unique nutritional (Gowrishankar *et al*., 2010; Dillard and German, 2000), therapeutical (Ayotunde *et al*., 2011; Anwar *et al*., 2007) and water coagulation properties (Santos *et al*., 2012; Ali *et al*., 2009). The use of *Moringa oleifera* as a water purifier is probably one of its major use. Natural adsorbents are used mostly in water treatment as they are cheap and readily available (Kumari *et al*., 2006). In contrast, traditional method of water purification using aluminium sulphate and calcium hypochlorite are very expensive, especially for rural communities in developing countries. This leaves no option for rural communities but look for alternative cheap methods of cleaning their drinking water. However, most readily available adsorbent sources lack in sorption capacities, thereby exposing people to waterborne diseases.



**Fig. 9.** *Moringa oleifera* tree and seed kernels

Huge volumes of waste and by-products are generated when agricultural products are processed. Use of it can be made by developing the biosorbents to treat polluted water (Reddy *et al*., 2010). Apart from low cost, the other advantages that biosorbents have over other conventional methods include; high efficiency, minimization of chemical and or/biological sludge, ability for regeneration of biosorbent and no additional nutrient requirement. There are no significant concentraion of $Cl^-$ and $SO_4^{2-}$ after water treatment, unlike when traditional coagulants like $FeCl_3$ and $Al_2(SO_4)_3$ are used.

Apart from being used as raw, the Moringa seeds are known to contain some proteins which have been extracted and used in water purification. In a study by Ndabigengesere *et al*. (1995), they found the net charge of the protein to be positive. This natural cationic protein acted as a flocculant, thereby decreasing the turbidity of the water. It was found to be capable of removing negatively charged particles including bacteria (Ndabigengesere *et al*., 1995). Ghebremichael *et al*. (2005) had the same observations that the proteins had a net positive charge when they were added to water.

Chemically modified Moringa seed powder, especially with amine-based surfactants, has been used for the sequestration of metal ions from aqueous solutions. This is owing to the strong binding properties of the amine functional groups. Mnisi *et al*. (2012) used unmodified and amine modified

(ethylenediamine, diethylenetriamine, triethylenetetramine and tetraethylenepentamine) *Moringa oleifera* bark as a potential alternative sorbent to the current costly methods of vanadium removal from polluted water solutions. Use of different coating agents was done to ascertain whether the different amines could functionalize the adsorbent and what effect this would have on the adsorption performance.

Activated carbon (AC) is a carbonaceous material which is characterized by high surface area. This physical transformation is another popular modification. Since *Moringa oleifera* seed husks are available in large amounts, they were used by Warhurst *et al*. (1997) to make AC. The product showed high micro-porous with some meso-porosity and showed fast adsorption of pollutants 4-nitrophenol and methylene blue. High-quality AC made from readily available waste husks of *Moringa oleifera* (Miquel and Wendy, 2010; Pollard *et al*., 1995) was used to clean contaminated water. Sumathi and Alagumuthu (2014) activated *Moringa oleifera* dried raw leaves by carbonizing them in a muffle furnace at 400°C for removal of arsenic from aqueous solutions.

## 2.7 Performance comparison of different extraction analytical methods

Table 5 summarizes the application of different sorbents (discussed above as new sorbent materials) for the removal of PAHs and NACs from aqueous solutions. There is a lot of literature concerning the extraction of PAHs from different matrices. For example Lau *et al*. (2010) gave a detailed review of the extraction of PAHs from soil samples where techniques like Soxhlet extraction, supercritical and subcritical fluid extraction and fluidized-bed extraction were details.

**Table 5** Comparison of different methods for the removal of PAHs and NACs

| PAH/NAC | Material | Separation method | Selectivity [Y/N] | LOD | Reference |
|---|---|---|---|---|---|
| 2,4-DNT | Functionalized multiwalled carbon Nanotubes/polyethyleneimine | Electrochemical sensors | Yes | $1.0 \times 10^{-9}$ mol $L^{-1}$ | Nie *et al*., 2016 |
| TNT | Porphyrin doped electrospun fibers | Adsorption | - | - | Tao *et al*., 2007 |
| NB | Raw and biocharred *Moringa oleifera* seed powder | Biosorption | No | xxx | Tavengwa *et al.*, 2016 |
| 16 priority | Multi-walled carbon nanotubes | | xx | xx | Ma *et al*., 2010 |
| TNT | MIP | Adsorption | Yes | 40.7 µM | Stringer *et al*., 2010 |
| 2,4-DNT | MIP | Adsorption | Yes | 30.1 µM | Stringer *et al*., 2010 |
| 2,4-DNT | Porous graphitic carbon | | | 0.07 ng $\mu L^{-1}$ | Tachon et al., 2007 |
| TNT | MIP | Adsorption | Yes | - | Bunte *et al*., 2007 |
| [§]Light PAHs | MIP | Adsorption | Yes | 1.5-270 ng $L^{-1}$ | Egli *et al*., 2015 |
| [ɤ]Probable | MIP | Adsorption | Yes | - | Krupadam *et al*., |

| | | | | | |
|---|---|---|---|---|---|
| human carcinogens | | | | | 2010 |
| Nitroaromatic compounds | Graphine oxide, reduced graphine oxide and graphine nanosheets | Adsorption | - | - | Chen and Chen, 2015 |
| Nitroaromatic compounds | Carbon nanotubes | Adsorption | - | - | Chen *et al*., 2007 |
| TNT | SiO2 aerogel/activated carbon | Adsorption | - | - | Zhou et al., 2013 |
| Nitroaromatic compounds | β-CD@CNF[ϰ] | Adsorption | - | 3-24 µg $L^{-1}$ | Tavengwa *et al*., 2016 |

ϰ: These are: B[a]A, benzo[a]anthracene; B[a]P, Benzo[a]pyrene; B[b]F, Benzo[b]fluoranthene; Chr, Chrysene; D[a]P, dibenzo[a,h]pyrene; and I[2]P and[§]These are: Nap, Flu, Phen and Pyr

-: not reported

ϰ: β-cyclodextrin functionalized on carbon nanofibers

Where ‘Nitroaromatic compounds` is mentioned, a mixture of >3 NAC was used

# Chapter 3

# 3 Research objectives

## 3.1 General objectives

The general objective of the study was to develop natural and synthetic sorbents for application in water treatment for the extraction and removal of organic pollutants (explosive compounds and polycyclic hydrocarbons).

## 3.2 Specific objectives

- To apply the characterized raw and biochared *Moringa oleifera* seeds to the removal of nitrobenzene from aqueous solutions (**paper I**).
- To study the selective extraction of 2,4-DNT explosive from aqueous solutions by application of magnetic molecularly imprinted polymers (**paper II**).
- To investigate the extraction of explosive compounds from aqueous solutions by solid phase extraction impregnated with β-cyclodextrin functionalized carbon nanofibers (**paper III**).
- To prepare the molecularly imprinted polymers-membrane assisted solvent extraction combination for the extraction of polycyclic aromatic hydrocarbons from sewage wastewater (**paper IV**).
- To electrospin polyacrylonitrile into nanofibers and characterize it before extraction of nitrotoluenes from aqueous solutions (**paper V**).

## 3.3 Research questions

- What are the factors that can be optimized in order to achieve better quantification and identification of the low concentrations of nitroaromatic compounds and polycyclic aromatic hydrocarbons in the environment?
- Does biocharring of *Moringa oleifera* seed powder have an effect in the extraction of nitrobenzene?
- Can the molecularly imprinted polymers selective of specific selected analyte be synthesized and perform as expected in batch adsorption studies?

## 3.4 General approach

- Selection/development of the desired sorbent material as outlined in the methodology sections of the respective papers.
- Modification (chemical or physical) of the starting material accordingly.
- Full characterization of the prepared material was carried out to gain the physico-chemical behaviour of the prepared materials.
- Optimization of the proposed methods was carried out. Parameters such as sample pH, contact time and weight of the sorbent were investigated.
- Where relevant, modelling of the kinetic data (e.g., pseudo-first-order and pseudo-second-order) and adsorption data (e.g., Langmuir and Freundlich) were carried out.
- The developed methods (optimized) were then applied to real environmental samples to test their applicability from parameters such as recovery and %RSD.

Figure 10 shows the general flow chart of the order of experiments. In **paper II**, **III** and **IV**, the work started with chemical synthesis of the material; MIPs for paper I and IV and fibrous materials **paper III**. Physical transformation of the moringa seed powder into activated carbon was also used to prepare the sorbent **paper I** and in **paper V**, PAN was converted into nanofibers through electrospinning. At times, the material needed further functionalization in order to improve the sorption of the target analyte. An example is when the synthesized CNF was further modified but addition of β-cyclodextrin (**paper III**). In **paper IV**, the synthesized MIPs were firstly added to a membrane bag and dispersed in toluene acceptor phase. Necessary characterization of the prepared materials were done and reported in the respective papers. Full optimization was done to find out the maximum values of parameters likely to affect the uptake of the investigated analytes. The optimized parameters were finally applied to real environmental samples.

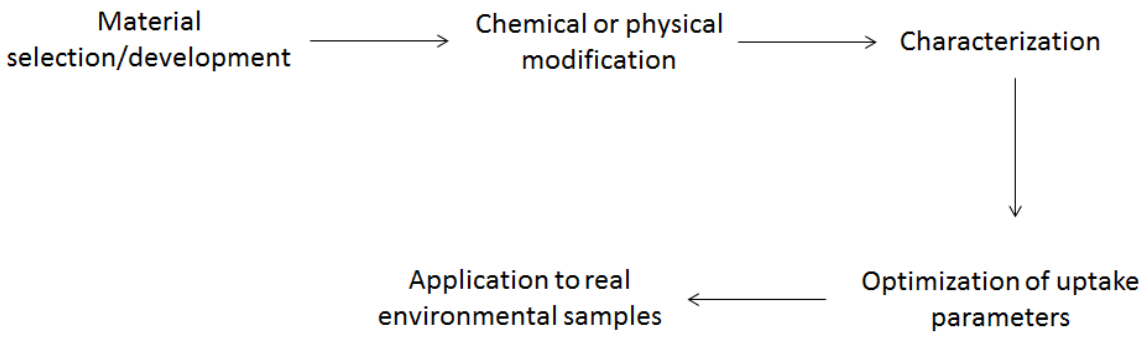



**Fig. 10** A general scheme for the research approach.

# Chapter 4

# 4 List of publications

This chapter lists all the five manuscripts submitted for examination. Each manuscript is formatted into the sytle requirement of the journal as per the requirements of the particular journal. Note also that the reference styles are also different. **Papers I** and **III** have already been published, **papers II** and **V** have been submitted and are currently under review, whilst **paper IV** is a manuscript that will be submitted soon.

**Paper I**

This paper "Application of raw and biochared *Moringa oleifera* seeds to the removal of nitrobenzene from aqueous solutions," was published in *Desalination and Water Treatment*. It explores the effect of biocharring of the natural sorbent *Moringa oleifera* seeds in the uptake of nitrobenzene model pollutant.

*Desalination and Water Treatment*
www.deswater.com
doi: 10.1080/19443994.2016.1151381

(2016) 1–10

Taylor & Francis
Taylor & Francis Group

# Application of raw and biochared *Moringa oleifera* seed powder for the removal of nitrobenzene from aqueous solutions

Nikita Tawanda Tavengwa, Ewa Cukrowska, Luke Chimuka*

*Molecular Sciences Institute, School of Chemistry, University of Witwatersrand, Private Bag 3, Johannesburg 2050, South Africa, emails: nikita.tavengwa@students.wits.ac.za (N.T. Tavengwa), ewa.cukrowska@wits.ac.za (E. Cukrowska), luke.chimuka@wits.ac.za (L. Chimuka)*

Received 14 September 2015; Accepted 2 February 2016

ABSTRACT

Low cost and locally available *Moringa* seed powder as a potential biosorbent was tested for its effectiveness in the removal of nitrobenzene (NB) from aqueous solution. Biochared *Moringa oleifera* seed powder was also used to compare its performance in the uptake of NB from aqueous solution. Fourier transform infrared spectroscopy fingerprint region of the biochared *M. oleifera* seed powder was clearer as compared to the raw. Pores observed by the scanning electron microscopy analysis were found to be 0.84 and 1.23 $cm^3 g^{-1}$ (by BET analysis) for the raw and biochared *M. oleifera* seed powder, respectively. The carbon elemental analysis by energy-dispersive X-ray spectroscopy was 80 and 70% for the raw and biochared *M. oleifera* seed powder, respectively. The removal efficiencies of the two sorbents were evaluated using factors such as solution pH, biosorbent dosage, contact time and initial NB concentration. A basic pH of 11 was found to be optimum for the uptake of NB for both sorbents. The sorption equilibration time of NB at 25°C was about 50 min, and the optimal NB removal efficiency was achieved with a dosage of 12.5 g $L^{-1}$. The pseudo-second-order was found to fit the kinetic data better with the calculated sorption capacity of NB of 0.084 and 0.071 mg $g^{-1}$ onto the raw and biochared *M. oleifera* seed powder sorbent. The limit of detection and limit of quantification values for NB determination by HPLC-UV were found to be 11.54 and 38.46 μg $L^{-1}$, respectively.

*Keywords:* Biosorption; *Moringa oleifera*; Biochar; Nitrobenzene

## 1. Introduction

Nitrobenzene (NB) is widely used in the manufacturing of dyes, pesticides, explosives and paper and textile [1,2]. However, the release of NB from these industries into the environment has drawn considerable attention due to its toxicity, persistence and accumulation in the food chain. Nitroaromatic compounds (NACs) are commonly found in the subsurface soil and pose a potential threat to human health [3]. Therefore, a variety of wastewater treatment technologies such as adsorption [4], biodegradation [5] and oxidation processes [6] have been employed for the purification of NACs contaminated water. Due to high costs and environmental side effects of the chemical coagulant compounds such as aluminium and iron salts, there has been an increase in interest in the use of organic coagulants derived from plant material [7].

*Corresponding author.

1944-3994/1944-3986 © 2016 Balaban Desalination Publications. All rights reserved.

Biomass, which is abundant in nature and produced in large quantities as a by-product or waste from agricultural activities could be used to make biosorbents for environmental remediation [8]. The use of biosorbents for the uptake of pollutants from aqueous medium was previously reported e.g. metal removal with biosorbents was reviewed by Veglio and Beolchini [9], and Wang and Chen [10].

Amongst other plant materials, powder form of *Moringa oleifera* seed has been proven to be one of the most effective and viable replacement of various chemical coagulants [11,12]. *Moringa*, the only genus belonging to the *Moringaceae* family, consists of 14 species [13]. Raw *M. oleifera* seed powder has been used extensively for the removal of various pollutants from wastewaters e.g. orange 7 dye [14], chromium [15] and copper [16]. However, most of the studies in literature have focused on metal ion remediation. Use have been made of the functional groups as a result of the presence of various amino acids, fatty acids, vitamins, glucosinolates and phenolics (flavonoids, anthocyanins, proanthocyanidins and cinnamates) [16]. In order to improve the sorption capacity, the *M. oleifera* seed powder has been chemically modified with different chemicals like alginate [17] and acetic anhydride [18].

Physical transformation of raw *M. oleifera* seed powder into biochar is receiving great research attention due to its potential in agronomic and environmental applications [19]. In this process, the generation of pores take place via selective elimination of the more reactive carbon and further gasification leading to the production of activated carbon with high porosity [20]. The cost of the activated carbon prepared from biomaterials is lower compared with that of commercial activated carbon [21].

In this work, factors affecting the biosorption of NB by the locally available, low cost and eco-friendly *M. oleifera* seed powder were investigated. Uptake performance of NB by biochar obtained by direct pyrolysis of *M. oleifera* seed powder was also investigated and compared with the raw material. Characterization of the raw and biochared *M. oleifera* seed powder was done by Brunauer–Emmett–Teller (BET) surface area analysis, Fourier transform infrared spectroscopy (FTIR), scanning electron microscopy (SEM) and zeta potential and energy dispersive X-ray spectroscopy (EDS).

## 2. Materials and methods

### 2.1. Chemicals and materials

NB (≥99%) was bought from Sigma-Aldrich (Johannesburg, South Africa) and acetonitrile (99.9%) was obtained from Sigma-Aldrich (Steinhein, Germany).

Deionized water was obtained from Milli-Q ultrapure water (Millipore, Billerica, Massachusetts, USA). pH measurements were done on a 766 Calimatic pH meter equipped with a Shott N61 pH electrode from Knick (Berlin, Germany). For mechanical agitation, a Wisecube Fuzzy Control System from Wisd Laboratory Instruments was used at 100 rpm at a fixed temperature of 25°C. A Rotofix 32A Centrifuge from Hettich Lab Technology (Tuttlingen, Germany) was used to separate the NB solution from the sorbents, and was set at 2,500 rpm.

### 2.2. HPLC conditions and preparation of solutions

A Bischoff HPLC with a UV detector set at 254 nm with an Ascentis@ RP-Amide column (25 cm × 4.6 mm × 5 µm) was used to quantify the NB. The mobile phase composition was acenotnitrile/water (65/35, v/v) with the flow rate maintained at 1 mL $min^{-1}$ in isocratic mode and the sample injection volume of 50 µL was used.

A 100-mg $L^{-1}$ stock solution of NB was prepared by dissolving the appropriate volume in 50/50, v/v acetonitrile/water solution. A 10-mg $L^{-1}$ NB working solution was then prepared from the stock solution and the same diluent, acetonitrile/water (50/50, v/v) was used to top up to the mark.

### 2.3. Biosorbent preparation

*M. oleifera* seeds were collected from a farm in Lebowakgomo in Limpopo Province, South Africa (24.3050°S, 29.5650°E). *M. oleifera* seeds were dried in sunlight for 3 d (average temperature was 26°C). The dehusked *M. oleifera* seeds were then washed several times with distilled water to remove all dirt. The cleaned *M. oleifera* seeds were oven dried at 80°C for 3 h. The seeds were powdered in mortar and pestle and sieved through a 2 mm mesh. Direct pyrolysis was used for the preparation of biochar from *M. oleifera* seeds. The heating process was carried out in the absence of air after purging with nitrogen for 10 min. The *M. oleifera* seed powder was biochared in a muffle furnace at 200°C for 2 h, and the average pyrolysis yield of biochar was 48.9% by mass. After biocharing, the material was repeatedly washed with distilled water.

### 2.4. Characterization

Through a FEI Quanta 200 ESEM scanning electron microscopy equipped with EDS, the surface morphological features of the raw and biochared *M. oleifera* seed powder were explored and elemental composi-

tions determined. The samples were mounted on a black double-sided carbon tape attached to a sample platform. To avoid charging, the samples were coated with gold palladium using a sputter coater Baltec Scutter SCD 050 to a thickness of approximately 30 nm. Fourier transform infrared spectra were recorded in the frequency range of 400–4,000 $cm^{-1}$ using a Tensor 27 Bruker FTIR spectrophotometer (Ettlingen, Germany). Zeta potentials were measured with the Zeta-Meter 3.0 system (Malvern ZS-90).

### 2.5. Swelling studies

The swelling behaviour was investigated by immersion of 1.5 g of *M. oleifera* seed powder (raw and biochared) in 25 mL of distilled water at 25°C for 3 d until swelling equilibrium was achieved. Elongated times were used (3 d) to make sure equilibrium was reached. The equilibrium times are normally shorter; in orders of few hours e.g. Ijarotimi et al. [22] who equilibrated the *M. oleifera* seed flour for 30 min. The sorbent weight increase allowed the calculation of the swelling percentage using Eq. (1) where $W_s$ and $W_d$ are the weights of the swollen and dry sorbent samples (in g), respectively.

$$\text{Swelling ratio } (\%) = \frac{(W_s - W_d)}{W_d} \times 100 \quad (1)$$

### 2.6. Batch adsorption studies

A typical batch adsorption was done by adding the dried biosorbent (raw and biochared *M. oleifera* seed powder) into a solution of NB under specific experimental conditions. The effect of pH was investigated using 0.2 M NaOH and/HCl to adjust the pH of the samples to acidic, neutral and basic conditions. The effect of biosorbent loading was studied using various dosages of biosorbents (1.0, 2.50, 6.25, 12.50, 18.75, 50.0 and 100.0 g $L^{-1}$). Contact time was investigated at different time levels (1, 2, 5, 10, 15, 20, 30, 45 and 90 min). The effect of concentration was also examined at different levels (1.0, 0.25, 0.5, 0.8, 1.0, 1.5, 2.0 and 3.0 mg $L^{-1}$).

After shaking the mixture, the sorbent was separated by centrifugation at 2,500 rpm for 10 min and the concentration of NB in the supernatant was measured by HPLC-UV. Eqs. (2) and (3) were used to calculate the uptake efficiency of NB from aqueous solution.

$$\text{Extraction efficiency } (\%) = \frac{(C_o - C_e) \times 100}{C_o} \quad (2)$$

$$\text{Adsorption capacity} = \frac{(C_o - C_e)V}{m} \quad (3)$$

where $C_o$ is the initial concentration of NB (mg $L^{-1}$), $C_e$ is the amount of NB after adsorption (mg $L^{-1}$), $V$ is the volume of NB solution (L) and $m$ is the weight of the sorbent (raw or biochared *M. oleifera* seed powder) used (g).

### 2.7. Point of zero charge determination

For the point of zero charge ($pH_{pzc}$) determination, a modified method from Rivera-Utrilla et al. [23] was used: 25 mL of 0.01 M NaCl solution was placed in a vessel. Nitrogen was bubbled through the solution to stabilize the pH by preventing the dissolution of $CO_2$. The pH was adjusted to values between 1 and 13 by addition of 0.1 M HCl or 0.1 M NaOH solutions. 100 mg of the raw or biochared *Moringa* seed powder was added to the solution and left shaking for 24 h at 140 rpm at 25°C. The final pH was then measured and plotted against the initial pH for the determination of the $pH_{pzc}$.

## 3. Results and discussion

### 3.1. Characterization

The swelling results are presented in Table 1 where the raw *M. oleifera* seed powder had a swelling ration of 27.2% whilst that of the biochared *M. oleifera* seed powder was 14.2%. The raw material had almost double the swelling capability as compared to the biochared because of the various functional groups which were absent in the biochared, as the FTIR result later showed. The initial rapid increase in the swelling of the polymeric sorbent synthesized by Anirudhan et al. [24] was attributed to the presence of the hydrophilic –COOH. The surface characterization of the biosorbents shown in Table 1 indicated the high porosity of the biochared sorbent as compared to the raw one.

The morphologies of raw and biochared *M. oleifera* seed powder were investigated by SEM analysis (Fig. 1(a) and (b)). The SEM micrographs showed an amorphous and heterogeneous nature of *M. oleifera* seed powder with clear, porous characteristic on the surfaces and the development of voids. The presence of a porous surface meant an increased surface area and this translated to an increased NB sorption capacity as this increased the mass transfer.

FTIR was used to investigate the functional groups present on the *M. oleifera* seed powder sorbents. The two spectra of *M. oleifera* seed powder (raw and

Table 1
Physical characteristics of the biosorbents

| *Moringa* powder biosorbent | Surface area ($m^2\ g^{-1}$) | Specific volume ($cm^3\ g^{-1}$) | Swelling ratio (%) |
|---|---|---|---|
| Raw | 6.3 | 0.84 | 27.2 |
| Biochared | 12.6 | 1.23 | 14.2 |

biochared) are shown in Fig. 1(c). The broad peak seen on the raw sorbent at around 3,430 $cm^{-1}$ indicated the presence of hydroxyl group (–OH) stretching. There was a great reduction of the hydroxyl group (–OH) stretching frequency for the biochared sorbent probably due to the elimination of moisture and –OH groups of the proteins from the biochared *M. oleifera* seed powder during biocharing. The absorption peaks at 2,920 and 2,851 $cm^{-1}$ were due to the C–H stretching off –C=O and/or $–CH_3$ of functional groups. The bands corresponding to the carbonyl group (–COO) of the proteins and other organic compounds in *Moringa* seed powder were detected at around 1,750 $cm^{-1}$. The band centred at 1,600 $cm^{-1}$ was assigned to the molecular vibration of ring stretching in C=C probably due to the presence of organic compounds in the *Moringa* seed powder. This band was intense for the raw materials and was subdued in the biochared sorbent. Biochar is a solid residue of biomass incomplete combustion or pyrolysis, which is produced alongside two other by-products, bio-oil and syngas [25]. As such, the spectrum of the biochared *M. oleifera* seed powder was observed to be cleaner in the fingerprint region. The FTIR band shifts at 3,450, 1,750 and 1,600 $cm^{-1}$ discussed above might also be due to denaturation of proteins at high temperatures.

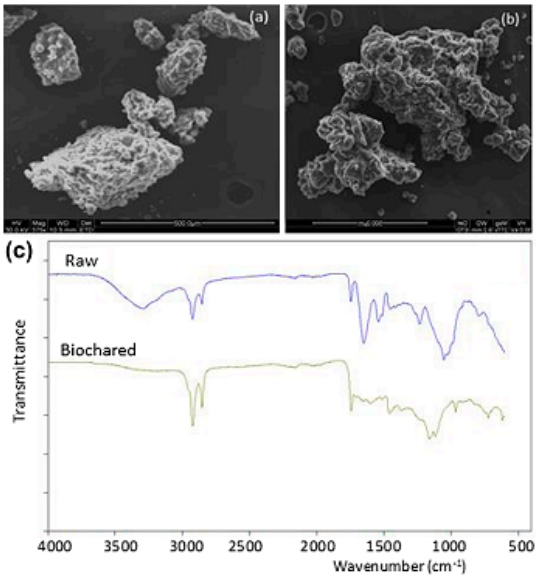



Fig. 1. SEM micrographs of (a) raw, (b) biochared *Moringa* seed and (c) FTIR of *Moringa* seed powder.

EDS was used to study the elemental composition of the *Moringa* seed powder (Fig. 2). Raw and biochared *Moringa* seed powder were dominated by carbon and moderate content of O, P, S and K were also present. Biochar is a carbonaceous material containing 65–90% carbon [26]. In the present study, the biochared sorbent had 80% carbon content, an increase from 70% for the raw sorbent. This increase has been reported by other researchers. For instance, Jouiad et al. [27] biochared date palm and Rhodes grass and

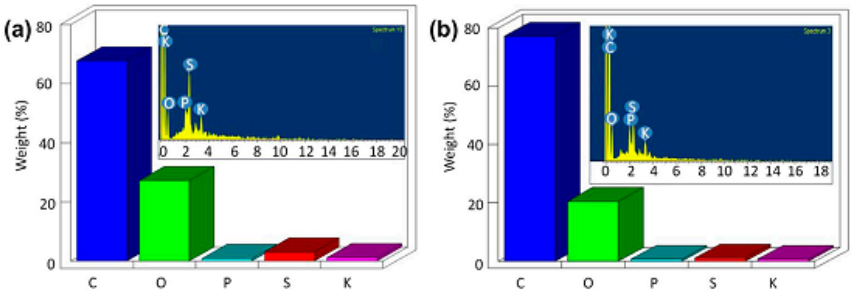



Fig. 2. Elemental composition of (a) raw and (b) biochared (inserts are the respective EDS spectra).

obtained a carbon content increase of 45.4–60.9% and 42.5–56.7%, respectively. Zhang et al. [28] also observed an increase in the fixed carbon content from 15.75 to 21.25% as the pyrolysis temperature was increased. In a research done by Břendová et al. [29], the elemental analysis done on the biochars of maize and meadow grass biomass, the content of carbon was also observed to increase.

The zeta potential of the *M. oleifera* seed powder was also determined. This surface property depends on the type and surface density of ionizable or polar functional groups on the *M. oleifera* seed powder. The zeta potential for the raw and biochared *M. oleifera* seed powder was 1.69 and 10.5 mV, respectively. The zeta potential of the biochared *M. oleifera* seed powder was quite high which indicated the absence of negatively charged functional groups on the surface which were present on the surface of the raw *M. oleifera* seed powder. This was in agreement with the findings of Gai et al. [19] who observed a decrease in the polar functional groups with an increase in pyrolysis temperature. Narrow peaks of the zeta potential (graphs not presented) indicated the high chemical homogeneity of the tested samples.

### 3.2. Point of zero charge determination and effect of pH

In order to understand the adsorption mechanism of the sorption of NB onto *M. oleifera* seed powder, it was necessary to determine the $pH_{pzc}$ (Fig. 3(a)). Due to the removal of some functional groups during biocharing, the $pH_{pzc}$ of the biochared *M. oleifera* was lower than that of the raw one, 6.9 and 4.1, respectively. The result was close to the one obtained by Junior et al. [30] who obtained a $pH_{pzc}$ of 4.4 for the raw *Moringa* powder. Therefore, at $pH > pH_{pzc}$ of the sorbents, the total surface charge was negative leading to the increased removal degree of NB due to the electrostatic force of attraction. Thus, the adsorption of NB was favoured at pH values above the $pH_{pzc}$. Electron accepting nitro group created a partial positive charge on the benzene ring of the NB. The deactivated ring was assumed to be the part which participated in the binding to both raw and biochared *M. oleifera* sorbents as the maximum sorption was determined to be in basic pH. Fig. 3(b) is a result of the experiment which was carried out to determine the pH value which gave the maximum removal efficiency of NB. It was observed that pH 11 gave the optimum performance which was in agreement with the $pH_{pzc}$ determination. Pan and Guan [31] also found the maximum adsorption of NB in the basic region (12.6–14.0) when they used modified activated sludge sorbent where the removal efficiency of NB was about 75%. In another research by Wang et al. [32], both biosorbents (maize stem and rice stem) performed similarly and NB was completely removed when treated at pH > 7. However, in this work, as the benzene ring was deactivated, the nitro group became a reservoir of the negative charge which probably was used to interact with the positive surface of the sorbent at low pH.

### 3.3. Effect of dosage

The dependence of dosage on the adsorption of NB on *M. oleifera* seed powder (raw and biochared) is shown in Fig. 4. From 1.0 to 100.0 g $L^{-1}$, an increase in the dosage of adsorbent yielded a corresponding increase in the amount of NB adsorbed onto the surface of the adsorbents since there were more sites for adsorption. Non-significant increase was observed when the adsorbent doses were increased beyond 12.5 g $L^{-1}$. This suggested that the maximum adsorption was attained with 12.5 g $L^{-1}$ for both raw and biochared *M. oleifera* seed powder. The small increase in percentage removal after biosorbent dosage of 12.5 g $L^{-1}$ might have been due to particle aggregation arising from an increased use of biosorbent quantity.

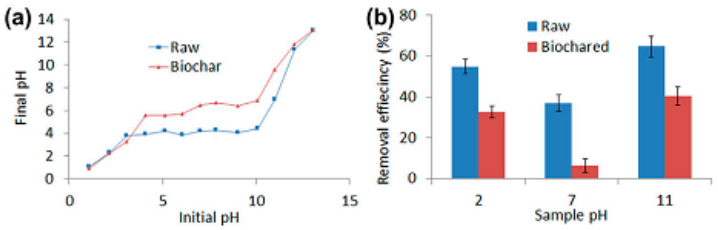



Fig. 3. (a) Point of zero charge determination of *M. oleifera* seed powder (raw and biochared) and (b) effects of pH on adsorption of NB from aqueous solutions (temperature = 25°C, adsorbent dose = 12.5 g $L^{-1}$, contact time = 30 min and initial NB concentration = 1 mg $L^{-1}$).

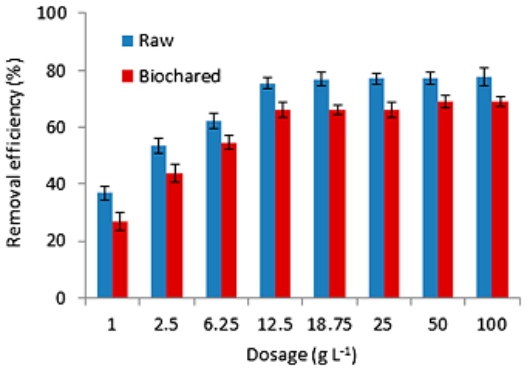



Fig. 4. Effect of sorbent dosage for the biosorption of NB from aqueous solutions (temperature = 25℃, sample pH 11, contact time = 30 min and initial NB concentration = 2 mg $L^{-1}$).

The formation of the aggregates was observed to reduce the total number of sorption sites available for biosorption and increased the diffusional path lengths.

### 3.4. Effect of the contact time and kinetic modelling

The uptake of NB by the *M. oleifera* seed powder (raw and biochared) was examined at different time intervals and the results are shown in Fig. 5. It was observed that, during the first 50 min of the experiment, the concentration of NB adsorbed on both the raw and biochared *M. oleifera* seed powder increased with time. After 50 min, no further appreciable biosorption was observed. Thus, 50 min was taken as the optimum contact time and was used in subsequent

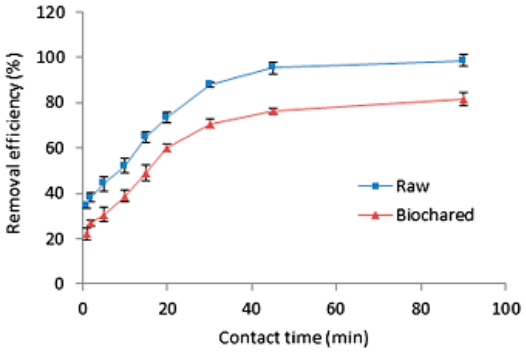



Fig. 5. Effect of contact time for the biosorption of NB from aqueous solutions (temperature = 25℃, sample pH 11, adsorbent dose = 12.5 g $L^{-1}$ and initial NB concentration = 1 mg $L^{-1}$).

experiments. In general, longer extraction times of NACs have been reported in literature, e.g. Fu et al. [33] used bamboo charcoal@$ZnCl_2$ and Yang et al. [34] used vermicompost-biochar and obtained optimal sorption times of 3 and 24 h, respectively.

For kinetic modelling, the data from the effect of contact time was used. Two most commonly used models; pseudo-first-order and pseudo-second-order were used in their linearized forms, Eqs. (4) and (5), respectively:

$$\log(q_e - q_t) = \log q_e - \frac{k_1}{2.303}t \quad (4)$$

$$\frac{t}{q_t} = \frac{1}{k_2 q_e^2} + \frac{1}{q_e}t \quad (5)$$

where $q_e$ (mg $g^{-1}$) represents the equilibrium sorption capacity and $q_t$ (mg $g^{-1}$) the instantaneous sorption capacity at time $t$ (min). The first- and second-order rate constants are $k_1$ ($min^{-1}$) and $k_2$ (g mg $min^{-1}$), respectively. Table 2 summarizes the most important constants for pseudo-first-order and pseudo-second-order models. Based on the correlation coefficients ($R^2 > 0.98$), the pseudo-second-order model fitted the data better than the pseudo-first-order. Again, the pseudo-second-order model was seen to model the kinetic data better as $q_{e,cal}$ (0.084 and 0.071 mg $g^{-1}$ for raw and biochared *M. oleifera* seed powder, respectively) was closer to $q_{e,exp}$ (0.08 and 0.05 mg $g^{-1}$ for raw and biochared *M. oleifera* seed powder, respectively). The adsorption kinetics study was also used to understand the mechanism of adsorption reactions. The pseudo-second-order kinetic model is based on the assumption that the rate-limiting step may be chemisorption involving hydrogen bonding between NB and the *M. oleifera* seed powder sorbent.

### 3.5. Effect of initial concentration and adsorption modelling

The influence of the initial concentration of NB sorption onto *M. oleifera* seed powder is shown in Fig. 6. At the initial stages of biosorption process, the biosorption capacity increased rapidly. High sorption capacities were observed with higher initial NB concentrations. It was explained by the equilibrium shift in either monolayer (Langmuir) or multilayer (Freundlich) adsorption [35]. The higher concentration of NB caused the increasing aqueous NB gradient at the surface of adsorbent, hence resulting in the higher binding affinity possibility on the active sorption sites and adsorption capacity [36]. At low NB concentration, the active sorption sites of the biosorbent were

Table 2
Kinetic model parameters for NB adsorption on *M. oleifera* seed powder

| | Pseudo-first-order | | | Pseudo-second-order | | |
|---|---|---|---|---|---|---|
| *Moringa* sorbent | $k_1$ ($min^{-1}$) | $q_e$ (mg $g^{-1}$) | $R^2$ | $k_2$ (g $mg^{-1}$ $min^{-1}$) | $q_e$ (mg $g^{-1}$) | $R^2$ |
| Raw | 0.018 | 2.70 | 0.542 | 1.88 | 0.084 | 0.991 |
| Biochared | 0.006 | 13.0 | 0.705 | 1.73 | 0.071 | 0.988 |

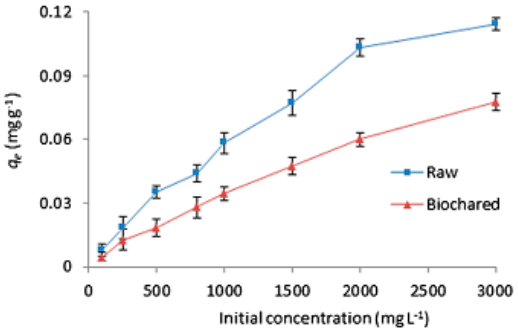



Fig. 6. Effect of initial concentration on adsorption of NB onto *M. oleifera* seed powder (temperature = 25°C, sample pH 11, adsorbent dose = 12.5 g $L^{-1}$ and contact time = 50 min).

not saturated and the NB removal efficiency was therefore increased with more occupation of the sites.

The Langmuir isotherm (Eq. (6)) was used to model the adsorption data and to determine whether the mechanism of adsorption was chemisorption. From the Langmuir isotherm equation, the value of $b$ of the raw sorbent was higher than that of the biochared material (Table 3) indicating the affinity of binding sites for NB (0.0145 vs. 0.0015). However, in both cases $b$ lied between zero and one, suggesting that the adsorption of NB onto *M. oleifera* seed powder sorbent was favourable.

$$\frac{1}{q_e} = \frac{1}{q_m b C_e} + \frac{1}{q_m} \tag{6}$$

The favourability of the sorption process was also to be measured by a dimensionless separation parameter $R_L$, which can be calculated by Eq. (7). Since $R_L$ values for both the raw (0.986) and biochared (0.999) *M. oleifera* seed powder, respectively, fell in the range of 0–1, the sorption of NB onto these sorbents was concluded to be favourable.

$$R_L = \frac{1}{1 + bC_o} \tag{7}$$

To ascertain whether the sorption was physisorption, the adsorption data was modelled by the Freundlich data, Eq. (8). The constant $n$ is the empirical parameter related to the intensity of adsorption, which varies with the heterogeneity of the material. When $1/n$ values are in the range $0.1 < 1/n < 1$, the adsorption process is favourable, which was the case in this work.

The statistical parameter chi-squared ($\chi^2$) (Eq. (9)) was used to quantify the degree of variation of the calculated from the experimental sorption capacity, $q_{m,cal}$ and $q_{m,exp}$, respectively. Since the deviation was smaller for the Langmuir isotherm model ($1.5 \times 10^{-5}$ and $1.2 \times 10^{-2}$) as compared to the Freundlich isotherm (0.51 and 6.15) (Table 3), the former was concluded to be the best.

$$\log q_e = \log K_F + \frac{1}{n} \log C_e \tag{8}$$

$$\chi^2 = \sum \frac{(q_{e,exp} - q_{e,cal})^2}{q_{e,cal}} \tag{9}$$

### 3.6. Method validation and application

A series of calibration standard solutions were made (a linear range of 50–500 μg $L^{-1}$ was used). All standard solutions were stored in a refrigerator at 4°C

Table 3
Constant parameters for the adsorption models for the adsorption of NB onto *M. oleifera* seed powder

| | Langmuir constants | | | | | Freundlich constants | | | |
|---|---|---|---|---|---|---|---|---|---|
| Sorbent | $q_m$ (mg $g^{-1}$) | $R_L$ | $b$ ($mg^{-1}$) | $R^2$ | $\chi^2$ | $K_F$ (mg $g^{-1}$) | $n$ | $R^2$ | $\chi^2$ |
| Raw *Moringa oleifera* | 0.0811 | 0.986 | 0.0145 | 0.944 | $1.5 \times 10^{-5}$ | 0.0097 | 3.12 | 0.950 | 0.51 |
| Biochared *Moringa oleifera* | 0.0816 | 0.999 | 0.0015 | 0.948 | $1.2 \times 10^{-2}$ | 0.0004 | 1.45 | 0.978 | 6.15 |

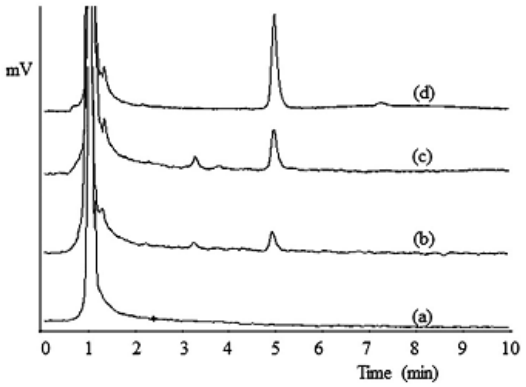



Fig. 7. Chromatogram of (a) unspiked, (b) 0.5 mg $L^{-1}$ spiked, (c) 1.0 mg $L^{-1}$ spiked wastewater sample subjected to biochared *M. oleifera* seed powder and (d) 1.0 mg $L^{-1}$ NB standard solution.

when not in use. The calibration curve found was $y = 0.1838x + 7.3464$ (where $x$ is the NB concentration and $y$ the instrument response) and a good correlation was obtained ($R^2 = 0.9923$).

In order to test the accuracy of the proposed method, real wastewater samples were spiked with NB at different concentration levels of 0.5 and 1.0 mg $L^{-1}$. These samples were analysed using the extraction and chromatographic procedure optimized in this work. Fig. 7 shows an example of chromatograms obtained after sorption of spiked and unspiked-NB wastewater samples by biochared *M. oleifera seed powder* together with a 1-mg $L^{-1}$ NB standard solution. Recoveries obtained from spiked wastewater samples at different concentration levels are shown in Table 4. It was observed that, good recoveries ranging between 59 and 81% were obtained for wastewater. High precision of the instrumental analysis was obtained, as shown by RSD ($n = 3$) of 2.1–8.2%.

Table 4
Recoveries of NB from spiked real wastewater samples using *M. oleifera* seed powder ($n = 3$)

| | Concentration (mg $L^{-1}$) | | | |
|---|---|---|---|---|
| | Spiked | Found | Recovery (%) | RSD (%) |
| Raw | – | – | – | – |
| | 0.5 | 0.41 | 81.0 | 8.2 |
| | 1.0 | 0.74 | 74.0 | 6.7 |
| Biochared | – | – | – | – |
| | 0.5 | 0.35 | 69.7 | 2.1 |
| | 1.0 | 0.58 | 58.8 | 5.4 |

### 3.7. *Comparison of* M. oleifera *seed powder with other sorbents*

In order to assess the performance of *M. oleifera* seed powder (raw and biochared) as an adsorbent for NB, a comparison with other adsorbents is given in Table 5. As can be seen, there is a wide range of adsorption capacities for the uptake of NB. This was expected as various sorption conditions were applied by different researchers. More so, different sorbents

Table 5
Uptake performance comparison of closely related sorbents

| Sorbent | Target pollutant | Adsorption conditions[a] | $q$ (mg $g^{-1}$) | Refs. |
|---|---|---|---|---|
| Modified cetyltrimethylammonium bromide | NB | Sample pH ≈ 11, dosage 2 g $L^{-1}$, time 24 h, [NB] 150 mg $L^{-1}$, Temp. 25°C | 24.8 | [31] |
| Bamboo charcoal@$ZnCl_2$ | | Sample pH 2.0, dosage 12 g $L^{-1}$, time 180 min | – | [33] |
| Vermicompost biochar | NB | Sample pH 5.47, dosage 2 g $L^{-1}$, time 24 h, [NB] 20 mg $L^{-1}$, Temp. 25°C[b] | 8.20 | [34] |
| Phenyltrimethoxysilane@magnetite | NB | Sample pH 5.47, dosage 2 g $L^{-1}$, time 24 h, [NB] 1,000 mg $L^{-1}$, Temp. 25°C | 0.45[c] | [37] |
| Raw *Moringa oleifera* seed powder | NB | Sample pH 11, dosage 12.5 g $L^{-1}$, time 50 min, [NB] 2 mg $L^{-1}$, Temp. 25°C | 0.09 | This work |
| Biochared *Moringa oleifera* seed powder | NB | Sample pH 11, dosage 12.5 g $L^{-1}$, time 50 min, [NB] 2 mg $L^{-1}$, Temp. 25°C | 0.078 | This work |

[a]Sample pH, dosage, time, concentration and temperature values are given, if not, the researchers concerned did not provide.
[b]Sample pH not optimized but was only fixed at the stated value.
[c]Calculated from mmol $g^{-1}$.

with different surface morphologies were used. The most important finding in this work was the raw *M. oleifera* seed powder sorbent which had a superior uptake of NB as compared to the biochared material.

### 3.8. *Toxicity of* Moringa *seed powder*

Application of high quantity of *Moringa* seed powder in aquaculture ponds leads to mortality of fish due to the presence of toxic substances or antinutritional factors [38]. Data on toxicity *of M. oleifera* seed extract on freshwater fish are still scarce. However, studies from Al-Anizi et al. [39] indicated that the main toxicity is from the insoluble fatty acid components of *M. oleifera*. The toxicological assessments by Berger et al. [40] and Grabow et al. [41] have already indicated that there is no threat to human health in using *M. oleifera* as a primary coagulant.

## 4. Conclusions

Raw and biochared *M. oleifera* seed powder were successfully used as biosorbents for the removal of NB from aqueous solutions. However, the former was seen to have a better uptake capability due to the organic functional groups which were not present in the biochared material. The optimum conditions for the NB uptake were pH 7, dosage of 12.5 g $L^{-1}$ and a contact time of 50 min. The pseudo-second-order and the Langmuir isotherm modelled the kinetic and the adsorption data better, respectively, pointing to a chemisorption type of interaction between the *M. oleifera* seed powder (raw and biochared) and NB. Owing to its low cost, high availability and biodegradable nature, this biosorbent can be considered a viable alternative for the treatment of contaminated aqueous solutions.

## Acknowledgements

The authors would like to thank the National Research Foundation (NRF) of South Africa for funding through the innovation scarce skills scholarship (grant ID number NFS13091843717). Appreciation is also extended to the University of Witwatersrand (Postgraduate Merit Award) for tuition fees paid to Nikita Tawanda Tavengwa for his doctoral studies.

## References

[1] S. Contreras, M. Rodríguez, E. Chamarro, S. Esplugas, UV- and UV/Fe(III)-enhanced ozonation of nitrobenzene in aqueous solution, J. Photochem. Photobiol., A 142 (2001) 79–83.
[2] B. Moodley, D.A. Mulholland, H.C. Brookes, The chemical oxidation of lignin found in Sappi Saiccor dissolving pulp mill effluent, Water SA 38 (2012) 1–8.
[3] A. Farkas, I. Dekany, Interlamellar adsorption of organic pollutants in hydrophobic montmorillonite, Colloid Polym. Sci. 279 (2001) 459–467.
[4] C. Rajagopal, J.C. Kapoor, Development of adsorptive removal process for treatment of explosives contaminated wastewater using activated carbon, J. Hazard. Mater. 87 (2001) 73–98.
[5] T. Richard, J. Weidhaas, Biodegradation of IMX-101 explosive formulation constituents: 2,4-Dinitroanisole (DNAN), 3-nitro-1,2,4-triazol-5-one (NTO), and nitroguanidine, J. Hazard. Mater. 280 (2014) 372–379.
[6] C. Hempfling, Ultraviolet/oxidation treatment of explosive wastewaters using a commercial process, Environ. Prog. 16 (1997) 164–170.
[7] K.A. Ghebremichael, K.R. Gunaratna, H. Henriksson, H. Brumer, G. Dalhammar, A simple purification and activity assay of the coagulant protein from *Moringa oleifera* seed, Water Res. 39 (2005) 2338–2344.
[8] R.M. Hlihor, M. Gavrilescu, Removal of some environmentally relevant heavy metals using low-cost natural sorbents, Environ. Eng. Manage. J. 8 (2009) 353–372.
[9] F. Veglio, F. Beolchini, Removal of metals by biosorption: A review, Hydrometallurgy 44 (1997) 301–316.
[10] J.L. Wang, C. Chen, Biosorption of heavy metals by *Saccharomyces cerevisiae*: A review, Biotechnol. Adv. 24 (2006) 427–451.
[11] E.N. Ali, S.A. Muyibi, H.M. Salleh, M.Z. Alam, M.R.M. Salleh, Production of natural coagulant from *Moringa Oleifera* seed for application in treatment of low turbidity water, J. Water Resour. Prot. 02 (2010) 259–266.
[12] K. Ravikumar, A.K. Sheeja, Water clarification using *Moringa oleifera* seed coagulant, Green Technologies (ICGT), in: 2012 International Conference, Trivandrum, India on 18–20 Dec. (2012), pp. 64–70.
[13] F. Anwar, S. Latif, M. Ashraf, A.H. Gilani, *Moringa oleifera*: A food plant with multiple medicinal uses, Phytother. Res. 21 (2007) 17–25.
[14] R. Marandi, S.M.B. Sepehr, Removal of orange 7 dye from wastewater used by natural adsorbent of *Moringa oleifera* seeds, Am. J. Environ. Eng. 1 (2011) 1–7.
[15] P. Sharma, P. Goyal, S. Srivastava, Biosorption of trivalent and hexavalent chromium from aqueous systems using shelled *Moringa oleifera* seeds, Chem. Speciation Bioavailability 19 (2007) 175–182.
[16] R.W. Gaikwad, *Moringa oleifera* seed as low cost and effective biosorbent for Cu(II) removal from acid mine drainage 15th Edition, Int. J. Inf. Futuristic Res. 2 (2014) 493–501.
[17] M. Franco, J. Beltran-Heredia, J.E.S. Paterniani, Use of alginate-*Moringa oleifera* beads on Cu(II) and Cd(II) adsorption from aquatic systems, Int. J. Chem. Eng. Appl. 4 (2013) 373–376.
[18] P. Sahni, S. Srivastava, M.M. Srivastava, Isolation and characterization of protein content of shelled *Moringa oleifera* seeds used for decontamination of arsenic water bodies, Proceeding of the International Conference on Environmental Parasitology and Community Health Care Initiatives, Taj Mahal, India, 13–15 October (2007), pp. 160.

[19] X. Gai, H. Wang, J. Liu, L. Zhai, S. Liu, T. Ren, H. Liu, Effects of feedstock and pyrolysis temperature on biochar adsorption of ammonium and nitrate, PLoS ONE 9 (2014) 1–19.
[20] J.R. Baseri, P.N. Palanisamy, P. Sivakuma, Preparation and characterization of activated carbon from *Thevetia peruviana* for the removal of dyes from textile waste water, Adv. Appl. Sci. Res. 3 (2012) 377–383.
[21] V.C. Renge, S.V. Khedkar, S.V. Pande, Removal of heavy metals from wastewater using low cost adsorbents, Sci. Rev. Chem. Commun. 2 (2012) 580–584.
[22] O.S. Ijarotimi, O.A. Adeoti, O. Ariyo, Comparative study on nutrient composition, phytochemical, and functional characteristics of raw, germinated, and fermented *Moringa oleifera* seed flour, Food Sci. Nutr. 1 (2013) 452–463.
[23] J. Rivera-Utrilla, I. Bautista-Toledo, M.A. Ferro-García, C. Moreno-Castilla, Activated carbon surface modifications by adsorption of bacteria and their effect on aqueous lead adsorption, J. Chem. Technol. Biotechnol. 76 (2001) 1209–1215.
[24] T.S. Anirudhan, P.L. Divya, J. Nima, Silylated montmorillonite based molecularly imprinted polymer for the selective binding and controlled release of thiamine hydrochloride, React. Funct. Polym. 73 (2013) 1144–1155.
[25] P. Khare, U. Dilshad, P.K. Rout, V. Yadav, S. Jai, Plant refuses driven biochar: Application as metal adsorbent from acidic solutions, Special Issue: Environmental Chemistry, Arabian J. Chem. (in press), doi: 10.1016/j.arabjc.2013.11.047.
[26] S. Sohi, E. Lopez-Capel, E. Krull, R. Bol, in: E. Krull (Ed.), Biochar, Climate Change and Soil: A Review to Guide Future Research. CSIRO Land and Water Science Report 05/09, Callingwood (2008), pp. 1–56.
[27] M. Jouiad, N. Al-Nofeli, N. Khalifa, F. Benyettou, L.F. Yousef, Characteristics of slow pyrolysis biochars produced from rhodes grass and fronds of edible date palm, J. Anal. Appl. Pyrol. 111 (2015) 183–190.
[28] J. Zhang, F. Lu, H. Zhang, L. Shao, D. Chen, P. He, Multiscale visualization of the structural and characteristic changes of sewage sludge biochar oriented towards potential agronomic and environmental implication, Sci. Rep. 5 (2015) 1–8.
[29] K. Břendová, P. Tlustoš, J. Száková, J. Habar, Biochar properties from different materials of plant origin, Eur. Chem. Bull. 1 (2012) 535–553.
[30] A.C.G. Junior, A.P. Meneghel, F. Rubio, L. Strey, D.C. Dragunski, G.F. Coelho, Applicability of *Moringa oleifera Lam.* pie as an adsorbent for removal of heavy metals from waters, Revista Brasileira de Engenharia Agrícola e Ambiental 17 (2013) 94–99.
[31] J. Pan, B. Guan, Adsorption of nitrobenzene from aqueous solution on activated sludge modified by cetyltrimethylammonium bromide, J. Hazard. Mater. 183 (2010) 3410–3410.
[32] S. Wang, S. Yang, X. Jin, L. Liu, F. Wu, Use of low cost crop biological wastes for the removal of Nitrobenzene from water, Desalination 264 (2010) 32–36.
[33] D. Fu, Y. Zhang, X. Meng, F. Lv, P.K. Chu, K. Tong, Investigation of organic matter adsorption from TNT red water by modified bamboo charcoal, Desalin. Water Treat. 56 (2015) 684–694.
[34] G. Yang, Z. Wang, Q. Xian, F. Shen, C. Sun, Y. Zhang, J. Wu, Effects of pyrolysis temperature on the physicochemical properties of biochar derived from vermicompost and its potential use as an environmental amendment, RSC Adv. 5 (2015) 40117–40125.
[35] L. Xu, C. Guo, F. Wang, S. Zheng, C.Z. Liu, A simple and rapid harvesting method for microalgae by *in situ* magnetic separation, Bioresour. Technol. 102 (2011) 10047–10051.
[36] Z. Lin, Y. Xu, Z. Zhen, Y. Fu, Y. Liu, W. Li, C. Luo, A. Ding, D. Zhang, Application and reactivation of magnetic nanoparticles in *Microcystis aeruginosa* harvesting, Bioresour. Technol. 190 (2015) 82–88.
[37] T. Sasaki, S. Tanaka, Adsorption behavior of some aromatic compounds on hydrophobic magnetite for magnetic separation, J. Hazard. Mater. 196 (2011) 327–334.
[38] E.O. Ayotunde, O.A. Fagbenro, O.T. Adebayo, Histological changes in *Oreochromis niloticus* (Linnaeus 1779) exposed to aqueous extract of *Moringa oleifera* seeds powder, Turk. J. Fish. Aquat. Sci. 11 (2011) 37–43.
[39] A.A. Al-Anizi, M.T. Hellyer, D. Zhang, Toxicity assessment and modelling of *Moringa oleifera* seeds in water purification by whole cell bioreporter, Water Res. 56 (2014) 77–87.
[40] M.R. Berger, M. Habs, S.A.A. Jahn, D. Schmalhl, Toxicological assessment of seeds from *Moringa oleifera* and *Moringa stenopetala*, two highly efficient primary coagulants for domestic water treatment of tropical raw waters, East Afr. Med. J. 61 (1984) 712–716.
[41] W.O.K. Grabow, J.L. Slabbert, W.S.G. Morgan, S.A.A. Jahn, Toxicity and mutagenicity evaluation of water coagulated with *Moringa oleifera* seed preparations using fish, protozoan, bacterial, coliphage, enzyme and Ames Salmonella, Water SA 11 (1985) 9–14.

## Paper II

This paper “Application of polymer-composites for the solid phase extraction of selected nitroaromatic compounds from contaminated aqueous environments,” was submitted *to Separation Science and Technology*. It describes the effect of imprinting polymers and application of these in the uptake of nitrobenzene, 2,4-DNT and 2-NT model pollutants.

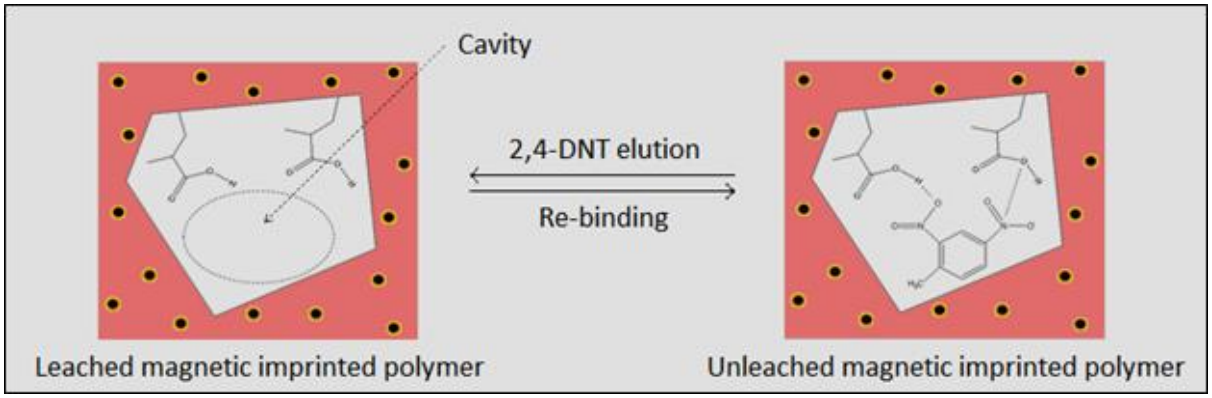
# Application of magnetic molecularly imprinted polymers for the solid phase extraction of selected nitroaromatic compounds from contaminated aqueous environments

Nikita Tawanda Tavengwa, Ewa Cukrowska, and Luke Chimuka*

Molecular Sciences Institute, School of Chemistry, University of Witwatersrand, Private Bag 3, Johannesburg 2050, South Africa

*E–mail address: luke.chimuka@wits.ac.za

**Graphical abstract**




**Highlights**

- The synthesized magnetic molecular imprinted polymers were used to extract nitroaromatic compounds and were loaded in solid extraction cartridges for elution.
- Low detection limits of 2,4–dinitrotoulene, nitrobenzene and 2–nitrotoulene were found to be 13.6, 7.7 and 27.2 µg $L^{-1}$, respectively.
- The magnetic molecular imprinted polymers showed good recoveries of 82%–90% when applied to real wastewater samples.

ABSTRACT

Magnetic molecularly imprinted polymers (MIPs) were successfully synthesized by bulk polymerization for the extraction of nitroaromatic compounds (NACs). Based on the HPLC method, the linear calibration range of 0.5–5 mg $L^{-1}$ for 2,4–dinitrotoluene, nitrobenzene and 2–nitrotoluene gave detection limits of 13.6, 7.7 and 27.2 µg $L^{-1}$, respectively and good correlation values of $R^2$ > 0.993 of all the analytes were obtained. The optimum sorption was at sorbent dosage of 5 g $L^{-1}$, contact time of 15 min and at pH 8. Recoveries for 2,4–dinitrotoluene, nitrobenzene and 2–nitrotoluene from spiked real water samples were all ≥ 82%.

*Keywords* Nitroaromatic compounds; Magnetic; Molecularly imprinted polymers, Solid phase extraction

**Introduction**

Nitroaromatic compounds (NACs) accumulate in the environment due to their wide use in industries that manufacture compounds like dyes, pesticides and explosives. They are mostly used as explosives in mining, projectiles and demolition of buildings (1, 2). A wide range of NACs are available e.g., 1,3,5–trinitroperhydro–1,3,5–triazine, octahydro 1,3,5,7–tetranitro–1,3,5,7–tetrazocine, 2,4,6,8,10,12–hexanitrohexaazaisowurtzitane, nitrotoluenes (e.g. 2–nitrotoluene, 2,4–dinitrotoluene, 3–nitrotoluene, 2,6–dinitrotoluene) and nitrobenzenes (e.g. 1,3–dinitrobenzene). These compounds are classified as explosives because they release large amounts of

energy in the form of heat, light and flame when they are exposed to chemical or physical stimuli (3).

Acute exposure to NACs can cause headaches, convulsions, circulatory collapse, nausea, liver failures and death in humans, while chronic exposure may cause hallucinations and skin rashes (4-6). The $–NO_2$ functional group in NACs can interact with DNA and result in the alterations of it or its expression (1, 7) and can cause infertility in animals (1). The $–NO_2$ group is reduced to more reactive carcinogenic compounds such as nitroso and hydroxyl amino groups (8). NACs such as nitrobenzene, dinitrotoluenes, and mono– and di– nitrophenols are toxic and powerful carcinogens, and are classified as priority pollutants by the United States Environmental Protection Agency (9). NACs are normally present at low concentration in complex environmental matrices such as river or industrial wastewater (10). Concentration levels of 50 $\mu g\ L^{-1}$ have been reported in surface water (11). According to Howard (12), nitrobenzene concentrations in various industrial effluents were: auto and other laundries 40.4 $\mu g\ L^{-1}$, pesticides manufacture 16.3 $\mu g\ L^{-1}$, explosives 51.7 $\mu g\ L^{-1}$ and organic chemicals 43.7 $\mu g\ L^{-1}$. The recommended maximum allowable concentrations for NACs were set at 0.0068 $\mu g\ L^{-1}$ for 2,6–DNT and 0.17 $\mu g\ L^{-1}$ for 2,4–DNT (13).

NACs are environmental hazards because industries that manufacture and use them do not dispose them adequately, so they end up in soil and ground water. Before these compounds can be degraded, there is need to develop efficient methods that can extract them from the environment. When exposed to light, nitrobenzenes in the

atmosphere are degraded to hydroxyl radicals. They are also degraded in the lithosphere by micro–organisms in the soil (1).

It is therefore important to come up with new ways to extract NACs from the environment. There has been an increase in developing methods to extract them from the environment. Some of these methods include solvent microextraction (14) supercritical fluid extraction (15), solid phase extraction (16), and ultrasound–assisted dispersive liquid–liquid microextraction (17). Polymers, especially molecularly imprinted polymers (MIPs), have the potential to selectively extract such compounds if properly synthesized and optimized (18). MIPs are materials that have specific recognition cavities within a polymer network (19,20). MIPs form sites which are chemically and physically complementary to the template molecule (21). They are used for binding specific molecules and are applied in many different fields ranging from environmental chemistry, electrochemistry, biochemistry and drug design, catalysis and sensors (22, 23). Magnetic MIPs are a modified version of MIPs where inorganic magnetic particles are coated by a polymer to make the whole sorbent magnetic (21). The addition of a magnetic particle overcomes some of the problems that are found in MIPs, and can provide controllable binding and rebinding of the templates (24). Other advantages provided by magnetic MIPs are that they have greater selectivity, shorter contact time with the analyte solution and can be reused many times (21, 25). Although imprinted polymers have been explored for the extraction of other organic compounds (26), not much has been reported on the use of these materials for the extraction of nitroaromatic compounds.

This research therefore attempted to prepare magnetic MIPs and then pack them in solid phase extraction cartridges for the extraction of selected NACs. This is important in the South African context as mining is an important pillar for its economy where the NACs normally end up polluting water bodies. The targeted NACs were 2,4–dinitrotoluene (2,4–DNT), nitrobenzene (NB) and 2–nitrotoluene (2–NT).

## Experimental

### *Materials and equipment*

$FeSO_4 \cdot 5H_2O$ was purchased from Riedel–de Haen (Seelze, Germany). Methanol (99%), acetonitrile (99%) and $Fe_2(SO_4)_3$ were purchased from The British Drug Houses (Poole, England). Ethlylene glycol dimethacrylate (EGDMA), N,N–dimethylformamide, oleic acid (OA), methacrylic acid (MAA) and 4,4'–azobis (4–cyanovaleric acid) were purchased from Sigma–Aldrich (Steinheim, Germany). The explosives NB, 2,4–DNT and 2–NT were also purchased from Sigma–Aldrich (Steinheim, Germany).

A Bischoff high–performance liquid chromatography (HPLC) equipped with a lambda 1010 detector set at $\lambda_{max}$ 254 nm with an Ascentis RP–amide column (25 cm x 4.6 mm x 5 µm) was used. An acetonitrile/water (50:50, v/v) mobile phase solution was used at a flow rate of 1 mL $min^{-1}$. Elution of the template from the synthesized magnetic polymers was done using a pressurized hot water extraction (PHWE) in a modified Hewlett Packard 5890 gas chromatography oven fitted with a GenTech

Scientific Waters 515 HPLC pump (Milford, USA). For grinding, a pulverrisette from Fritsch (Darmstadt, Germany) was used. A Retsch AS 200 mechanical sieve from Monitoring and Control Laboratories (Pty) Ltd (Johannesburg, South Africa) was used to sieve the ground polymers for 4 min at an amplitude of 1000 at 600 rpm. Deionized water from Millipore system (Molsheim, France) was used. A Rotofix 32 A Centrifuge from Hettich Lab Technology (Tuttlingen, Germany) was used for centrifuging. The pH meter from Knick (Germany) was used to measure the pH. Thermogravimetric analysis (TGA) for the prepared materials was performed with Perkin Elmer Pyris 1 TGA Thermogravimetric Analyser (Massachusetts, USA). Fourier transform infrared (FTIR) spectra were recorded in the frequency range of 400–4000 $cm^{-1}$ using a Tensor 27 Bruker FTIR spectrometer (Ettlingen, Germany). Scanning electron microscopy (SEM) images were obtained from a FEI Quanta 200 SEM (FEI, Hillsboro, OR, USA). All samples were first coated with Cr with A Q150T ES from Quorum Technologies Ltd (East Sussex, UK) to avoid charging.

*Preparation of solutions and sampling*

Explosive compounds were prepared by dissolving them in 50/50 acetonitrile/water (v/v) solution to make 100 mg $L^{-1}$ stock solutions and 0.5–5 mg $L^{-1}$ calibration standards were prepared. Stock solutions were stored at 4ºC when not used and working solutions prepared whenever needed from the stock solutions. Table 1 summarizes the validation data of the three explosive compounds.

Real samples were collected from a local river which passed through an explosives manufacturing company in East Rand, South Africa. Prior to extraction of

NACs, the river water was filtered through the 0.45 μm filter paper. The application was only tested with the magnetic MIPs for the extraction of NACs spiked at three different levels of 50 μg $L^{-1}$, 100 μg $L^{-1}$ and 200 μg $L^{-1}$.

**Table 1.** Validation parameters for HPLC determination of a mixture of three explosive compounds.

| | $t_R$ (min) | Equation | $R^2$ | LOD (μg $L^{-1}$) | LOQ (μg $L^{-1}$) |
|---|---|---|---|---|---|
| NB | 9.7 | y = 0.1726x + 0.1225 | 0.9998 | 13.6 | 45.5 |
| 2,4–DNT | 11.6 | y = 0.2112x + 0.2319 | 0.9997 | 7.7 | 25.6 |
| 2–NT | 12.7 | y = 0.1164x + 0.2429 | 0.9998 | 27.2 | 89.8 |

Note: LOD Limits of detection, LOQ Limits of quantification.

*Synthesis of nano–magnetic particles*

$FeSO_4 \cdot 5H_2O$ (6 g) and $Fe_2(SO_4)_3$ (4.2 g) were placed in a one neck 250 mL round bottomed flask in the presence of a magnetic stirrer and were dissolved in 100 mL of distilled water. The solution was heated to 80ºC and purged for 5 min with nitrogen gas. After purging, 10 mL of ammonium solution was added and the mixture was stirred for 20 min. The synthesized iron oxide particles were removed magnetically from the solution. They were then washed with 50 mL portions of water and then 50 mL portions of ethanol.

*Coating of nano–magnetic particles*

Coating was done by dispersing the synthesized iron oxide nano–particles in 100 mL distilled water where the solution was heated to 80ºC with stirring. The mixture was then purged for 3 min with nitrogen gas before 20 mL of oleic acid (OA) was added

and the temperature was maintained at 80ºC for 30 min. The resulting coated iron oxide particles were washed with water/ethanol (35/15 v/v), then with (15/35 v/v) and finally with 50 mL of ethanol.

*Synthesis of magnetic molecularly imprinted polymers*

A mass of 0.75 g of the OA coated iron oxide ($Fe_3O_4$) particles was dispersed in 12 mL of N,N–dimethylformamide in a 250 mL round bottomed flask and heated to 40ºC. 50 mg 2,4–DNT, 35 µL of methacrylic acid and 3.15 mL of ethylene glycol methacrylate were then added to the flask and purged with nitrogen gas for 3 min. After purging, 50 mg of 4,4'–azobis (4–cyanovaleric acid) was added to the solution and was heated at 80ºC for 35 min. Once polymerization finished, the magnetic polymer was removed and dried at 55ºC, ground and sieved to limit the particle diameter between 25 and 50 µm. The template was then eluted from the polymer using pressurized hot water extraction unit where the eluent composition was initially 1% acetic acid and then increased to 10% acetic acid. Magnetic NIPs were prepared in the same as way as magnetic MIPs with the exclusion of 2,4–DNT.

*Point of zero charge ($pH_{PZC}$) determination*

14 mL of 0.01 M NaCl solution was aliquoted into a series of vials. The initial pH ($pH_i$) was adjusted from 2 to 12 by addition of 0.1 M NaOH or HCl. A 10 mg sample of magnetic MIP was added to each vial followed by 170 rpm agitation for 24 h at 25ºC. After filtration, the final pH ($pH_f$) of the supernatant was then measured. The $pH_{PZC}$ was defined as the point at which the curve of $pH_i$ vs $pH_f$ plateaued.

*Optimization of the NACs uptake by the magnetic polymers*

The pH optimization studies were done by adjusting the solutions of all the three NACs (2,4–DNT, 2–NT and NB) with HCl and NaOH (Fixed parameters: mass of the magnetic polymer = 30 mg; concentration = 1 mg $L^{-1}$; sample volume 20 mL; contact time = 30 min). The amount of magnetic MIPs and NIPs was varied between 10 and 100 mg, (Fixed parameters: concentration = 1 mg $L^{-1}$; sample volume 20 mL; contact time = 30 min; sample pH = 8). The contact time was investigated between 5 and 30 min (Fixed parameters: mass of the magnetic polymer = 100 mg; concentration = 1 mg $L^{-1}$; sample volume 20 mL; sample pH = 8). The initial concentration of 2,4–DNT was varied between 0.1 and 2 mg $L^{-1}$ (Fixed parameters: Mass of the magnetic polymer = 100 mg; sample volume 20 mL; contact time = 15 min; sample pH = 8). All experiments were done in batch mode in triplicate in a fixed volume of 20 mL and shaken on an elliptical benchtop shaker at 300 rpm. After the sorption of the NACs, the polymers were loaded in SPE cartridges where the solution was drained and the loaded MIPs were then eluted with 3 mL of a 9/1 methanol/water (v/v) solution. The filtrate was then analyzed by an HPLC–UV. Extraction efficiency and adsorption capacity $q$ (mg $g^{-1}$) were calculated using Eqs. (1) and (2), respectively.

$$Extraction\ efficiency\ (\%) = \frac{C_A V_A}{C_D V_D} \times 100 \quad (1)$$

$$\text{Adsorption capacity } (q) = \frac{(C_o - C_e)V}{W} \quad (2)$$

where $C_A$ (mg $L^{-1}$) and $V_A$ (L) are the NACs concentration and volume after solid phase extraction. $C_D$ (mg $L^{-1}$) and $V_D$ (L) denote the NACs concentration and volume in the donor solution before solid phase extraction. *Ce* (mg $g^{-1}$) is the final concentration, *V* (L) is the sample volume and *W (g)* is the magnetic polymer mass.

## Results and discussion

### *Synthesis and characterization of MIPs*

#### *Preparation of magnetic polymers*

The magnetic MIPs and NIPs were successfully synthesized using the scheme shown in Fig. 1. $Fe_3O_4$ was synthesized by co–precipitation of the ferric and ferrous sulphate salts before coating with oleic acid surfactant. The OA@$Fe_3O_4$ were then included as pre–polymerization reagent for the synthesis of the magnetic polymers.

Pressurized hot water extraction was chosen as a method for 2,4–DNT elution from the magnetic MIPs because it is environmentally friendly (27). Fresh solvent was used for each washing, collected in 15 mL vials and analyzed with HPLC–UV. The 2,4–DNT in the first washing was lower than in the second (graph not presented) as the solvent was still wetting and penetrating the pores of the polymer powder. To increase the elution amount per cycle, the amount of the organic modifier (acetic acid) was increased from 1% to 10%. 16 cycles were enough to get a complete template removal and a general exponential decay curve was observed.

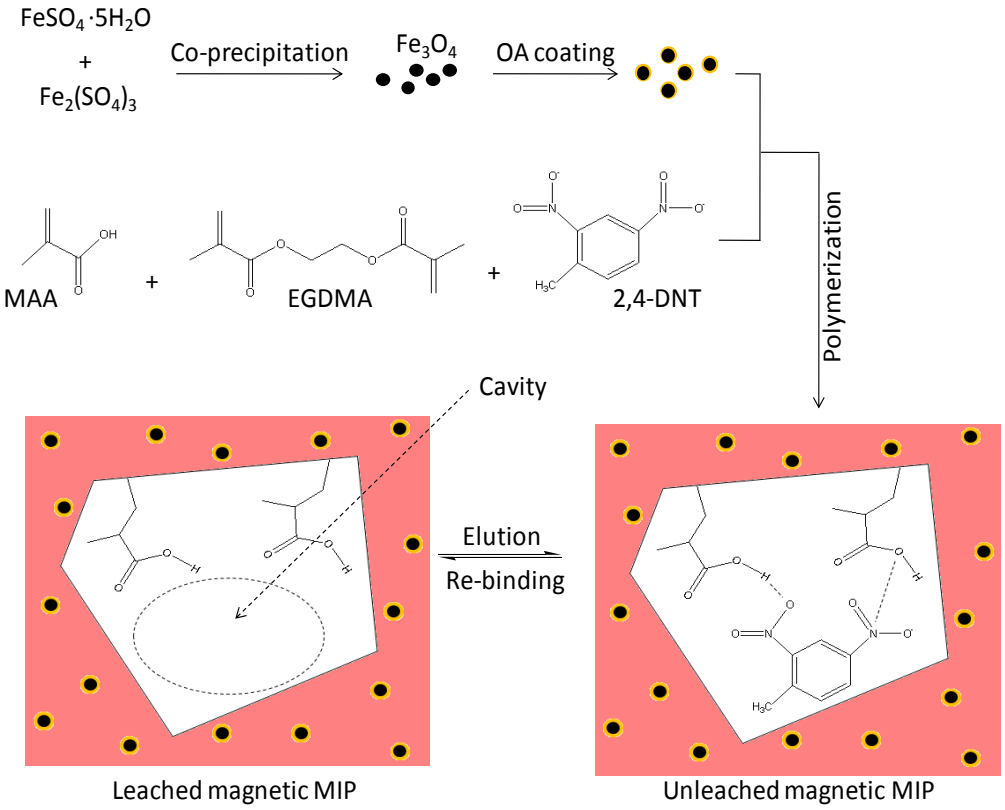



**Figure 1.** Proposed schematic diagram for the synthesis of magnetic MIPs with 2,4–DNT as a template.

*Fourier transform infrared spectroscopy*

It can be seen that the Fourier transform infrared (FTIR) spectra of the three polymers are highly similar as a result of the presence of the high ratio of the cross–linking monomer. No drastic differences were observed between the eluted MIPs and washed NIPs, which show that there was no template in the former which could be detected. The elution of the MIP using hot water extraction system with 1%, and later 10% acetic acid at 25ºC was therefore effective. However, according to the FTIR spectra, one distinct difference is glaring between the uneluted and eluted MIP and the

highlighted areas show these peaks of interest (Fig. 2). The bands around 1600 $cm^{-1}$ was observed in the unleached MIP, while it was absent in the spectrum of the leached MIP. This band was assigned to $–NO_2$ functional group on the aromatic ring of 2,4–DNT. Almost similar results were obtained by Ebrahimzadeh et al. (28) who obtained the $–NO_2$ band at 1531 $cm^{-1}$. The absence of the $–NO_2$ band in the leached MIPs confirmed successful elution of 2,4–DNT from the polymer matrix. The intense singlet at about 1725 $cm^{-1}$ indicated the stretching vibrations of the carboxyl groups C=O presented in functional monomer (MAA) and cross–linker (EGDMA) for the three polymers.

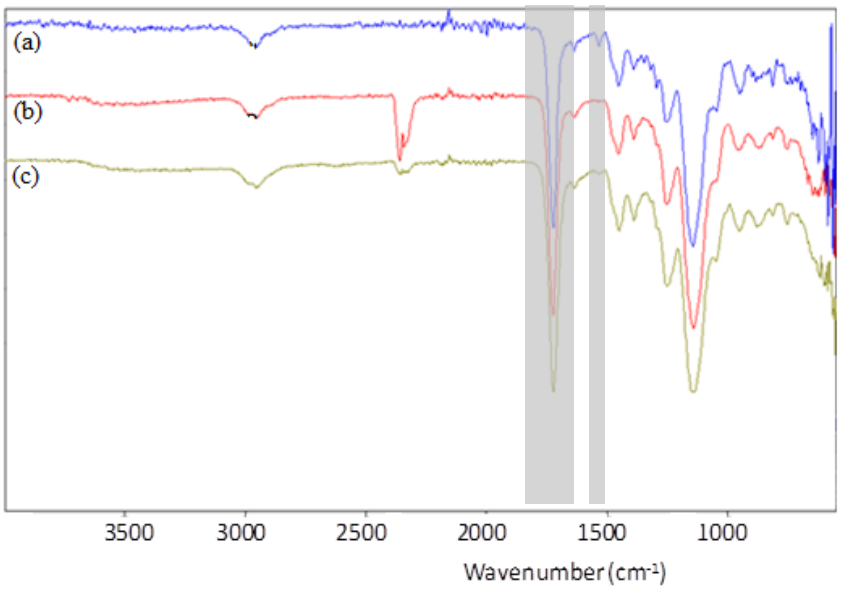



**Figure 2.** FTIR spectra of (a) uneluted magnetic MIP (b) eluted magnetic MIP and (c) washed magnetic NIP.

*Scanning electron microscopy and size distribution*

The morphology of the synthesized polymers was characterized using scanning electron microscopy (SEM) imaging analysis and the micrographs of the particles are shown in Fig. S1. There was a dramatical change of surface morphology as a result of elution of the template. The uneluted magnetic MIPs were generally smoother than the eluted magnetic MIPs. The cavities in the magnetic MIPs were caused by of the template molecule which was eluted from the polymeric matrix. This proved that elution of the imprinted polymer particle was successful. In order to facilitate the transfer of NACs such as 2,4–DNT, the magnetic MIPs should have a porous structure. The size distribution of the synthesized MIPs was determined by use of a zeta meter and a narrow size distribution was found (Fig. S1c) with an average diameter of about 48 μm. This was within the size range of the sieves used to select the magnetic MIP particles (25 to 50 μm).

*Thermogravimetric analysis*

Thermogravimetric analysis (TGA) plots with identical characteristics were obtained for the magnetic polymers (Fig. 3) as they all had a great percentage of EGDMA cross–linker for structural rigidity and were all synthesized in N,N–dimethylformamide porogen. The stability of the polymer followed the order: Uneluted magnetic MIP > washed magnetic NIP > eluted magnetic MIP. The eluted magnetic MIP was least stable because it had a porous surface, and hence their structures were easily decomposed. The residual weight difference between the eluted magnetic MIP and NIP was confirmed to be due to the presence of 2,4–DNT template and the embedded nano–magnetic $Fe_3O_4$ particles by comparing the two TGA

profiles. A TGA conducted on the corresponding magnetic NIP showed a lower residual weight, a feature consistent with the successful removal of 2,4–DNT template.

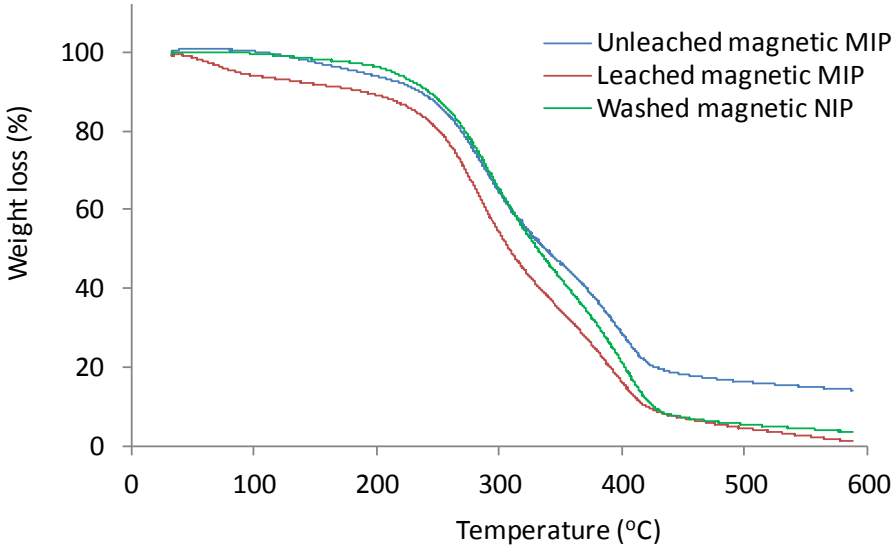



**Figure 3.** TGA spectra of magnetic polymers.

*Adsorption properties of NACs by MIPs*

*Influence of pH on the binding of NACs*

Surface charge of the adsorbent and its degree of ionization was significantly influenced by pH which in turn affected the sorption of NACs unto the magnetic polymers from aqueous solutions (Fig. 4a). Since magnetic MIPs have specific sites for 2,4–DNT compounds, they bind more explosives than magnetic NIPs which have no specific binding sites. However, it should be noted that, because of the presence of water in the aqueous samples, selectivity of magnetic MIPs was reduced during

binding. In both NIPs and MIPs, 2,4–DNT has the highest extraction efficiency as compared to other explosives (NB and 2–NT). At high pH values, the carboxyl groups of MAA are deprotonated and are able to uptake the NACs which by inductive effect, the $–NO_2$ group withdraws electrons from the benzene ring thereby making it partially positive. The positive ring then interacted with the negatively charged MIP sorbent at pH values > $pH_{PZC}$ (7.3). The higher the number of the nitro groups the higher the partial positive charge on the benzene ring (29). pH 8 was found to be the optimum and was used in subsequent experiments. The order of sorption of the NACs was: 2,4–DNT > 2–NT > NB which coincidentally followed the π–acceptor strength order. This order was consistent with the findings of Chen and Chen (30) and Zhu and Pignatello (31) who exhaustively investigated the π–acceptor strengths of nitro based sorbates. On the other hand, at pH < $pH_{PZC}$ (7.3), the carboxylic acid functional groups existing in the selective cavities of the imprinted polymeric were protonated. They were therefore capable of repelling the NACs and this resulted in low extraction efficiencies.

*Influence of polymer amount*

The results on the influence of polymer amount on the binding for both magnetic polymers are shown in Fig. 4b. Magnetic MIPs which have specific binding sites for the template molecule bound more explosives than the magnetic NIPs. 2,4–DNT which was the template molecule had the highest extraction efficiency in the magnetic MIPs. Based on the results (Fig. 4b), an increase in the adsorption with the increase of adsorbent dosage from 0.015–0.1 g was attributed to greater surface area

and the availability of more adsorption sites generated during elution. 100 mg was chosen as the optimal mass and was used for further experiments.

*Influence of contact time and kinetic modelling*

The results of the influence of contact time on binding of the NACs are shown in Fig. 4c. 2,4–DNT which was used as a template molecule showed the highest extraction efficiency in the MIPs as compared to NB and 2–NT. The optimal contact time the MIPs was found to be 15 min. The results again showed that the MIPs which have specific binding sites for the template molecule binds more explosives than the NIPs which has non–specific binding sites. However, the superiority of MIPs over NIPs with respect to the uptake of NACs was small because the solvent used in the binding experiments had water. Since water is a polar solvent, it makes binding of molecules on the MIPs surface non–selective, implying the selectivity of the MIPs was slightly reduced.

Based on the $R^2$ values, it can be seen from Table S1 that the pseudo–second–order fitted the kinetic data better than the pseudo–first–order. The $R^2$ for the pseudo–second–order were all high (> 0.993). Further, the pseudo–first–order was dismissed on the basis of $q_{e,\,cal}$ values for NB, 2,4–DNT and 2–NT being lower than $q_{e,\,exp}$ which were 0.142 mg $g^{-1}$, 0.11 mg $g^{-1}$ and 0.222 mg $g^{-1}$, respectively. There was no much deviation of $q_{e,\,cal}$ from $q_{e,\,exp}$ for all the three NACs in the pseudo–second–order case. The implication of the pseudo–second–order fitting the data better was that a chemisorption type of mechanism was followed. This was most likely to be through the H–bonding of the $–NO_2$ group with the H atoms of the functional monomers in

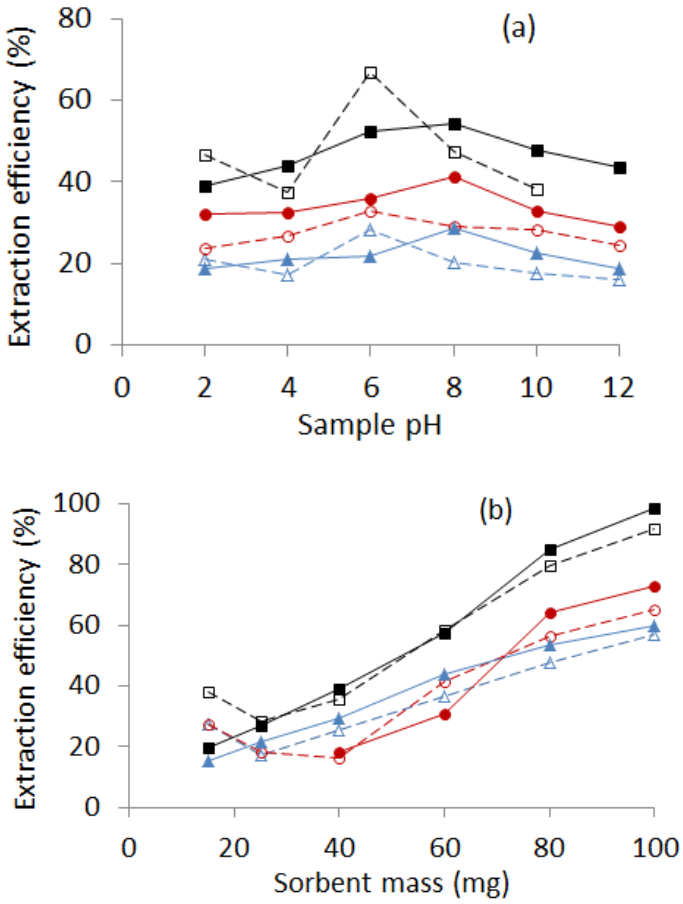
the cavities of the imprinted polymer or alternatively, ionic bonding of the de–activated benzene ring with the heteroatoms of the functional monomers.

*Influence of initial concentration and adsorption modelling*

From Fig. 4d, it can be observed that the sorption of NACs was dependent on its initial concentration. The initial concentration of NACs provided a driving force that overcame mass transfer resistance between the bulk solution and the magnetic imprinted polymer. In the range of the investigated initial concentration (0.1–2 mg $L^{-1}$), $q_e$ increased sharply from 0.008 mg $g^{-1}$ to 0.23 mg $g^{-1}$, 0.02 mg $g^{-1}$ to 0.39 and 0.01 mg $g^{-1}$ to 0.29 mg $g^{-1}$ for the MIPs for NB, 2,4–DNT and 2–NT, respectively. In all the three NACs, an increase in the initial concentration resulted in an increase in the driving force which led to an increased uptake rate.

Linear plots of the Langmuir and Freundlich adsorption models were used to test their applicability to fit the adsorption data. A summary of the theoretical parameters of adsorption isotherms along with regression coefficients are listed in Table S2. Langmuir isotherm parameter fits for NACs adsorption on magnetic imprinted polymers yielded isotherms that were in good agreement with observed behaviour with all $R^2 > 0.99$. Since all $R_L$ values fell in the range of 0–1, the sorption of nitroaromatics compounds onto magnetic polymers was concluded to be favourable. Nearly all the Freundlich constants ($n$) were < 1 indicating the unsuitability of this model. More so, the correlation coefficients for this model were lower than those of the Langmuir implying its unsuitability.

The performance of the magnetic MIP for the uptake of NACs was compared with a variety of other materials reported recently in the literature for pre–concentration and determination of NACs. The optimum pH and adsorption capacities of these materials are summarized in Table 2.



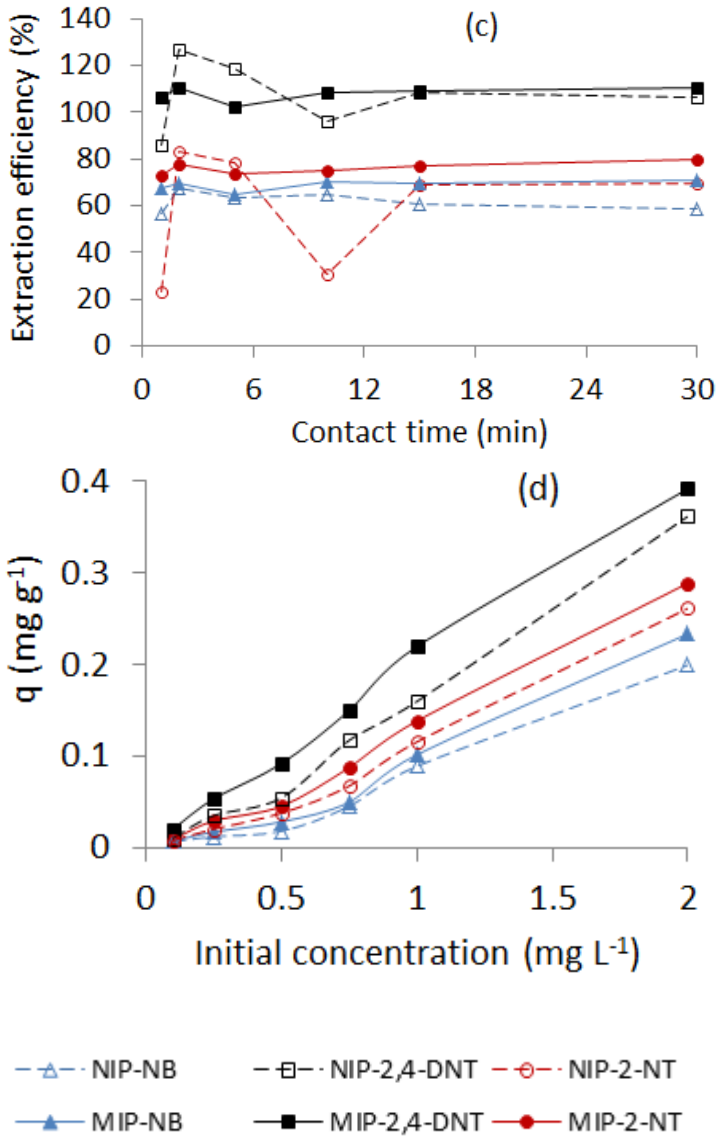



**Figure 4.** (a) Effect of initial sample pH (b) mass (c) contact time and (d) initial concentration on the extraction of NACs by magnetic polymers.

**Table 2.** Comparison of the uptake of NACs from aqueous solutions using different materials.

| Sorbent | Target explosive compound | Optimum pH | Adsorption capacity (mg $g^{-1}$) | Reference |
|---|---|---|---|---|
| PEI/$SiO_2$ | 2,4,6–trinitrotoluene | 6 | 14.5 | (32) |
| PAM/$SiO_2$ | 2,4,6–trinitrotoluene | 12 | 0.87 | (33) |
| Mesoporous molecular sieves (MCM-41) | nitrobenzene | 1 | 0.46[¥] | (34) |
| Maize stem | nitrobenzene | pH > 7 | 10.4 | (34) |
| Rice stem | nitrobenzene | pH > 7 | 1.31 | (35) |
| Anthracite | nitrobenzene | pH independent | 0.58 | (36) |
| Anthracite | 1,3–dinitrobenzene | pH independent | 0.67 | (36) |
| MIP | 2–nitrotoulene | 8–10 | 0.16 | Present study |
| MIP | nitrobenzene | 8–10 | 0.14 | Present study |
| MIP | 2,4–dinitrotoulene | 8–10 | 0.22 | Present study |

[¥]Converted from µmol $g^{-1}$ to mg $g^{-1}$

*Real sample analysis*

In literature, the concentration of some NACs has been reported to be in the ppt orders Liang et al. (2011). In this work, limits of detection and quantification of 7–28 µg $L^{-1}$ and 25–90 µg $L^{-1}$, respectively, were obtained for the three investigated NACs. The results showed that only 2,4–DNT was detected in real water (364 µg $L^{-1}$) whereas the other NACs were below the limits of detection. The results presented in Fig. 5 and Table 3 shows that the method can be used in real wastewater samples as high recoveries (82%–90%) were obtained with low relative standard deviation (RSD < 12%). Since the recommended maximum allowable concentrations were set at 0.0068 µg $L^{-1}$ and 0.17 µg $L^{-1}$ for 2,6–DNT and 2,4–DNT, respectively (13), the method was able to detect some of the NACs.

The selectivity of the MIPs towards NACs was demonstrated by the cleanliness of the chromatograms in Fig. 5. Real wastewater samples are known to have interfering matrix. Application of MIPs is generally known to be selective of target analytes, in this case NACs.

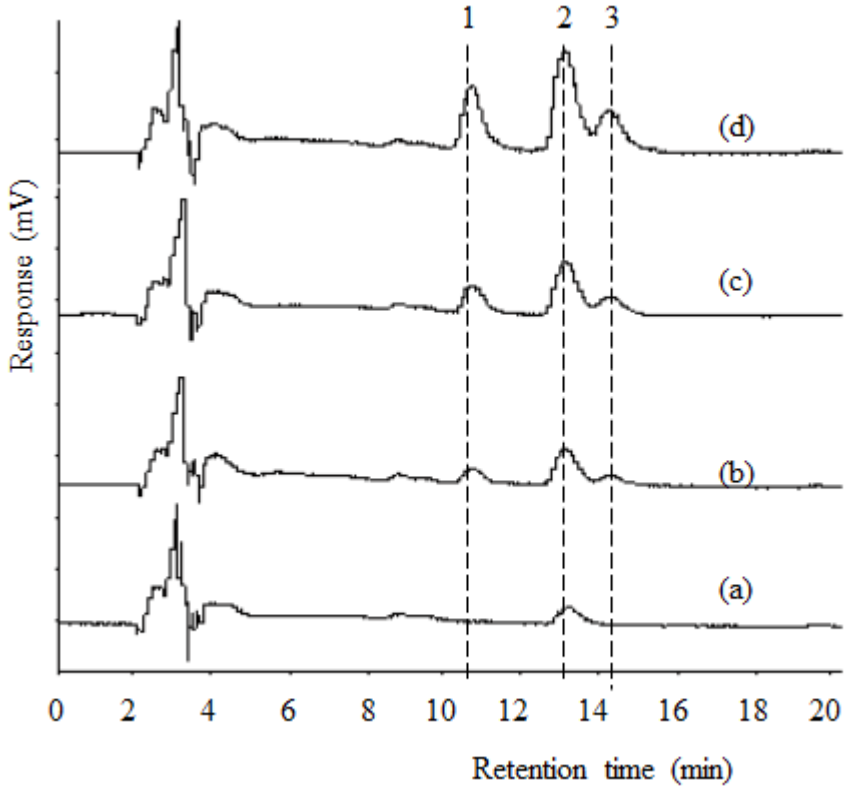



**Figure 5.** Chromatograms of (a) unspiked wastewater sample (b) 50 µg $L^{-1}$ spiked wastewater sample (b) 100 µg $L^{-1}$ spiked wastewater sample and (b) 200 µg $L^{-1}$ spiked wastewater sample, all passed through SPE. Peak 1: NB, Peak 2: 2,4–DNT, Peak 3: 2–NT.

**Table 3.** Recovery of explosive compounds from real wastewater sample.

| Compound | Spiked concentration ($\mu g\ L^{-1}$) | Recovery (%) | RSD (%) |
|---|---|---|---|
| NB | – | – | – |
| | 50 | 84.9 | 3.7 |
| | 100 | 80.5 | 2.4 |
| | 200 | 82.6 | 11.9 |
| 2,4–DNT | – | – | – |
| | 50 | 89.9 | 3.1 |
| | 100 | 87.2 | 1.4 |
| | 200 | 87.2 | 9.9 |
| 2–NT | – | – | – |
| | 50 | 82.3 | 4.8 |
| | 100 | 81.3 | 5.4 |
| | 200 | 82.4 | 9.5 |

## Conclusions

2,4–dinitrotoluene MIPs embedded with oleic acid (OA) functionalized magnetic $Fe_3O_4$ nano–particles were successfully synthesized through a bulk polymerization approach. Acetic acid solution was used as a leachant for the removal of 2,4–DNT template molecule using a pressurized hot water extraction unit. The synthesized polymers were characterized for physico–chemical characteristics using Fourier transform infrared spectroscopy (FTIR), thermogravimetric analysis (TGA), scanning

electron microscopy (SEM) and the zeta potential. Batch adsorption investigations, for the binding of NACs, were done at different levels of sample pH, amount of the polymer, contact time and concentration in order to find the optimum sorption conditions. Generally, the sorption order was: 2,4–DNT > 2–NT > NB. Fast NACs transfer was determined to be 15 min. Pseudo–second–order provided a good description from kinetic modelling while the Langmuir model was found to describe satisfactorily the adsorption isotherm of NACs. Recoveries for 2,4–DNT, NB and 2–NT from spiked real water samples were 82.7%, 88.1% and 82.0%, respectively with %RSD values ranging from 1.4%–11.9%. This implied that they can be potential sorbents in the extraction of NACs.

**Acknowledgements**

The authors would like to thank the National Research Foundation (NRF) South Africa for funding Nikita Tawanda Tavengwa through the innovation Doctoral Scholarship, grant ID number NFS13091843717. Department of Science and Technology (DST) of South Africa is also acknowledged for funding (Grant DST/CON 0054/2014).

**References**

(1) Talmage, S. S.; Opresko, D. M.; Maxwell, C. J.; Welsh, C. J.; Cretella, F. M.; Reno, P. H.; Daniel, F. B. (1999) Nitroaromatic munition compounds: environmental effects and screening values. *Rev. Environ. Contam. Toxicol*., 161: 1.

(2) Ju, K.; Parales, R. E. (2010) Nitroaromatic compounds, from synthesis to biodegradation. *Microbiol. Mol. Biol. Rev*., 74: 250.

(3) Pitchell, J. (2012) Distribution and fate of military explosives and propellants in soil. *Appl. Environ. Soil Sci*., 2012: 1.

(4) Sittig, M. (1981) *Handbook of toxic and hazardous chemicals*, 3rd ed.; Noyes Publications, Park Ridge, NJ, USA.

(5) Rom, W. N. (1992) *Environmental and occupational medicine*, 2nd ed.; Little Brown and Company, Boston, USA.

(6) OSHA, *Occupational safety and health guideline for nitroglycerin*, http://www.osha.gov/SLTC/healthguidelines/nitroglycerin/recognition.html

(7) Purohit, V.; Basu, A. K. (2000) Mutagenicity of nitroaromatic compounds. *Chem. Res. Toxicol*., 13: 673.

(8) Kulkarni, M.; Chaudhari, A. (2007) Microbial remediation of nitro–aromatic compounds: An overview. *J. Environ. Manage*., 85: 496.

(9) U.S. EPA. (2006) *Water Quality Standards Database*, Washington, DC. USA.

(10) Nie, D.; Li, P.; Zhang, D.; Zhou, T.; Liang, Y.; Shi, G. (2010) Simultaneous determination of nitroaromatic compounds in water using capillary electrophoresis with amperometric detection on an electrode modified with a mesoporous nano–structured carbon material. *Electrophoresis*, 31: 2981.

(11) Douglas, T. A.; Johnson, L.; Walsh, M.; Collins, C. (2009) A time series investigation of the stability of nitramine and nitroaromatic explosives in surface water samples at ambient temperature. *Chemosphere*, 76: 1.

(12) Howard, P. H. (1989) *Handbook of environmental fate and exposure data for organic chemicals, large production and priority pollutants,* Lewis Publishers, Inc., Chelsea, Michigan, USA.

(13) U.S. Environmental Protection Agency (1980) Ambient water quality criteria for dinitrotoluene. Office of Water Regulations and Standards, Criteria and Standards Division, Washington, DC, EPA 440/5–80–045.

(14) Psillakis, E.; Kalogerakis, N. (2001) Application of solvent microextraction to the analysis of nitroaromatic explosives in water samples. *J. Chromatogr. A*, 907: 211.

(15) Batlle, R.; Nerin, C.; Crescenzi, C.; Carlsson, H. (2005) Supercritical fluid extraction of energetic nitroaromatic compounds and their degradation products in soil samples. *Anal. Chem*., 77: 4241.

(16) Walsh, M. E.; Ranney, T. (1998) Determination of nitroaromatic, nitramine, and nitrate ester explosives in water using solid–phase extraction and gas chromatography–electron capture detection: Comparison with high–performance liquid chromatography. *J. Chromatogr. Sci*., 36: 406.

(17) Cortada, C.; Vidal, L.; Canals, A. (2011) Determination of nitroaromatic explosives in water samples by direct ultrasound–assisted dispersive liquid–liquid microextraction followed by gas chromatography–mass spectrometry. *Talanta*, 85: 2546.

(18) Liang, Y.; Gu, L.; Liu, X.; Yang, Q.; Kajiura, H.; Li, Y.; Zhou, T.; Shi, G. (2011) Composites of polyaniline nanofibers and molecularly imprinted polymers for recognition of nitroaromatic compounds. *Eur. J*., 17: 5989.

(19) Shi, X.; Song, S.; Sun, A.; Liu, J.; Li, D.; Chen, J. (2012) Characterisation and application of molecularly imprinted polymers for group–selective recognition of antibiotics in food samples. *Analyst*, 137: 3381.

(20) Chen, L.; Xu, S.; Li, J. (2011) Recent advances in molecular imprinting technology: current status, challenges and highlighted applications. *Chem. Soc. Rev*., 40: 2922.

(21) Ansell, R.J.; Mosbach, K. (1998) Magnetic molecularly imprinted polymer beads for drug radioligand binding assay. *Analyst*, 123: 1611.

(22) Chen, L.; Li, B. (2012) Application of magnetic molecularly imprinted polymers in analytical chemistry. *Anal Methods*, 4: 2613.

(23) Chen, L.; Wang, X.; Lu, W.; Wu, X.; Li, J. (2016) Molecular imprinting: perspectives and applications. *Chem. Soc. Rev*., 45: 2137.

(24) Phutthawong, N.; Pattarawarapan, M. (2012) Facile synthesis of magnetic molecularly imprinted polymers for caffeine via ultrasound–assisted precipitation polymerization. *Polym. Bull*., 70: 691.

(25) Li, J.; Dong, R.; Wang, X.; Xiong, H.; Xu, S.; Shen, D.; Song, X.; Chen, L. (2015) One-pot synthesis of magnetic molecularly imprinted microspheres by RAFT precipitation polymerization for the fast and selective removal of 17β-estradiol. *RSC Adv*., 5: 10611.

(26) Wu, X.; Wang, X.; Lu, W.; Wang, X.; Li, J.; You, H.; Xiong, H.; Chen, L. (2016) Water-compatible temperature and magnetic dual-responsive molecularly imprinted polymers for recognition and extraction of bisphenol A. *J. Chromatogr. A*, 1435: 30.

(27) Matshediso, P. G.; Cukrowska, E.; Chimuka, L. (2015) Development of pressurised hot water extraction (PHWE) for essential compounds from Moringa oleifera leaf extracts. *Food Chem*., 172: 423.

(28) Ebrahimzadeh, H.; Abedi, H.; Yamini, Y.; Adlnasa, L. (2010) Molecular–imprinted polymer extraction combined with dispersive liquid–liquid micro–extraction for ultra–preconcentration of mononitrotoluene. *J. Sep. Sci*., 33: 3759.

(29) Tavengwa, N. T.; Hintsho, N.; Durbach, S.; Weiersbye, I.; Ewa Cukrowska, E.; Chimuka, E. (2016) Extraction of explosive compounds from aqueous solutions by solid phase extraction impregnated with functionalized nanofibres, *J. Environ. Chem. Eng*., 4(2): 2450.

(30) Chen, X.; Chen, B. (2015) Macroscopic and spectroscopic investigations of the adsorption of nitroaromatic compounds on graphene oxide, reduced graphene oxide, and graphene nanosheets. *Environ. Sci. Technol*., 49: 6181.

(31) Zhu, D.; Pignatello, J. J. (2005) Characterization of aromatic compound sorptive interactions with black carbon (charcoal) assisted by graphite as a model. *Environ. Sci. Technol*., 39: 2033.

(32) An, F.; Gao, B.; Feng, X. (2009a) Adsorption of 2,4,6–trinitrotoluene on a novel adsorption material PEI/$SiO_2$. *J. Hazard. Mater.*, 166: 757.

(33) An, F.; Feng, X.; Gao, B. (2009b) Adsorption mechanism and property of a novel adsorption material PAM/$SiO_2$ towards 2,4,6–trinitrotoluene. *J. Hazard. Mater*., 168: 352.

(34) Qin, Q.; Ma, J.; Liu, K. (2007) Adsorption of nitrobenzene from aqueous solution by MCM–41. *J. Colloid. Interface Sci.*, 315: 80.

(35) Wang, S.; Yang, S.; Jin, X.; Liu, L.; Wu, F. (2010) Use of low cost crop biological wastes for the removal of nitrobenzene from water. *Desalination*, 264: 32.

(36) Parham, H.; Saeed, S. (2013) Simultaneous removal of nitrobenzene, 1,3–dinitrobenzene and 2,4–dichloronitrobenzene from water samples using anthracite as a potential adsorbent. *J. Environ. Chem. Eng*., 1: 1117.

**Supplementary section**

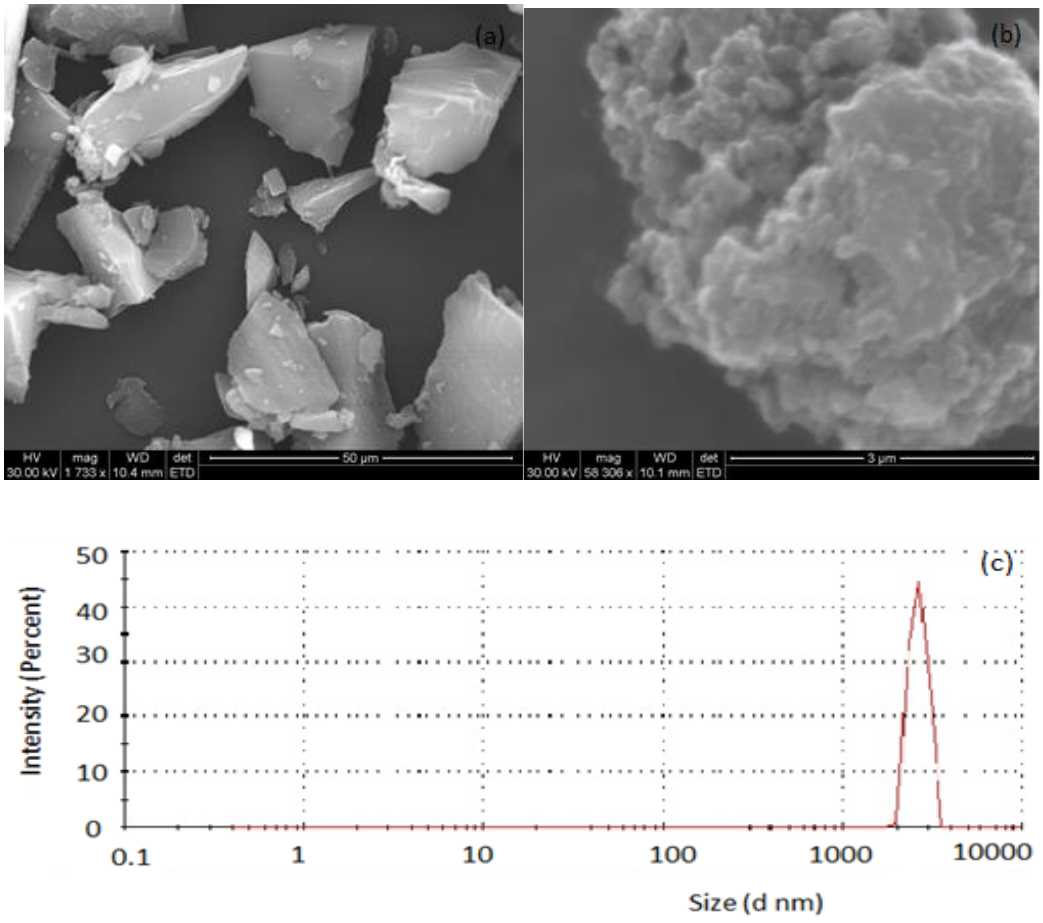



**Figure S1.** SEM micrograph of (a) uneluted magnetic MIPs (b) eluted magnetic MIPs and (c) size distribution of eluted magnetic MIPs.

**Table S1.** List of kinetic parameters and correlation coefficients for the adsorption of NACs onto magnetic imprinted polymers.

| Model | Parameter | NB | | 2,4–DNT | | 2–NT | |
|---|---|---|---|---|---|---|---|
| | | MIP | NIP | MIP | NIP | MIP | NIP |
| Pseudo–first–order | $q_{e,\,cal}$ (mg $g^{-1}$) | 0.005 | 0.027 | 0.011 | 0.080 | 0.023 | 0.103 |
| | $k_1$ ($min^{-1}$) | 0.087 | 0.106 | 0.085 | 0.022 | 0.117 | 0.047 |
| | $R^2$ | 0.9197 | 0.9078 | 0.9955 | 0.6549 | 0.9469 | 0.7583 |
| Pseudo–second–order | $q_{e,\,cal}$ (mg $g^{-1}$) | 0.142 | 0.117 | 0.222 | 0.212 | 0.16 | 0.142 |
| | $k_2$ (g $mg^{-1}$ $min^{-1}$) | 36.9 | 21.9 | 27.2 | 400 | 22.4 | 14.9 |
| | $R^2$ | 0.9998 | 0.9988 | 0.9998 | 0.9973 | 0.994 | 0.9933 |

**Table S2.** The Langmuir and Freundlich constants for adsorption of NACs on magnetic polymers.

| Model | Parameter | NB | | 2,4–DNT | | 2–NT | |
|---|---|---|---|---|---|---|---|
| | | MIP | NIP | MIP | NIP | MIP | NIP |
| Langmuir | $q_{e,\,cal}$ (mg $g^{-1}$) | 0.39 | 0.12 | 3.29 | 0.33 | 0.41 | 5.44 |
| | $b$ (L $mg^{-1}$) | 0.21 | 0.62 | 0.06 | 0.33 | 0.24 | 0.02 |
| | $R_L$ | 0.82 | 0.62 | 0.94 | 0.75 | 0.80 | 0.98 |
| | $R^2$ | 0.998 | 0.993 | 0.999 | 0.992 | 0.994 | 0.997 |
| Freundlich | $k_F$ (L $mg^{-1}$) | 0.09 | 0.07 | 0.20 | 0.16 | 0.13 | 0.11 |
| | $n$ | 0.89 | 0.88 | 1.02 | 0.87 | 0.89 | 0.88 |
| | $R^2$ | 0.964 | 0.929 | 0.996 | 0.989 | 0.989 | 0.985 |

**Paper III**

This paper “Extraction of explosive compounds from aqueous solutions by solid phase extraction impregnated with β-cyclodextrin functionalized carbon nanofibers,” was submitted *to Journal of Environmental Chemical Engineering*. It investigates the synthesis, characterization of carbon nanofibers functionalized with β-cyclodextrin packed in solid pase extraction cartridges for the extraction of six nitroaromatic compounds and subsequent application to real wastewater samples.

Journal of Environmental Chemical Engineering 4 (2016) 2450–2457

Contents lists available at ScienceDirect

Journal of Environmental Chemical Engineering

journal homepage: www.elsevier.com/locate/jece

# Extraction of explosive compounds from aqueous solutions by solid phase extraction using β-cyclodextrin functionalized carbon nanofibers as sorbents

Nikita Tawanda Tavengwa[a], Nomso Hintsho[b], Shane Durbach[b], Isabel Weiersbye[c], Ewa Cukrowska[a], Luke Chimuka[a,*]

[a] Molecular Sciences Institute, School of Chemistry, University of the Witwatersrand, Private Bag 3, Johannesburg 2050, South Africa
[b] DST-NRF Centre of Excellence in Strong Materials, University of the Witwatersrand, Private Bag 3, Johannesburg 2050, South Africa
[c] Ecological Engineering & Phytotechnology Programme, School of Animal, Plant and Environmental Sciences, University of the Witwatersrand, Private Bag 3, Johannesburg 2050, South Africa

ARTICLE INFO

*Article history:*
Received 25 December 2015
Received in revised form 17 April 2016
Accepted 19 April 2016
Available online 21 April 2016

*Keywords:*
Explosive compounds
Solid phase extraction
Pre-concentration
β-Cyclodextrin
Nanofibers

ABSTRACT

This work describes the synthesis of carbon nanofibers (CNFs) which was functionalized with β-cyclodextrin (β-CD). The resultant composite, β-CD@CNFs, was then used for the extraction of selected nitro-based explosive compound pollutants from aqueous solutions. The extraction was through an off-line solid-phase extraction (SPE) procedure followed by high-performance liquid chromatography with ultraviolet detection. Scanning electron microscopy (SEM) and thermogravimetric analysis (TGA) were used to characterize the synthesized materials. Three independent variables: SPE elution solvent, sample pH and sample volume were investigated to determine their influence on the adsorption of the explosive compounds from aqueous samples. The breakthrough volume of 40 mL was considered as optimum. Under the optimized conditions, good calibration linearities were obtained in the range 30–150 $\mu g\,L^{-1}$ with coefficients of determination ($R^2$) > 0.997 for 3-nitrotoluene (3-NT), 1,3-dinitrobenzene (1,3-DNB), 2,6-dinitrotoluene (2,6-DNT), 4-nitrotoluene (4-NT), nitrobenzene (NB) and 2-nitrotoluene (2-NT). Low limits of detection of 3.3, 7.1, 8.6, 9.7, 23.1 and 13.0 $\mu g\,L^{-1}$ were found for the respective compounds. The applicability of the developed method using β-CD@CNF as a sorbent was investigated using spiked real water samples collected within the vicinity of an operational gold mine and recoveries of 36.6–102.2% were obtained.

© 2016 Published by Elsevier Ltd.

## 1. Introduction

Nitroaromatic compounds (NACs) have been found to be ubiquitous pollutants in the aquatic environment [1]. NAC explosives are found as contaminants in sludges, soil surfaces and ground water [2]. These compounds are extremely weakly basic and have been used to measure Hammett acidity functions [3]. They are widely used as pesticides, explosives, chemical intermediates and dyes. NACs and their transformation products are widespread environmental pollutants of significant toxicological concern, especially in soil and ground water. In addition, NACs are among the 127 priority pollutants included on the United States Environmental Protection Agency (USEPA) priority list [4].

There has been interest in developing sensitive detection techniques for explosive compounds like 2,4,6-trinitrotoluene (TNT), picric acid and other nitroaromatic compounds [5,6]. Chemical sensors for the rapid detection of explosives are important because they have potential applications, such as in remediation of explosives manufacturing sites [7]. Recently, carbon nanotubes have been explored as new materials in sensors for explosives [8,9].

In the last decade, a variety of extraction methods have been developed for preparing environmental samples. However, adsorbents with superior properties play a key role in solid phase extraction (SPE) for enhancing the enrichment efficiency and analytical performance. SPE is a well-established method for sample clean-up and pre-concentration in the analysis of biological as well as trace environmental samples [10,11]. The SPE method is convenient, requires less volume of organic solvents, and is time-saving and simple to use [12].

* Corresponding author.
*E-mail address:* luke.chimuka@wits.ac.za (L. Chimuka).

http://dx.doi.org/10.1016/j.jece.2016.04.024
2213-3437/© 2016 Published by Elsevier Ltd.

Fly ash is typically a by-product of several energy and power generation industries [13]. It can be used as an adsorbent due to its structure and charge behaviour. However, it has also been observed that fly ash can be effective at producing carbon nanofibers (CNFs) [14–17]. This is due to the transition metals that are found in fly ash which act as catalysts during synthesis. Typically, fly ash consists of: $SiO_2$, $Al_2O_3$, $Fe_2O_3$ and $TiO_2$, but may also include trace amounts of: CaO, BaO and Mn [18]. In general, some of the catalysts used for carbon nanotubes (CNTs) and CNF synthesis include metals such as: Fe/Ni, Ni, Co, Mn, Cu, Mo and Pd; hence, the potential of fly ash to be used as a catalyst in such reactions. CNFs usually have larger diameters, are longer in length and are lower in cost to make than the multi-walled CNTs, thus making them practical for more applications [19]. CNFs and CNTs have potential application in catalysis [20], transparent conducting films as supports [21], and in bio-sensing [22]. CNF has also been used in environmental analysis as SPE sorbents [23,24]. Recently, a comprehensive study on the synthesis and full characterization of CNFs was conducted in our school [17].

Because CNFs exist in bundles or aggregations after the growth process [25], there is need to disentangle them for further use, otherwise this limits their potential application, e.g. as reinforcements in polymers [26]. One way of overcoming this is through the chemical modification of the surfaces and edges of CNFs [27]. For instance, the introduction of oxygen-containing groups on these surfaces through oxidation, has afforded further modification with other organic compounds such as: aspartic acid [28], β-cyclodextrin (β-CD) [29] and 4,4′-methylenedianiline [30] which have altered the surface chemistry as well as properties of different carbon materials. Insoluble β-CD polymers have also been used for selective sorption and release of a broad range of organic guests [31].

In this work, β-CD was selected as a coating agent over other saccharides and polymers because of its encapsulation abilities [32]. β form of CD was chosen ahead of the γ and α forms because of its lower solubility in water. The first objective of the work was to synthesis CNFs from natural abundant waste fly ash from Duvha electricity generating power station in South Africa. The raw CNFs were then functionalized with β-CD to make composite β-CD@CNF sorbents which was used for the extraction of selected explosive compounds from aqueous solutions by SPE. On its own CNFs are hydrophobic, it was therefore necessary to transform it into a hydroplilic form in order to extract NACs. To our best knowledge, this is the first systematic research on β-CD functionalized CNFs as SPE sorbents for the extraction of NACs.

## 2. Experimental

### 2.1. Materials and equipment

Six explosive compounds: 3-nitrotoluene (3-NT), 1,3-dinitrobenzene (1,3-DNB), 2,6-dinitrotoluene (2,6-DNT), 4-nitrotoluene (4-NT), nitrobenzene (NB) and 2-nitrotoluene (2-NT) were bought from Sigma Aldrich (Johannesburg, South Africa). Methanol (99%) was purchased from Fischer Scientific (Loughborough, UK) and acetonitrile (99.9%) was obtained from Sigma-Aldrich (Steinheim, Germany). Dimethylsulfoxide (99.9%) and *N*,*N*-dimethylformamide (99.9%) were purchased from Fluka (Steinheim, Germany).

The SPE cartridges used were bought from Supelco (Bellefonte, PA, USA). Deionized water was obtained from Milli-Q ultrapure water (Millipore, Billerica, Massachusetts, USA). The pH measurements were performed on a 766 Calimatic pH meter equipped with a Shott N61 pH electrode from Knick (Berlin, Germany). A modified method from Gaurav et al. [33] was used by using a Bischoff HPLC, with a UV detector set at 254 nm and an Ascentis RP-amide column (25 cm × 4.6 mm × 5 μm) was used to separate and quantify the explosive compounds. The mobile phase composition was acetonitrile/water (50/50, v/v) where the flow rate was maintained at 1 mL $min^{-1}$ in isocratic mode and the sample injection volume was 50 μL.

### 2.2. Instruments for characterization

Surface morphological information of the sorbent material was investigated using a FEI Quanta 200 SEM (FEI, Hillsboro, OR, USA). A FEI TECNAI SPIRIT (TEM-EDS) electron microscope (Eindhoven, Netherlands) was used for morphological determination of raw CNFs and β-CD@CNFs. Fourier-transform infrared spectra were recorded in the frequency range of 400–4000 $cm^{-1}$ using a Bruker FTIR spectrometer, Model Tensor 27 (Ettlingen, Germany) at a resolution of 2 $cm^{-1}$. Zeta potentials were measured with the Zeta-Meter 3.0 system (Malvern ZS-90). The thermal stabilities of the raw and functionalized CNF materials were determined by using a Perkin Elmer Pyris 1 Thermogravimetric Analyzer (Massachusetts, USA). In this analysis, a 10 mg sample was heated to 900 °C at a rate of 10 °C $min^{-1}$ under air (20 mL $min^{-1}$).

### 2.3. Preparation of standards and real environmental solutions

A stock solution of each explosive compound was prepared by dissolving the appropriate mass or volume in 50 mL of 50/50 (v/v) acetonitrile/water solution. A 10 mg $L^{-1}$ mixture of working stock solution was then prepared from the individual stock solutions and the same diluent was used to top up to the mark. A series of calibration standard solutions were made (30–150 μg $L^{-1}$). All standard solutions were stored in a refrigerator at 4 °C when not in use. Environmental water samples were first filtered through a 0.45 μm filter paper and 5% acetonitrile (v/v) was added for complete dissolution of the explosive compounds.

### 2.4. Synthesis of CNFs from fly ash

Waste coal fly ash was obtained from the Electricity Supply Commission of South Africa (ESCOM) Duvha power station and was used as-received (i.e. without modification). Carbon deposition was achieved by the chemical vapour decomposition of acetylene over the waste coal fly ash. In this reaction, coal fly ash was the catalyst, acetylene the carbon source and hydrogen was the carrier gas. In the synthesis run, 500 mg of as-received fly ash was uniformly spread in a small quartz boat and placed at the centre of a horizontal furnace. The fly ash was then heated at 10 °C $min^{-1}$ in $H_2$ at 100 mL $min^{-1}$ to 650 °C, where upon acetylene gas was introduced into the reaction zone at 100 mL $min^{-1}$ for 45 min. After 45 min of reaction time, the flow of acetylene was terminated and the reactor was cooled under $H_2$ to ambient temperature. The resultant carbonaceous material was then harvested for characterization and further modification.

### 2.5. Functionalization and the addition of β-cyclodextrin (β-CD) unto carbon nanofibers

In a modified method by Atieh et al. [34], 300 mL of concentrated nitric acid (55%) was added to 2 g of the synthesized CNFs. Since the CNFs were hydrophobic, some were observed to float on top of the acid. However, with a steady stirring at 54 °C, they began to mix with the acid over time. The reaction was only stopped when all the CNFs were mixed together with the acid after 3 h. Further heating was detrimental as there was a likelihood for the functionalized CNFs to be dissolved [35,36]. After oxidation, centrifugation was used to separate the CNFs. This was then followed by subsequent washing with distilled water until the pH was almost neutral [37], followed by drying in a vacuum oven at

90 °C. For further functionalization, a modified method by Wang et al. [38] was used where 0.2 g of CNFs were dispersed in 100 mL of an aqueous β-CD solution (2%) with the aid of ultrasonic agitation.

### 2.6. Point of zero charge (pHpzc)

For the point of zero charge (pHpzc) determination, a 0.01 mol $L^{-1}$ $KNO_3$ solution was prepared and its initial pH ($pH_i$) was adjusted to between 2 and 12 by the addition of 0.1 mol $L^{-1}$ HCl and 0.1 mol $L^{-1}$ NaOH in different test tubes. A volume of 12 mL of the pH adjusted of $KNO_3$ and 20 mg of β-CD@CNFs were then mixed together. The samples were kept at 25 °C for 24 h, after which the solution was separated from the β-CD@CNFs by centrifugation. After decanting, the final pH ($pH_f$) of solution was then measured.

### 2.7. SPE preparation

A 20 μm polyethylene frit was placed at the bottom of a 3 mL empty polyethylene SPE cartridge. A mass of 100 mg of dry β-CD@CNFs was then loaded into the cartridge, and another frit was placed on the top of the cartridge to cover the sorbent bed. Prior to the extraction procedure, the sorbent was sequentially pre-washed with 6 mL of methanol and 10 mL Milli-Q water at a flow rate of 1 mL $min^{-1}$. The β-CD@CNFs were then conditioned with two 10 mL aliquots of the 50/50 (v/v) acetonitrile/water mixture. During the conditioning step and the following extraction step, the SPE material was prevented from running dry.

A portion of the aqueous sample solution containing explosive compounds was prepared, and its pH was adjusted to the desired value. An aliquot of the solution containing different amounts of explosive compounds was then passed through the column at a flow rate of 1 mL $min^{-1}$. The explosive compounds which were retained were then eluted with 3 × 1000 μL of different organic solvents. The analytes in the effluent were then determined by HPLC-UV.

### 2.8. Optimization of the SPE procedure

In order to achieve accurate and sensitive chromatographic quantification of the trace explosive compounds in aqueous solutions, the optimum conditions for SPE using β-CD@CNF as a sorbent were determined. The investigated conditions affecting extraction efficiency included elution solvent, sample pH, and sample volume. One parameter was varied while the others were held constant and all experiments were performed in triplicate (n = 3).

## 3. Results and discussion

### 3.1. Characterization of sorbent materials

As observed in the FTIR spectrum of the raw CNF (Fig. 1), there was almost no signal except for C—H stretch and anti-stretching frequencies at 2949 $cm^{-1}$ and 2886 $cm^{-1}$, respectively, and a few bands (1033–1202 $cm^{-1}$) in the fingerprint region. However, as the raw CNF was oxidized by acid treatment and subsequently functionalized by β-CD, a number of new peaks started appearing. According to Gomes et al. [39], the oxidation of CNTs results in functional groups such as carboxylic (—COOH), carbonyl (—CO), and hydroxylic (—OH) are formed on their surface and is likely to be the case with CNFs. The peaks at 1006 and 1034 $cm^{-1}$ can be assigned to C—OH stretch modes in CNF-$COO^-$ and β-CD@CNF, respectively. The hydroxyl groups which appeared at 3469 $cm^{-1}$ for the CNF-$COO^-$ was absent in the raw CNF. For β-CD@CNF, an anti-symmetric stretch C—O was also clearly distinguishable at 1587 $cm^{-1}$. According to Liu et al. [40], they found that the two main interaction mechanisms between β-CD and the carbonaceous material, multi-walled CNTs, involved the van der Waals forces and hydrogen bonding.

According to Memişoğlu et al. [41], the zeta potential of β-CD was −31.6 mV and da Silveira et al. [42] determined it to be −(24.7 ± 8.2) mV. The zeta potentials for the raw CNFs and CNF-$COO^-$ were 0 and −17.3 mV, respectively. The negative zeta potential was caused by the deprotonation of the —COOH. This was an indication of successful activation of the raw CNFs. The sorption performance of carbon nano-materials has been shown to be mainly determined by the nature and concentration of the surface functional groups [43]. The introduction of the carboxylate/hydroxy groups made it possible for further functionalization when β-CD was added. The final products of functionalization were β-CD@CNF fragments where terminals were loaded with various oxygen containing carboxyl groups. The percentage of carboxylic functions on the oxidized CNTs surface does not exceed 4% in the best cases [44] and we assume it is the same with CNFs. Oxidation of CNTs with nitric acid is an effective method to remove the amorphous carbon, carbon black and carbon particles introduced by their preparation process [45].

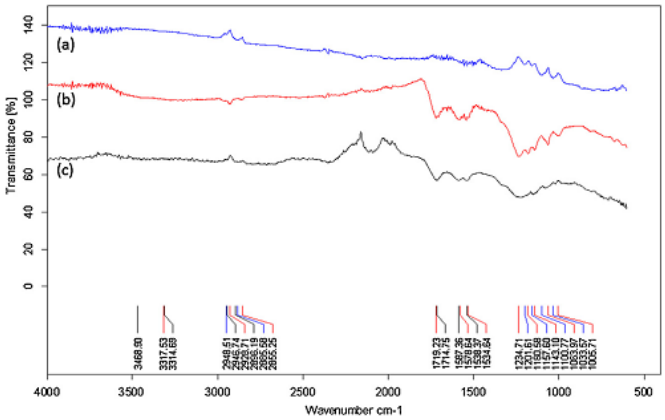



**Fig. 1.** FTIR spectra of (a) raw CNFs (b) oxidized CNFs and (c) β-CD modified CNFs.

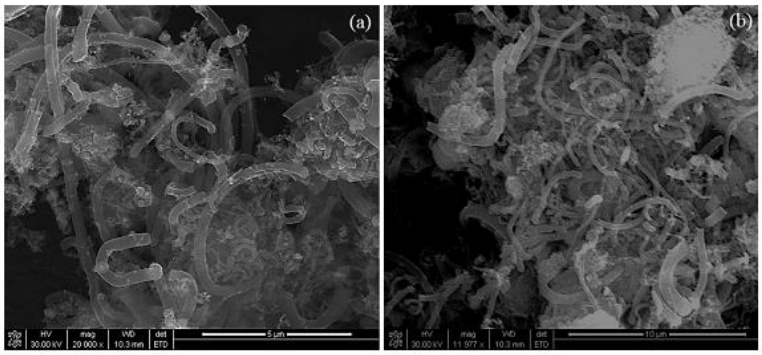



**Fig. 2.** SEM micrographs of (a) raw CNFs and (b) β-CD modified CNFs.

The surface morphology of the raw CNFs and the β-CD functionalized CNFs were characterized by scanning electron microscopy (SEM) (Fig. 2). The diameters of the raw CNFs were observed to be in the range of 180–800 nm. After acid treatment, a few of the CNFs were cut into short segments, otherwise their morphologies and diameters remained essentially the same. This suggested that the acid treatment process was mild and predominantly non-destructive to the CNF structure. The same applied after β-CD modification.

TEM analysis confirmed the success of the grafting of β-CD to CNFs. The β-CD molecules were randomly incorporated along the stretch of the CNFs (Fig. 3) and not as a film. The dark contrast on the surface of the CNFs was due to linkage with β-CD moieties (Fig. 3(b)).

The thermal stabilities of the variously prepared materials were measured by thermogravimetric analysis. Based upon the thermograms (Fig. 4(a)), it was observed that the raw CNFs were the most thermally stable, with decomposition having begun at 630 °C. CNFs are known to decompose above 500 °C, which was the same finding by Van et al. [46]. Oxidation of these CNFs (Fig. 4(b)), as well as the addition of β-CD (Fig. 4(c)) led to a decrease in their thermal stability. For example, the decomposition of functionalized CNFs started as low as 270 °C (Fig. 4). This was most likely due to the disorder introduced by the functional groups. In each case, the residual weight% that remained after full combustion was due to coal fly ash and a small amount of metal and metal oxides. All the carbonaceous materials have been removed. The residual weight after 900 °C for the raw CNFs (11%) was the highest, followed by the carboxyl functionalized CNFs (9%) and the least was β-CD modified CNF (6%). From the TGA thermograms, an estimation of the amount of the organic coating on the CNF was 1.97% leaving the bulky of the material (98.03%) of β-CD@CNF to be CNF.

### 3.2. Effect of pH on sorption

Oxidation of the CNFs led to surface modifications with more oxygen-containing groups which were further modified with β-CD. The surface charge of the sorbent depended on the pH of the surrounding solution (Fig. 5). Likewise, the different molecular forms and charges of the explosive compounds were also affected by the pH environment. The graph of initial pH ($pH_i$) versus final pH ($pH_f$) was plotted, and the point of zero charge (pHpzc) was determined to be a value where $pH_f$ was almost constant; this was found to be 4.01. Van et al. [46] found the $pH_{PZC}$ for all the CNF samples they investigated to vary between pH 3 and 4. At pH < 4.01, the surface of the β-CD@CNF was positively charged due to protonation, while at pH > 4.01 the surface of the β-CD@CNF was negatively charged. When the pH of the solution was higher than pHpzc (i.e. pH > 4.01), the negative charge on the surface of the β-CD@CNF provided electrostatic interactions which were favourable for adsorbing cationic species. The probable sorption mechanism included: van der Waals forces, inclusion complex formation (like 2,4-DCP, an analyte closely related to NACs, which has been proven to have formed an inclusion complex with β-CD

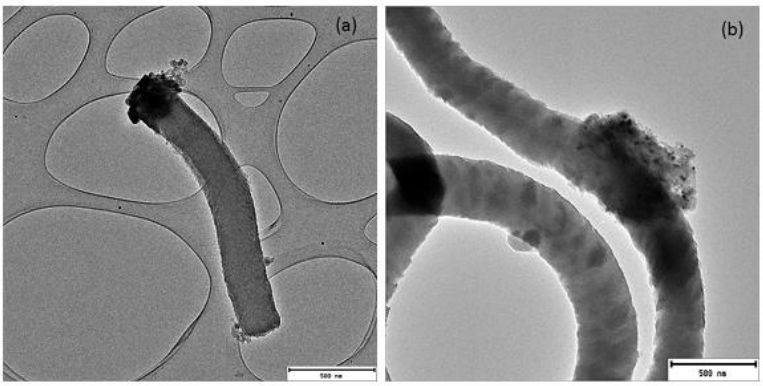



**Fig. 3.** TEM images of (a) raw CNFs and (b) β-CD@CNFs.

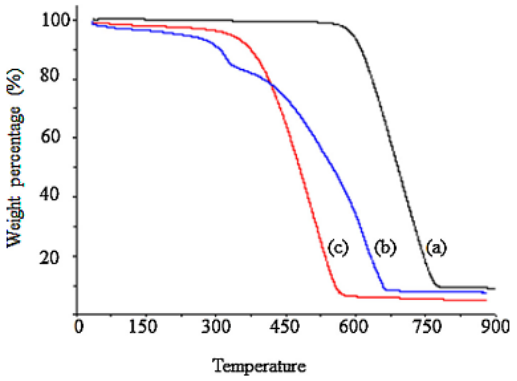



**Fig. 4.** TGA of (a) raw CNFs (b) oxidized CNFs and (c) β-CD modified CNFs.

[47]), and hydrogen bonding [48]. However, when the various explosive compounds were added onto the β-CD@CNF packed in the SPE cartridge, it was observed that its adsorption capacity was lower in both acidic and basic solutions, but was greatest at pH of 7 (Fig. 6) where the NACs are in their neutral forms. However, because of the inductive effect, the nitro-groups tend to withdraw electrons from the benzene ring thereby de-activating it. In the process, the benzene ring becomes partially positively charged. This is the part which was proposed to electrostatically interact with the negative surface of the β-CD@CNF (pH > pHpzc). In this experiment, the general order of elution was determined to be: 2,6-DNT > 2-NT > 3-NT > NB > 4-NT > 1,3-DNT. In other work, Shen et al. [49] found that the elution order for NACs from multi-walled nanotubes (MWCNT) sorbents was: DNB > 2-NT > 3-NP > NB. They concluded that the molecular size of the NACs and the number of nitro groups on the NACs influenced the sorption affinity of NACs to MWCNT.

### 3.3. Elution solvent

Selecting the most appropriate solvent is quite essential for the optimization of the desorption process in SPE. In this study, 60 mL of six selected explosive compounds mixed at 100 μg $L^{-1}$ concentration level in 50/50 (v/v) acetonitrile/water solution were added directly into the SPE cartridge. Because of the different polarities and water solubilities, methanol (MeOH), dimethylsulfoxide (DMSO), N,N-dimethylformamide (DMF) and acetonitrile (ACN) were selected as possible eluents in this SPE experiment in

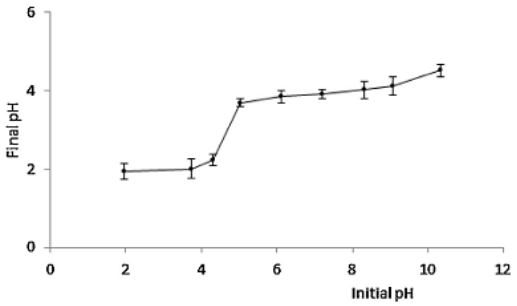



**Fig. 5.** $pH_i$ versus $pH_f$ for the determination of point of zero charge of the β-CD@CNF sorbent (n = 3).

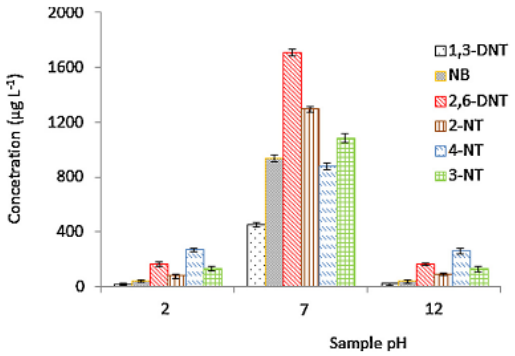



**Fig. 6.** Effect of sample pH on SPE performance in extraction of explosive compounds. Extraction conditions: sample volume, 60 mL; NACs concentration, 50 μg $L^{-1}$; extraction rate, 1 mL $min^{-1}$; elution solvent, ACN; eluent volume, 3 mL. Error bars indicate standard deviation (n = 3).

order to find the most appropriate solvent for extraction. When eluting with another solvent other than acetonitrile (MeOH, DMSO and DMF), the extracts were evaporated to dryness under nitrogen at 45 °C and were finally reconstituted to a volume of 3 mL with ACN. It was observed that ACN exhibited a superior extracting ability (Fig. 7); hence, it was chosen as the best eluent and was used in subsequent optimization experiments. The full elution order was: ACN > DMF > MeOH > DMSO. The NACs are hydrophilic compounds, and are strongly adsorbed on the β-CD@CNFs. This interaction makes their elution difficult. ACN was the best solvent to break the interactions between the NACs and the CD@CNFs sorbent.

### 3.4. Effect of loading volume

In order to explore the possibility of enriching low concentration of analytes from large volumes, the maximum applicable sample volume was determined as the enrichment efficiency relies on the volume of the loading solvent. For this purpose, 20–100 mL of sample volumes were used to test the effect of sample volume (Fig. 8). Sample solutions containing 50 μg $L^{-1}$ of the standard solutions at pH 7 were passed through SPE loaded with 100 mg β-CD@CNF sorbent. A loading volume of 40 mL was found to have given maximum recoveries (>75%) for all explosive compounds (Fig. 8). Lower recovery percentages were recorded with volumes

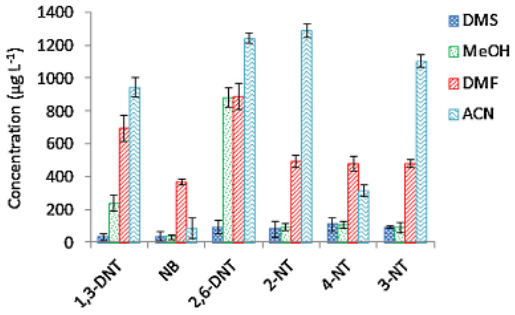



**Fig. 7.** Effect of different eluting solvents on SPE performance. Extraction conditions: sample pH, 7; sample volume, 60 mL; NACs concentration, 50 μg $L^{-1}$; elution rate, 1 mL $min^{-1}$; eluent volume, 3 mL. Error bars indicate standard deviation (n = 3).

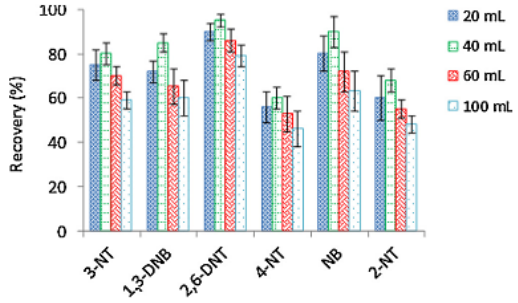



**Fig. 8.** The effect of sample volume on the recovery of explosive compounds extracted with ACN at a flow rate of 1 mL $min^{-1}$. Extraction conditions: sample pH, 7; NACs concentration, 50 $\mu g\,L^{-1}$; extraction rate, 1 mL $min^{-1}$; elution solvent, ACN; eluent volume, 3 mL. Error bars indicate standard deviation (n = 3).

<40 mL and >40 mL. Generally, smaller sample volumes allowed greater amounts of analytes to interact with a larger number of binding sites than when higher sample volumes were used.

### 3.5. Method validation and application

The calibration curves were constructed by measuring different concentrations of standard solutions (30–150 $\mu g\,L^{-1}$), and the resulting coefficients of determination ($R^2$) were >0.997 for all the explosive compounds (Table 1). The limit of detection (LOD) and the limit of quantification (LOQ), which was defined as a signal to noise ratio of 3:1 and 10:1, were obtained, respectively. This validation data is shown in Table 1.

In order to study the effectiveness of the developed method, the synthesized β-CD@CNFs were added to mine tailings impacted water samples under the optimized conditions. In situ measurements were taken of stream water in recently planted artificial reedbeds constructed to treat acid mine drainage from a gold and uranium mine tailings facility at the West Wits Mining Operations near Carletonville in Gauteng Province. The pH of the surface water was 6.6 and the redox potential was 487 V. The electrical conductivity of the real water sample of 4.63 mS $cm^{-1}$ suggested the presence of more ionic compounds. HPLC-UV chromatograms of the unspiked and spiked real water samples at 10 and 100 $\mu g\,L^{-1}$ levels after extraction of the explosive compounds on CD@CNFs packed in SPE cartridges are shown in Fig. 9. The recoveries of the nitrobenze and the dinitritoluene isomers were higher than the mono-substituted toluenes (Table 1). The presence of the matrix in sorption of NACs by β-CD@CNF could explain the low recoveries of the mono substituted toluenes whose one nitro group did not deactivate the aromatic ring sufficiently. The developed method was suitable for the determination of explosive compounds in complex samples since the LOD (3.1-23.1 $\mu g\,L^{-1}$) were lower than the recommended maximum allowable concentrations for NACs (e.g. 0.0068 mg $L^{-1}$ for 2,6-DNT and 0.17 mg $L^{-1}$ for 2,4-DNT, USEPA

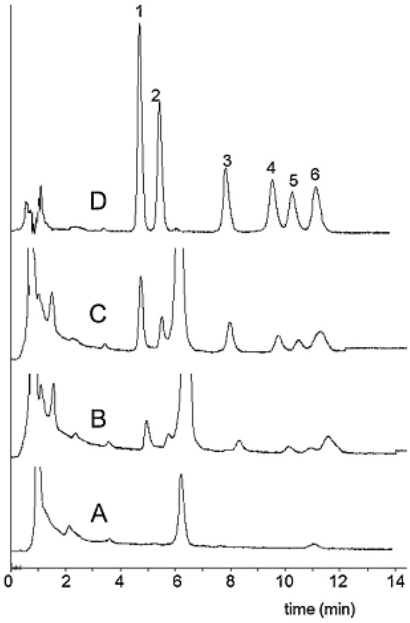



**Fig. 9.** Chromatograms of (A) unspiked real water (B) 10 $\mu g\,L^{-1}$ spiked real water (C) 100 $\mu g\,L^{-1}$ spiked real water and (D) 800 $\mu g\,L^{-1}$ standard solution. Peak 1: 1,3-dinitrobenzene (1,3-DNB), peak 2: dinitrobenzene (NB), peak 3: 2,6-dinitrotoulene (2,6-DNT), peak 4: 2-nitrotoulene (2-NT), peak 5: 4-nitrotoulene (4-NT) and peak 6: 3-nitrotoulene (3-NT).

[50]). The repeatability of the proposed method was satisfactory and the relative standard deviation (RSD) of three runs was >20%.

### 3.6. Interactions of nitroaromatic based explosive compounds and β-CD@CNF

There are at least three different types of possible interactions that could have taken place between the β-CD@CNF sorbent and the explosive compounds as shown in Fig. 10. Due to the hydrophilic nature of the explosive compounds and the hydrophilic exterior of β-CD, the explosive compounds could have been sorbed through H-bonding. Here, the formation of hydrogen bonds could have taken place between the nitrogen atom of the NAC and the hydrogen atom on the hydroxyl group of the β-CD@CNF (Fig. 10(a)). Apart from the neutral explosive compound, the ionized resonance form could also possibly have interacted with β-CD though ionic interactions (Fig. 10(b)). Another possible interaction mechanism was that of inclusion of the hydrophobic part of the explosive compound into the hydrophobic interior of the cyclodextrin. The inclusion complex formation would then

**Table 1**
Validation parameters for HPLC determination of six explosive compounds and their recoveries from real water sample spiked at 10 $\mu g\,L^{-1}$.

| | $t_R$ (min) | Equation | $R^2$ | LOD ($\mu g\,L^{-1}$) | LOQ ($\mu g\,L^{-1}$) | Recovery (%) | RSD (%) |
|---|---|---|---|---|---|---|---|
| 1,3-DNB | 5.0 | y = 0.247x – 11.279 | 0.9984 | 3.8 | 12.8 | 87.7 | 0.3 |
| NB | 5.7 | y = 0.148x + 4.594 | 0.9992 | 7.1 | 23.8 | 32.6 | 7.7 |
| 2,6-DNT | 8.1 | y = 0.090x – 3.076 | 0.9994 | 8.6 | 28.6 | 102.2 | 2.9 |
| 2-NT | 9.8 | y = 0.072x + 2.335 | 0.9972 | 9.7 | 47.6 | 64.4 | 18.2 |
| 4-NT | 10.5 | y = 0.097x – 1.478 | 0.9990 | 23.1 | 76.9 | 43.0 | 17.9 |
| 3-NT | 11.4 | y = 0.118x – 0.319 | 0.9987 | 13.0 | 43.5 | 61.8 | 6.3 |

*Note*: LOD—limit of detection, LOQ—limit of quantification.

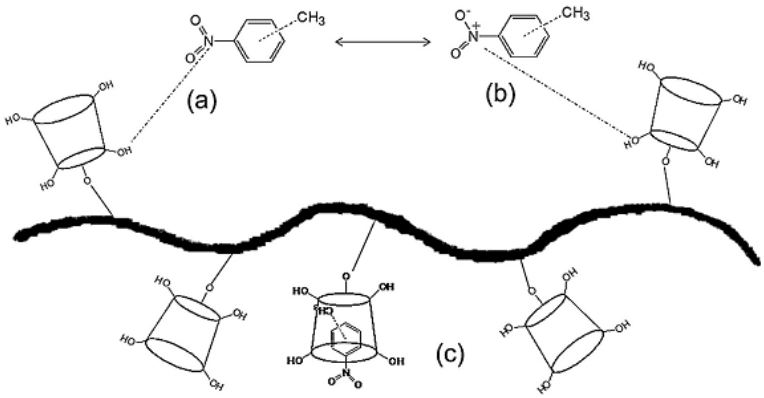



**Fig. 10.** Possible interaction mechanisms between the explosive compounds and β-CD@CNFs.

have been between the β-CD cavity of β-CD@CNF and the explosive compound molecules (Fig. 10(c)). Hydrophobic effects (not shown) may also have played an important role in the process of adsorption, through π-π interactions between the aromatic ring of β-CD functionalized on the CNF and the benzene ring of the explosive compounds.

## 4. Conclusions

In this work, it was demonstrated that the waste abundant coal fly ash from South African power stations can be made good use of by synthesizing CNFs as sorbents for the extraction of NACs from aqueous solutions. Explosive compounds were found to be extracted simultaneously by solid phase extraction with β-CD@CNFs as an SPE sorbent. Extraction of the NACs unto β-CD@CNFs was pH dependent and was greatest at around pH 7 when the sorbent charge was positive. At this neutral pH, the number of nitro-groups attached to the benzene ring was a big factor; di-nitroaromatic compounds were adsorbed more than the mono-nitroaromatic compounds. Acetonitrile was found to be the best SPE eluting solvent. This method was successfully applied to extraction and pre-concentration of explosive compounds from real water samples with recoveries of >80% for 1,3-DNB and 2,6-DNT. However, the matrix affected the mono-substituted toluenes more, hence lower recoveries were obtained.

## Acknowledgements

The authors would like to thank the National Research Foundation (NRF) South Africa for funding Nikita Tawanda Tavengwa through the innovation Doctoral Scholarship, grant ID number NFS13091843717, as well as AngloGold Ashanti Ltd. S.A. region and the NRF/Department of Trade and Industry (DTI) "THRIP" (TP13080525596) awards to I. Weiersbye and E.T.F. Witkowski. Department of Science and Technology (DST) of South Africa is also acknowledged for funding (Grant DST/CON 0054/2014).

## References

[1] C.G. Heijman, E. Grieder, C. Holliger, R.P. Schwarzenbach, Reduction of nitroaromatic compounds coupled to microbial iron reduction in laboratory aquifer columns, Environ. Sci. Technol. 29 (1995) 775–783.
[2] A. Michalkova, J.J. Szymczak, J. Leszczynski, Adsorption of 2,4-dinitrotoluene on Dickite: the role of H-bonding, Struct. Chem. 16 (2005) 325–337.
[3] C.H. Rochester, Acidity Functions, Academic Press, London, 1970.
[4] R.K. Jain, D. Paul, A. Ghosh, J. Pandey, Biodegradation of nitroaromatic pesticides, in: V.L. Chopra, R.P. Sharma, S.R. Bhat, B.M. Prasanna (Eds.), Search for New Genes, National Academy of Agricultural Sciences (NAAS), 2007.
[5] E.R. Goldman, I.L. Medintz, J.L. Whitley, A. Hayhurst, A.R. Clapp, H.T. Uyeda, J.R. Deschamps, M.E. Lassman, H.J. Mattoussi, A hybrid quantum dot-antibody fragment fluorescence resonance energy transfer-based TNT sensor, Am. Chem. Soc. 127 (2005) 6744–6751.
[6] K.S. Focsaneanu, J.C. Scaiano, Potential analytical applications of differential fluorescence quenching: pyrene monomer and excimer emissions as sensors for electron deficient molecules, Photochem. Photobiol. Sci. 4 (2005) 817–821.
[7] A.M. Rouhi, Seeking drugs in natural products, Chem. Eng. News 75 (1997) 14–20.
[8] J. Wang, S.B. Hocevar, B. Ogorevc, Carbon nanotube-modified glassy carbon electrode for adsorptive stripping voltammetric detection of ultratrace levels of 2,4,6-trinitrotoluene, Electrochem. Commun. 6 (2004) 176–179.
[9] E.E. Snow, F.K. Perkins, E.J. Houser, S.C. Badescu, T.L. Reinecke, Chemical detection with a single-walled carbon nanotube capacitor, Science 307 (2005) 1942–1945.
[10] F. Omidi, M. Behbahani, H.S. Abandansari, A. Sedighi, S.J. Shahtaheri, Application of molecular imprinted polymer nanoparticles as a selective solid phase extraction for preconcentration and trace determination of 2,4-dichlorophenoxyacetic acid in the human urine and different water samples, J. Environ. Health Sci. Eng. 12 (2014) 137.
[11] K. Pyrzynska, E. Pobozy, On-line coupling of solid phase extraction sample processing with high-performance liquid chromatography, Crit. Rev. Anal. Chem. 32 (2002) 227–243.
[12] E.C. Figueiredo, D.M. de Oliveira, M.E. de Siqueira, M.A. Arruda, On-line molecularly imprinted solid-phase extraction for the selective spectrophotometric determination of nicotine in the urine of smokers, Anal. Chim. Acta 635 (2009) 102–107.
[13] D.C. Nath, V. Sahajwalla, Application of fly ash as a catalyst for synthesis of carbon nanotube ribbons, J. Hazard. Mater. 192 (2011) 691–697.
[14] O.M. Dunens, K.J. MacKenzie, A.T. Harris, Synthesis of multiwalled carbon nanotubes on fly ash derived catalysts, Environ. Sci. Technol. 43 (2009) 7889–7894.
[15] A. Yasui, Y. Kamiya, S. Sugiyama, S. Ono, H. Noda, Y. Ichikawa, Synthesis of carbon nanotubes on fly ashes by chemical vapor deposition processing, IEEJ Trans. 4 (2009) 787–789.
[16] N. Salah, S.S. Habib, Z.H. Khan, A. Memic, M.N. Nahas, Growth of carbon nanotubes on catalysts obtained from carbon rich fly ash, Dig. J. Nanomater. Biostruct. 7 (2012) 1279–1288.
[17] N. Hintsho, A. Shaikjee, H. Masenda, D. Naidoo, D. Billing, P. Franklyn, S. Durbach, Direct synthesis of carbon nanofibers from South African coal fly ash, Nanoscale Res. Lett. 9 (2014) 387–398.
[18] R. Iyer, The surface chemistry of leaching coal fly ash, J. Hazard. Mater. 93 (2002) 321–329.
[19] Y. Gao, P. He, J. Lian, M.J. Schulz, J. Zhao, W. Wang, X. Wang, J. Zhang, X. Zhou, D. Shi, Effects of surface modification carbon nanofiber concentration, and dispersion time on the mechanical properties of carbon-nanofiber-polycarbonate composites, J. Appl. Polym. Sci. 103 (2007) 3792–3797.
[20] O. Babajide, L. Petrik, N. Musyoka, B. Amigun, F. Ameer, Use of coal fly ash as a catalyst in the production of biodiesel, Pet. Coal 52 (2010) 261–272.
[21] Z. Wu, Z. Chen, X. Du, J.M. Logan, J. Sippel, M. Nikolou, K. Kamaras, J.R. Reynolds, D.B. Tanner, A.F. Hebard, A.G. Rinzler, Transparent, conductive carbon nanotube films, Science 305 (2004) 1273–1276.
[22] J. Wang, Y. Lin, Functionalized carbon nanotubes and nanofibers for biosensing applications, Trends Anal. Chem. 27 (2008) 619–626.
[23] S. Chen, M. Xiao, D. Lu, X. Zhan, Carbon nanofibers as solid-phase extraction adsorbent for the preconcentration of trace rare earth elements and their

determination by inductively coupled plasma mass spectrometry, Anal. Lett. 40 (2007) 2105–2115.
[24] A. Sarafraz-Yazdi, T. Rokhian, A. Amiri, F. Ghaemi, Carbon nanofibers decorated with magnetic nanoparticles as a new sorbent for the magnetic solid phase extraction of selected polycyclic aromatic hydrocarbons from water samples, New J. Chem. 39 (2015) 5621–5627.
[25] K.R. Jacobsen, D.G. Walters, Carbon nanofiber filled materials for charge dissipation, 8th Spacecraft Charging Technology Conference (2003) 1–6.
[26] Y. Nie, T. Hübert, Surface modification of carbon nanofibers by glycidoxysilane for altering the conductive and mechanical properties of epoxy composites, Compos. A: Appl. Sci. Manuf. 43 (2012) 1357–1364.
[27] J.S. An, B. Nam, S.H. Tan, S.C. Hong, Study on the functionalization of multi-walled carbon nanotube with monoamine terminated poly(ethylene oxide), Macromol. Symp. 249–250 (2007) 276–282.
[28] Jacob M. Ngoy, Sunny E. Iyuke, Wilhelm E. Neuse, Clarence S. Yah, Covalent functionalization for multi-walled carbon nanotube (f-MWCNT)-folic acid bound bioconjugate, J. Appl. Sci. 11 (2011) 2700–2711.
[29] J. Cheng, P.R. Chang, P. Zheng, X. Ma, Characterization of magnetic carbon nanotube-cyclodextrin composite and its adsorption of dye, Ind. Eng. Chem. Res. 53 (2014) 1415–1421.
[30] R. Chaos-Morán, M. Campo, S.G. Prolongo, M.D. Escalera, A. Ureña, The functionalization of carbon nanofibers with 4,4′-diaminodiphenylmethane, a curing agent for epoxy resins, J. Mater. Res. 24 (2009) 1435–1445.
[31] D. Koradecki, W. Kutner, Inclusion of the regioisomeric nitrobenzene derivatives and ferrocene guests by β-cyclodextrin polymer and their transport through the polymer matrix, J. Incl. Phenom. Mol. Recognit. Chem. 10 (1991) 79–96.
[32] H.K.S.V. Mohan, J. An, K. Liao, C.H. Wong, L. Zheng, Detection and classification of host-guest interactions using β-cyclodextrin-decorated carbon nanotube-based chemiresistors, Curr. Appl. Phys. 14 (2014) 1649–1658.
[33] Gaurav, A.K. Malik, P.K. Rai, Development of a new SPME-HPLC-UV method for the analysis of nitro explosives on reverse phase amide column and application to analysis of aqueous samples, J. Hazard. Mater. 172 (2009) 1652–1658.
[34] M.A. Atieh, O.Y. Bakather, B. Al-Tawbini, A.A. Bukhari, F.A. Abuilaiwi, M.B. Fettouhi, Effect of carboxylic functional group functionalized on carbon nanotubes surface on the removal of lead from water, Bioinorg. Chem. Appl. 2010 (2010) 1–9.
[35] M.N. Tchoul, W.T. Ford, D. Lolli, E. Resasco, S. Arepalli, Effect of mild nitric acid oxidation on dispersability size, and structure of single-walled carbon nanotubes, Chem. Mater. 19 (2007) 5765–5772.
[36] S. Kopaieemalek, A.M. Yusof, R.N.A. Abdul, M.J. Abbasi, M.T. Kopaiee, Study of stability and dispersibility of oxidized multiwall carbon nanotube and characterization with analytical methods for bioapplication, J. Chem. Health Risks 1 (2011) 17–22.
[37] K.L. Salipira, B.B. Mamba, R.W. Krause, T.J. Malefetse, S.H. Durbach, Cyclodextrin polyurethanes polymerised with carbon nanotubes for the removal of organic pollutants in water, Water SA 34 (2008) 113–118.
[38] G.Y. Wang, X.J. Liu, B. Yu, G.A. Luo, Electrocatalytic response of norepinephrine at a β-cyclodextrin incorporated carbon-nanotube modified electrode, J. Electroanal. Chem. 567 (2004) 227–231.
[39] H.T. Gomes, P.V. Samant, P. Serp, P. Kalck, J.L. Figueiredo, J.L. Faria, Carbon nanotubes and xerogels as supports of well-dispersed Pt catalysts for environmental applications, Appl. Catal. B: Environ. 54 (2004) 175–182.
[40] K. Liu, H. Fu, Y. Xie, L. Zhang, K. Pan, W. Zhou, Assembly of β-cyclodextrins acting as molecular bricks onto multiwall carbon nanotubes, J. Phys. Chem. C 112 (2008) 951–957.
[41] E. Memişoğlu, A. Bochot, M. Şen, D. Duchêne, A.A. Hıncal, Non-surfactant nanospheres of progesterone inclusion complexes with amphiphilic β-cyclodextrins, Int. J. Pharm. 251 (2003) 143–153.
[42] A.M. da Silveira, G. Ponchel, F. Puisieux, D. Duchêne, Combined poly(isobutylcyanoacrylate) and cyclodextrins nanoparticles for enhancing the encapsulation of lipophilic drugs, Pharm. Res. 15 (1998) 1051–1055.
[43] A. Stafiej, K. Pyrzynska, Adsorption of heavy metal ions with carbon nanotubes, Sep. Purif. Technol. 58 (2007) 49–52.
[44] F.A. Abuilaiwi, T. Laoui, M. Al-Harthi, M.A. Atieh, Modification and functionalization of multiwalled carbon nanotube (MWCNT) via Fischer esterification, Arab. J. Sci. Eng. 35 (2010) 37–48.
[45] Y.H. Li, S. Wang, Z. Luan, J. Ding, C. Xu, D. Wu, Adsorption of cadmium(II) from aqueous solution by surface oxidized carbon nanotubes, Carbon 41 (2003) 1057–1062.
[46] T.D.N. Van, S. Sufian, N. Mansor, N. Yahya, Characterization of carbon nanofibers treated with thermal nitrogen as a catalyst support using point-of-zero charge analysis, J. Nanomater. 2014 (2014) 1–6.
[47] N. Li, Z. Mei, S.G. Ding, 2,4-Dichlorophenol sorption on cyclodextrin polymers, J. Incl. Phenom. Macrocycl. Chem. 68 (2010) 123–129.
[48] T. Nakagawa, S. Immel, F.W. Lichtenthaler, H.J. Lindner, Topography of the 1:1 alpha-cyclodextrin-nitromethane inclusion complex, Carbohydr. Res. 324 (2000) 141–146.
[49] X. Shen, D. Shan, X. Dong, Kinetics and thermodynamics of sorption of nitroaromatic compounds to as-grown and oxidized multiwalled carbon nanotubes, J. Colloid Interface Sci. 330 (2009) 1–8.
[50] U.S. Environmental Protection Agency Ambient Water Quality Criteria for Dinitrotoluene, Office of Water Regulations and Standards, Criteria and Standards Division, Washington, DC, 1980 EPA 440/5-80-045.

**Paper IV**

This paper “Application of molecularly imprinted polymers - membrane assisted solvent extraction combination for the extraction of polycyclic aromatic hydrocarbons from domestic wastewater,” is still in preparation. It investigates the extraction of PAHs extraction across a membrane into an acceptor organic phase where further preconcentration is achieved by molecularly imprinted polymers.

# Application of molecularly imprinted polymers - membrane assisted solvent extraction combination for the extraction of polycyclic aromatic hydrocarbons from domestic wastewater

Nikita Tawanda Tavengwa, Somandla Ncube, Ewa Cukrowska, Luke Chimuka*

*Molecular Sciences Institute, School of Chemistry, University of Witwatersrand, Private Bag 3, Johannesburg 2050, South Africa. *Corresponding author. Email: luke.chimuka@wits.ac.za*

ABSTRACT

A novel and selective extraction for polycyclic aromatic hydrocarbons (PAHs) based on combination of membrane assisted solvent extraction (MASE) and molecularly imprinted polymer (MIP) was optimized. MIPs were prepared using benzo[k]fluoranthene as template. The extraction procedure involved diffusion of the analytes from the aqueous donor solution through a hydrophobic polypropylene membrane into the organic acceptor solution dispersed with MIP particles. The movement of PAHs across the membrane was driven by a concentration gradient. In the acceptor solution, the diffused PAHs were selectively bound on MIP particles. Thus, the technique combined extraction and clean-up in a single format. Important parameters such as type of organic solvent in the acceptor phase, type and amount of organic modifier in the aqueous sample, amount of MIP particles, extraction time, stirring rate and SPE elution solvent

type were investigated. The optimum parameters were found to be toluene as acceptor solution with 80 mg of MIP particles dispersed into it. 25% N,N-dimethylformamide in aqueous sample as organic modifier was found optimum. An extraction time of 90 min at a stirring rate of 1000 rpm gave the optimum pre-concentration of the PAHs. Low detection limits were obtained (0.16–90.2 mg $L^{-1}$) and good linearities ($R^2 > 0.992$) were obtained for all the seventeen PAHs.

*Keywords:* Polycyclic aromatic hydrocarbons, molecularly imprinted polymers, membrane assisted solvent extraction, selectivity

## 1. Introduction

Polycyclic aromatic hydrocarbons (PAHs) are a group of xenobiotic chemicals representing a group of contaminants with high melting and boiling points, low vapour pressure, and very low water solubility. In most urban area setups, the main source of indoor PAHs has been attributed to emissions from traffic [1].

Analytes of interest nearly always occur in the presence of other species. In analytical analysis, it is therefore important to do sample preparation and clean-up of the sample prior to analysis in order to remove these interferences [2]. A number of such techniques have been reported in literature for different target analytes such as solid phase extraction with selective or non-selective sorbents [3], solid phase micro-extraction [4] and membrane based extraction [5]. However, as more applications are being done in sample preparation using selective sorbents, in some cases, results have revealed that these selective sorbents may not always offer the desired selectivity, a common problem in the extraction of chemicals from plant materials, sludge and wastewater [3,5]. Plant

material, sludge and wastewater samples are composed of many interferring compounds present as both micro- and macro-molecules and selective sorbents are ineffective in some cases [3,5].

Molecularly imprinted polymers (MIPs) are synthetic polymers with judiciously fabricated sites that can be used as selective sorbents. However, since the backbone polymer is non-specific, inteferring matrix compounds which are usually present in higher amounts compared to the target analytes, are adsorbed on the backbone. The MIP is usually washed with an appropriate solvent after sample extraction to remove some of the inteferring compounds. However, in some cases, it has been shown that it is difficult to wash out all of these interfering compounds without also losing the target compounds [3,5].

The new approach proposed in this study is becoming more common in dealing with complex samples and prevents both the matrix and the target analyte from being extracted simultaneously in the first place [5–10]. This approach makes more sense where matrix components are prevented from adsorbing on the sorbent altogether. Surely it does not make sense to pre-concentrate the matrix components, already in high concentration and then try to make a cleanup afterwards.

Our proposed novel extraction technique has been optimized for the extraction of PAHs in wastewater samples is based on this new approach. Our research group has been one of the pioneers in membrane combination with molecularly imprinted materials [5-7] but here is taken to a new level.

## 2. Materials and methods

### 2.1. Chemicals and materials

A 2000 mg $L^{-1}$ PAHs mixture was obtained from Supelco (Bellefonte, PA, USA): Acenaphthene (99.9%), Acenaphthylene (99.9%), Anthracene (99.9%), 2-bromonaphthalene (99.9%). Benzo(a)anthracene (99.9%), Benzo(a)pyrene (99.9%), Benzo(b)fluoranthene (99.9%), Benzo(g,h,i)perylene (99.9%), Benzo(k)fluoranthene (99.9%), chrysene (99.9%), Dibenzo(a,h)anthracene (99.9%), Fluoranthrene (99.9%), Fluorene (99.9%), Indeno(1,2,3-cd)pyrene (99.9%), Phenanthrene (99.9%), Pyrene (99.9%), Naphthalene (99.9%). Acetonitrile, N,N-dimethylformamide, methanol, dichloromethane, heptane, hexane, toluene and cyclohexane were purchased from Sigma-Aldrich (Darmstadt, Germany). Empty 3 mL cartridges with 10 μm frits were from Sorbent AB (Frölunda, Sweden). Membrane bags and their accessories were supplied by Gerstel (Mülheim, Germany). Stirring of the solutions was done on a WiseStir MS MP8 stirrer.

### 2.2. Stock solution and standard solutions

A working stock solution of 20 mg $L^{-1}$ of 17 PAH mixture was prepared in methanol from a 2000 μg $mL^{-1}$ stock solution in methylene chloride. From this, an external calibration was made with standard solutions of 0.5–4 mg $L^{-1}$.

### 2.3. Synthesis of molecularly imprinted polymers

50 mg (0.198 mmol) benzo[k]fluoranthene was added to 15 mL of N,N–dimethylformamide (DMF) in a 50 mL round bottomed flask and heated to 40ºC. 35 μL (0.411 mmol) of methacrylic acid, 3.15 mL (16.7 mmol) of ethylene glycol methacrylate were then added to the flask and purged with nitrogen gas for 5 min. After purging, 50 mg of 4,4'–azobis (4–cyanovaleric acid) was added to the solution and was heated at 80ºC for 35 min. Once polymerization finished, the product was removed and dried overnight at 25ºC. The resultant bulk polymer was then ground and sieved through a 150 mm mesh and collected on a 100 mm mesh. The template was then removed from the polymer using a Wisecube shaker in hexane and the eluent was analyzed for benzo[k]fluoranthene. The elution was repeated and only stopped when the template detection was zero. NIPs were prepared using the same procedure used for MIPs, except that the template molecule, benzo[k]fluoranthene, was excluded.

### 2.4. MASE-MIP extraction procedure

The membrane assisted solvent extraction–molecularly imprinted polymer (MASE–MIP) system was set up as follows: The membrane extraction cell consisted of a 20 mL headspace vial filled with 15 mL of spiked donor phase solution. The membrane bag was attached to a metal funnel and fixed with a PTFE ring. A dense polypropylene membrane bag with MIP particles and 1 mL organic solvent was placed inside the extraction cell containing the donor solution and stirred for preset times. After extraction, the acceptor content (MIP and the acceptor solvent) was transferred into a 3 mL empty solid phase extraction (SPE)

cartridge with a 10 µm frit at the bottom and mounted onto solid phase extraction unit. The acceptor solvent was separated from MIP particles by opening the SPE valve slowly and allowing it to flow out by gravity at about 1 mL $min^{-1}$. A full vacuum was then applied for 5 min to dry off the MIP particles completely. The trapped PAHs were then eluted with 3 × 1000 µL fractions of methanol before analyzed directly by HPLC–UV.

### 2.5. HPLC analysis of PAHs

The HPLC system was used for the separation and quantification of PAHs. An injection volume of 20 µL and a VUV variable wavelength UV–VIS detector set to 254 nm for detection of PAHs. Clarity software was used for acquiring of the data. A supelcosil$^{TM}$ LC–PAH column (25 cm × 46 mm, 5 µm) from Supelco (Darmstadt, Germany) was used. The mobile phase was composed of acetonitrile and water pumped with a flow rate of 1 mL $min^{-1}$ at different composition with the aid of a Dionex P580 pump. The gradient elution program started at 50/50, V/V acetonitrile/water held for 1.5 min then ramped up to 70% acetonitrile for 0.5 min. this was further increased to 90% acetonitrile in 10 min and held at this composition for 8 min. the composition was then adjusted to 50/50, V/V acetonitrile/water held for 1.5 min.

### 2.6. Sample collection and preparation

The influent and effluent wastewater samples were collected from Goudkoppies treatment plant (GPS). This plant is the biggest in South Africa and it receives untreated domestic and industrial sewage from the city of

Johannesburg. The treated effluent is discharged into the river where some nutrients cause eutrophication. The collected samples were fully homogenized, stored in amber glass bottles, and cooled at 4ºC until the laboratory analysis was performed.

Immediately prior to extraction, some wastewater samples were spiked with the mixture of standard solution of 17 PAHs at a concentration of 100 μg $L^{-1}$. The samples were extracted and subjected to a MIP–MASE extraction and cleanup process described above. Spiked and non-spiked samples were systematically compared.

### 2.7. Extraction efficiency and enrichment factors

Quantification of the PAHs was in other instances expressed from peak areas to either extraction efficiency or enrichment factors. The enrichment factor (*EF*) is defined as the ratio between the concentrations in the acceptor phase after extraction to the initial concentration of the analyte in the donor phase. *EF* is related to the extraction efficiency (*E*) defined as the ratio of analyte extracted to the total analyte.

$$E = \frac{n_A}{n_D} = \frac{C_A V_A}{C_D V_D} = EF \frac{V_A}{V_D} \quad (1)$$

where $C_A$, $V_A$ and $n_A$ are the analyte concentration, volume and analyte amount in the acceptor solution after extraction. $C_D$, $V_D$ and $n_D$ denote the analyte concentration, volume and amount of analyte in the donor solution before extraction.

### 2.8. Method validation

The concentrations of the calibration standard solutions were 0.5 mg $L^{-1}$, 1.0 mg $L^{-1}$, 2 mg $L^{-1}$, 3 mg $L^{-1}$ and 4 mg $L^{-1}$. An example of a 4 mg $L^{-1}$ chromatogram used for the plotting of the calibration curve is shown in Fig. 1. The peaks were identified by the retention times. All seventeen PAHs exhibited good linearity (Table 1) with correlation coefficients ($R^2$) > 0.992. For recovery calculation, a 1.0 mg $L^{-1}$ standard solution was also passed through the SPE. The limits of detection (LODs) and limits of quantification (LOQs) were calculated using the background noise level estimated from the peak-to-peak baseline near the analyte peaks.

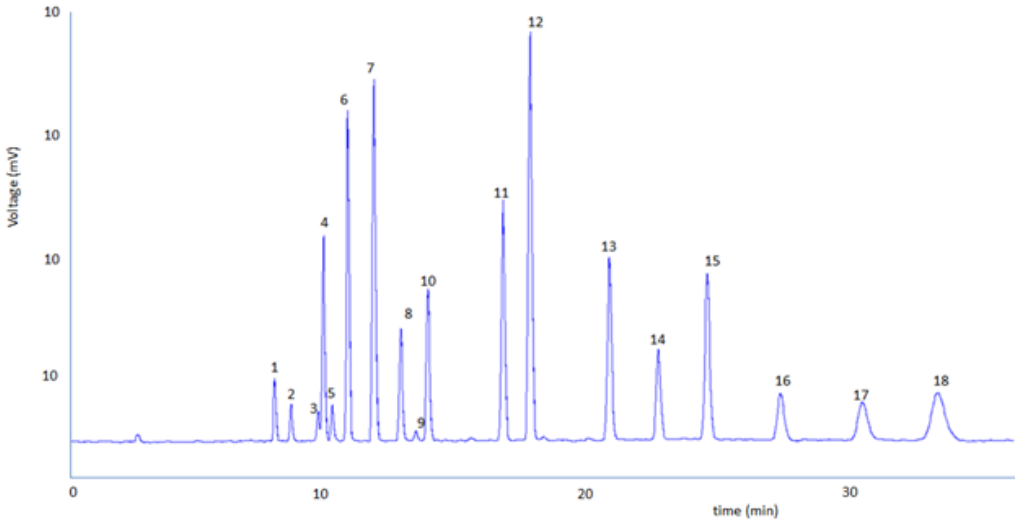



**Fig. 1.** Chromatogram of a 4 mg $L^{-1}$ standard PAH solution. 1. Nap, 2. Acy, 3. 2-Bnap, 4. Ace, 5. Fln, 6. Phe, 7. Ant, 8. Flu, 9. Pyr, 10. B[a]A, 11. Chr, 12. B[b]F, 13. B[k]F, 14. B[a]P, 15. D[ah]A, 16. B[ghi]P, 17. I[123-cd]P.

**Table 1**

Validation parameters for HPLC determination of eighteen PAH compounds

| PAH | $t_R$ (min) | Equation | $R^2$ | LOD (mg $L^{-1}$) | LOQ (mg $L^{-1}$) |
|---|---|---|---|---|---|
| Nap | 7.9 | y = 44.657x + 4.3698 | $R^2$ = 0.9988 | 3.14 | 7.08 |
| Acy | 8.6 | y = 28.912x + 0.4312 | $R^2$ = 0.9969 | 90.2 | 415.1 |
| 2-Bnap | 9.6 | y = 20.701x + 6.2514 | $R^2$ = 0.9957 | - | - |
| Ace | 9.8 | y = 154.28x + 15373 | $R^2$ = 0.9921 | 2.14 | 4.07 |
| Fln | 10.1 | y = 30.008 + 3.0523 | $R^2$ = 0.9964 | 4.65 | 15.9 |
| Phe | 10.7 | 263.05x + 17.215 | $R^2$ = 0.9996 | 1.10 | 3.41 |
| Ant | 11.7 | y = 320.78x + 94.318 | $R^2$ = 0.995 | 0.23 | 2.29 |
| Flu | 12.7 | y = 99.751x + 8.3336 | $R^2$ = 0.9976 | 2.26 | 8.44 |

| | | | | | |
|---|---|---|---|---|---|
| Pyr | 13.7 | y = 137.85x + 15.446 | $R^2$ = 0.9997 | 1.81 | 6.30 |
| B[a]A | 16.5 | y = 230.82x + 11.478 | $R^2$ = 0.9981 | 0.62 | 3.75 |
| Chr | 17.4 | y = 426.27x + 25.398 | $R^2$ = 0.9993 | 0.84 | 2.03 |
| B[b]F | 20.3 | y = 200.64x + 33.186 | $R^2$ = 0.9986 | 0.43 | 3.54 |
| B[k]F | 22.9 | y = 104.49x + 41.518 | $R^2$ = 0.9992 | 0.58 | 3.40 |
| B[a]P | 23.9 | y = 217.93x + 35.567 | $R^2$ = 0.9977 | 1.57 | 5.80 |
| D[ah]A | 26.2 | y = 89.917x + 0.4459 | $R^2$ = 1.0000 | 0.84 | 3.43 |
| B[ghi]P | 29.0 | y = 110.31x + 16.048 | $R^2$ = 0.9994 | 0.16 | 3.23 |
| I[123-cd]P | 30.9 | y = 178.53x + 77.446 | $R^2$ = 0.9958 | - | - |

Note: LOD Limits of detection, LOQ Limits of quantification

## 3. Results and discussion

### 3.1. Elution of benzo[k]fluoranthene

Benzo[k]fluoranthene elution from the polymers was monitored as outlined in the method section. An exponential decay curve was obtained (Fig. 1). It can be seen that there was a tremendous decrease of benzo[k]fluoranthene after 19 h, were the template content was almost zero. Template elution is critical in imprinted polymer preparation as incomplete removal will always lead to bleeding of the template during the use of the prepared material. Similar trends as that seen in Fig. 2 were observed by other researchers using various templates [11,12].

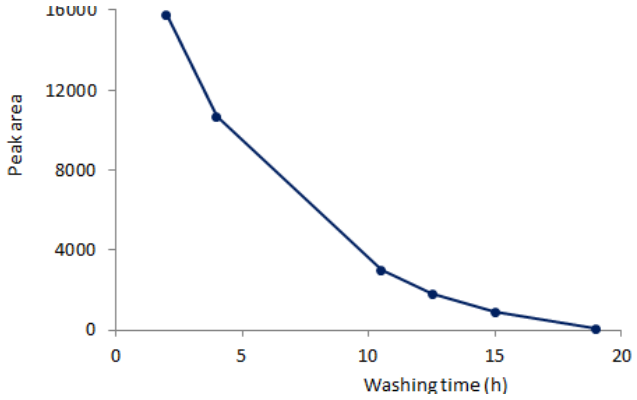



**Fig. 2.** Elution of benzo[k]fluoranthene from the imprinted polymer over time.

### 3.2. Characterization of the molecularly imprinted polymers

BET surface area is normally solved graphically by plotting $1/[Q(p/p_o) - 1]$ versus $p/p_o$. The BET specific surface areas of the polymeric adsorbents were calculated from the isothermal adsorption of nitrogen within the partial pressure range of 5% to 35% ($p/p_o$). The monomolecular volume ($v_m$) and the BET constant ($c$) were calculated from the BET equations and the results are

summarized in Table 2. The BET surface area characterization study was carried out to know the effect of imprinting on the polymer surface area, pore volume and pore width. The leached MIP exhibited more surface area (386.6 $m^2$ $g^{-1}$) when compared to NIP (360.6 $m^2$ $g^{-1}$) and the unleached MIP (332.5.6 $m^2$ $g^{-1}$) (Table 1). BET surface area result indicated an enhancement in surface area for MIP due to imprinting.

**Table 2** The BET surface area for the synthesized polymers.

| Polymer | Surface area ($m^2$ $g^{-1}$) | Pore volume ($cm^3$ $g^{-1}$) | $v_m$ | $c$ |
|---|---|---|---|---|
| MIP unleached | 332.5 | 0.74 | 75.6 | 661 |
| MIP leached | 386.6 | 0.61 | 86.0 | 388 |
| NIP leached | 360.6 | 0.55 | 81.2 | 616 |

MIPs and NIPs were prepared via bulk polymerization using a non-covalent approach. Scanning electron microscopy (SEM) was used to determine the surface morphology and the size of the synthesized particles. The micrography of the control polymer (NIP) in Fig. 3 shows a smooth surface with large particles compared to the molecular imprinted polymer which had a rough surface. The roughness was due to the fact that the MIP was washed in order to remove the template and NIP had no template to be removed [13]. The shapes of the particles obtained after preparation of polymers by bulk polymerization (after grinding) are all irregular [14]. Sikiti et al. [15] observed that MIP had a rough surface

compared to NIP and this was due to the presence of cavities during the synthesis process. The average size of the MIP particles was found to be 110 mm (The particles were sieved between 100–150 mm mesh).

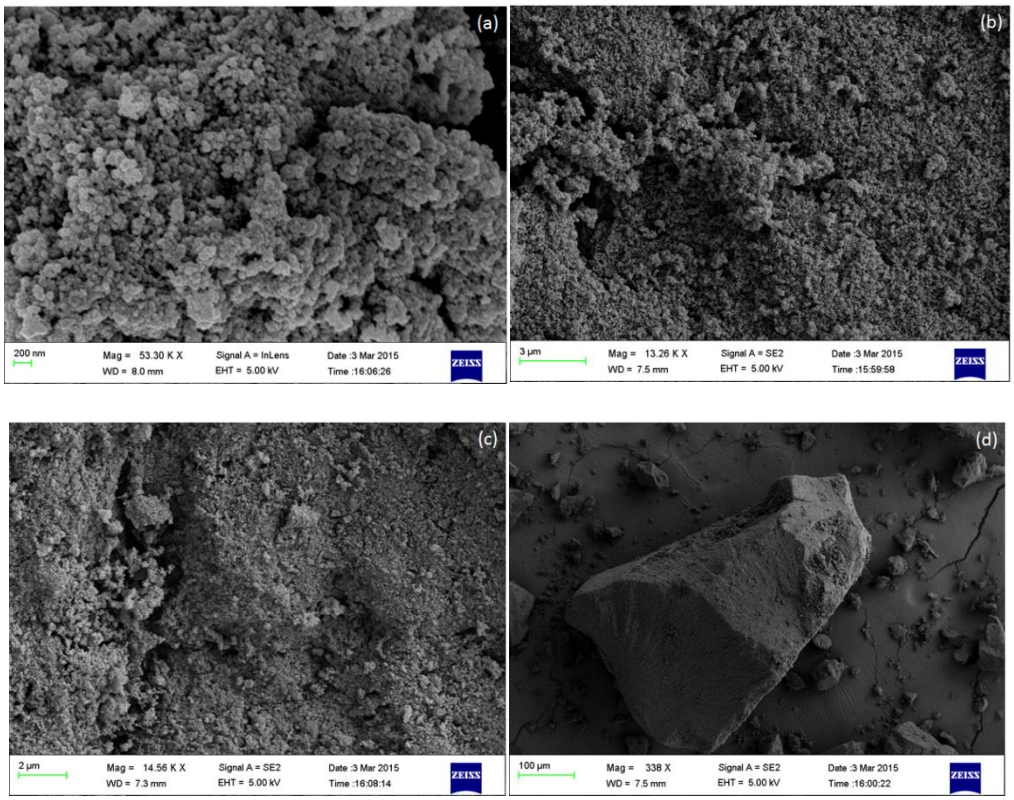



**Fig. 3.** SEM micrographs of (a) eluted MIP (b) uneluted MIP (c) eluted NIP and (d) uneluted NIP.

For the FTIR analysis, it was shown that the bands at 1724 $cm^{-1}$ featured prominently for the unleached MIP as well as the washed NIP. However, for the leached MIP, this band shifted to 1730 $cm^{-1}$. This band was probably due the carboxylate group ($-COO^-$). Another band which occurred in all tree spectra is that at 1665 $cm^{-1}$ which is as a result of the double bonds. As a result of the leaching action, this band was diminished greatly in the washed polymer as compared to the unleached MIP. The CH- stretching frequency band is shown at

2935 $cm^{-1}$ while the –OH is shown around 3430 $cm^{-1}$. The spectrum of the leached NIP was cleaner both in the fingerprint and the functional group regions as compared to the unleached NIP. This was attributed to the elution of the imprint from the polymer.

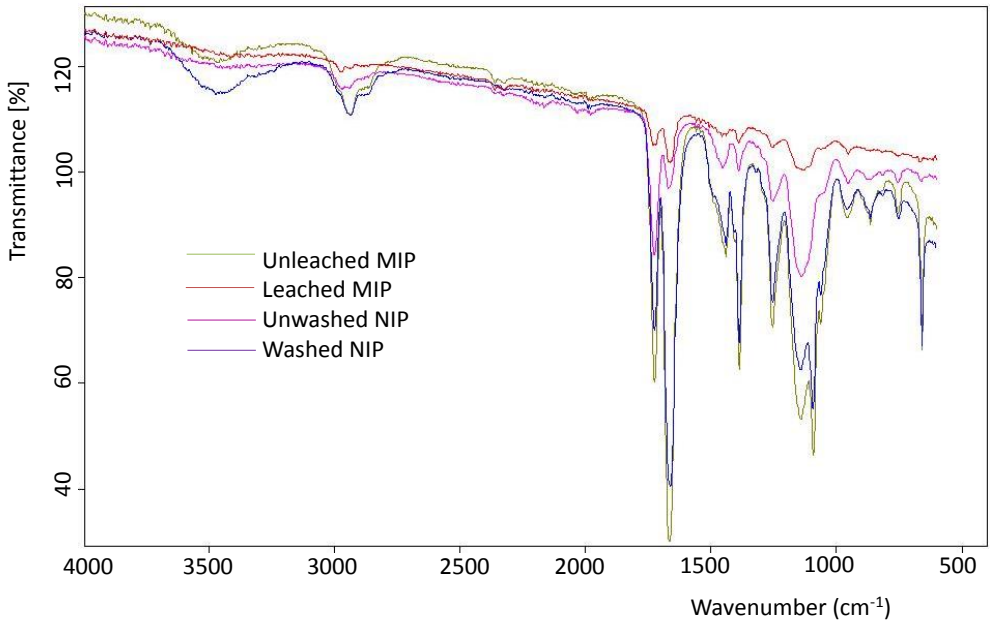



**Fig.3.** FTIR spectra of the four polymer material.

The swelling behaviour of the imprinted polymers was investigated in six solvents. This was achieved by immersion of 1.2 g of the in 12 mL of distilled water at 25ºC for 12 h. The sorbent weight increase allowed the calculation of the swelling percentage using Eq. (2) where $W_s$ and $W_d$ are the weights of the swollen and dry sorbent samples (in g), respectively. The results are presented in Fig. 4.

$$\text{Swelling ratio (\%)} = \frac{(W_s - W_d)}{W_d} \text{ x } 100 \qquad (2)$$

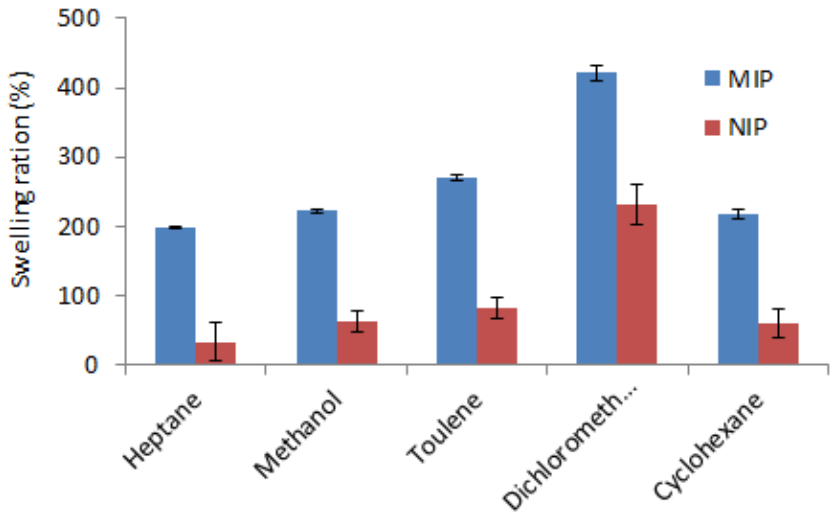



**Fig. 4.** Swelling behaviour of the imprinted polymer in different solvents.

### 3.3. Selection of extraction solvent

The solubility of the analytes in organic solvent is a major variable since the relation of solubilities of the analytes between the acceptor and the donor phases determines the efficiency of the extraction at the equilibrium [16]. Selection of the proper acceptor phase is an important exercise, so six solvents were investigated in this work; *n*-hexane, methanol, heptane, cyclohexane, dichloromethane and toluene. This was carried out as follows: 0.5 mg $L^{-1}$ of a mixture of 18 PAHs was made by diluting the 20 mg $L^{-1}$ using 15% methanol in water as a diluent to top up to the mark. This solution (15 mL) was used as a donor phase. A wide range of solvents were used as acceptor phases (1 mL) in plastic bags loaded with 50 mg of the MIP sorbent. Pre-concentration of the PAHs was done at a preset time of 60 min using the WiseStir MS MP8 at 420 rpm. PAHs are non-polar with mostly hydrophobic interactions through pi bonds being involved. This may explain why best performing solvents, with pi bonds and linear in geometry, gave slightly better extractions (Fig. 5). A water miscible solvent, such as methanol, was not

suitable, because it diffused through the membrane into the aqueous phase. Further, polar solvents were avoided since the target analytes PAHs are non-polar. Toulene was the best acceptor phase for the pre-concentration of PAHs. Large PAHs were not detected in this analysis as they have a dissolution problem in aqueous phase. This was despite addition of an organic modifier (15% methanol). March et al. [16] had an observation that for higher viscosities, the transference of the organic solvent to the acceptor phase can be avoided, but the diffusion of the analytes is slower, and consequently so is the kinetics of the extraction. They found higher extraction efficiencies for decane than for 1-octanol. However, all their extraction efficiencies were very low (5.8-16.1%). For similar target analytes Rodil et al. [17] found toluene and *n*-hexane to perform poorly in terms of the enrichment factors for the target analytes, particularly for the compounds with high log $K_{ow}$ values. Hollender et al. [18] obtained a combination of 1:1 toulene: acetone as the best for the extraction of PAHs from soil samples.

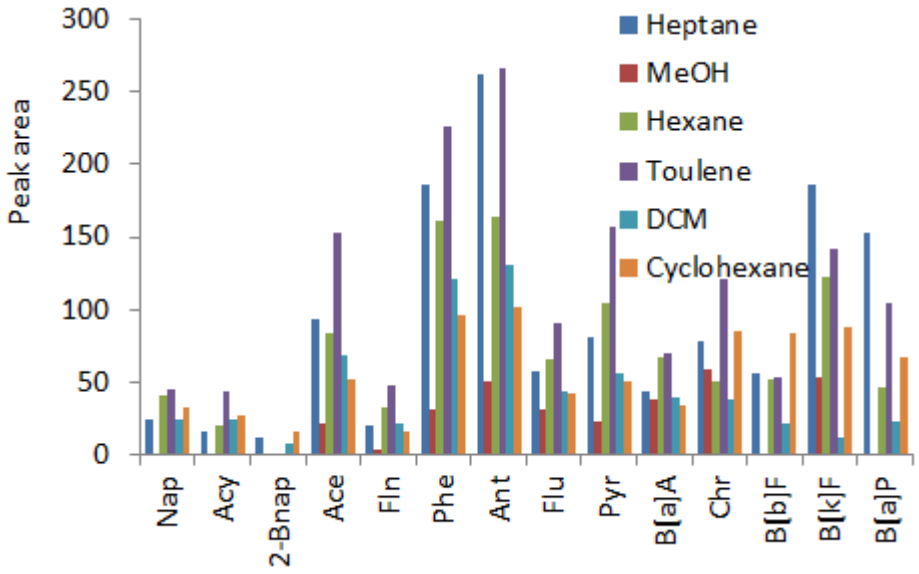



**Fig. 5.** Effect of different acceptor solvents in the uptake of PAHs (Experimental conditions: concentration of PAHs = 0.5 mg $L^{-1}$, donor phase = 15 mL of 15% methanol, acceptor phases = 1 mL with 50 mg of the MIP sorbent, pre-concentration time = 60 min and stirring rate = 420 rpm).

### 3.4. Addition of the organic modifier

The addition of miscible organic solvents to aqueous samples has been reported to minimize adsorption of organic analytes on the walls of glass flasks [19]. Fig. 6 shows the results obtained when various organic modifiers were used. It is evident that DMF gave the maximum PAHs extraction. March et al. [14] investigated the presence of ethanol increased the extraction efficiency and found 5% to give the optimum uptake. They related the amount of ethanol for maximum extraction seems to be related to the analyte polarity. Addition of an organic modifier is very important especially for heavier PAHs that have poor solubility in water. With an organic modifier, they are forced to be in solution and thus get extracted into the membrane bag.

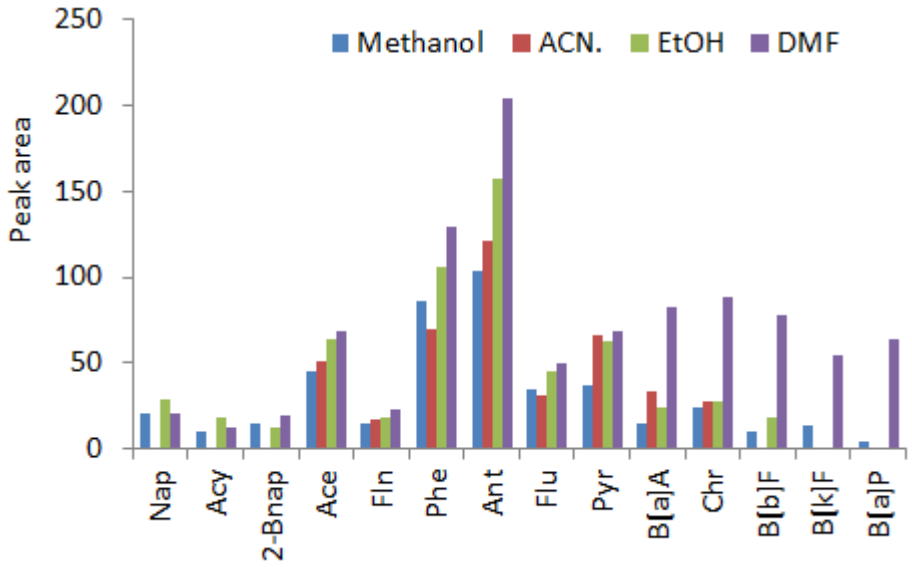



**Fig. 6.** Effect of change of the organic modifier in the donor phase aqueous solution (Experimental conditions: concentration of PAHs = 0.5 mg $L^{-1}$, donor phase = 15 mL of 15% organic modifier, acceptor phases = 1 mL toluene with 50 mg of the MIP sorbent, pre-concentration time = 60 min and stirring rate = 420 rpm).

### 3.5. Organic modifier content

In this study, the influence on the extraction efficiency was studied in the range of 5–50% (v/v) of DMF (Fig. 7(a) and (b)). The extraction behavior of the eighteen PAHs followed two trends. Effect of the amount of the organic modifier had a maximum uptake with 15% DMF for light and medium weight PAHs. However, the heavier PAHs were extracted more with a 25% DMF organic modifier. This was because of their increased dissolution at high organic modifier content. As the amount of DMF was increased in the donor solution, so was the dissolution of the PAHs. This was illustrated in Fig. 7(b) where 5% DMF solution was opaque but became clearer at 50% content. PAHs have remained one of the most difficult

compounds to analyze. According to Li et al. [20], one well-known reason is that they tend to adsorb on the walls of containers. At low DMF content, there was no imprinting phenomenon as the target template; benzo[k]fluoranthene was unavailable in solution due to its low dissolution. Thus a 25% DMF was taken as the optimum.

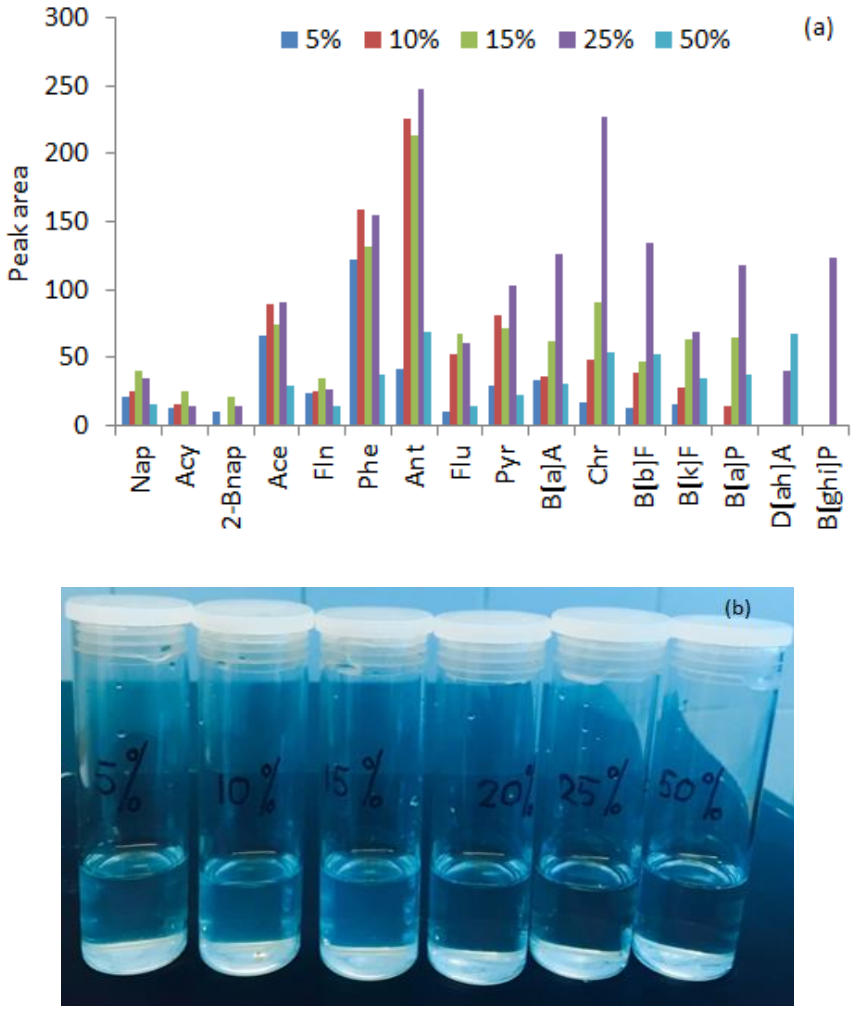



**Fig. 7.** (a) Effect of variation of the DMF organic phase content in the extraction of PAHs (Experimental conditions: concentration of PAHs = 0.5 mg $L^{-1}$, donor phase = 15 mL of DMF, acceptor phases = 1 mL toluene with 50 mg of the MIP sorbent, pre-concentration time = 60 min and stirring rate = 420 rpm) (b) Clarity of the multi–PAH mixture as the percentage of DMF is varied).

### 3.6. Effect of the weight of MIP

From Fig. 8, it was observed that an increase in the amount of the MIP sorbent increased the extraction efficiency of the PAHs. This was the case for all eighteen analytes investigated. The sorbent mass was only investigated up to 80 mg as the capacity of the MASE membrane bag would have been exceeded especially when factoring the swell capacity which was observed to be 200% for toluene which was used as the receiver phase. 80 mg was taken as the optimum.

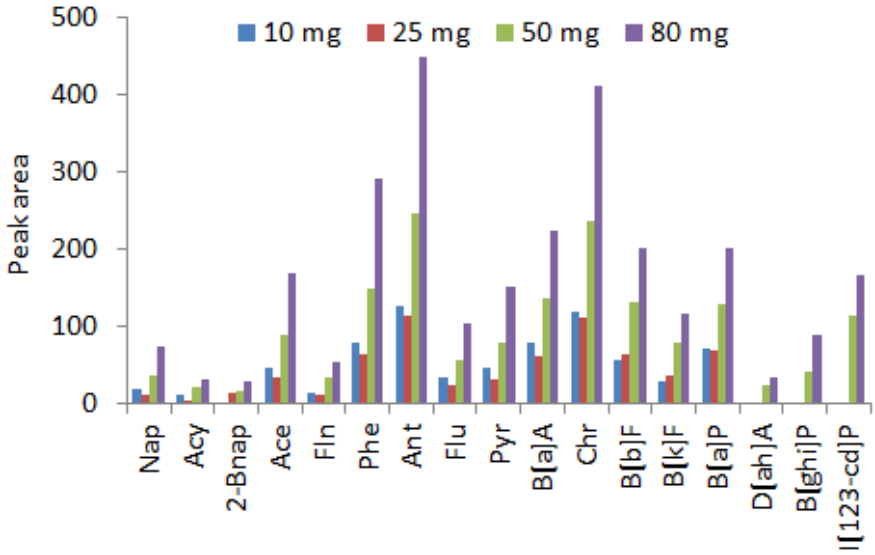



**Fig. 8.** Effect of the amount of MIP in the acceptor phase (Experimental conditions: concentration of PAHs = 0.5 mg $L^{-1}$, donor phase = 15 mL of 25% DMF, acceptor phases = 1 mL toluene with a MIP sorbent, pre-concentration time = 60 min and stirring rate = 420 rpm).

### 3.7. Effect on the extraction time

The effect of sorption time is illustrated in Fig. 9. For the time investigated, there was an almost linear dependency of the extraction of PAHs with time. This

can be explained by the fact that longer exposure time of the receiver system (MASE–MIP) to the donor sequestrated the PAHs. Inversely, shorter exposure time yielded low recoveries. Thus 90 min seemed optimum as longer extraction time than this was seen as not practical unless under many simultaneous extractions.

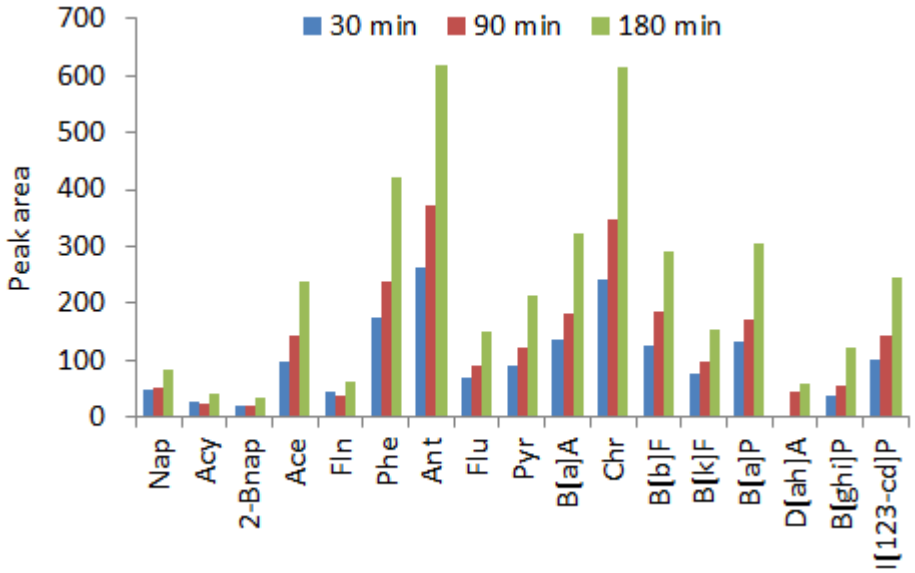



**Fig. 9.** Effect of the sorption time of PAHs (Experimental conditions: concentration of PAHs = 0.5 mg $L^{-1}$, donor phase = 15 mL of 25% DMF, acceptor phases = 1 mL toluene with 80 mg of the MIP sorbent, stirring rate = 420 rpm).

### 3.8. Effect of the stirring rate

Fig. 10 shows the results obtained when the stirring rate was varied while keeping other parameters constant. There was a great variation in recovery as the stirring speed was increased from 420 to 1000 rpm. Stirring aids the movement of the PAH analytes from the donor to the MIPs in the toluene receiver phase across the membrane. The increase was more pronounced with medium non–polar to

more non–polar PAHs. This was expected since these have high dissolution into the membrane bag and transport is limited by diffusion to the membrane surface. Thus a stirring speed of 1000 rpm was taken as optimum.

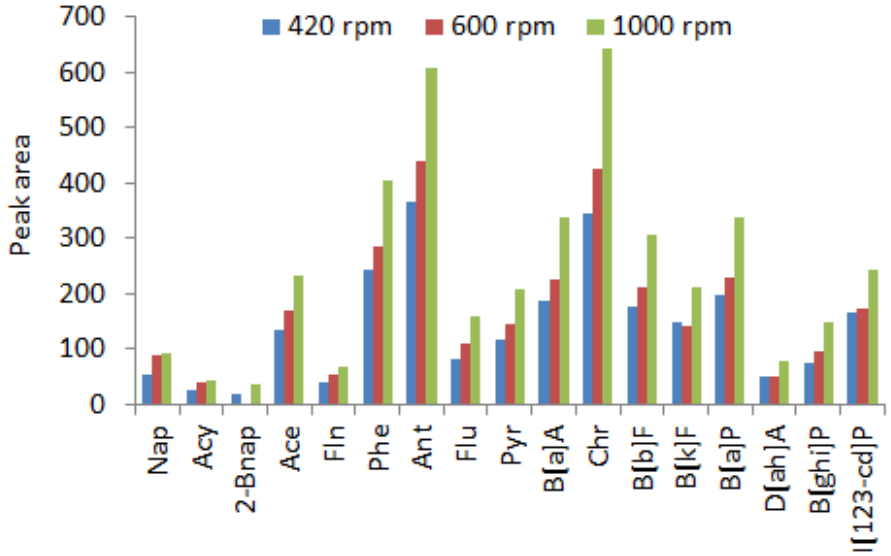



**Fig. 10.** Effect of stirring rate on the uptake of PAHs (Experimental conditions: concentration of PAHs = 0.5 mg $L^{-1}$, donor phase = 15 mL of 25% DMF, acceptor phases = 1 mL toluene with 80 mg of the MIP sorbent and pre-concentration time = 60 min).

### 3.9. Influence of SPE elution solvent

The type of SPE elution solvent is very important to make sure that minimal solvent is used to avoid dilution, but at the same time able to elute the target analytes in one goal. Elution with methanol was found to be much superior compared to other solvents (Fig. 11). Toluene, which was found to be superior during binding onto MIP particles, was less effective during the elution step. This also shows the imprinting effect on the prepared polymers. More polar solvents

are recommended during elution as they help to break the analyte–monomer interactions. The order of preference of SPE solvent extraction was: methanol > heptane > chloroform ≈ toulene. In a similar study, Oluseyi et al. [21] also found methanol to be the best SPE extraction solvent. The same authors explained the low recoveries of low molecular weight PAHs as due to their loss as they are more volatile. In this work a stream of $N_2$ gas was blown to the PAHs solution to near dryness for solvent exchange. It was a good thing that methanol was found to be the optimum as there was no need for reconstitution of the solvent as the solvent is compatible with the instrument, HPLC.

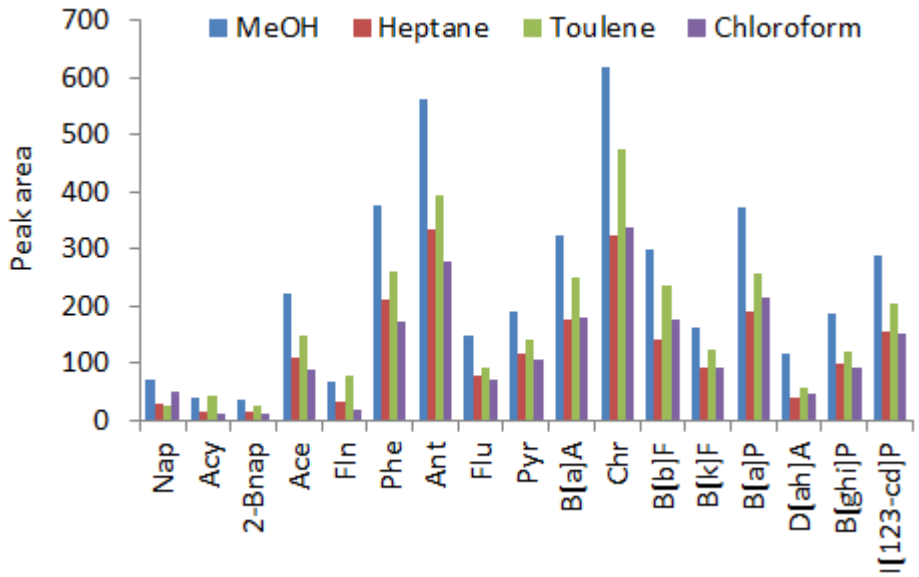



**Fig. 11.** Influence of elution solvent (Experimental conditions: concentration of PAHs = 0.5 mg $L^{-1}$, donor phase = 15 mL water with 25% DMF, acceptor phases = 1 mL toluene with 80 mg of the MIP sorbent, extraction time = 90 min and stirring rate = 1000 rpm).

### 3.10. Reproducibility of the MASE–MIPs combination

The extraction of eighteen PAHs spiked at 50 µg $L^{-1}$ level was done in triplicate. Figure 12 shows the reproducibility of the method. The results generally indicated good reproducibility except two compounds. In most cases it is one such experiment that can result either higher or lower than other two experiments. This indicated random error and is common with any analytical technique. Thus the MASE–MIP combination has demonstrated good consistency in giving the amount extracted each time despite double extraction occurring in a single step.

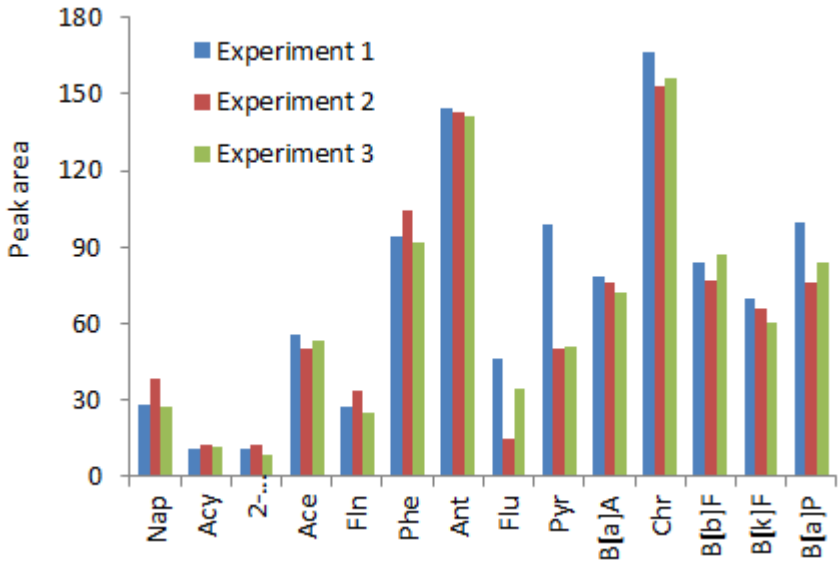



**Fig. 12.** Reproducibility of the MASE-MIP combination after extraction of water sample spiked with 50 mg $L^{-1}$ of PAHs mixture at optimized conditions.

### 4. Conclusions

The MASE-MIP combination for selective extraction of PAHs in aqueous samples solution was succesfully been optimized. Heavy molecular weight PAHs were most of the times not recovered due to their poor solubilities in aqueous

samples. As such, 25% (v/v) N,N-dimethylformamide in aqueous was found optimum as it improved the solubilities of heavy molecular weight PAHs. The extraction efficiency of PAHs was optimum with 80 mg of MIP particles dispersed in 1 mL toluene solution. Maximum recovery was found after 90 min of extraction time at a stirring rate of 1000 rpm. The method can be applied for the determination of trace analysis of PAHs as low detection limits were obtained (0.16–90.2 mg $L^{-1}$).

**Acknowledgements**

The authors would like to thank the Water Research Commission of South Africa (WRC project number K5–7025) of South Africa for funding the project.

**References**

[1] S.D. Dubowsky, L.A. Wallace, T.J. Buckley, J. Expo. Anal. Environ. Epidemiol. 9 (1999) 312–321.

[2] L. Chimuka, M. van Pinxteren, J. Billing, E. Yilmaz, J.Å. Jönsson, J. Chromatogr. A 1218 (2011) 647–653.

[3] C. Cacho, E. Turiel, A. Martin-Esteban, C. Perez-Conde, C. Camara, Anal. Bioanal. Chem. 376 (2003) 491–496.

[4] G. Ouyang, J. Pawliszyn, Anal. Chem. 78 (2006) 5783–5788.

[5] A. Poliwoda, A.M. Chrzanowska, K. Orłowska, P.P. Wieczorek, CHEMIK 68 (2014) 312–320.

[6] B. Mhaka, E. Cukrowska, B. T. Sum Bui, O. Ramström, K. Haupt, H. Tutu, L. Chimuka, J. Chromatogr. A 1216 (2009) 6796–6801.

[7] O. Nemulenzi, B. Mhaka, E. Cukrowska, O. Ramström, H. Tutu, L. Chimuka, J. Sep. Sci. 32 (2009) 1941–1948.

[8] Y. Hu, Y. Wang, Y.Hu, G. Li, J. Chromatogr. A 1216 (2009) 8304–8311.

[9] H.H. See, M.M. Sanagi, W.A.W. Ibrahim, A.A. Naim, J. Chromatogr. A 1217 (2010) 1767–1772.

[10] F. Barahona, E. Turiel, A. Martin-Esteban, Anal. Chim. Acta 694 (2011) 83–89.

[11] N.T. Tavengwa, L. Chimuka, E. Cukrowska, Talanta 116 (2003) 670–667.

[12] N.T. Tavengwa, L. Chimuka, E. Cukrowska, J. Hazardous Mater. 267 (2014) 221–228.

[13] M. Kawaguchi, R. Ito, K. Saito, H. Nakazawa, J. Pharm. Biomed. Anal. 40 (2006) 500–508.

[14] M. Kayali-Sayadi, S. Rubio-Barroso, C. Diaz-Diaz, L. Polo-Diez, J. Anal. Chem. 368 (2000) 697–701.

[15] P. Sikiti, A.M. Msagati, B. Mamba, A.J. Mishra, J. Environ. Health Sci. Eng. 12(82) (2014) 1–8.

[16] J.G. March, F. Moukhchan, V. Cerdà, Anal. Chim. Acta 685 (2011) 132–137.

[17] R. Rodil, M. Schellin, P. Popp, J. Chromatogr. A 1163 (2007) 288–297.

[18] J. Hollender, B. Koch, C. Lutermann, W. Dott, Intern. J. Environ. Anal. Chem. 83 (2003) 21–32.

[19] D. Benanou, F. Acobas, M.R. de Roubin, F. David, P. Sandra, Anal. Bioanal. Chem. 376 (2003) 69–77.

[20] N. Li, H.K. Lee, J. Chromatogr. A 921 (2001) 255–263.

[21] T. Oluseyi, K. Olayinka, B. Alo, R.M. Smith, African J. Environ. Sci. Technol. 5 (2011) 482–493.

**Paper V**

This paper "Miniaturized pipette tip–based electrospun polycrylonitrile nanofibers for micro–solid–phase extraction of nitro based explosive compounds," investigates the extraction of four nitroaromatic compounds from acqueous solutions using a small amount of electrospun polycrylonitrile nanofiber loaded in the pipette tips. The manuscript has been submitted to *Journal of Separation Science*.

# Miniaturized pipette tip–based electrospun polyacrylonitrile nanofibers for micro–solid–phase extraction of nitro based explosive compounds

**Nikita Tawanda Tavengwa[1], Pardon Nyamukamba[2], Ewa Cukrowska[1], Luke Chimuka[1]**

[1]Molecular Sciences Institute, School of Chemistry, University of Witwatersrand, Private Bag 3, Johannesburg 2050, South Africa

[2]Department of Pure and Applied Chemistry, University of Fort Hare, Alice Campus, Private Bag X1314, Alice 5700, South Africa

Corresponding author: Prof Luke Chimuka, Molecular Sciences Institute, School of Chemistry, University of Witwatersrand, Private Bag 3, Johannesburg 2050, South Africa

**E-mail:** luke.chimuka@wits.ac.za, **Fax number:** +27 117176749

**Keywords:** Electrospinning / Explosive compounds / Miniaturized / Polyacrylonitrile / Solid Phase Extraction

**Abbreviations: ACN,** acetonitrile; **DMF,** N,N–dimethylformamide; **2,6–DNT,** 2,6–dinitrotoluene; **DLLME,** dispersive liquid–liquid micro–extraction; **MeOH,** methanol; **MIP–DLLME,** molecular–imprinted polymer extraction with dispersive liquid–liquid micro–extraction; **2–NT,** 2–nitrotoluene; **3–NT,** 3–nitrotoluene; **4–NT,** 4–nitrotoluene; **PAN,** polyacrylonitrile; **PT–SPE,** pipette tip–solid phase extraction; **SDME,** single drop micro–extraction; **SPME,** solid–phase micro–extraction; **SE,** solvent extraction; **THF,** tetrahydrofuran; **TNT,** 2,4,6–trinitrotoluene

**Abstract** In this study, a self–assembly of miniaturized pipette tip–based solid phase extraction for the simultaneous extraction of nitroaromatic compounds was developed, with electrospun polyacrylonitrile nanofibers used as sorbents. The electrospun polyacrylonitrile nanofibers were characterized by scanning electron microscopy, Fourier transform infrared analysis and surface area analysis. Good linearities for the four nitroaromatic compounds (2,6–dinitrotoluene, 2–nitrotoluene, 3–nitrotoluene, and 4–nitrotoluene) were obtained in a range of 250–1000 μg $L^{-1}$ with coefficients of determination $R^2 > 0.99$. The limits of detection of these analytes were between 21 μg $L^{-1}$ and 38 μg $L^{-1}$. The results showed that pipette tip–based solid phase extraction was effective in extracting nitrotoluenes in the pH regime of environmental interest (≈ 6). The investigation also revealed that the optimum mass of electrospun polyacrylonitrile nanofibers sorbent was 15 mg and 20 aspirating/dispensing cycles gave the maximum recovery of nitrotoluenes with 200 μL acetonitrile as the best eluting solvent. Moreover, the performance of the present method was studied for the extraction and determination of nitroaromatic compounds in real environmental water samples and good recoveries ranging from 70% to 115% were found. The respective relative standard deviations of < 12% were obtained.

## 1 Introduction

Nitrocompounds, especially nitroaromatic compounds encountered in drugs, dyes and explosives, represent a group of hazardous contaminants which can be discharged into the environment during production, processing, destruction and recycling [1] thereby polluting water bodies. Decontamination of polluted water is considered as one of the most challenging problems facing the world. Owing to the severe toxicity and doubtful carcinogenicity of 2,4,6–trinitrotoluene (TNT), 2,4–dinitrotoluene (2,4–DNT) and 2,4–dinitrotoluene (2,6–DNT), nitroaromatic compounds should be removed from wastewater to acceptable levels before their disposal into the environment which has proven to be a challenge. As a result, the US Environmental Protection Agency (US EPA) has set a limit of 2 μg $L^{-1}$ for TNT, and 0.05 μg $L^{-1}$ for 2,4–DNT and 2,6–DNT in drinking water [2,3].

The sensitivity and selectivity of most of the current analytical and separation methods are usually insufficient for direct determination of the target compounds at low concentration levels in complex matrix samples, implying that a sample pre–treatment step prior to analysis is usually necessary [4]. Several methods have been used for the extraction of nitrotoluenes from aqueous solutions and these include dispersive liquid–liquid micro–extraction (DLLME) [5], solid–phase micro–extraction (SPME) [6], solvent extraction (SE) [7], combination of molecular–imprinted polymer extraction with dispersive liquid–liquid micro–extraction (MIP–DLLME) [8] and single drop micro–extraction (SDME) [9].

In the area of water treatment, nanotechnology offers the possibility of an efficient extraction of pollutants that may cause health problems. Recently, various engineering fields have been paying a great deal of attention to these

nano–scale materials due to their small physical sizes which offer much improved and even new functions that cannot be achieved by bulk materials. Electrospun nanofibers are one of the many nano–sized materials that have attracted a lot of attention and application. The electrospinning technique involves application of a high voltage between a nozzle of a pasteur pipette, where the sample exits the capillary, and a collector where electrospun nanofibers are accumulated and collected. An electrically charged jet of polymer or composite solution is formed between the two charged sites and migrates towards the collector. The solvent is lost through evaporation before reaching the grounded collector which is the reason why the humidity should be contolled during the electrospinning process.

An electrospinning technique conveniently allows the preparation of non–woven fibrous materials with interesting characteristics such as small diameters ranging from submicron to several nanometers, having an advantage of offering large surface area per unit mass, high porosity, high gas permeability and small interfibrous pore size. The use of electrospun nanofibers with high specific surface area allows for a reduction in sorbent mass in sorption studies [10]. Many materials have been used as candidates for electrospinning e.g., naturally abundant chitosan [11], amidoxime–modified polyacrylonitrile [12], a solution of polyamide containing polyethylene glycol [13] and molecularly imprinted sol–gel nanomembrane with nylon 6 backbone [14].

Sorbents are normally loaded in cartridges such as in solid phase extraction. However, in cases where small amounts of sorbents are available, pipette tip solid phase extraction (PT–SPE) can be used. This method is a miniaturized form of SPE and has become an essential tool for purification and concentration of

proteins and peptides in the study of genomics, proteomics and metabolomics. In this method, the pipette tip with a small outlet diameter requires tiny amount of sorbent to be used and the PT–SPE setup has low solution consumption. By using this approach, a large number of reusable SPE tips can be prepared simultaneously [15]. However, no previous applications of PT–SPE for nitrotoluenes analysis have been reported thus far. In this work, electrospun PAN nanofibers were used as sorbents because of the easiness to electrospin, and were loaded in pipette tips. The PAN PT–SPE was then evaluated for its pre–concentration efficiency in the extraction of four nitrotoluenes; 2,6–dinitrotoluene (2,6–DNT), 2–nitrotoluene (2–NT), 3–nitrotoluene (3–NT) and 4–nitrotoluene (4–NT) from solutions. The PAN PT–SPE method was then applied to real wastewater samples to determine the recovery of nitroaromatic compounds.

## 2 Materials and methods

### 2.1 Reagents

Four explosive compounds: 2,6–dnitrotoluene (2,6–DNT), 2–nitrotoluene (2–NT), 3–nitrotoluene (3–NT) and 4–nitrotoluene (4–NT) were bought from Sigma–Aldrich (Johannesburg, South Africa). Polyacrylonitrile (PAN), HCl and NaOH were also purchased from Sigma–Aldrich (Johannesburg, South Africa). N,N–dimethylformamide (DMF), acetonitrile (ACN), tetrahydrofuran (THF) and methanol (MeOH) were bought from Fluka (Steinheim, Germany). All chemicals were used as received without further purification. Ultrapure water (Milli–Q, MA, USA) was used in all experiments. All pH measurements were performed on a

766 Calimatic pH meter equipped with a Shott N61 pH electrode from Knick (Berlin, Germany).

### 2.2 Preparation of stock and real solutions

Four stock solutions (100 mg $L^{-1}$) of 2,6–DNT, 2–NT, 3–NT and 4–NT were prepared by dissolving an appropriate amount of the explosive compound and made up to the mark with a 50% (v/v) acetonitrile/water solution. A 10 mg $L^{-1}$ working solution mixture was then prepared from the stock solutions and the same diluent was used to top up to the mark. A series of calibration standard solutions (250–1000 µg $L^{-1}$) were then prepared by appropriate dilutions of the working stock solution. The working stock solution was stored in a refrigerator at 4°C when not in use and standard solutions were prepared whenever required. Environmental water samples were first filtered through a 0.45 µm filter paper and 5% acetonitrile (v/v) was added for complete dissolution of the explosive compounds.

### 2.3 Instruments

A Bischoff HPLC with a UV detector set at 254 nm with an Ascentis@RP–amide column (25 cm x 4.6 mm x 5 µm) was used to separate and quantify the four explosive compounds. The mobile phase composition was methanol/water (50/50, v/v) with the flow rate maintained at 1 mL $min^{-1}$ in an isocratic mode, and the sample injection volume of 50 µL was used.

For morphological studies of the electrospun nanofibers, a FEI Nova Nanolab 600 FIB/SEM scanning electron microscopy (SEM) was used at 5 kV. Fourier transform infrared spectroscopy (FTIR) studies, for functional group analysis,

were performed by using a Tensor 27 Bruker FTIR spectrometer (Ettlingen, Germany).

### 2.4 Surface area analysis

For surface area analysis, a modified method by Alzaydien [16] was used, where 50 mg of electrospun PAN nanofibers were treated with 15 mL of methylene blue of concentration 10 mg $L^{-1}$ for 60 min after standard solutions were prepared and measured at $k_{max}$ = 664 nm. The surface area of the electrospun PAN nanofibers was calculated using Eq. (1).

$$A_S = \frac{G\ x\ N_{AV}\ \text{x}\ Ø\ x\ 10^{23}}{mM_W} \quad (1)$$

where $A_s$ is the surface area of electrospun PAN nanofibers in $m^2\ g^{-1}$, $G$ the mass of adsorbed methylene blue (g), $N_{AV}$ the Avogadro's number (6.02 x $10^{23}$ moles), $Ø$ the methylene blue molecular cross section (197.2 $A^2$), $M_W$ the molecular weight of methylene blue (373.9 g $mol^{-1}$) and $m$ is the mass of the electrospun PAN nanofibers (g).

### 2.5 Preparation of polyacrylonitrile nanofibers

A 10% (w/v) PAN–DMF solution was prepared by dissolving 2 g of PAN powder in 18.98 mL of N,N–dimethylformamide. To ensure that all PAN was dissolved so as to get an electrospinnable homogenous solution, stirring was carried out overnight. The setup of the electrospinning process consisted of a syringe needle, a high voltage power supply that was capable of generating voltages of up to 50 kV and an aluminum foil for collecting the nanofibers. The PAN solution was

placed in a glass pasteur pipette whose diameter was 0.5 mm inclined at 45º to minimize dripping of the PAN solution. The distance from the tip of the pasteur pipette and the aluminum foil collector was fixed at 25 cm. A copper wire electrode was inserted into the pasteur pipette until it was 5 cm from the tip of the pipette. The voltage was then set at 20 kV to start the electrospinning process. To ensure that all the solvent evaporated thereby preventing the nanofibers from being re–dissolved, a heater was used to maintain the temperature between 30ºC and 35ºC.

**2.6 Miniaturized pipette tip preparation**

A modified method by Lee et al. [17] was used. Polypropylene pipette tips were washed with 1 mL of water and 1 mL of acetonitrile, and then dried in an oven at 30ºC for 24 hours. A total mass of ≈ 3 mg of the electrospun PAN nanofibers was loaded into a 1000 µL pipette tip which was pre–loaded with a fixed mass of 3 mg of glass wool. The pipette tips loaded with electrospun PAN nanofibers were then washed with 200 µL of distilled water twice and pre–conditioning of the sorbent was carried out by aspirating and dispensing 200 µL of 50% (v/v) water/acetonitrile solution three times. A 200 µL aliquot of the solution with four explosive compounds was aspirated onto the conditioned electrospun PAN nanofibers and dispensed back into the same sample tube. This aspiration/dispensing cycle was repeated five times to allow the nitro explosive compounds to be adsorbed onto the electrospun PAN nanofibers. For the real environmental sample analysis, two aspirating/dispensing using 200 µL methanol/water (1/9, v/v) were carried out to remove the co–adsorbed matrix

materials. The trapped explosive compounds were then eluted with acetonitrile in one aspirating/dispensing cycle before analyzing the eluate with HPLC–UV.

### 2.7 Optimization of the extraction conditions

The effects of different parameters capable of influencing the recovery of the four nitroaromatic compounds from spiked standard solutions were investigated using electrospun PAN PT–SPE. The effect of sample pH (adjusted using 0.5 M HCl and 0.5 M NaOH), mass of electrospun PAN nanofibers, choice of eluent, and the number of aspirating/dispensing cycles, loading volume and elution volume were investigated and optimized. All experiments were done in triplicate and the recovery (%) was calculated according to Eq. (2).

$$\text{Recovery (\%)} = \frac{n_E \text{ x } 100}{n_O} \qquad (2)$$

where $n_O$ (moles) is the number of moles in the original solution and $n_E$ (moles) is the number of moles pre–concentrated onto electrospun PAN nanofibers.

## 3 Results and discussion

### 3.1 Characterization of electrospun polyacrylonitrile fibers

Fourier transform infrared (FTIR) (Fig. 1) was used to determine the important functional groups in neat electrospun PAN nanofibers and that loaded with four explosive compounds. The peaks at 2243 $cm^{-1}$ and 1452 $cm^{-1}$ were due to the stretching vibration of nitrile groups (–CN–) and the bending vibration of methylene (–$CH_2$–), respectively. This was in consistency with the findings of other researchers [18]. In other work, the characteristic band of nitrile was

exhibited at 2260 $cm^{-1}$ [12]. The broad band at 3370 $cm^{-1}$ was due to the hydroxyl groups from water in which the explosive compounds were spiked. Its presence indicated that the electrospun PAN nanofibers were not completely dry before the FTIR analysis. For the loaded electrospun PAN nanofibers, the small peak at 1539 $cm^{-1}$ was due to the asymmetric stretching frequency of the $–NO_2$ groups of the nitroaromatic compounds. Walsh and Hamilton [19] had almost similar findings for the $–NO_2$ stretching frequency. The presence of the characteristic $–NO_2$ asymmetric stretch at 1542 $cm^{-1}$ was also observed by Turner et al. [20].

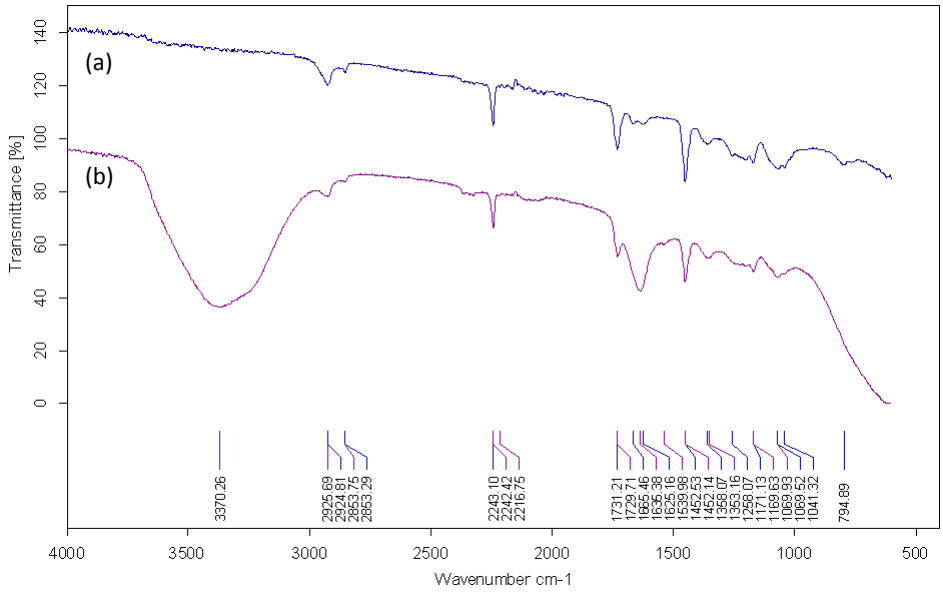



**Figure 1.** FTIR spectra of (a) neat electrospun PAN nanofibers and (b) electrospun PAN nanofibers loaded with four explosive compounds.

The scanning electron microscopy (SEM) micrographs of the electrospun PAN nanofibers with beads are shown in Fig. 2. When the beads effect was not taken into account, the size of the electrospun PAN nanofibers had a narrow diameter range. The uniformity of the electrospun PAN nanofiber was probably

due to the fact that the polymer was forced through the same fixed diameter of an orifice during electrospinning. The average diameter of the electrospun PAN nanofibers was found to be 670 nm. The phenomenon of beading has been reported by other researchers [21]. As exhibited in the SEM image, a large surface area provided by the specific agglomerate structure suggested an enormous adsorption capacity. According to the methylene blue sorption studies, the surface area of the electrospun PAN nanofibers was 8.95 $m^2$ $g^{-1}$. According to earlier research by Possi–Pezzali et al. [22], the extraction efficiency was found to decrease as the diameter of the fibers increased, probably due to the reduction in surface area. Their optimum value was 1.3 μm. The average diameter of the electrospun PAN nanofibers in this research was well below this and it was assumed that the extraction efficiency was even better. However, as the value becomes smaller, the extraction time becomes longer because the sorbent tends to agglomerate and lump together.

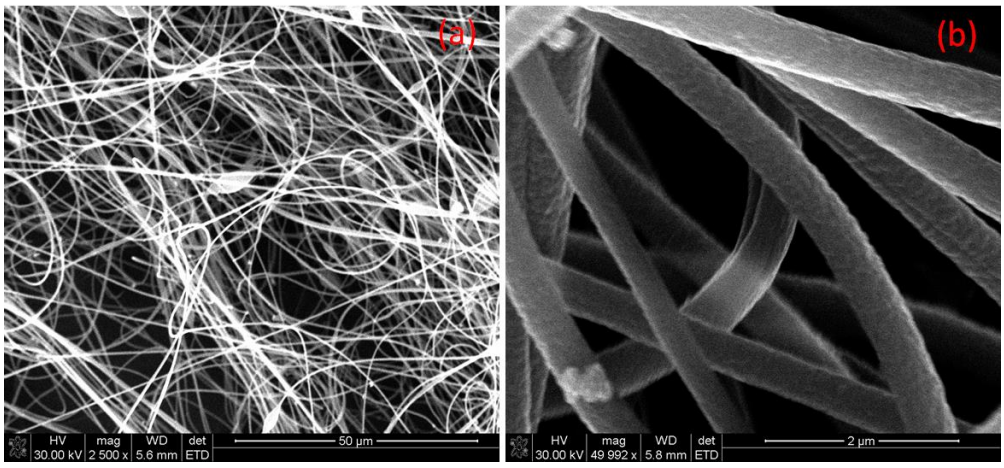



**Figure 2.** SEM micrographs of the electrospun PAN nanofibers at (a) low magnification (x 2500) and (b) high magnification (x 50000).

### 3.2 Effect of pH

The recovery of nitroaromatic compounds as a function of pH from the spiked solutions is demonstrated in Fig. 3(a). The experiment was performed by changing the pH (2–12) of the 1000 µL spiked (1000 µ $L^{-1}$) 50% (v/v) water/acetonitrile, mass of electrospun PAN = 3 mg, conditioning solution = 400 µL 50% (v/v) water/acetonitrile, elution solution = 200 µL acetonitrile. Different trends that were difficult to generalize were observed for 2,6–DNT, 2–NT, 3–NT and 4–NT. However, a pH of 6 was considered to be the optimum and was used in subsequent experiments. Specifically for 2–NT, there was no much difference in the recovered amount as the pH was varied. This finding was in agreement with the results of Chen and Chen [23] who investigated the binding of nitroaromatic compounds onto graphene oxide or reduced graphene oxide and found that the adsorbed amount was unchanged at all pH values. Similarly, Chen et al. [24] ruled out H–bonding mechanisms in the adsorption of 2,4–DNT onto carbon nanofibers because the value of the $\log K_d$ remained constant when the pH changed. As for 2,6–DNT, 3–NT and 4–NT, there was a slight variation of the amount adsorbed as the pH was varied, and still a pH of 6 was considered as a compromise. The order of the loading capacity of the nitroaromatic compounds was 2,6–DNT ≈ 3–NT > 2–NT > 4–NT. Electrostatic attraction was proposed to be the interaction mechanism since 2,6–DNT with two electron witdrawing $–NO_2$ groups was the highest adsorbed analyte. The positively charged benzene rings of the nitroaromatic compounds interact with the negatively charged surface (due to lone electrons on the nitrogens) of the electrospun PAN nanofibers. The extent of adsorption was higher in the vicinity of neutral pH as also observed by Boddu et

al. [25] who investigated the sorption of 2,4–dinitroanisole on surface modified granular activated carbon. A similar finding was obtained by Zhou et al. [26] who used a $SiO_2$ aerogel/activated carbon composite to adsorb TNT explosive.

### 3.3 Effect of mass of electrospun polyacrylonitrile nanofibers

In order to investigate the effect of sorbent mass on the recovery of nitroaromatic compounds, 5 mg, 10 mg and 15 mg of electrospun PAN nanofibers were packed in pipette tips, and the results are presented in Fig. 3(b). The experimental conditions were as follows: Initial concentration of nitroaromatic compounds = 1000 µg $L^{-1}$, sample pH = 6, conditioning solution = 400 µL 50% (v/v) water/acetonitrile, loading volume = 1000 µL, elution solution = 200 µL acetonitrile. It was found that the extraction efficiency increased with increasing fiber mass of the packing quantity. Thus, a mass of 15 mg of the nanofibers was selected for extraction of nitroaromatic compounds. On 15 mg electrospun PAN nanofibers, 0.060, 0.050, 0.072 and 0.066 µg were loaded for 2,6–DNT, 2–NT, 3–NT and 4–NT, respectively. It is readily understood that the number of available adsorption sites increases with the increase of the adsorbent dosage, consequently leading to an increase in the amount of adsorbed nitroaromatic compounds. In addition, the number of the nitro substituent groups on the benzene ring has a bearing on the recovery of the nitroaromatic compounds [27]. Among the four nitroaromatic compounds studied, 2,6–DNT had more $–NO_2$ groups than the others, so its acceptor strength would be stronger and consequentially, it was retained on the electrospun PAN nanofibers more than the other three nitroaromatic compounds.

### 3.4 Aspirating/dispensing cycles

The number of aspirating/dispensing cycles is a critical parameter for loading and subsequently recovery of the nitroaromatic compounds in PT–SPE. Figure 3(c) shows the recovery of nitroaromatic compounds when 1 to 30 aspirating/dispensing cycles (at the loading stage) were investigated. This experiment was perfomed under the following experimental conditions: Initial concentration of nitroaromatic compounds = 1000 µg $L^{-1}$, mass of electrospun PAN = 15 mg, sample pH = 6, conditioning solution = 400 µL 50% (v/v) water/acetonitrile, loading volume = 1000 µL, elution solution = 200 µL acetonitrile. The extraction of all nitroaromatic compounds were maximally recovered after twenty aspirating/dispensing cycles of the sample, and this value was taken as the optimum for use in subsequent experiments. Coincidentally, the same optimum number of cycles was obtained by Hasegawa et al. [28] though they were enriching dextromethorphan onto C18–bonded monolithic silica gel. In this work, there was seen a reduction of the extraction of nitroaromatic compounds as > 20 aspirating/dispensing cycles were perfomed. This was probably due to the elution of the analytes during the dispensing actions which was undesirable on the loading stage.

### 3.5 Effect of elution solvent

The elution solvent also has an important effect on the extraction efficiency, and must ensure that all the nitroaromatic compounds are eluted from the pipette tip and available for the subsequent analysis. Four polar elution solvents which were compatible with the HPLC mobile phase were investigated; MeOH, ACN, THF

and DMF, and the results are presented in Fig. 3(d). The investigation was carried out under the following experimental conditions: Initial concentration of nitroaromatic compounds = 1000 µg $L^{-1}$, sample pH = 6, mass of electrospun PAN = 15 mg, conditioning solution = 400 µL 50% (v/v) water/acetonitrile, loading volume = 1000 µL, elution solution = 200 µL acetonitrile. It was clear that ACN gave the highest recovery of the nitroaromatic compounds, and was used as the elution solvent in subsequent experiments. This was in agreement with the findings from our previous study Tavengwa et al. [29] where ACN was found to be the best elution solvent ahead of DMF, MeOH and dimethylsulphoxide (DMSO).

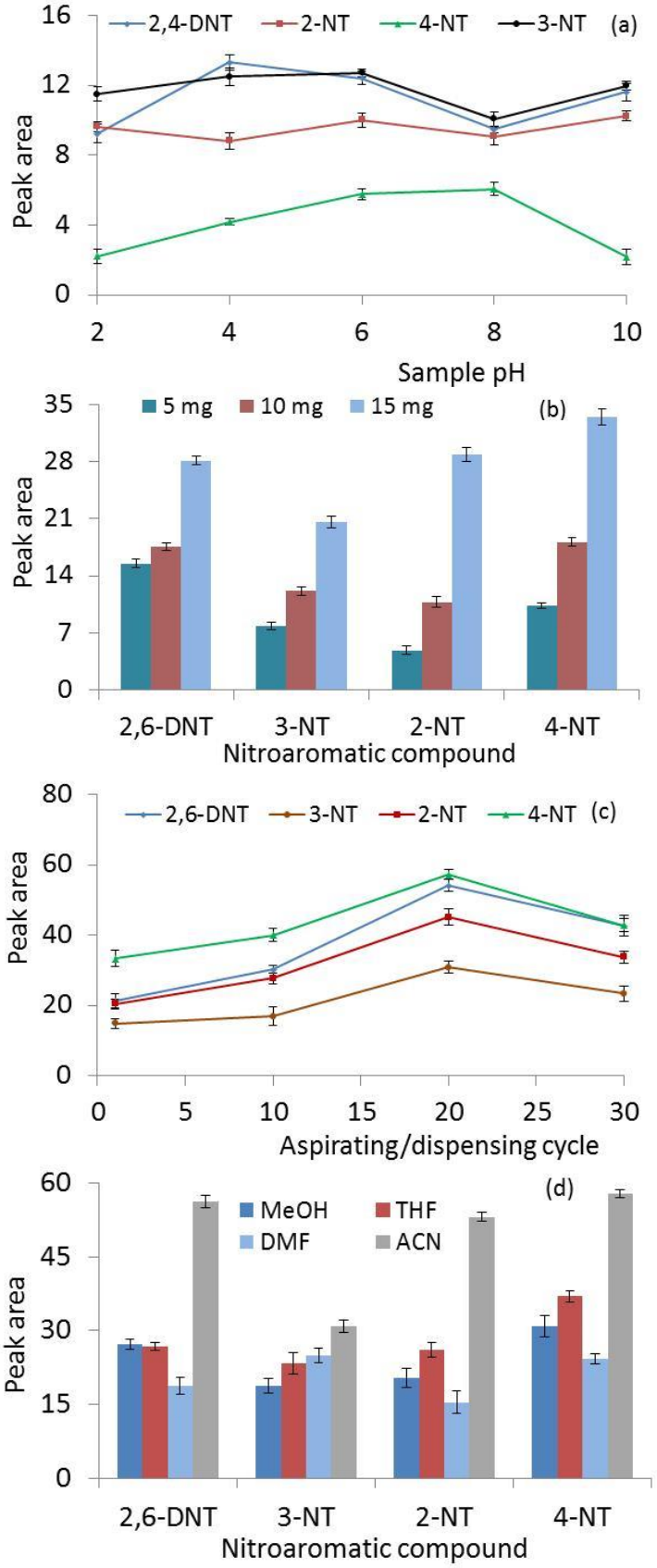
### 3.6 Effect of loading volume

Figure 3(e) shows the dependency of on the recovery of nitrotoluenes on the loading volume (Experimental conditions: Initial concentration of nitroaromatic compounds = 1000 µg $L^{-1}$, sample pH = 6, mass of electrospun PAN = 15 mg, conditioning solution = 400 µL 50% (v/v) water/acetonitrile). The sample volume should be sufficient for target analytes to be determined at low levels saving time. The chromatographic peak areas of the analytes increased remarkably with the increase of sample volume from 200 µL to 1000 µL. Accordingly, 1000 µL of water samples was selected for the following experiments because it showed better recovery which was also the case with Andrade et al. [30].

### 3.7 Effect of elution volume

The dependency of the elution volume on the extraction efficiency of nitroaromatic compound was investigated (Fig. 3(f)). The experimental conditions

were: Initial concentration of nitroaromatic compounds = 1000 µg $L^{-1}$, sample pH = 6, mass of electrospun PAN = 15 mg, conditioning solution = 400 µL 50% (v/v) water/acetonitrile, elution solution = acetonitrile. The amount of the nitroaromatic compounds enriched of the PAN PT–SPE was found to increase from 100 µL to 200 µL then decrease as the eluent volume was increased from 200 µL to 500 µL. This trend and observation was also found by Smith et al. [31] who used a semi–automated microcolumn SPE system for the extraction of six nitroaromatic compounds. Large volumes of the eluate solvent generally leads to low concentration of nitroaromatic compounds, and this resulted in high limits of detection. Hence, 200 µL of acetonitrile was used to obtain low limits of detection. The adsorption capacities of 2,6–DNT, 2–NT, 3–NT and 4–NT on electrospun PAN nanofibers were 0.017 µg $mg^{-1}$, 0.012 µg $mg^{-1}$, 0.015 µg $mg^{-1}$ and 0.013 µg $mg^{-1}$, respectively.


2,4-DNT
2-NT
4-NT
3-NT
(a)
Peak area
Sample pH
5 mg
10 mg
15 mg
(b)
2,6-DNT
3-NT
2-NT
4-NT
Nitroaromatic compound
(c)
Aspirating/dispensing cycle
MeOH
THF
DMF
ACN
(d)

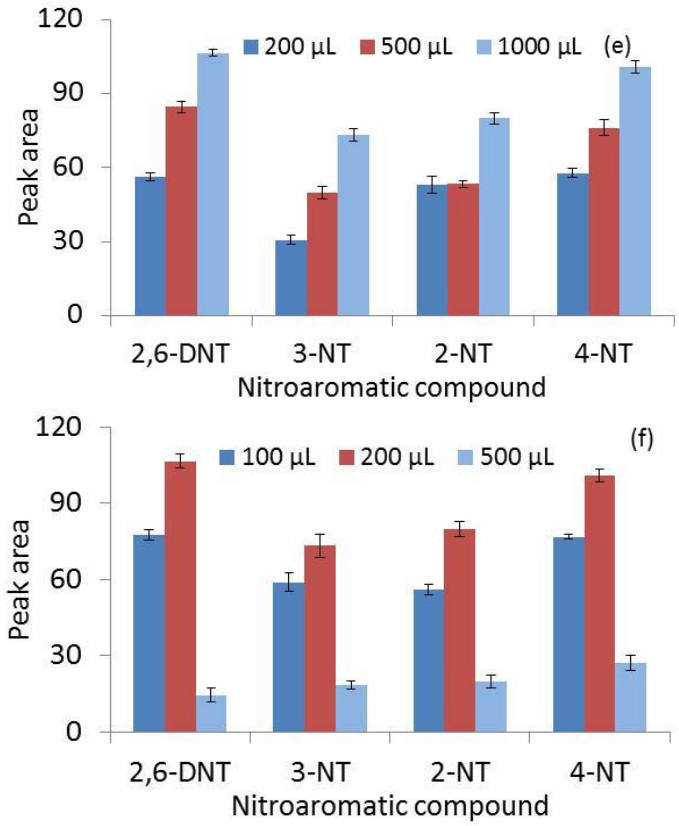



**Figure 3. (a)** Effect of pH **(b)** mass of electrospun PAN **(c)** number of aspirating/dispensing cycles **(d)** elution solvent **(e)** loading volume and **(f)** elution volume (n = 3, RSD).

### 3.8 Method validation

The analytical characteristics of the PT–SPE method were evaluated with respect to linearity, repeatability, and detection limits under the optimum conditions. Table 1 summarizes some calibration and chromatographic constants. Regression equations for 2,6–DNT, 4–NT, 3–NT and 2–NT exhibited good linearity ($R^2$ = 0.99) which indicated good relationship between the peak area (y) and the nitroaromatic compounds concentration (x, µg $L^{-1}$). The linear dynamic range (LDR) of the investigated nitroaromatic compounds was 250–1000 µg $L^{-1}$. Low limits of detection (LOD) of 21 µg $L^{-1}$ to 38 µg $L^{-1}$ were determined based on S/N

= 3, and limits of quantification (LOQ) were found to be between 250 µg $L^{-1}$ and 210 µg $L^{-1}$, based on S/N = 10.

To ascertain the perfomance of the developed PAN PT–SPE method for the extraction of nitrotoluenes from water samples, it was compared to other selected conventional analytical techniques common in literature (Table 2). As demonstrated in Table 2, the proposed method demonstrated to be simple and had a wide linearity dynamic range (LDR), low sensitivity, and an acceptable reproducibility with an important emphasis on the extraction time which seems to be quite short. Other advantages of the developed method are that it has low solvent consumption, low cost, no evaporation step, the tools are very accessible, and short extraction times are required. A large number of reusable SPE tips can also be used at one goal in PT–SPE format [15].

**Table 1** Validation parameters for HPLC determination of four nitroaromatic compounds

| | $t_R$ (min) | Equation | $R^2$ | LOD (µg $L^{-1}$) | LOQ (µg $L^{-1}$) |
|---|---|---|---|---|---|
| 2,6–DNT | 19.98 | y = 0.0813x + 3.8571 | 0.9989 | 21.4 | 70.6 |
| 2–NT | 20.67 | y = 0.0818x + 0.06968 | 0.9965 | 63.7 | 210 |
| 4–NT | 22.21 | y = 0.0645x + 5.5536 | 0.9926 | 25.2 | 83.5 |
| 3–NT | 24.08 | y = 0.1029x – 0.7162 | 0.9909 | 37.6 | 124 |

LOD: Limits of detection, LOQ: Limits of quantification, direct injection

**Table 2.** Comparison of different analytical methods applied for the determination of nitroaromatic compounds in water samples.

| Analytical technique | Target analyte | LOD | LDR (μg $L^{-1}$) | RSD (%) | Reference |
|---|---|---|---|---|---|
| SPME–GC–MS | 2,6–DNT | 4.5 ng $L^{-1}$ | 75 ng $L^{-1}$ – 7.5 μg $L^{-1}$ | 3.7 | [6] |
| *Microcolumn–SPE–HPLC | p–NT | 1100 ng $L^{-1}$ | – | 0.63 | [31] |
| MIP–Fluorescent | 2,4–DNT | ≈0.5–1.0 mg $L^{-1}$ | – | – | [32] |
| DLLE–GC–FID | ᵡMNT | 0.5 μg $L^{-1}$ | 1–400 (μg $L^{-1}$) | 8.0–9.4 | [33] |
| DLLME– GC–FID | 2,4–DNT | 0.5 μg $L^{-1}$ | 1–400 (μg $L^{-1}$) | 3.9[#] | [34] |
| Electrospun PAN–PT–SPE–HPLC–UV | 4–NT | 25.2 μg $L^{-1}$ | 250–1000 μg $L^{-1}$ | 6.6 | Present work |

–: not reported
LDR: linear dynamic range
*seawater analysis
ᵡMNT: mononitrotoluene (o–: ortho, m–: meta and p–: para)
[#]well water

### 3.9 Real sample analysis

In order to investigate the applicability and reliability of the proposed method in the presence of the matrix effect, wastewater spiked with 100 µg $L^{-1}$, 150 µg $L^{-1}$ and 200 µg $L^{-1}$ of the four explosive compounds was enriched on the electrospun PAN nanofibers at optimized conditions. Figure 4 shows the chromatograms of (a) unspiked real water, (b) 200 µg $L^{-1}$ spiked real water and (c) 250 µg $L^{-1}$ standard solution with the corresponding retention times shown. Recoveries of 2,6–DNT, 4–NT, 3–NT and 2–NT from a real wastewater samples using the present method are presented in Table 3. These recoveries were between 70% and 115% and were considered satisfactory as they demonstrated little effect of the matrix. The respective relative standard deviations (RSD) were < 6.3%, indicated that the method was reliable and could be used for the determination of nitroaromatic compounds in real environmental wastewater samples.

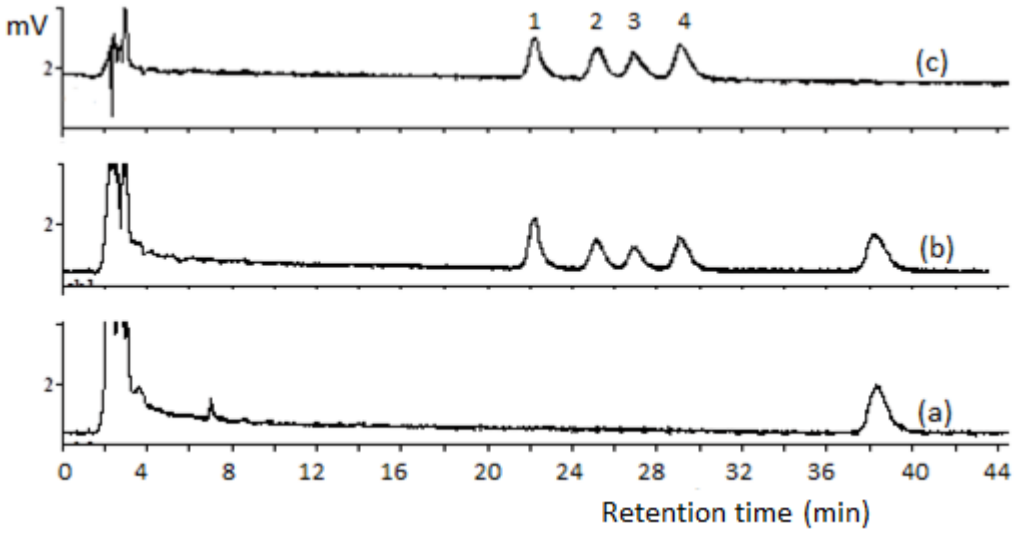



**Figure 4.** Chromatograms of (a) unspiked real water (b) 200 µg $L^{-1}$ spiked real water and (c) 250 µg $L^{-1}$ standard solution. Peak 1: 2,6–DNT, peak 2: 2–NT, peak 3: 4–NT and peak 4: 3–NT. Experimental conditions: Sample pH = 6, mass of electrospun PAN = 15 mg, conditioning solution = 400 µL 50% (v/v) water/acetonitrile, loading volume = 4000 µL, elution solution = 200 µL acetonitrile.

**Table 3.** Recovery of explosive compounds from real wastewater sample.

| Compound | Spiked concentration (μg $L^{-1}$) | Recovery (%) | RSD (%) |
|---|---|---|---|
| NB | – | – | – |
| | 50 | 84.9 | 3.7 |
| | 100 | 80.5 | 2.4 |
| | 200 | 82.6 | 11.9 |
| 2,4–DNT | – | – | – |
| | 50 | 89.9 | 3.1 |
| | 100 | 87.2 | 1.4 |
| | 200 | 87.2 | 9.9 |
| 2–NT | – | – | – |
| | 50 | 82.3 | 4.8 |
| | 100 | 81.3 | 5.4 |
| | 200 | 82.4 | 9.5 |

## 4 Conclusions

The study demonstrated that the electrospun PAN nanofibers impregnated in the pipette tip were effective for simultaneous extraction of nitroaromatic compounds from aqueous solutions. In this PAN PT–SPE method, a small mass of the sorbent and solvents (washing, conditioning, loading and elution) were used. The pH had different effects on the adsorption of nitroaromatic compounds. The investigation revealed that the optimum mass of electrospun PAN sorbent was 15 mg and 20 aspirating/dispensing cycles gave the maximum recovery of nitrotoluenes with acetonitrile as the best eluting solvent. Low LODs of nitroaromatic compounds

were achieved, and it was confirmed that the method could be used for the determination of trace level nitroaromatic compounds in real wastewater samples as satisfactory relative recoveries of different nitroaromatic compounds from real wastewater samples were obtained.

*The authors would like to thank the National Research Foundation (NRF) of South Africa for funding Nikita Tawanda Tavengwa and Pardon Nyamukamba, grant IDs NFS13091843717 and NFS13090633524 respectively. The University of Witwatersrand is also appreciated for providing financial support through the Wits Postgraduate Merit Award.*

*The authors have declared no conflict of interest.*

## 5 References

[1] Sviatenko, L. K., Isayev, O., Gorb, L., Hill, F. C., Leszczynska, D., Leszczynski, J., Are the reduction and oxidation properties of nitrocompounds dissolved in water different from those produced when adsorbed on a silica surface? A DFT M05–2X computational study. *J. Comput. Chem.* 2015, *36*, 1029–1035.

[2] Agency for Toxic Substances and Disease Registry (ATSDR) (1995) Toxicological profile for 2,4,6–trinitrotoluene (TNT) (Trans: U.S. Department of Health and Human Services). Public Health Service, Atlanta.

[3] U.S. Environmental Protection Agency (2008) Drinking water health advisory for 2,4–dinitrotoluene and 2,6–dinitrotoluene (Trans: Health and Ecological Criteria Division). Washington, DC.

[4] Chimuka, L., van Pinxteren, M., Billing, J., Yilmaz, E., Jönsson, J. A., Selective extraction of triazine herbicides based on a combination of membrane assisted solvent extraction and molecularly imprinted solid phase extraction. *J. Chromatogr. A* 2011, *1218*, 647–653.

[5] Wen, Y., Li, J., Zhang, W., Chen, L., Dispersive liquid–liquid microextraction coupled with capillary electrophoresis for simultaneous determination of sulfonamides with the aid of experimental design. *Electrophoresis* 2011, *32*, 2131–2138.

[6] Jönsson, S., Gustavsson, L., van Bavel, B., Analysis of nitroaromatic compounds in complex samples using solid–phase microextraction and isotope dilution quantification gas chromatography–electron–capture negative ionisation mass spectrometry. *J. Chromatogr. A* 2007, *1164*, 65–73.

[7] Chen, W., Chiang, W., Lai, C., Recovery of nitrotoluenes in wastewater by solvent extraction. *J. Hazard. Mater.* 2007, *145*, 23–29.

[8] Ebrahimzadeh, H., Abedi, H., Yamini, Y., Adlnasab, L., Molecular–imprinted polymer extraction combined with dispersive liquid–liquid micro–extraction for ultra preconcentration of mononitrotoluene. *J. Sep. Sci.* 2010, *33*, 3759–3766.

[9] Psillakis, E., Kalogerakis, N., Application of solvent microextraction to the analysis of nitroaromatic explosives in water samples. *J. Chromatogr. A* 2001, *907*, 211–219.

[10] Ifegwu, O. C., Anyakora, C., Chigome, S., Torto, N., Application of nanofiber–packed SPE for determination of urinary 1–hydroxypyrene level using HPLC. *Anal. Chem. Insights* 2014, *9*, 17–25.

[11] Haider, S., Park, S., Preparation of the electrospun chitosan nanofibers and their applications to the adsorption of Cu(II) and Pb(II) ions from an aqueous solution. *J. Membr. Sci.* 2009, *328*, 90–96.

[12] Saeed, K., Haider, S., Oh, T., Park, S., Preparation of amidoxime–modified polyacrylonitrile (PAN–oxime) nanofibers and their applications to metal ions adsorption. *J. Membr. Sci.* 2008, *322*, 400–405.

[13] Bagheri, H., Najarzadekan, H., Roostaie, A., Electrospun polyamide–polyethylene glycol nanofibers for headspace solid–phase micro–extraction. *J. Sep. Sci.* 2014, *37*, 1880–1886.

[14] Moein, M.M., Javanbakht, M., Karimi, M., Akbari-adergani, B., Fabrication of a novel electrospun molecularly imprinted nanomembrane coupled with high-performance liquid chromatography for the selective separation and determination of acesulfame. *J. Sep. Sci.* 2015, *38*, 1372–1379.

[15] Ekström, S., Wallman, L., Hök, D., Marko–Varga, G., Laurell, T., Miniaturized solid–phase extraction and sample preparation for maldi ms using a microfabricated integrated selective enrichment target. *J. Proteome Res.* 2006, *5*, 1071–1081.

[16] Alzaydien, A. S., Physical, chemical and adsorptive characteristics of local oak sawdust based activated carbons. *Asian J. Sci. Res.* 2016, *9*, 45–56.

[17] Lee, X. P., Hasegawa, C., Kumazawa, T., Shinmen, N., Shoji, Y., Seno, H., Sato, K., Determination of tricyclic antidepressants in human plasma using

pipette tip solid–phase extraction and gas chromatography–mass spectrometry. *J. Sep. Sci.* 2008, *31*, 2265–2271.

[18] Zhang, D., Karki, A. B., Rutman, D., Young, D. P., Wang, A., Cocke, A., Ho, T. H., Guo, Z., Electrospun polyacrylonitrile nanocomposite fibers reinforced with $Fe_3O_4$ nanoparticles: Fabrication and property analysis. *Polymer* 2009, *50*, 4189–4198

[19] Walsh, G., Hamilton, S., Adsorption of 2,4,6–trinitrotoluene on MFI zeolite. *Propellants Explos. Pyrotech.* 2011, *36*, 182–186.

[20] Turner, N. W., Holmes, N., Brisbane, C., McGeachie, A. B., Bowyer, M. C., McCluskey, A., Holdswort, C. I., Effect of template on the formation of phase–inversed molecularly imprinted polymer thin films: an assessment. *Soft Matter* 2009, *5*, 3663–3671.

[21] Gomes, D. S., da Silva, A. N. R., Morimoto, N. I., Mendes, L. T. F., Furlan, R., Ramos, I., Characterization of an electrospinning process using different PAN/DMF concentrations. *Polímeros* 2007, *17*, 206–211.

[22] Possi–Pezzali, T., Chigome, S., Rodríguez–Haralambides, A., Nelson Torto, T., Evaluation of electrospunfibers as solid phase extraction sorbents for sample preparation in HPLC–MS/MS confirmatory doping control analysis of dexamethasone and betamethasone. *Anal. Methods* 2013, *5*, 4230–4237.

[23] Chen, X., Chen, B., Macroscopic and spectroscopic investigations of the adsorption of nitroaromatic compounds on graphene oxide, reduced graphene oxide, and graphene nanosheets. *Environ. Sci. Technol.* 2015, *49*, 6181–6189.

[24] Chen, W., Duan, L., Zhu, D., Adsorption of polar and nonpolar organic chemicals to carbon nanotubes. *Environ. Sci. Technol.* 2007, *41*, 8295–8300.

[25] Boddu, V. M., Abburi, K., Fredricksen, A. J., Maloney, S. W., Damavarapu, R., Equilibrium and column adsorption studies of 2,4–dinitroanisole (DNAN) on surface modified granular activated carbons. *Environ. Technol.* 2009, *30*, 173–181.

[26] Zhou, X. F., Cui, S., Liu, Y., Liu, X. Y., Shen, X. D., Wu, Z. W., Adsorption capacity of hydrophobic $SiO_2$ aerogel/activated carbon composite materials for TNT. *Sci. China Tech. Sci. 2013*, 56, 1767–1772.

[27] Shen, X. E., Shan, X. Q., Dong, D. M., Hua, X. Y., Owens, G., Kinetics and thermodynamics of sorption of nitroaromatic compounds to as–grown and oxidized multiwalled carbon nanotubes. *J. Colloid. Interface Sci*. 2009, *330*, 1–8.

[28] Hasegawa, C., Kumazawa, T., Uchigasaki, S., Lee, X. P., Sato, K., Terada, M., Kurosaki, K., Determination of dextromethorphan in human plasma using pipette tip solid–phase extraction and gas chromatography–mass spectrometry. *Anal. Bioanal. Chem.* 2011, *401*, 2215–2223.

[29] Tavengwa, N. T., Hintsho, N., Durbach, S., Weiersbye, I., Cukrowska, E., Chimuka, L., Extraction of explosive compounds from aqueous solutions by solid phase extraction using β–cyclodextrin functionalized carbon nanofibers as sorbents. *J. Environ. Chem. Eng.* 2016, *4*, 2450–2457.

[30] Andrade, R. T., da Silva, R. C. S., Pereira, A. C., Borges, K. B., Self–assembly pipette tip–based cigarette filters for micro–solid phase extraction of ketoconazole cis–enantiomers in urine samples followed by high–

performance liquid chromatography/diode array detection. *Anal. Methods* 2015, *7*, 7270–7279.

[31] Smith, M., Collins, G. E., Wang, J., Microscale solid–phase extraction system for explosives. *J. Chromatogr. A* 2003, *991*, 159–167.

[32] Stringer, R. C., Gangopadhyay, S., Grant, S. A., Detection of nitroaromatic explosives using a fluorescent–labeled imprinted polymer. *Anal. Chem.* 2010, *82*, 4015–4019.

[33] Sobhi, H. R., Kashtiaray, A., Farahani, H., Javaheri, M., Ganjali, M. R., Quantitation of mononitrotoluenes in aquatic environment using dispersive liquid–liquid microextraction followed by gas chromatography–flame ionization detection. *J. Hazard. Mater*. 2010, 175, 279–283.

[34] Ebrahimzadeh, H., Yamini, Y., Kamarei, F., Optimization of dispersive liquid–liquid microextraction combined with gas chromatography for the analysis of nitroaromatic compounds in water. *Talanta* 2009, *79*, 1472–1477.

# Chapter 5

# 5 General conclusions and future work

In this section, conclusions based on experimental findings are discussed. The work carried out in this research and a discussion of the achieved objectives is also presented. The recommended future work is also presented in this section.

## 5.1 Conclusions

In this work, natural abundant agricultural waste *Moringa oleifera* seed powder was used as a possible sorbent for the reomoval of nitrobenzene (**paper I**). Biocharing of this sorbent into activated carbon had an effect of reduction in the nitrobenzene uptake performance. This indicated that chemisorption was the pre-dominant form of interaction. Since this material is cheap and abundant, it can be an alternative to commercial activated carbons.

The selectivity of the molecular imprinted polymer was demonstrated in **paper II** and **paper IV**. 2,4-dinitrotoluene was used as an imprint in **paper I** and this analyte was selectively extracted when the sorbent was applied to an aqueous solution having two other closely related analogues (2-nitrotoluene and nitrobenzene). In all investigated optimization parameters, the imprinting effect was evident as the control polmers extracted the nitroaromatic compounds less as compared to the imprinted one. In **paper IV**, a novel combination of the molecular imprinted polymer dispersed in toluene held in a membrane extraction assisted solvent extraction bags was applied succesfully for the extraction of of polycyclic aromatic hydrocarbons from domestic wastewater.

Another material with vast potential in use as a sorbent is carbon nanofiber (**paper III**). This material is a waste in power stations but can find good use in water purification with the aim of reducing costs. Furthermore, it can be functionalized with srfactants like β-cyclodextrin which increased the sorption capacity of nitroaromatic compounds. The extraction efficiency of the β-cyclodextrin functionalized carbon nanofiber was superior as compared to the raw sorbent. This was possible since the β-cyclodextrin has a reserviuor of hydroxyl groups on it. Furthermore, the cyclic nature of β-cyclodextrin can make it possible for the formation of inclusion complexes.

Application of electrospun polyacrylonitrile was successfully applied for the extraction of four explosive compounds. The PAN fibers were loads in pipette tips in miniaturized pipette tip solid phase extraction (**paper V**).

## 5.2 Future work

To try other combinations of techniques/sorbents other than the MIP-MASE combination investigated in **paper IV** and see the effect in sample matrix concentration minimization. Comparison of the chromatograms of the MASE alone, MIP alone and that of the MIP MASE combination to be given to investigate selectivity. Quantification of PAHs in real environmental samples is to be done

Apart from *Moringa oleifera* seed powder investigated in **paper I**, use can be made of other cheap (at times free) and readily available agricultural and agro-waste materials as sorbents for remediation of different organic pollutants. These materials can be used as raw in a ground form or they can either be chemically or physically modified.

Fly ash, which is another ubandant waste material from power generating stations should be full utilized as a raw sorbent or converted into nano-fibers like in **paper III** for the extraction of contaminants in aquatic environments. Further, some functionalization agents can be added to make the sortion more specific.

# References

Agency for Toxic Substances and Disease Registry (ATSDR). (1995) Toxicological Profile for TNT.

Ahmedna, M., Marshall, W.E. and Rao, M. (2000) Production of granular activated carbon from select agricultural by-products and evaluation of their physical, chemical and adsorption properties, *Bioresource Technology*, 71, 113-123.

Ali, E.N. Muyibi, A.S., Hamzah M. Salleh, H.M., Salleh, M.R.M. and Alam, M.Z. (2009) *Moringa oleifera* seeds as natural coagulant for water treatment, *Thirteenth International Water Technology Conference*, IWTC 13 2009, Hurghada, Egypt, 163-168.

Amagloh, F.K. and Benang, A. (2009) Effectiveness of Moringa oleifera seed as coagulant for water purification, *African Journal of Agricultural Research*, 4, 119-123.

Angerer, J. and Weismantel, A. (1998) Biological monitoring of dinitrotoluene by gas chromatographic-mass spectrometric analysis of 2,4-dinitrobenzoic acid in human urine, *Journal of Chromatography B: Biomedical Sciences and Applications*, 713, 313-22.

Anwar, F., Latif, S., Ashraf, M. and Gilani, A.H. (2007) *Moringa oleifera*: A food plant with multiple medicinal uses, *Phytotherapy Research*, 21, 17-25.

Arthur, C.L. and Pawliszyn, J. (1990) Solid phase microextraction with thermal desorption using fused silica optical fibers, *Analytical Chemistry*, *62*, 2145-2148.

Ayotunde, E.O., Fagbenro, O.A. and Adebanyo, O.T. (2011) Toxicity of aqueous extract of *Moringa oleifera* seed powder to Nile tilapia (*Oreochromis niloticus*) fingerlings, *International Research Journal of Agricultural Science*s, 1, 142-150.

Bahmaei, M., Mashayekhi, H.A. and Khalilian, F. (2015) Application of ultrasound-assisted emulsification microextraction based on applying low density organic solvents to the extraction and determination of mononitrotoluenes in water samples, *Journal of the Brazilian Chemical Society*, 26, 1475-1481.

Balamurugan, K., Gokulakrishnan, K. and Prakasam, T. (2011) Preparation and evaluation of molecularly imprinted polymer liquid chromatography column for the separation of ephedrine enantiomers, *Arabian Journal of Chemistry*, In Press.

Batlle, R., Nerín, C., Crescenzi, C. and Carlsson, H. (2005) Supercritical fluid extraction of energetic nitroaromatic compounds and their degradation products in soil samples, *Analytical Chemistry*, 77, 4241-4247.

Belardi, R.P. and Pawliszyn, J.B. (1989) Application of chemically modified fused silica fibers in the extraction of organics from water matrix samples and their rapid transfer to capillary columns, *Water Pollution Research Journal of Canada*, 24 179-191.

Bhattacharjee, P.K. and Rutledge, G.C. (2011) Electrospinning and Polymer Nanofibers: Process Fundamentals, *Comprehensive Biomaterial*, 1, 497-512.

Boparai, H., Comfort, S., Shea, P. and Szecsody, J. (2008) Remediating explosive-contaminated groundwater by in situ redox manipulation (ISRM) of aquifer sediments, *Chemosphere*, 71, 933-941.

Brannon, J.M. and Pennington, J.C. (2002) Environmental fate and transport process descriptors for explosives, ERDC/EL TR-02-10, U.S Army Engineer Research and Development Center, Vicksburg, Miss, USA.

Bunte, G., Hürttlen, J., Pontius, H., Hartlieb, K. and Krause, H. (2007) Gas phase detection of explosives such as 2,4,6-trinitrotoluene by molecularly imprinted polymers, *Analytica Chimica Acta*, 591, 49–56.

Cappiello, A., Famiglini, G., Palma, P. and Trufelli, H. (2010) Matrix effects in liquid chromatography-mass spectrometry, Journal of Liquid Chromatography and Related Technologies, 33, 1067-1081.

Casari, C. and Andrews, A.R. (2001) Application of solvent microextraction to the analysis of amphetamines and phencyclidine in urine, Forensic Science International, 120, 165-71.

Chen, M., Wang, C., Fang, W., Wang, J., Zhang, W., Jin, G. and Diao, G. (2013) Electrospinning of calixarene-functionalized polyacrylonitrile nanofiber membranes and application as an adsorbent and catalyst support, *Langmuir*, 29, 11858-11867.

Chen, W., Duan, L. and Zhu, D. (2007) Adsorption of polar and nonpolar organic chemicals to carbon nanotubes, *Environmental Science and Technology*, 41, 8295-8300.

Chen, X. and Chen, B. (2015) Macroscopic and spectroscopic investigations of the adsorption of nitroaromatic compounds on graphene oxide, reduced graphene oxide, and graphene nanosheets, *Environmental Science and Technology*, 49, 6181-6189.

Clark, B. and Boopathy, R. (2007) Evaluation of bioremediation methods for the treatment of soil contaminated with explosives in Louisiana Army Ammunition Plant, Minden, Louisiana, *Journal of Hazardous Materials*, 643-648.

Cortada, C., Vidal, L. and Canals, A. (2011) Determination of nitroaromatic explosives in water samples by direct ultrasound-assisted dispersive liquid-liquid microextraction followed by gas chromatography-mass spectrometry, *Talanta*, 85, 2546-2552.

Cuervo, R.M., Asedegbega-Nieto, E., Díaz, E., Vega, A., Ordóñez, S., Castillejos-López, E. and Rodríguez-Ramos, I. (2008) Effect of carbon nanofiber functionalization on the adsorption properties of volatile organic compounds, *Journal of Chromatography A*, 1188, 264-273.

Darrach, M.R., Chutjian, A. and Plett, G.A. (1998) Trace explosives signatures from World War II unexploded undersea ordnance, *Environmental Science and Technology*, 32, 1354-1358.

Deng, C., Gong, P., He, Q., Cheng, J., He, C., Shi, L., Zhu, D. and Lin, T. (2009). Highly fluorescent TPA-PBPV nanofibers with amplified sensory response to TNT, *Chemical Physics Letters*, 483, 219-223.

Dillard, C.J. and German, J.B. (2000) Phytochemicals: Nutraceuticals and human health, *Journal of the Science of Food and Agriculture*, 80, 1744-1756.

Dolatto, R.G., Messerschmidt, L., Pereira, B.F., Martinazzo, R. and Abate, G. (2016) Preconcentration of polar phenolic compounds from water samples and soil extract by liquid-phase microextraction and determination via liquid chromatography with ultraviolet detection, *Talanta*, 148, 292-300.

Ebrahimzadeh, H. and Behbahani, M. (2013) A novel lead imprinted polymer as the selective solid phase for extraction and trace detection of lead ions by flame atomic absorption spectrophotometry: Synthesis, characterization and analytical application, *Arabian Journal of Chemistry*, In Press.

Ebrahimzadeh, H., Yamini, Y. and Kamarei, F. (2009) Optimization of dispersive liquid–liquid microextraction combined with gas chromatography for the analysis of nitroaromatic compounds in water. *Talanta*, 79, 1472–1477.

Egli, S.N., Butler, E.D. and Bottaro, C.S. (2015) Selective extraction of light polycyclic aromatic hydrocarbons in environmental water samples with pseudo-template thin-film molecularly imprinted polymers, *Analytical Methods*, 7, 2028-2035.

Feng, L., Xie, N. and Zhong, J. (2014) Carbon nanofibers and their composites: A review of synthesizing, properties and applications, *Materials*, 7, 3919-3945.

Formhals, A. (1938) Electrical spinning of fibers such as those produced from cellulose acetate, US Patent, 2116942.

García-Vázquez, A., Borrull, F., Calull, M. and Aguilar C. (2016) Single-drop microextraction combined in-line with capillary electrophoresis for the determination of nonsteroidal anti-inflammatory drugs in urine samples, *Electrophoresis*, 37, 274-281.

Ghebremichael, K., Gunaratna, K., Henrikson, H., Burmer, H. and Dalhammar, G. (2005) A simple purification and activity assay for the coagulant protein from *Moringa oleifera* seed, *Water Research*, 32, 2338-2344.

Gholz, H.L. (Ed.) (1987) Agroforestry: Realities, possibilities and potentials. Dordrecht, the Netherlands, Martinus Nijhoff Publishers in cooperation with ICRAF.

Gowrishankar R., Kumar M., Menon V., Divi S. M. and Saravanan M., Magudapathy P., Panigrahi B. K., Nair K. G., Venkataramaniah K. (2010) Trace element studies on *Tinospora cordifolia* (Menispermaceae), *Ocimum sanctum* (Lamiaceae), *Moringa oleifera* (Moringaceae), and *Phyllanthus niruri* (Euphorbiaceae) using PIXE, *Biological Trace Element Research*, 133, 357-363.

Guatemala-Morales, G.M., Elisa Alejandra Beltrán-Medina, E.A., Mario Alfonso Murillo-Tovar, M.A., Priscilla Ruiz-Palomino, P.R., Rosa Isela Corona-González, R.I. and Arriola-Guevara, E. (2016) Validation of analytical conditions for determination of polycyclic aromatic hydrocarbons in roasted coffee by gas chromatography-massspectrometry, *Food Chemistry*, 197, 747-775.

Hajjar, N.P., Brewer, M.E., Turck, P.A., Kruger, C.L., Hartley, W.R. and Roberts, W.C. (1991) Office of Drinking Water, US EPA, Report Number PB91-159640, Washington, D.C. 20460.

Hennion, M.C. (1999) Solid-phase extraction: method development, sorbents, and coupling with liquid chromatography, *Journal of Chromatography A*, 856, 3-54.

Hou, L. and Lee, H.K. (2002) Application of static and dynamic liquid-phase microextraction in the determination of polycyclic aromatic hydrocarbons, 7th International Symposium on Hyphenated Techniques in Chromatography and Hyphenated Chromatographic Analyzers, *Journal of Chromatography A*, 976, 377–385.

Hsueh, K.A., Chang, F.C., Wang, H.P., Wang, H.C., Huang, Y.J., Huang, H.L. and Tuan, Y.J. (2013) Enhanced extraction of PAHs hindered in fly ashes with supercritical water, *Journal of Supercritical Fluids*, 73, 116-119.

Hung, C.Y., Huang, H.H. and Hwang, C.C. (2005) Chiral separations of mandelic acid by HPLC using molecularly imprinted polymers, *Eclética Química*, 30, 67-73.

Hyder, M., Aguilar, L.L., Genberg, J., Sandahl, M., Wesén, C. and Jönsson, J.Å. (1999) Determination of polycyclic aromatic hydrocarbons (PAHs) from organic aerosols using hollow fiber micro-porous membrane liquid-liquid extraction (HF-MMLLE) followed by gas chromatography-mass spectrometry analysis, *Talanta*, 85, 919-926.

Itoh, N., Numata, M., Aoyagi, Y. and Yarita, T. (2008) Comparison of low-level polycyclic aromatic hydrocarbons in sediment revealed by Soxhlet extraction, microwave-assisted extraction, and pressurized liquid extraction, *Analytica Chimica Acta*, 612, 44-52.

Jeannot, M.A. and Cantwell, F.F. (1996) Solvent microextraction into a single drop, *Analytical Chemistry*, 68, 2236-2240.

Jenkins, A.L., Ellzy, M.W. and Buettner, L.C. (2012) Molecularly imprinted polymer sensors for detection in the gas, liquid, and vapor phase, *Journal of Molecular Recognition*, 25, 330-335.

Jing, T., Wang, J., Liu, M., Zhou, Y., Zhou, Y. and Mei, S. (2014) Highly effective removal of 2,4-dinitrophenolic from surface water and wastewater samples using hydrophilic molecularly imprinted polymers, *Environmental Science Pollution Research International*, 21, 1153-62.

Jönsson, S., Gustavsson, L. and van Bavel, B. (2007) Analysis of nitroaromatic compounds in complex samples using solid-phase microextraction and isotope dilution quantification gas chromatography-electron-capture negative ionisation mass spectrometry. *Journal of Chromatography A*, 1164, 65-73.

Jowkarderis, M. and Raofie, F. (2012) Optimization of supercritical fluid extraction combined with dispersive liquid-liquid microextraction as an efficient sample preparation method for determination of 4-nitrotoluene and 3-nitrotoluene in a complex matrix, *Talanta*, 15, 50-53.

Juhasz, A.L. and Naidu, R. (2007) Explosives: Fate, dynamics, and ecological impact in terrestrial and marine environments, *Reviews of Environmental Contamination and Toxicology*, 191, 163-215.

Kafilzadeh, F., Shiva, A.H. and Malekpour, R. (2011) Determination of polycyclic aromatic hydrocarbons (PAHs) in water and sediments of the Kor River, Iran, *Middle-East Journal of Scientific Research*, 10, 1-7.

Kalderis, D., Juhasz, A.L., Boopathy, R. and Comfort, S. (2011) Soils contaminated with explosives: Environmental fate and evaluation of state-of-the-art remediation processes (IUPAC technical report), *Pure and Applied Chemistry*, 83, 1407-1484.

Khajeh, M., Yamini, Y. and Hassan, J. (2006) Trace analysis of chlorobenzenes in water samples using headspace solvent microextraction and gas chromatography/electron capture detection, *Talanta*, 69, 1088-1094.

King, A.J., Readman, J.W. and Zhou, J.L. (2004) Determination of polycyclic aromatic hydrocarbons in water by solid-phase microextraction-gas chromatography-mass spectrometry, *Analytica Chimica Acta*, 523, 259–267.

Kjellström, A., Brantlind, M. and Eldsäter, C. (2008) Optimized microwave extraction for trace detection of 2,4,6-trinitrotoluene in soil samples, *Chemosphere*, 71, 1701-1708.

Kootstra, P.R., Straub, M.H.C., Stil, G.H., van der Velde, E.G., Hesselink, W. Land, C.C.J. (1995) Solid-phase extraction of polycyclic aromatic hydrocarbons from soil samples, *Journal of Chromatography A*, 697, 123-129.

Kouzayha, A., Iskandarani, M.A., Mokh, S., Rabaa, A.R., Budzinski, H. and Jaber, F. (2011) Optimization of a solid-phase extraction method using centrifugation for the determination of 16 polycyclic aromatic hydrocarbons in water, *Journal of Agricultural and Food Chemistry*, 59, 7592-760.

Krupadam, R.J., Khan, M.S. and Wate, S.R. (2010) Removal of probable human carcinogenic polycyclic aromatic hydrocarbons from contaminated water using molecularly imprinted polymer, *Water Research*, 44, 681-688.

Kumari, P., Sharma, P., Srivastava, S., and Srivastava, M.M. (2006). Biosorption studies on shelled *Moringa oleifera* Lamarck seed powder: Removal and recovery of arsenic from aqueous system, *International Journal of Mineral Processing*, 78, 131-139.

Larki, A., Nasrabadi, M.R. and Pourreza, N. (2015) UV-vis spectrophotometric determination of trinitrotoluene (TNT) with trioctylmethylammonium chloride as ion pair assisted and disperser agent after dispersive liquid-liquid microextraction, *Forensic Science International*, 251, 77-82.

Lau, E.V., Gan, S. and Ng, H.K. (2010) Extraction techniques for polycyclic aromatic hydrocarbons in soils, *International Journal of Analytical Chemistry*, 2010, 1-9.

Lee, B. (2010) (Villanyi, V. (Ed.)) Sources, distribution and toxicity of polyaromatic hydrocarbons (PAHS) in particulate matter,

Lenardão, E.J., Freitag, R.A., Dabdoub, M.J., Batista, A.C.F. and Silveira, C.C. (2003) Greenchemistry - The 12 principles of green chemistry and it insertion in the teach and research activities, *Química Nova*, 26, 123-129.

Letzel, S., Göen, T., Bader, M., Angerer, J. and Kraus, T. (2003) Exposure to nitroaromatic explosives and health effects during disposal of military waste, *Occupational and Environmental Medicine*, 60, 483-488.

Liang, P., Liu,Y., Guo, L., Zeng, J. and Lu, H. (2004) Multiwalled carbon nanotubes as solid-phase extraction adsorbent for the preconcentration of trace metal ions and their determination by inductively coupled plasma atomic emission spectrometry, *Journal of Analytical Atomic Spectrometry*, 19, 1489-1492.

Librando, V., Hutzinger, O., Tringali, G. and Aresta, M. (2004) Supercritical fluid extraction of polycyclic aromatic hydrocarbons from marine sediments and soil samples, *Chemosphere*, 54, 1189-1197.

Liu, L. (2015) Extraction and enrichment of polycyclic aromatic hydrocarbons by ordered mesoporous carbon reinforced hollow fiber liquid-phase microextraction, *Journal of Separation Science*, 38, 683-689.

López-Montilla, J.C., Pandey, S., Shah, D.O. and Crisalle, O.D. (2005) Removal of non-ionic organic pollutants from water via liquid-liquid extraction, *Water Research*, 39, 1907-1913.

Luo, X., Zhan, Y., Huang, Y., Yang, L., Tu, X. and Luo, S. (2011) Removal of water-soluble acid dyes from water environment using a novel magnetic molecularly imprinted polymer, *Journal of Hazardous Materials*, 187, 274-282.

Ma, J., Ronghui Xiao, R., Jinhua Li, J., Junbao Yu, J., Yanqing Zhang, Y. and Chen, L. (2010) Determination of 16 polycyclic aromatic hydrocarbons in environmental water samples by solid-phase extraction using multi-walled carbon nanotubes as adsorbent coupled with gas chromatography-mass spectrometry, *Journal of Chromatography A*, 1217, 5462-5469.

Mahmoud, M.E., Osman, M.M. and Amer, M.E. (2000) Selective pre-concentration and solid phase extraction of mercury(II) from natural water by silica gel-loaded dithizone phases, *Analytica Chimica Acta*, 415, 33-40.

Manahan, S.E. (1994) Environmental Chemistry, sixth ed. Lewis Publisher, New York.

Marchand, N., Besombes, J.L., Chevron, N., Masclet, P., Aymoz, G. and Jaffrezo, J.L. (2004) Polycyclic aromatic hydrocarbons (PAHs) in the atmospheres of two French alpine valleys: Sources and temporal patterns, *Atmospheric Chemistry and Physics*, *European Geosciences Union*, 4, 1167-1181.

Marvin, C.H., Allan, L., McCarry, B.E. and Bryant, D.W. (1992) A comparison of ultrasonic extraction and soxhlet extraction of polycyclic aromatic hydrocarbons from sediments and air particulate material, *International Journal of Environmental Analytical Chemistry*, 49, 221-230.

Matsui, J., Kato, T., Takeuchi, T., Suzuki, M., Yokoyama, K., Tamiya, E. and Karube, I. (1993) Molecular recognition in continuous polymer rods prepared by a molecular imprinting technique, *Analytical Chemistry*, 65, 2223-2225.

Mills, E. (2012) Lighting the way to explosive detection, Available on: http://www.rsc.org/chemistryworld/2012/06/lighting-way-explosive-detection, Accessed 14 Jun. 2013.

Miquel, L. and Wendy, B. (2010) Anti-cyanobacterial activity of *Moringa oleifera* seeds, *Journal of Applied Phycology*, 22, 503-510.

Mnisi, R.L., Ndibewu P.P. and Mokgalaka, N.S. (2010) Functionalization of a natural biopolymer with aliphatic polyamines and its sorption properties for vanadium removal from aqueous solutions, *South African Journal of Chemistry*, 65, 62-67.

Moja, S.J. and Mtunzi, F. (2013) Application of solid phase extraction (SPE) method in determining polycyclic aromatic hydrocarbons (PAHs) in river water samples, *Journal of Environmental Chemistry and Ecotoxicology*, 5, 278-283.

Nasr, I.N., Arief, M.H. Abdel-Aleem, A.H. and Malhat, F.M. (2010) Polycylic aromatic hydrocarbons (PAHs) in aquatic environment at El Menofiya Governorate, Egypt, *Journal of Applied Sciences Research*, 6, 13-21.

National Environmental Management: Waste Act, 2008 (Act No.59 of 2008) National norms and standards for the assessment of waste for landfill disposal.

Ndabigengesere, A., Narasiah, K.S. and Talbot, B.G. (1995) Active agents and mechanism of coagulation of turbid waters using *Moringa oleifera*, *Water Research*, 29, 703-710.

Nie, D., Han, Z., Yu, Y. and Shi, G. (2016) Composites of multiwalled carbon nanotubes/polyethyleneimine (MWCNTs/PEI) and molecularly imprinted polymers for dinitrotoluene recognition, *Sensors and Actuators B: Chemical*, 224, 584-591.

Nikolaou, A., Kostopoulou, M., Lofrano, G. and Meric, S. (2009) Determination of PAHs in marine sediments: Analytical methods and environmental concerns, *Global NEST Journal*, 11, 391-405.

Norzilah, A.H., Fakhru'l-Razi, A., Choong, T.S.Y. and Chuah, A.L. (2011) Surface modification effects on cnts adsorption of methylene blue and phenol, *Journal of Nanomaterials*, 2011, 1-18.

Oluseyi, T., Olayinka, K., Alo, B. and Smith, R.M. (2011) Comparison of extraction and clean-up techniques for the determination of polycyclic aromatic hydrocarbons in contaminated soil samples, *African Journal of Environmental Science and Technology*, 5, 482-493.

Oxley, J.C. (1993) Non-traditional explosives: Potential detection problems, *Terrorism and Political Violence*, 5, 30-47.

Paden, N.E., Smith, E.E. and Kendall, R.J. (2008), Acute toxicity of 2,4,6-trinitrotoluene, 2,4-dinitrotoluene, and 2,6-dinitrotoluene in the adult bullfrog (Lithobates catesbeiana), *Bulletin of Environmental Contamination and Toxicology*, 80, 487-491.

Parera, J., Santos, F.J. and Ganceran, M.T. (2004) Microwave-assisted extraction versus Soxhlet extraction for the analysis of short-chain chlorinated alkanes in sediments, *Journal of Chromatography A*, 1046, 19-26.

Payán, M.R., López, M.Á.B., Fernández-Torres, R., Mochón, M.C. and Ariza, J.L.G. (2010) Application of hollow fiber-based liquid-phase microextraction (HF-LPME) for the determination of acidic pharmaceuticals in wastewaters, *Talanta*, 82, 854-858.

Pedersen-Bjergaard, S. and Rasmussen, KE. (1999) Liquid-liquid-liquid microextraction for sample preparation of biological fluids prior to capillary electrophoresis, *Analytical Chemistry*, 71, 2650-2656.

Pennington, J.C. and Brannon, J.M. (2002) Environmental fate of explosives, *Thermochimica Acta*, 384, 163-172.

Pichtel, J. (2012) Distribution and fate of military explosives and propellants in soil: A Review, *Applied and Environmental Soil Science*, 2012, 1-33.

Pollard, S.J.T., Thompson, F.E. and McConnachie, G.L. (1995) Microporous carbons from Moringa oleifera husks for water purification in less developed countries, *Water Research*, 29, 337-347.

Psillakis, E. and Kalogerakis, N. (2001) Solid-phase microextraction versus single-drop microextraction for the analysis of nitroaromatic explosives in water samples, *Journal of Chromatography A*, 938, 113-120.

Qiu, Y.W., Zhang, G., Liu, G.Q., Guo, L.L., Li, X.D. and Wai, O. (2009) Polycyclic aromatic hydrocarbons (PAHs) in the water column and sediment core of Deep Bay, South China, *Estuarine, Coastal and Shelf Science*, 83, 60-66.

Rai, A., Mohanty, B. and Bhargava, R. (2016) Supercritical extraction of sunflower oil: A central composite design for extraction variables, *Food Chemistry*, 192, 647-659.

Rashed, M.N. (2013) Adsorption technique for the removal of organic pollutants from water and wastewater. In: Organic pollutants - monitoring, risk and treatment.

Rasmussen, K.E. and Pederson-Bjergaard, S. (2004) Developments in hollow fibre-based, liquid-phase microextraction, *Trends in Analytical Chemistry*, 23, 1-10.

Ravindra, K., Sokhi, R. and Van Grieken, R. (2008) Atmospheric polycyclic aromatic hydrocarbons: Source attribution, emission factors and regulation, *Atmospheric Environment*, 42, 2895-2921.

Reddy, D.H.K., Seshaiah, K., Reddy, A.V.R., Rao, M.M. and Wang M.C. (2010) Biosorption of $Pb^{2+}$ from aqueous solutions by *Moringa oleifera* bark: Equilibrium and kinetic studies, *Journal of Hazardous Materials*, 174, 831–838.

Rengarajan, T., Rajendran, P., Nandakumar, N., Lokeshkumar, B., Rajendran, P., and Nishigaki, I. (2015) Exposure to polycyclic aromatic hydrocarbons with special focus on cancer, *Asian Pacific Journal of Tropical Biomedicine*, 5, 182–189.

Rezaee, M., Assadi, Y., Hosseini, M.R.M., Aghaee, E. Ahmadi, F. and Berijani, S. (2006) Determination of organic compounds in water using dispersive liquid-liquid microextraction, *Journal of Chromatography A*, 1116, 1-9.

Riah, S., Eynollahi, S., Ganjali, M.R. and Norouzi, P. (2010) Computational approach to investigation of template/monomer complex in imprinted polymers; dinitrobenzene sensor, *International Journal of Electrochemical Science*, 5, 509-516.

Richter, B.E., Jones, B.A., Ezzell, J.L., Porter, N.L., Avdalovic, N. and Pohl, C. (1996) Accelerated solvent extraction: A technique for sample preparation, *Analytical Chemistry*, 68, 1033-1039.

Richter-Torres, P., Dorsey, A. and Hodes, C. (1995) Toxicological profile for 2,4,6-trinitrotoluene (TNT), US Department for Health and Human Services, Agency for Toxic Substances and Disease Registry.

Rodriguez, N.M. (1993) A review of catalytically grown carbon nanofibres, *Journal of Materials Research*, 8, 3233-3250.

Rutledge, G.C. and Fridrikh, S.V. (2007) Formation of fibers by electrospinning, *Advanced Drug Delivery Reviews*, 59, 1384-1391.

Saleh, A., Yamini, Y., Faraji, M., Rezaee, M. and Ghambarian, M. (2009) Ultrasound-assisted emulsification microextraction method based on applying low density organic solvents followed by gas chromatography analysis for the determination of polycyclic aromatic hydrocarbons in water samples, *Journal of Chromatography A*, 1216, 6673-6679.

Santos, A.F., Paiva, P.M., Teixeira, J.A., Brito, A.G., Coelho, L.C. and Nogueira, R. (2012) Coagulant properties of Moringa oleifera protein preparations: application to humic acid removal, *Environmental Technology*, 33, 69-75.

Santos, D.T., Veggi, P.C. and Meireles, M.A.A. (2012) Optimization and economic evaluation of pressurized liquid extraction of phenolic compounds from jabuticaba skins, *Journal of Food Engineering*, 108, 444-452.

Sarafraz-Yazdi, A. and Amiri, A. (2010) Liquid-phase microextraction, *Trends in Analytical Chemistry*, 29, 1-14.

Serp, P., Corrias, M. and Kalck, P. (2003) Carbon nanotubes and nanofibers in catalysis, *Applied Catalysis A: General*, 253, 337-358.

Sheikh, F.A., Ju, H.W., Moon, B.M., Park, H.J., Kim, J.H., Lee, O.J. and Park, CH. (2013) A novel approach to fabricate silk nanofibers containing hydroxyapatite nanoparticles using a three-way stopcock connector, *Nanoscale Research Letters*, 8, 303.

Shen, X.E., Shan, X.Q., Dong, D.M., Hua, X.Y. and Owens, G. (2009) Kinetics and thermodynamics of sorption of nitroaromatic compounds to as-grown and oxidized multiwalled carbon nanotubes, *Journal of Colloid and Interface* Science, 330, 1-8.

Shi, Y., Wu, H. , Wang, C., Guo, X., Du, J. and Du, L. (2016) Determination of polycyclic aromatic hydrocarbons in coffee and tea samples by magnetic solid-phase extraction coupled with HPLC-FLD, *Food Chemistry*, 199, 75-80.

Sibiya, P., Chimuka, L., Cukrowska, E. and Tutu, H. (2013) Development and application of microwave assisted extraction (MAE) for the extraction of five polycyclic aromatic hydrocarbons in sediment samples in Johannesburg area, South Africa, *Environmental Monitoring and Assessment*, 185, 5537-5550.

Singh, S. (2007) Sensors - an effective approach for the detection of explosives, *Journal of Hazardous Materials*, 144, 15-28.

Smith-Simon, C. and Goldhaber, S. (1995) Toxicological profile for RDX, US Department for Health and Human Services, Agency for Toxic Substances and Disease Registry.

Sobhi, H.R., Kashtiaray, A., Farahani, H., Javaheri, M. and Ganjali, M.R. (2010) Quantitation of mononitrotoluenes in aquatic environment using dispersive liquid-liquid microextraction followed by gas chromatography-flame ionization detection, *Journal of Hazardous Materials*, 175, 279-283.

Stringer, R.C., Gangopadhyay, S. and Grant, S.A. (2010) Detection of nitroaromatic explosives using a fluorescent-labeled imprinted polymer, *Analytical Chemistry*, 82, 4015-4019.

Sumathi, T. and Alagumuthu, G. (2014) Adsorption studies for arsenic removal using activated *Moringa oleifera*, *International Journal of Chemical Engineering*, 2014, 1-6.

Sun, F.D., and Gibson, M.D. (1998) Ultrasonication extraction and solid phase extraction clean-up for determination of US EPA 16 priority pollutant polycyclic aromatic hydrocarbons in soils by reversed-phase liquid chromatography with ultraviolet absorption detection, *Analytica Chimica Acta*, 364, 1-11.

Sun, J.Q., Qiao, B. and Sun, D.S. (2014) determination of polycyclic aromatic hydrocarbons in wastewater by single-drop microextraction coupled to capillary gas chromatography, *Advanced Materials Research*, 838-841, 2582-2585.

Tachon, R., Pichon, V., Le Borgne, M.B. and Mine, J.J. (2007) Use of porous graphitic carbon for the analysis of nitrate ester, nitramine and nitroaromatic explosives and by-products by liquid chromatography–atmospheric pressure chemical ionisation-mass spectrometry, *Journal of Chromatography A*, 1154, 174-181.

Tao, S., Li, G. and Yin, J. (2007) Fluorescent nanofibrous membranes for trace detection of TNT vapor, *Journal of Materials Chemistry*, 17, 2730-2736.

Tavengwa, N.T., Cukrowska, E. and Chimuka, L. (2016) Application of raw and biochared *Moringa oleifera* seed powder for the removal of nitrobenzene from aqueous solutions, *Desalination and Water Treatment*, In Press.

Tavengwa, N.T., Hintsho, N., Durbach, S., Weiersbye, I., Cukrowska, E. and Chimuka, L. (2016) Extraction of explosive compounds from aqueous solutions by solid phase extraction using β-cyclodextrin functionalized carbon nanofibers as sorbents, *Journal of Environmental Chemical Engineering*, 4, 2450-2457.

Thurman, E.M. and Ferrer, I. (2012) Adapting EPA Method 833B for analysis of explosives in water to SPE and LC/MC/MS, Agilent Technologies.

Timofeeva, I., Medinskaia, K., Nikolaeva, L., Kirsanov, D. and Bulatov, A. (2016) Stepwise injection potentiometric determination of caffeine in saliva using single-drop microextraction combined with solvent exchange, *Talanta*, 150, 655-660.

Tobiszewski, M., Bigus, P. and Namieśnik, J. (2014) Determination of parent and methylated polycyclic aromatic hydrocarbons in water samples by dispersive

liquid–liquid microextraction-two dimensional gas chromatography-time-of-flight mass spectrometry, *Analytical Methods*, 6, 6678-6687.

Townsend, D.M. and Myers, T.E. (1996) Recent developments in formulating model descriptors for subsurface transformation and sorption of TNT, RDX, and HMX, Tech. Rep. IRRP- 96-1, US Army Engineer Waterways Experiment Station, Vicksburg, Miss, USA.

Tudoran, M.A. and Putz, M.V. (2012) Polycyclic aromatic hydrocarbons: from *In Cerebro* to *In Silico* eco-toxicity fate, *Chemical Bulletin of "Politehnica" University of Timisoara, ROMANIA*, 57, 50-53.

U.S. Environmental Protection Agency, 1986. Quality Criteria for Water 1986, Office of Water Regulations and Standards, Washington, D.C., EPA 440/5-86-001.

Wackerlig, J. and Schirhagl, R. (2016) Applications of molecularly imprinted polymer nanoparticles and their advances toward industrial use: A Review, *Analytical Chemistry*, 88, 250-261.

Wang, G.J., Tian, L., Fan, Y.M. and Qi, M.L. (2013) Headspace single-drop microextraction gas chromatography mass spectrometry for the analysis of volatile compounds from Herba Asari, *Journal of Analytical Methods in Chemistry*, 2013, 1-6.

Wang, N., Guo, Y., Wang, L., Liang, X., Liu S. and Jiang, S. (2004) Preparation of an aminopropyl imidazole-modified silica gel as a sorbent for solid-phase extraction of carboxylic acid compounds and polycyclic aromatic hydrocarbons, *Analyst*, 139, 2531-2537.

Wang, X.Y., Kim, Y.G., Drew, C., Ku, B.C., Kumar, J. and Samuelson, L.A. (2004) Electrostatic assembly of conjugated polymer thin layers on electrospun nanofibrous membranes for biosensors, *Nano Letters*, 4, 331-334.

Wang, G.J., Tian, L., Fan, Y.M. and Qi, M.L. (2013) Headspace single-drop microextraction gas chromatography mass spectrometry for the analysis of volatile compounds from Herba Asari, *Journal of Analytical Methods in Chemistry*, 2013, 1-6.

Ward, K.J. (1943) Occurrence of Cellulose, in: Cellulose and cellulose derivatives, Ott, E. (ed.), Interscience, New York, 7-25.

Warhurst, A.M., McConnachie, G.L. and Pollard, S.J.T. (1997) Characterisation and applications of activated carbon produced from *Moringa oleifera* seed husks by single-step steam pyrolysis, *Water Research*, 31, 759-766.

Wu, H., Li, G., Liu, S., Hu, N., Geng, D., Chen, G., Sun, Z., Zhao, X., Lian Xia, L. and You, J. (2016) Monitoring the contents of six steroidal and phenolic endocrine disrupting chemicals in chicken, fish and aquaculture pond water samples using pre-column derivatization and dispersive liquid-liquid microextraction with the aid of experimental design methodology, *Food Chemistry*, 192, 98-106.

Wu, S. and Yu, W. (2012) Liquid-liquid extraction of polycyclic aromatic hydrocarbons in four different edible oils from China, *Food Chemistry*, 134, 597-601.

Wu, Y., Xia, L., Chen, R., Hu, B. (2008) Headspace single drop microextraction combined with HPLC for the determination of trace polycyclic aromatic hydrocarbons in environmental samples, *Talanta*, 74, 470-477.

Wynn, C.M., Palmacci, S., Kunz, R.R. and Rothschild, M.A. (2008) Novel method for remotely detecting trace explosives. Available on: http://www.ll.mit.edu/ publications/journal/pdf/vol17_no2/17_2_1Wynn.pdf.

Xia, X., Zhou, C., Huang, J., Wang, R. and Xia, N. (2013) Mineralization of phenanthrene sorbed on multiwalled carbon nanotubes, *Environmental Toxicology*, 32, 894-901.

Xiao, Q. and Hu, B. (2010) Hollow fiber-liquid phase microextraction combined with gas chromatography for the determination of phenothiazine drugs in urine, *Journal of Chromatography B*, 878, 1599-1604.

Xu, L., Basheer, C. and Lee, H.K. (2007) Developments in single-drop microextraction, *Journal of Chromatography A*, 1152, 184-192.

Yang, H.H., Zhou, W.H., Guo, X.C., Chen, F.R., Zhao, H.Q., Lin, L.M. and Wang, X.R. (2009) Molecularly imprinted polymer as SPE sorbent for selective extraction of melamine in dairy products, *Talanta*, 80, 821-825.

Yin, J., Yang, G. and Chen, Y. (2005) Rapid and efficient chiral separation of nateglinide and its L-enantiomer on monolithic molecularly imprinted polymers, *Journal of Chromatography A*, 1090, 68-75.

Zhao, R., Chu, S. and Xu, X. (2004) Optimization of nonequilibrium liquid-phase microextraction for the determination of nitrobenzenes in aqueous samples by gas chromatography-electron capture detection, *Analytical Sciences*, 20, 663-666.

Zheng, J., Liu, B., Ping, J., Chen, B., Hongjing Wu, H. and Zhan, B. (2015) Vortex- and shaker-assisted liquid–liquid microextraction (vsa-llme) coupled with gas chromatography and mass spectrometry (GC-MS) for analysis of 16 polycyclic aromatic hydrocarbons (PAHs) in offshore produced water, *Water, Air, and Soil Pollution*, 226, 318.

Zhou, X.F., Cui, S., Liu, Y., Liu, X.Y., Shen, X.D. and Wu, Z.W. (2013) Adsorption capacity of hydrophobic $SiO_2$ aerogel/activated carbon composite materials for TNT, *Science China Technological Science*, 56, 1767-1772.

# Appendix

**Paper VI**

This paper “Equilibrium and kinetic studies on the adsorption of humic acid unto cellulose and activated carbon sorbents,” was published in *Desalination and Water Treatment*. It investigated the sorption of humic acid unto a natural and synthetic sorbents: cellulose and activated carbon, respectively. Full concentration and time dependent models were studied.

*Desalination and Water Treatment*
www.deswater.com
doi: 10.1080/19443994.2015.1082510

57 (2016) 16843–16854
August

Taylor & Francis
Taylor & Francis Group

# Equilibrium and kinetic studies on the adsorption of humic acid onto cellulose and powdered activated carbon

Nikita Tawanda Tavengwa[a,b,*], Luke Chimuka[b], Lilian Tichagwa[a,c]

[a]*Department of Pure and Applied Chemistry, University of Fort Hare, Alice Campus, Private Bag X1314, Alice 5700, South Africa, email: nikita.tavengwa@students.wits.ac.za (N.T. Tavengwa)*
[b]*Molecular Sciences Institute, School of Chemistry, University of Witwatersrand, Private Bag 3, Johannesburg 2050, South Africa*
[c]*Department of Polymer Science & Engineering, Harare Institute of Technology, P.O. Box BE 277, Belvedere, Harare, Zimbabwe*

Received 18 March 2015; Accepted 7 August 2015

ABSTRACT

The removal of humic acid (HA) from aqueous solution onto cellulose (CE) and powdered activated carbon (PAC) was investigated in a batch adsorption system as a function of pH, sorbent mass and contact time. The optimum conditions for HA uptake by CE were 2–3, 50 mg and 30 min, respectively. For PAC, they were 2, 50 mg and 30 min, respectively. PAC and CE sorbents were characterized by Fourier transform infrared spectroscopy and scanning electron microscopy. The kinetic adsorption data was analysed on the basis of Lagergren pseudo-first-order, pseudo-second-order, Bangham and the interparticle diffusion models. The Lagergren pseudo-first-order fitted the kinetic data best. Experimental sorption data were fitted on different adsorption isotherm models, and it was established that the fitting followed the order: Langmuir > Freundlich > Temkin > Dubinin–Radushkevich (D–R). According to the Langmuir isotherm models, the maximum adsorption capacities of CE and PAC for HA were 89.3 and 30.4 mg $g^{-1}$, respectively.

*Keywords:* Humic acid; Cellulose; Activated carbon; Kinetics; Adsorption; Modelling

## 1. Introduction

Humic acids (HAs) are complex products of decaying vegetation, and are usually aromatic and acidic in nature [1]. The presence of HA in water resources has been of concern in water supply and there is considerable practical interest to minimize the presence of these compounds in drinking water [2]. Humic substances adversely affect water quality in several ways, causing undesirable colour and taste [3]. The presence of HAs in water does not directly cause toxicity but can (after disinfection process) result in the production of undesirable and dangerous post reactive molecules called disinfectant by-products [4]. HA can react with chlorine during water treatment producing trihalomethanes (THMs) which are carcinogenic substances [5]. The United States Environmental Protection Agency (USEPA) commends a maximum contamination level of below 80 μg $L^{-1}$ for THMs in drinking water [6]. THMs can be reduced by removing humic materials prior to chlorination [7]. HAs have many organic functional groups that provide abundant potential binding sites for various pollutants, which also influences contaminants' dispersion and mobility in the environment. HA elimination from aqueous solution is of great significance. Furthermore,

*Corresponding author.

1944-3994/1944-3986 © 2015 Balaban Desalination Publications. All rights reserved.

HA is thought to be one of the major reasons for the transport of metal ions in the environment [8]. There are several methods used to remove HA in natural water, including electrocoagulation [9], membrane technologies [10], photocatalytic degradation on Ti-modified silica [11] and adsorption [12,13]. Among these methods, adsorption is generally regarded as a promising method, and has been extensively studied for the removal of humic substances.

Activated carbon (AC) is a widely used adsorbent for industrial water treatment as well as municipal water purification [1,14]. It is a highly porous amorphous solid consisting of microcrystallites with a graphite lattice structure. The preparation involves carbonization where a carbonaceous material is exposed to elevated temperatures of between 400 and 600°C in an oxygen-deficient atmosphere. This is followed by activation, where carbonized particles are subjected to a stream of $CO_2$ at high temperatures. AC can be in powdered (PAC) or granulated (GAC) form which is a form of AC with a high surface area and adsorbs many toxic compounds. Since it is from a non-renewable source, there is need for an alternative. AC is also expensive [15,16] which is becoming unaffordable to poor municipalities in developing countries in Asia and Africa. The fouling rate of AC adsorbent is high so the replacement rate or the regeneration efficiency is also high. Since AC is in the powdered form, it makes handling a big problem.

Cellulose (CE) was selected as a sorbent in this work because it is a natural organic compound with the formula $(C_6H_{10}O_5)_n$ and is the most abundant organic polymer on earth [17,18]. This insoluble polysaccharide consists of a linear chain of several hundreds to over ten thousands β(1 → 4) glycosidicly linked D-glucose units. CE is mainly obtained from wood pulp and cotton because structural component of plants are formed primarily from cellulose. It forms crystals (cellulose $I_a$) where intramolecular (O3–H → O5′ and O6 →H–O2′) and intrastrand (O6–H → O3′) hydrogen bonds hold the network flat, allowing the more hydrophobic ribbon faces to stack [19]. Each residue is oriented 180° to the next with the chain synthesized two residues at a time [20]. Although individual strands of cellulose are intrinsically no less hydrophilic, or no more hydrophobic, than some other soluble polysaccharides (such as amylase), this tendency to form crystals utilizing extensive intra- and intermolecular hydrogen bonding makes it completely insoluble in normal aqueous solutions.

In the light of the above-mentioned negative effects of the HA's presence in water, this research aims to study the effects of parameters such as initial pH, sorbent mass (PAC and CE), contact time and initial concentration on adsorption efficiency of HA by cellulose and powdered activated carbon (PAC). Kinetic and adsorption modelling studies were done to determine the rate limiting steps and gain some mechanistic information.

## 2. Materials and methods

### 2.1. Chemicals and reagents

HA was bought from Sigma Aldrich (Steinheim, Germany). The pH of the $KNO_3$ solution was adjusted with NaOH and HCl. Cellulose was bought from Merck (Darmastadt, Germany), while AC was obtained from Sigma Aldrich (Steinheim, Germany). All other chemicals used were of analytical reagent grade from Merck (Darmastadt, Germany), and were used without further purification.

Perkin Elmer UV–vis Lamda 25 spectrophotometer (MA, USA) was used for the analysis of humic acid concentration. For mechanical agitation, a Wisecube Fuzzy Control System from Wisd Laboratory Instruments was used at 155 rpm at a fixed temperature of 37°C. A Rotofix 32 A Centrifuge from Hettich Lab Technology (Tuttlingen, Germany) was used to separate the HA solution from the sorbent, and was set at 3,000 rpm. Fourier transform infrared spectroscopy (FTIR) analysis was done as KBr disc on a Perkin Elmer Paragon 2000 FTIR spectrophotometer (Shelton, USA) in the range 400–4,000 $cm^{-1}$. For morphological feature studies of the sorbents, scanning electron microscopy (SEM), FEI Quanta 200 at 5 kV was used. Ultrapure water (Milli-Q, MA, USA) was used in all experiments. A 766 Calimatic pH meter, equipped with a Shott N61 pH electrode from Knick (Berlin, Germany) was used to measure pH.

### 2.2. Preparation of HA stock and standard solutions

HA (0.25 g) was transferred to a 250-mL volumetric flask where 3.3 mL of 1 M NaOH was added to necessitate its complete dissolution. The flask was shaken then topped up to the mark with distilled water. The stock solution was stored at 25°C in a dark cupboard when not in use. Standard solutions (5–250 mg $L^{-1}$) were then prepared in 100-mL volumetric flasks from the HA stock solution. The calibration curve for the absorption of HA gave a good linear curve with a correlation coefficient ($R^2$) value of 0.999, and was confidently used for quantification. The molar absorption coefficient of HA is equal to the gradient of the calibration curve, and was determined to be 0.0053 L $mol^{-1}$ $cm^{-1}$.

### 2.3. Determination of physicochemical properties of the sorbents

#### 2.3.1. Determination of moisture content

Moisture content of PAC and CE was determined by weighing 3 g of the sorbent into a crucible. This was placed in the oven and heated for 3 h at a constant temperature of 120°C. The sample was then removed and put into a desiccator in order to prevent moisture uptake from the atmosphere before the sample was reweighed. This procedure was repeated until a constant weight was obtained. The difference in the mass constituted the amount of moisture content of the adsorbent.

#### 2.3.2. Determination of loss of mass on ignition

The determination of loss of mass on ignition was done by weighing 5 g of the PAC adsorbent and put inside a furnace at constant temperature of 600°C for 1.5 h. After heating, the sample was removed and put in a desiccator to cool. The residual product was then weighed, and the difference in mass represented the mass of organic material.

#### 2.3.3. Determination of point of zero charge ($pH_{pzc}$)

For the point of zero charge ($pH_{pzc}$) determination, 0.1 mol $L^{-1}$ $KNO_3$ solution was prepared, and its initial pH ($pH_i$) was adjusted to between 1 and 12 using NaOH and HCl in different test tubes. A 12 mL aliquot of pH-adjusted $KNO_3$ and 100 mg of adsorbent were then mixed in a test tube and placed in a Wisecube shaker at 37°C set at 155 rpm. After 24 h, the mixture was centrifuged for 5 min at 3,000 rpm, and the final pH ($pH_f$) of the solution was measured. This was done for each pH.

### 2.4. Batch adsorption

HA solution was transferred to a 100-mL conical flask were 50 mg of the sorbent (PAC or CE) was placed. The mechanical agitation of the mixture in a Wisecube Fuzzy Control System for maximum sorption of HAs was ensured through a steady shaking of 155 rpm. At too high stirring speed, the shaking became violent and the HA sorption was affected by the generation of air bubbles. The HA-adsorbent mixture was then allowed to equilibrate for preset HA initial pH (2–11). Mass of sorbent (10–500 mg), agitation time (5–120 min) and initial HA concentration (20–250 mg $L^{-1}$) were also optimized. After sorption, the mixture was centrifuged for 5 min before the supernatant was analysed for HA using a Perkin Elmer UV–vis spectrophotometer set at a wavelength of 465 nm which was a wavelength used by other researchers [21,22]. All experiments were done in triplicate at 37°C by varying one parameter and fixing the rest. The influence of adsorption parameters was evaluated by calculating the adsorption capacity, $q$ (mg $g^{-1}$) defined as mass of substrate bound on a gram of adsorbent (Eq. (1)).

$$q = \frac{(C_o - C_e)V}{m} \tag{1}$$

where $C_o$ (mg $L^{-1}$) is the initial concentration, and $C_e$ (mg $L^{-1}$) represents the final equilibrium concentration after adsorption. $V$ (L) is the volume of the sample solution and $m$ (g) the mass of the adsorbent.

### 2.5. Kinetic model estimation

The kinetics of adsorption is important as it controls process efficiency. Kinetic studies were carried out to determine the rate and mechanism of reactions. In the present investigation, pseudo-first-order, pseudo-second-order, intraparticle diffusion and the Bangham's models were studied to determine the rate-limiting step of HA sorption onto surfaces of CE and PAC sorbents across the liquid phase.

A simple kinetic analysis of adsorption can be expressed by a pseudo-first-order equation (Lagergren equation) [23], as shown in Eq. (2):

$$\log(q_e - q_t) = \log q_e - \frac{k_1}{2.303}t \tag{2}$$

where $q_e$ and $q_t$ are the loading capacities (in mg $g^{-1}$) at equilibrium and at time $t$ (min), respectively. The rate constant $k_1$ ($min^{-1}$) was determined from the slope of a plot of $\log(q_e - q_t)$ vs. $t$.

For the pseudo-second-order chemisorption kinetic, the rate equation can be expressed as [24]:

$$\frac{t}{q_t} = \frac{1}{k_2 q_e^2} + \frac{1}{q_e}t \tag{3}$$

where $k_2$ is the rate constant of pseudo-second-order (g mg $min^{-1}$) obtained from the intercept of the plot of $t/q_t$ vs. $t$. The other terms are as previously defined.

To examine the diffusion mechanism of the adsorption process, the Weber and Morris intraparticle diffusion model [25] was applied to analyse the kinetic results:

$$q_t = k_{id} t^{1/2} + C \quad (4)$$

where $k_{id}$ (mg g$^{-1}$ min$^{-0.5}$) is the diffusion rate constant, and $C$ reflects the boundary layer effect. If intraparticle diffusion is involved, then the plot $q_t$ vs. $t^{1/2}$ gives a straight line with the slope $k_{id}$ and the intercept, $C$.

The slowest step in the adsorption process can be determined by plotting the kinetic data with Bangham equation [26] which is expressed as:

$$\log \log \frac{C_o}{C_o - q_t m} = \log \frac{k_o}{2.303V} + \alpha \log t \quad (5)$$

where $C_o$ is the initial concentration of the solution (mg L$^{-1}$), $V$ (L) is the volume of the solution, $m$ is the mass of the adsorbent used per litre of the solution (g L$^{-1}$), $q_t$ (mg g$^{-1}$) is the amount of the adsorbent retained at time $t$ (min), and $\alpha$ and $k_o$ are constants.

### 2.6. Adsorption modelling

Sorption equilibrium is usually described by isotherm equations whose parameters express the surface properties and affinity of the sorbent at a fixed temperature and pH [27]. Distribution of HA between the liquid phase and the solid phase (PAC and CE) can be described by several isotherm models, four of which were considered in this study; Langmuir, Freundlich, Dubinin–Radushkevich and Temkin isotherms.

The Langmuir isotherm assumes that the highest adsorption happens when a saturated monolayer of solute molecules exists on the adsorbent surface (homogenous system) [28].

$$\frac{1}{q_e} = \frac{1}{q_m b C_e} + \frac{1}{q_m} \quad (6)$$

where $q_e$ is the adsorbed amount (mg g$^{-1}$) of HA and $C_e$ is the equilibrium concentration in solution (mg L$^{-1}$). $q_m$ is the monolayer adsorption capacity (mg g$^{-1}$) and $b$ is the constant related to the free energy of adsorption (L mg$^{-1}$) obtained from the plot of Eq. (6). The essential features of Langmuir adsorption isotherm parameter can be used to predict the affinity between the sorbate and sorbent using a dimensionless constant called separation factor or equilibrium parameter ($R_L$), which is expressed by the following relationship:

$$R_L = \frac{1}{(1 + bC_o)} \quad (7)$$

where $b$ (L mg$^{-1}$) is the Langmuir constant and $C_o$ (mg L$^{-1}$) is the initial concentration. The value of $R_L$ provides information as to whether the adsorption is irreversible ($R_L = 0$), favourable ($0 < R_L < 1$), linearly favourable ($R_L = 1$) or unfavourable ($R_L > 1$).

The Freundlich isotherm model is an empirical relationship describing the adsorption of solutes from a liquid to a solid surface, and assumes that different sites with several adsorption energies are involved, and is represented by Eq. (8) [29].

$$\log q_e = \log k_F + \frac{1}{n} \log C_e \quad (8)$$

where $q_e$ is the amount of HA adsorbed per unit mass of adsorbent (mg g$^{-1}$) and $C_e$ is the concentration of HA at equilibrium (mg L$^{-1}$). $k_F$ (L mg$^{-1}$) roughly shows the adsorption capacity and $1/n$ represents the adsorption intensity.

Dubinin–Radushkevich isotherm does not assume a homogeneous surface or constant sorption potential. It is commonly applied in the following form [30]:

$$\ln q_e = \ln q_m - \beta_D \varepsilon^2 \quad (9)$$

where $q_m$ (mg g$^{-1}$) is maximum adsorption capacity and $\beta_D$ (mol$^2$ J$^{-2}$) is the activity coefficient associated with adsorption energy. The Polanyi potential ($\varepsilon$) is given in Eq. (10), $R$ (J mol$^{-1}$ K$^{-1}$) is the universal gas constant and $T$ (K) is temperature. $\beta_D$ and $q_m$ are calculated from the slope and intercept of the plot $\ln q_e$ vs. $\varepsilon^2$, respectively. The mean adsorption energy, $E$ (kJ mol$^{-1}$), is obtained from Eq. (11) and its value determines the type of adsorption process as physical ($E < 8$ kJ mol$^{-1}$) or chemical ($E > 16$ kJ mol$^{-1}$).

$$\varepsilon = RT \ln\left(1 + \frac{1}{C_e}\right) \quad (10)$$

$$E = \frac{1}{\sqrt{(2B_D)}} \quad (11)$$

By ignoring the extremely low and large values of concentration, the Temkin isotherm model assumes that the heat of adsorption of all molecules in a layer would decrease linearly rather than logarithmically with coverage. Its derivation is characterized by a uniform distribution of binding energies up to some maximum binding energy, which was determined by plotting the quantity sorbed $q_e$ against $\ln C_e$. The constants were determined from the slope and intercept of Eq. (12) [31].

$$q_e = \frac{RT}{b_T} \ln A_T + \frac{RT}{b_T} \ln C_e \quad (12)$$

where $A_T$ (L g$^{-1}$) and $b_T$ are the Temkin isotherm equilibrium binding constants.

## 3. Results and discussion

### 3.1. Characterization studies

HA can be characterized as a loose assembly of aromatic polymer of varying acidity and reactivity with a hypothetical structure as shown in Fig. 1. Table 1 summarizes some important physicochemical characteristics of the sorbents (PAC and CE).

Moisture content is an essential component of any sorbent material which determines the ability of the sorbent to hold the moisture. Moisture content depends on many factors such as the composition of the sorbent, thus the different values for CE and PAC which were 6.7 and 7.0%, respectively. A material with high moisture content has a high porosity and the active groups are spaced further apart from each other [33].

FTIR spectra of CE, HA, and CE–HA complex were investigated to determine the functional groups which participated in the formation of the complex (Fig. 2). The shaded bands are included to highlight the several differences in the three spectra. For HA, the prominent peak at 3,439.03 cm$^{-1}$ confirmed that it had hydroxyl groups. This band, due to –OH, was one of the functional groups used in the adsorption of HA to the CE adsorbent. The peak at 1,611.57 cm$^{-1}$ signified the presence of double bonds. The bond at 1,622.18 cm$^{-1}$ suggested the presence of double bonds in CE. HA itself have been found to be a good sorbent for different analytes such as metal ion contaminants [34] because of its functional groups. Previous FTIR studies have shown absorbance wavelengths at 3,416, 2,916, 1,638, 1,417, 1,323, 1,161, 1,046 and 895 cm$^{-1}$ to be associated with native cellulose [35,36]. The FTIR spectrum of CE–HA was basically an overlap of the CE's and HA's. There were bonds in HA which were not present in its spectrum but appeared in that of the CE–HA complex (1,430 and 1,300 cm$^{-1}$). However, bands at 900, 825, 700, 450 and 440 cm$^{-1}$ were strongly present in the pure HA spectrum but their intensity

Table 1
Physicochemical properties of the sorbents

| Sorbent property | Sorbent | |
|---|---|---|
| | CE | PAC |
| Colour | White | Black |
| Specific gravity (g cm$^{-3}$) | 1.62 | 0.8–2.1 |
| Moisture content (%) | 6.7 | 7.0 |
| Loss of mass on ignition (%) | – | 8.9 |
| Point of zero charge ($pH_{pzc}$) | 7.8 | 9.2 |
| BET surface area (m$^2$ g$^{-1}$) | 102 | 834 |

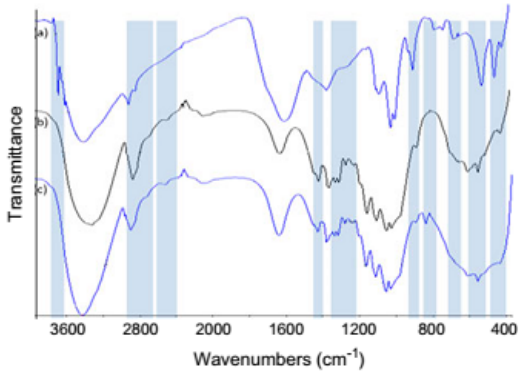



Fig. 2. FTIR spectra of (a) HA, (b) CE and (c) CE–HA complex (shaded regions highlight the differences).

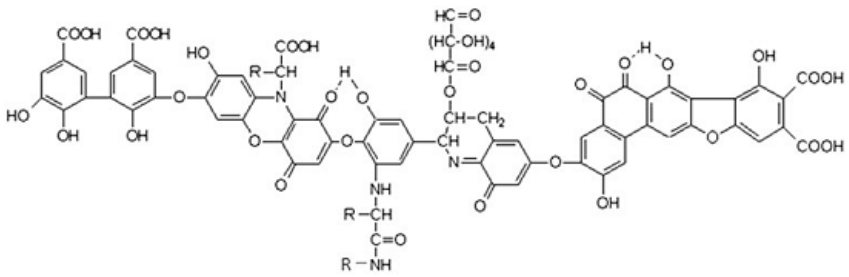



Fig. 1. A model structure of HA [32].

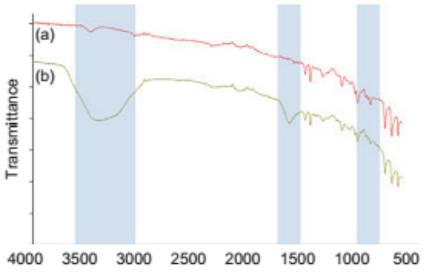



Fig. 3. FTIR spectra of (a) PAC and (B) PAC–HA complex (shaded regions highlight the differences).

were greatly diminished in the spectrum of the complex. The absorption band of the carboxyl group at 1,700 $cm^{-1}$ for CE remained considerably strong after reaction with HA indicating that only part of the carboxyl group participated in the bonding process.

Fig. 3 shows an FTIR spectrum of PAC with no detail in the functional group region. However, after adsorption of HA from a solution, several adsorption bands appeared both in the functional group and the fingerprint regions. The presence of the band around 3,350 $cm^{-1}$ was indicative of the hydroxyl ions from water where the HA was spiked. The C=C bond of the HA was observed in the PAC–HA complex and was an indication of bonding between PAC and HA.

The surface physical morphology of the sorbents was evaluated by SEM. Both the SEM images showed surfaces that were not smooth (Fig. 4). This is an important surface feature, as the roughness of the sorbent meant high available surface area for HA adsorption. The pores on the surface enhanced the mass transfer of the HA from the bulk solution to the pores of the sorbent.

### 3.2. Effect of pH and point of zero charge ($pH_{pzc}$)

The surfaces of the sorbents (CE and PAC) and HA were affected differently by basic and acidic conditions, as such, different adsorption values were observed at different pH values. Solution pH strongly influences the surface charge of the adsorbing material, degree of ionization process of HA molecules, and this parameter was investigated in the pH range of 2–11 (Fig. 5). For the determination of point of zero charge ($pH_{pzc}$), a plot of ΔpH vs. $pH_i$ was used (Fig. 6). The pH value where ΔpH = 0 was the point of zero charge ($pH_{pzc}$), which is the pH at which the total number of positive and negative charges on its surface becomes zero was found to be 9.2 for CE. It has been found that the $pH_{pzc}$ of chitosan, which is structurally related to cellulose, was 6.6 [2]. At pH < 9.2, the surface of the cellulose was taken as positive, and the HA, which is negatively charged due to its $pH_{pzc} \approx 2$ [37] was adsorbed strongly by electrostatic attraction. It can be seen from the hypothetical structure of HA that the –COOH, –OH and –NH groups are negative centre carriers. The increase in the number of negatively charged sites on cellulose beyond $pH_{pzc}$ resulted in electrostatic repulsion with the HA molecules and lower adsorption capacities were thus recorded. The same pH trend was found by Song et al. [38] who modified graphene oxide nanosheets with cyclodextrin in an investigation of HA removal.

Effect of pH on HA sorption onto PAC followed a similar trend to that of CE (Fig. 5). HA molecules generally gain excess negative surface charge as the pH is increased due to deprotonation, firstly by the carboxylic groups at pH values of 4–6, followed by the dissociation of phenolic groups at higher pH [39,40]. From Fig. 6, the $pH_{pzc}$ of PAC was found to be 7.8. In another research, it was observed that $pH_{pzc}$ of AC cloth in $KNO_3$ aqueous solutions was at pH 7.0 [41]. $pH_{pzc}$ of 7.98 of

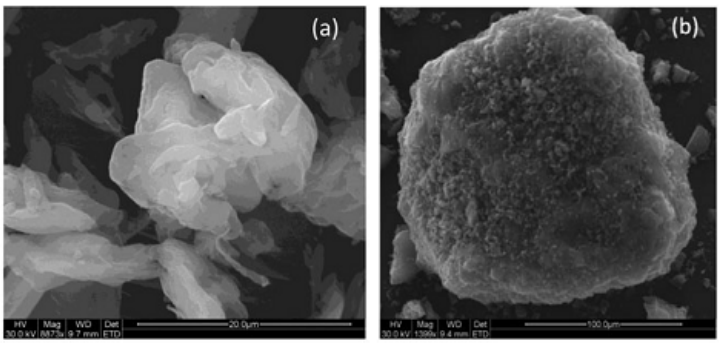



Fig. 4. SEM micrography of (a) CE and (b) PAC.

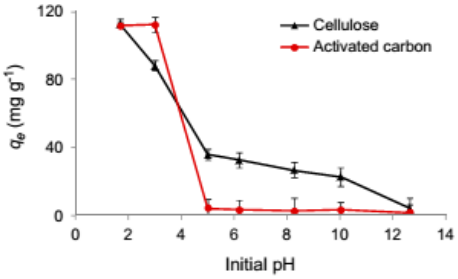



Fig. 5. Effect of initial pH on the adsorption of HA on PAC and cellulose ($n$ = 3). (Sample volume = 25 mL, HA concentration = 200 mg L$^{-1}$, contact time = 50 min, sorbent (CE and PAC) weight = 50 mg, temperature = 37°C.)

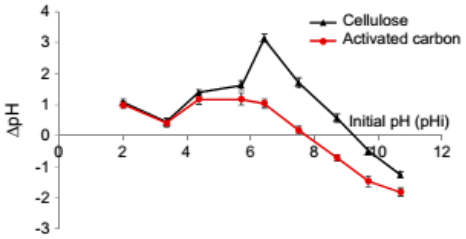



Fig. 6. Determination of point of zero charge ($pH_{pzc}$) of HA adsorbed on PAC and cellulose by varying the inital pH ($n$ = 3).

pyrolytically prepared AC from *Fagopyrum esculentum* Moench was obtained by Kibami et al. [42]. Just like in this study, Diaz-Flores et al. [43] used an anionic molecule, 2,4-dichlorophenoxyacetic acid, for sorption unto AC cloth and reported a $pH_{pzc}$ of 9.41 and the maximum sorption they recorded was at pH 2–3.

### 3.3. Effect of sobent mass

The effect of the sobent mass on the removal of HA from aqueous solution was investigated by varying the mass of the adsorbent (CE and PAC) from 10 to 500 mg (Fig. 7). It is expected that an increase in the mass of adsorbent should yield a corresponding increase in the amount of HA adsorbed onto the surface of the adsorbent since there will be more adsorption sites available. Therefore, competition for binding sites between molecules of the adsorbate decreased with increase in mass of the adsorbent. With increasing adsorbent dose, the removal efficiency increased and corresponding adsorbed quantity per unit mass decreased. The best mass was found to be 50 mg for both sorbents and was used in subsequent experiments.

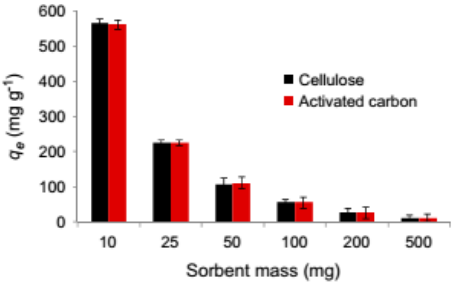



Fig. 7. Effect of sorbent mass on the adsorption of HA on PAC and cellulose ($n$ = 3). (Sample volume = 25 mL, HA concentration = 200 mg L$^{-1}$, contact time = 50 min, temperature = 37°C.)

### 3.4. Effect of contact time

The contact time between HA adsorbate and the sorbent (CE and PAC) is of great importance in the design of a sorption systems and large-scale applications. Therefore, time-dependent experiments were conducted in the range of 5–120 min at 37°C (Fig. 8). As can be seen, the maximum sorption was achieved after 30 min for both sorbents. This was an indication that the sorption of HA on both sorbents was a fast mass transfer. The fast sorption rate could have been due to a great availability of surface area/binding sites on the sorbents during the initial stages. Generally, HA molecules will bind to all the active sites until they are fully occupied. Hence, with time, fewer active sites are available leading to a reduction in the amount of HA adsorbed.

### 3.5. Effect of initial concentration

Initial concentration is an important parameter which may provide an important driving force to overcome all mass transfer resistance of adsorbate

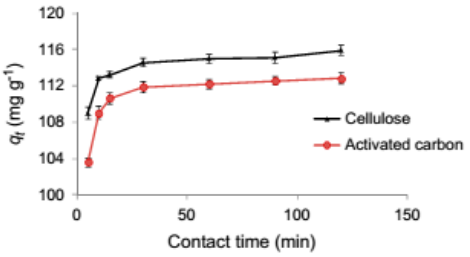



Fig. 8. Effect of contact time of HA adsobed on PAC and cellulose ($n$ = 3). (Sample pH 4, sample volume = 25 mL, HA concentration = 200 mg L$^{-1}$, sorbent (CE and PAC) weight = 50 mg, temperature = 37°C.)

between the aqueous and solid phases. It influences the rate at which adsorbate molecules move from the bulk solution to the adsorbent surface [27]. Increasing initial concentration enhanced the adsorption capacity of HA (Fig. 9). This trend was also observed by Mousavi et al. [4]. The almost linear dependency might have been due to the unsaturation of binding sites of CE and PAC which resulted in an increase in the HA removal. As shown in Fig. 9, when the initial concentration of aqueous HA solution was changed from 20 to 250 mg $L^{-1}$, the absolute amount of HA adsorbed per unit mass of cellulose and PAC also increased.

### 3.6. Kinetic modelling

The rate constants of pseudo-first-order ($k_1$) were found to be 0.029 and 0.030 $min^{-1}$ for HA adsorption onto CE and AC, respectively (Table 2). The comparison of $q_e$ values from experimental work ($q_{e,exp}$ = 109.4 and 111.8 mg $g^{-1}$) of this study and the calculated ones ($q_{e,cal}$ = 5.06 and 5.32 mg $g^{-1}$) of pseudo-first-order kinetic model showed a large difference. This did not show the suitability of this model. Furthermore, the degree of linearity for these kinetic model plots was judged from the value of the correlation coefficients. The correlation coefficients ($R^2$) were 0.895 and 0.868 for CE and AC, respectively. Therefore, the fitting of the experimental data to the pseudo-first-order was not good. The $q_{e,exp}$ (109.4 and 111.8 mg $g^{-1}$) and the $q_{e,cal}$ (113.6 and 116.3 mg $g^{-1}$) values from the pseudo-second-order kinetic model were close to each other. In addition, the calculated correlation coefficients ($R^2$) were both unity (for CE and AC) for this model (Fig. 10(a) and Table 2). These findings suggested that the pseudo-second-order adsorption mechanism was predominant and that the overall rate of the HA adsorption process was most likely to be controlled by the chemisorption process for both sorbents. The intraparticle diffusion is only rate-limiting step if the plot passes through the origin. Alternatively, both the external diffusion and the intraparticle diffusion contribute to the whole adsorption process when the straight line deviates from the origin. The larger $C$ values (105.7 and 110.1) indicated the greater effect of the boundary layer on diffusion. Since the plots are not totally linear and do not pass through their respective origins, intraparticle diffusion could not be the phenomena at play. As a rule of thumb, if equilibrium is achieved within 3 h, the process is usually kinetic controlled and above 24 h, it is diffusion controlled [44]. Bangham's equation was used to evaluate whether the adsorption was pore-diffusion controlled. Plots of log log[$C_o/(C_o - q_t m)$] vs. log $t$ for the sorption of HA onto CE and AC gave correlation values of 0.820 and 0.899, respectively (Fig. 10(d) and Table 2) which confirmed that the adsorption was pore-diffusion controlled. The constants $\alpha$ and $k_o$ are obtained from Fig. 10(d) and are given in Table 2 as 0.094 and 0.056 for CE, and 0.093 and 0.066 for AC.

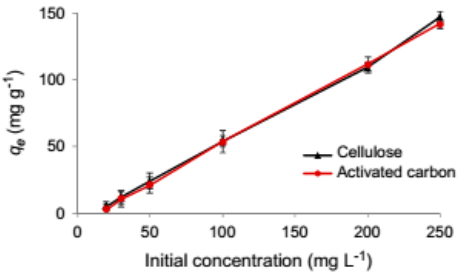



Fig. 9. Effect of initial concentration of HA adsorbed on cellulose and PAC ($n$ = 3). (Sample pH 4, sample volume = 25 mL, contact time = 50 min, sorbent (CE and PAC) weight = 50 mg, temperature = 37°C.)

Table 2
Pseudo-first-order, pseudo-second-order, intraparticle model, and the Bangham's model constants for the adsorption of HA onto CE and PAC

| Adsorption model | Modelling parameter | CE | PAC |
|---|---|---|---|
| Pseudo-first-order | $q_m$ (mg $g^{-1}$) | 5.06 | 5.32 |
| | $k_1$ ($min^{-1}$) | 0.029 | 0.030 |
| | $R^2$ | 0.895 | 0.868 |
| | RMSE | 46 | 48 |
| Pseudo-second-order | $q_e$ (mg $g^{-1}$) | 113.6 | 116.3 |
| | $k_2$ (g $mg^{-1}$ $min^{-1}$) | 0.022 | 0.023 |
| | $R^2$ | 1 | 1 |
| Intraparticle model | $k_{id}$ (mg $g^{-1}$ $min^{-0.5}$) | 0.76 | 0.59 |
| | $C$ | 105.7 | 110.1 |
| | $R^2$ | 0.604 | 0.702 |
| | RMSE | 1.88 | 2.01 |
| Bangham's model | $\alpha$ | 0.094 | 0.093 |
| | $k_o$ | 0.056 | 0.066 |
| | $R^2$ | 0.820 | 0.899 |

For the pseudo-first and pseudo-second-orders, the residual root mean square errors (RMSE) of the adsorption capacities were determined (Eq. (13)). RMSE represents the match between the experimental data and the calculated data obtained from plotting the isotherm and is defined as [45]:

$$\mathrm{RMSE} = \sqrt{\frac{1}{n-2}\sum_{i=1}^{N}(q_{e,exp} - q_{e,cal})^2} \quad (13)$$

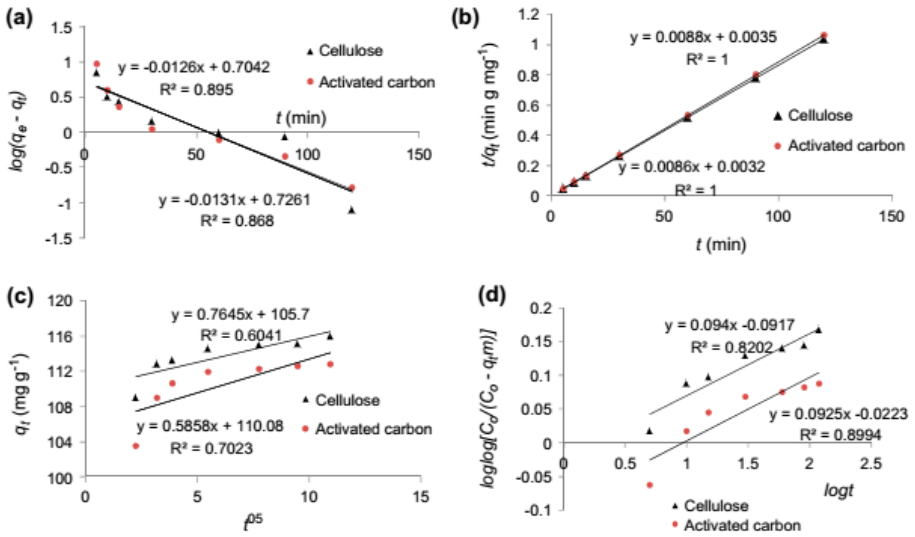



Fig. 10. Kinetic models of (a) pseudo-first-order, (b) pseudo-second-order, (c) intraparticle model and (d) Bangham's plot.

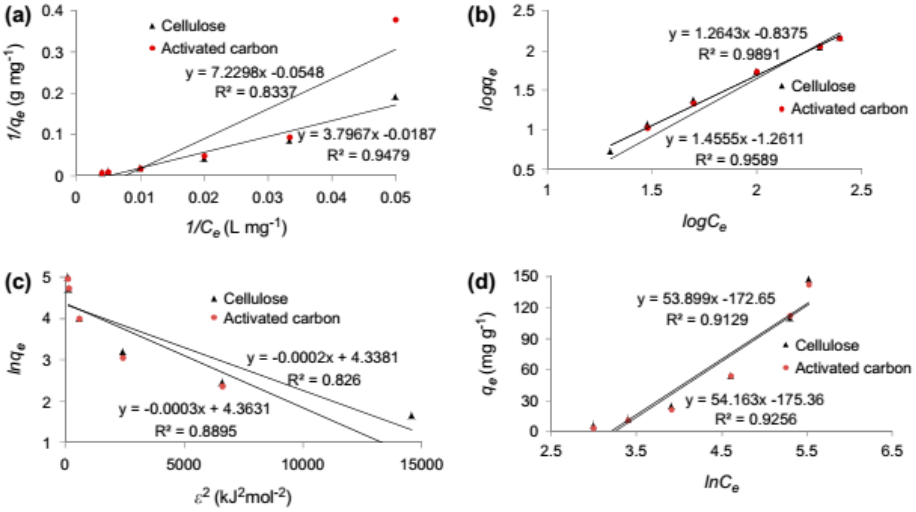



Fig. 11. Adsorption models (a) Langmuir, (b) Freundlich, (c) Dubinin–Radushkevich and (d) Temkin isotherms.

where $n$ is the number of data points. If the estimated data are very similar to the experimental data, then the RMSE value is small. The smaller RMSE values obtained from the pseudo-second-order (1.88 and 2.01 for the CE and PAC, respectively) further emphasizing the better fitting of this model to the kinetic data.

### 3.7. Adsorption modelling

Linear plots of the investigated models are shown in Fig. 11 and a summary of the theoretical parameters of adsorption isotherms along with regression coefficients are listed in Table 3. Langmuir isotherm parameter fits for HA adsorption on CE and AC

Table 3
Equilibrium isotherm parameters

| Adsorption model | Modelling parameter | CE | PAC |
|---|---|---|---|
| Langumuir | $q_m$ (mg g$^{-1}$) | 89.3 | 30.4 |
| | $b$ (L mg$^{-1}$) | 0.0076 | 0.0049 |
| | $R_L$ | 0.397 | 0.504 |
| | $R^2$ | 0.8337 | 0.9479 |
| Freundlich | $k_F$ (L mg$^{-1}$) | 4.13 | 10.9 |
| | $n$ | 0.791 | 0.69 |
| | $R^2$ | 0.9891 | 0.9589 |
| Dubinin–Radushkevich | $B_D$ (mol$^2$ kJ$^{-2}$) | 0.0002 | 0.0003 |
| | $q_m$ (mg g$^{-1}$) | 128 | 131 |
| | $E$ (kJ mol$^{-1}$) | 50 | 41 |
| | $R^2$ | 0.826 | 0.8895 |
| Temkin | $b_T$ (J mol$^{-1}$) | 27.6 | 27.5 |
| | $A_T$ (L g$^{-1}$) | 24.6 | 25.5 |
| | $R^2$ | 0.9129 | 0.9256 |

yielded isotherms that were in good agreement with observed behaviour with $R^2 > 0.83$ and $R^2 > 0.94$ as correlation coefficients, respectively. Since $R_L$ values for CE and AC, 0.397 and 0.504, respectively, fell in the range of 0–1, the sorption of HA onto these sorbents was concluded to be favourable. The adsorption capacities of HA onto CE and AC were found to be 89.3 and 30.4 mg g$^{-1}$. These values were close to the experimental values obtained in this study (109.4 and 111.8 mg g$^{-1}$). The HA adsorption capacity on CE and AC were compared to other similar sorbents (Table 4). Though the correlation coefficients for the Freundlich models were high for CE and AC ($R^2 > 0.98$ and $R^2 > 0.95$, respectively), the Freundlich constants ($n$) were <1 (0.79 and 0.69 for CE and AC, respectively) indicating the unsuitability of this model. Moreso, the Freundlich $k_F$ values for CE and AC (4.1 and 10.9 L g$^{-1}$, respectively) which approximates the adsorption capacities were lower than the experimental values. For Dubinin–Radushkevich model, values of $E$ between 1 and 8 kJ mol$^{-1}$ indicate physical adsorption; those higher than 8 kJ mol$^{-1}$ indicate that the process is chemical in nature [46]. The values obtained in this experiment were 50 kJ mol$^{-1}$ for the cellulose and 41 kJ mol$^{-1}$ for the AC; therefore, the type of HA adsorption on the adsorbent materials was likely to be chemisorption. Linear plots for Temkin adsorption isotherm (Fig. 11(c)), which refer to

Table 4
Comparison with other similar sorbents used for HA removal

| Sorbent | $q_{max}$ (mg g$^{-1}$) | pH | Refs. |
|---|---|---|---|
| *Carbon based sorbent* | | | |
| Single-walled carbon nanotubes | 33.2 | 4 | [4] |
| Fly ash | 10.7 | 3 | [47] |
| Activated carbon | 97.4 | ≈2 | [48] |
| Activated carbon | 30.4 | 2 | This work |
| *Glucose based sorbent* | | | |
| Chitosan-coated granules | 0.41 | <6 | [2] |
| Cyclodextrin modified graphene oxide nanosheets | 32.6 | 5 | [38] |
| Chitosan | 3,300 | ≈7.3[a] | [49] |
| Chitin | 189 | ≈7.3[a] | [49] |
| Crosslinked chitosan-epichlorohydrin beads | 44.8 | 6 | [50] |
| Cellulose | 89.3 | 2 | This work |

[a]Not optimized but chosen to simulate the environment of the upper intestinal tract.

chemisorption of an adsorbate onto the adsorbent, fitted quite well with correlation coefficients >0.91 and >0.92, for CE and AC, respectively.

## 4. Conclusions

In this study, cellulose and PAC were found to have good adsorption capacity for HA from an aqueous solution. These sorbents can be used for HA removal before chlorination to avoid the formation of cancerous trihalomethanes. The high sorption of HA at low pH values can also be attributed to its precipitation from solution. From the initial concentration data, the Langmuir adsorption isotherms provided the best fitting model which indicated that a chemisorption mechanism was mainly involved in the adsorption of HA onto the two sorbents. From the effect of contact time, kinetics of sorption followed the pseudo-second-order model, further emphasizing the chemisorption mechanism.

## References


[1] M.A. Ferro-García, J. Rivera-Utrilla, I. Bautista-Toledo, C. Moreno-Castilla, Adsorption of humic substances on activated carbon from aqueous solutions and their effect on the removal of Cr(III) ions, Langmuir 14 (1998) 1880–1886.

[2] X. Zhang, R. Bai, Mechanisms and kinetics of humic acid adsorption onto chitosan-coated granules, J. Colloid Interface Sci. 264 (2003) 30–38.

[3] M.A. Zulfikar, Effect of temperature on adsorption of humic acid from peat water onto pyrophyllite, IJCEBS 1 (2013) 88–90.

[4] S.P. Moussavi, M.H. Ehrampoush, A.H. Mahvi, M. Ahmadian, S. Rahimi, Adsorption of humic acid from aqueous solution on single-walled carbon nanotubes, Asian J. Chem. 25 (2013) 5319–5324.

[5] M.Y. Chang, R.S. Juang, Adsorption of tannic acid, humic acid, and dyes from water using the composite of chitosan and activated clay, J. Colloid Interface Sci. 278 (2004) 18–25.

[6] J. Kim, Y. Chung, D. Shin, M. Kim, Y. Lee, Y. Lim, D. Lee, Chlorination by-products in surface water treatment process, Desalination 151 (2002) 1–9.

[7] S.E. Manahan, Fundamentals of Environmental Chemistry, Lewis Publishers, Boca Raton, Florida, 1993.

[8] M.A. Rashid, Geochemistry of Marine Humic Compounds, Springer-Verlag, New York, 1985, p. 62.

[9] F. Ulu, S. Barışçı, M. Kobya, H. Särkkä, M. Sillanpää, Removal of humic substances by electrocoagulation (EC) process and characterization of floc size growth mechanism under optimum conditions, Sep. Purif. Technol. 133 (2014) 246–253.

[10] A. Mehrparvar, A. Rahimpour, M. Jahanshahi, Modified ultrafiltration membranes for humic acid removal, J. Taiwan Inst. Chem. Eng. 45 (2014) 275–282.

[11] T. Moriguchi, K. Yano, M. Tahara, K. Yaguchi, Metal-modified silica adsorbents for removal of humic substances in water, J. Colloid Interface Sci. 283 (2005) 300–310.

[12] J. Wang, L. Bi, Y. Ji, H. Ma, X. Yin, Removal of humic acid from aqueous solution by magnetically separable polyaniline: Adsorption behavior and mechanism, J. Colloid Interface Sci. 430 (2014) 140–146.

[13] X. Qin, F. Liu, G. Wang, G. Huang, Adsorption of humic acid from aqueous solution by hematite: Effects of pH and ionic strength, Environ. Earth Sci. 73 (2015) 4011–4017.

[14] F.S. Baker, C.E. Miller, A.J. Repik, E.D. Tolles, Activated carbon, Kirk-Othmer Encyc. Chem. Technol. 4 (1992) 1015–1037.

[15] D. Mohan, K.P. Singh, Single- and multi-component adsorption of cadmium and zinc using activated carbon derived from bagasse—An agricultural waste, Water Res. 36 (2002) 2304–2318.

[16] J.H. Potgieter, S.O. Bada, S.S. Potgieter-Vermaak, Adsorptive removal of various phenols from water by South African coal fly ash, Water SA 35 (2009) 89–96.

[17] C. Satgé, B. Verneuil, P. Branland, R. Granet, P. Krausz, J. Rozier, C. Petit, Rapid homogeneous esterification of cellulose induced by microwave irradiation, Carbohydr. Polym. 49 (2002) 373–376.

[18] J. Credou, T. Berthelot, Cellulose: From biocompatible to bioactive material, J. Mater. Chem. B 2 (2014) 4767–4788.

[19] A. Isogai, R.H. Atalla, Preparation of cellulose-chitosan polymer blends, Carbohyd. Polym. 19 (1992) 25–28.

[20] R.A. Festucci-Buselli, W.C. Otoni, C.P. Joshi, Structure, organization, and functions of cellulose synthase complexes in higher plants, Braz. J. Plant Physiol. 19 (2007) 1–13.

[21] L.F. Zara, A.H. Rosa, I.A.S. Toscano, J.C. Rocha, A structural conformation study of aquatic humic acid, J. Braz. Chem. Soc. 17 (2006) 1014–1019.

[22] S.S. Fong, L. Seng, W.N. Chong, J. Asing, M.F.M. Nor, A.S.M. Pauzan, Characterization of the coal derived humic acids from Mukah, Sarawak as soil conditioner, J. Braz. Chem. Soc. 17 (2006) 582–587.

[23] S. Lagergren, Zur theorie der sogenannten adsorption geloster stoffe (About the theory of so-called adsorption soluble substances), Kungliga Svenska Vetenskapsakademiens, Handlingar 24 (1898) 1–39.

[24] Y.S. Ho, G. McKay, D.A.J Wase, C.F. Foster, Study of the sorption of divalent metal ions on to peat, Adsorp, Sci. Technol. 18 (2000) 639–650.

[25] W.J. Weber, J.C. Morris, Kinetics of adsorption on carbon from solution, Sanit. Eng. Div. Am. Soc. Civ. Eng. 89 (1963) 31–40.

[26] C. Aharoni, S. Sideman, E. Hoffer, Adsorption of phosphate ions by colloid ion-coated alumina, J. Chem. Technol. Biotechnol. 29 (1979) 404–412.

[27] J. Wu, H.Q. Yu, Biosorption of 2,4-dichlorophenol from aqueous solution by Phanerochaete chrysosporium biomass: Isotherms, kinetics and thermodynamics, J. Hazard. Mater. 137 (2006) 498–508.

[28] I. Langmuir, The constitution and fundamental properties of solids and liquids. Part I. Solids, J. Am. Chem. Soc. 38 (1916) 2221–2295.

[29] H.M.F. Freundlich, Über die adsorption in lösungen (Over the adsorption in solution), Zeitschrift für Physikalische Chemie 57 (1906) 385–470.
[30] M.M. Dubinin, The potential theory of adsorption of gases and vapors for adsorbents with energetically nonuniform surfaces, Chem. Rev. 60 (1960) 235–241.
[31] M.J. Tempkin, V. Pyozhev, Kinetics of ammonia synthesis on promoted iron catalyst, Acta Physicochim. USSR 12 (1940) 327–352.
[32] F.J. Stevenson, Humus Chemistry. Genesis, Composition, Reactions, John Wiley and Sons, New York, NY, 1982.
[33] B.A. Shah, A.V. Shah, P.M. Shah, Sorption isotherms and column separation of Cu(II) and Zn(II) using ortho substituted benzoic acid chelating resins, Arch. Appl. Sci. Res. 3 (2011) 327–341.
[34] J.H. Chen, J.C. Ni, Q.L. Liu, S.X. Li, Adsorption behavior of Cd(II) ions on humic acid-immobilized sodium alginate and hydroxyl ethyl cellulose blending porous composite membrane adsorbent, Desalination 285 (2012) 54–61.
[35] S.Y. Oh, D.I. Yoo, Y. Shin, H.C. Kim, H.Y. Kim, Y.S. Chung, W.H. Park, J.H. Youk, Crystalline structure analysis of cellulose treated with sodium hydroxide and carbon dioxide by means of X-ray diffraction and FTIR spectroscopy, Carbohydr. Res. 340 (2005) 2376–2391.
[36] C.F. Liu, R.C. Sun, A.P. Zhang, J.L. Ren, Z.C. Geng, Structural and thermal characterization of sugarcane bagasse cellulose succinates prepared in ionic liquid, Polym. Degrad. Stab. 91 (2006) 3040–3047.
[37] W.L. Yan, R. Bai, Adsorption of lead and humic acid on chitosan hydrogel beads, Water Res. 39 (2005) 688–698.
[38] W. Song, D. Shao, S. Lu, X. Wang, Simultaneous removal of uranium and humic acid by cyclodextrin modified graphene oxide nanosheets, Sci. China Chem. 57 (2014) 1291–1299.
[39] A.A.M. Daifullah, B.S. Girgis, H.M.H. Gad, A study of the factors affecting the removal of humic acid by activated carbon prepared from biomass material, Colloids Surf., A 235 (2004) 1–10.
[40] A. Jada, R.A. Ait Akbour, J. Douch, Surface charge and adsorption from water onto quartz sand of humic acid, Chemosphere 64 (2006) 1287–1295.
[41] B.M. Babić, S.K. Milonjić, M.J. Polovina, B.V. Kaludierović, Point of zero charge and intrinsic equilibrium constants of activated carbon cloth, Carbon 37 (1999) 477–481.
[42] D. Kibami, C. Pongener, K.S. Rao, D. Sinha, Preparation and characterization of activated carbon from *Fagopyrum esculentum* Moench by $HNO_3$ and $H_3PO_4$ chemical activation, Der Chem. Sin. 5 (2014) 46–55.
[43] P.E. Diaz-Flores, R. Leyva-Ramos, J.R. Rangel-Mendez, M.M. Ortiz, R.M. Guerrero-Coronado, J. Mendoza-Barron, Adsorption of 2,4-dichlorophenoxyacetic acid from aqueous solution on activated carbon cloth, J. Environ. Eng. Manage. 16 (2006) 249–257.
[44] Y.S. Ho, J.C.Y. Ng, G. McKay, Kinetics of pollutant sorption by biosorbents: Review, Sep. Purif. Rev. 29 (2000) 189–232.
[45] D.C. Montgomery, Design and Analysis of Experiments, John Wiley & Sons, New York, NY, 2001.
[46] M.S. Onyango, Y. Kojima, A. Kumar, D. Kuchar, M. Kubota, H. Matsuda, Uptake of fluoride by $Al^{3+}$ pretreated low-silica synthetic zeolites: Adsorption equilibrium and rate studies, Sep. Sci. Technol. 41 (2006) 683–704.
[47] S. Wang, Z.H. Zhu, Humic acid adsorption on fly ash and its derived unburned carbon, J. Colloid Interface Sci. 315 (2007) 41–46.
[48] M.S. Rauthula, V.C. Srivastava, Studies on adsorption/desorption of nitrobenzene and humic acid onto/from activated carbon, Chem. Eng. J. 168 (2011) 35–43.
[49] J. Chen, C. Yeh, L. Wang, T. Liou, C. Shen, C. Liu, Chitosan, the marine functional food, is a potent adsorbent of humic acid, Mar. Drugs 9 (2011) 2488–2498.
[50] N.W.S. Wan, M.A.K.M. Hanafiah, S.S. Yong, Adsorption of humic acid from aqueous solutions on cross-linked chitosan-epichlorohydrin beads: Kinetics and isotherm studies, Colloids Surf., B 65 (2008) 18–24.

**Paper VII**

This paper "QuEChERS method development for bio-monitoring of low molecular weight polycyclic aromatic hydrocarbons in South African carp fish using HPLC-fluorescence: An initial assessment," was published in *South African Journal of Chemistry*. It investigated the optimum parameters that were applied for the QuEChERS method in the extraction of low molecular weight PAHs from carp fish.

RESEARCH ARTICLE A.O. Oduntan, N.T. Tavengwa, E. Cukrowska, S.D. Mhlanga and L. Chimuka, *S. Afr. J. Chem.*, 2016, **69**, 98–104, <http://journals.sabinet.co.za/sajchem/>. 98

# QuEChERS Method Development for Bio-monitoring of Low Molecular Weight Polycyclic Aromatic Hydrocarbons in South African Carp Fish using HPLC-fluorescence: An Initial Assessment

**Afolake Olufunmilola Oduntan[a], Nikita Tawanda Tavengwa[a], Ewa Cukrowska[a], Sabelo Dalton Mhlanga[b] and Luke Chimuka[a,*]**

[a]*Molecular Sciences Institute, School of Chemistry, University of Witwatersrand, Private Bag 3, Johannesburg, 2050, South Africa.*

[b]*Nanotechnology and Water Sustainability Research Unit, College of Science Engineering and Technology, University of South Africa, Florida, Johannesburg, 1709, South Africa.*

Received 7 October 2015, revised 29 December 2015, accepted 6 April 2016.

ABSTRACT

**Matrix components in the analysis of polycyclic aromatic hydrocarbons (PAHs) in fish require analytical methods with high selectivity and sensitivity. A quick, easy, cheap, effective, rugged and safe (QuEChERS) sample treatment method was optimized and applied, using HPLC-fluorescence for quantification of five low molecular weight PAHs: naphthalene (Nap), acenaphthene (Ace), phenathrene (Phe), fluoranthene (Flu) and pyrene (Pyr) in muscle of carp fish. Important in this study was the testing of different sorbents for clean-up in QuEChERS and comparison with Soxhlet extraction. Polymers and magnetite modified with γ-methacryloxypropyltrimethoxysilane (γ-MPS) were equally as selective towards PAHs as primary secondary amine (PSA) and multiwalled carbon nanotubes were the least selective. The concentration of PAHs in carp fish from Hartebeespoort Dam using QuEChERS extraction method was comparable to Soxhlet extraction and ranged from 0.8–739 $\mu$g kg$^{-1}$. In this study, the minimum concentration of PAHs in carp fish was 0.8 $\mu$g kg$^{-1}$ for fluoranthene and the maximum was 739 $\mu$g kg$^{-1}$ for Ace using QuEChERS method. The study revealed that polymers and magnetite modified with γ-MPS could be used as alternative clean-up sorbent in QuEChERs and that the concentration of PAHs in carp fish in the dam are a source of concern.**

KEYWORDS

**QuEChERS, PAHs, carp fish, HPLC-fluorescence, sorbents, selectivity.**

## 1. Introduction

PAHs are a large group of semi-volatile organic compounds consisting of fused aromatic rings in linear, angular or clustered arrangements.[1] They are lipophilic and have a high affinity for organic matter.[2] They can also penetrate biological membranes, making them bio-available, and bio-accumulate in fish and other marine organisms through the food chain.[3–8]

Excluding smokers and occupationally exposed populations, most individuals are exposed to PAHs predominantly from dietary sources such as fish.[9] In 1995, PAHs were included to the list of hazardous substance by the Agency for Toxic Substances and Disease Registry (ATSDR) and the United States Environmental Protection Agency (USEPA). USEPA has identified 16 unsubstituted PAHs as priority pollutants. It is against this background that their distribution in the environment as potential risks to human health has been the focus of much attention.[10] PAHs are an important concern due to their mutagenic and carcinogenic properties to humans and animals.[11] In light of these concerns, evaluation of PAHs levels in fish muscle is an important objective for environmental and health sciences.

Isolation of PAHs from biological matrices most often involves complicated extraction and clean-up procedures to provide extracts ready for the accurate analytical determination.[12] Sample preparation processes, therefore, have a direct impact on the accuracy, precision and quantification limits, and they are often a limiting step for many analytical methods.[13] Considering low concentration levels of PAH residues in food matrices, the determination of these residues often requires extensive sample extraction from environmental samples and purification prior to analysis. For complex matrices, an extraction and clean-up steps is generally required.[14] Techniques for PAH sample preparation include Soxhlet extraction, microwave assisted extraction,[15] ultrasonic extraction,[16] pressurized fluid extraction,[17] pressurized hot water extraction,[18] supercritical fluid extraction,[19] and QuEChERS (Quick, Easy, Cheap, Effective, Rugged and Safe).[20–22]

The QuEChERS extraction technique is known to utilize a minimal amount of solvent and it also uses less time. The QuEChERS extraction method originally developed was introduced by Anastassiades *et al.*[23] for extraction of a wide range of pesticides in fruit and vegetables. This technique has been used for the determination of a wide spectrum of analytes from different matrices such as pesticides and metabolites from meat-based baby food,[24] PAHs from tea,[25] simultaneously determination of pesticide and PAHs in fresh herbs.[20]

Few studies have been done on the risk assessment of PAHs in South African aqueous environmental compartments.[26,27] Most of the analyses of PAHs in the South African environment have focused on sediment and soil samples.[27–29] In this study, a QuEChERS extraction method was developed and optimized for the extraction of five PAHs: Nap (naphthalene), Ace (acenaphthene), Phe (phenathrene), Flu (fluoranthene) and Pyr (pyrene). These pollutants were extracted from carp fish from

* To whom correspondence should be addressed. E-mail: luke.chimuka@wits.ac.za

ISSN 0379-4350 Online / ©2016 South African Chemical Institute / http://saci.co.za/journal
DOI: http://dx.doi.org/10.17159/0379-4350/2016/v69a12

Hartebeespoort Dam (HPB) in Johannesburg West. The optimized parameters were the extraction speed, extraction time, volume of solvent, type of solvent, mass of salt ($MgSO_4$), the mass of fish used for extraction, mass of sorbent primary secondary amine (PSA). Other sorbents were also investigated for selectivity of PAHs from carp fish. The optimized QuEChERS extraction method was then applied for the analysis of PAHs in carp fish samples.

## 2. Materials and Methods

### 2.1. Chemicals and Instrumentation

All PAHs used, namely naphthalene (99.9 %), acenapthene (99.9 %), phenanthrene (99.9 %), fluoranthene (99.9 %) and pyrene (99.9 %) were purchased from Sigma-Aldrich (Steinhein, Germany). Acetone (99 %) was purchased from Fischer Scientific (Loughborough, UK), while acetonitrile (99.9 %) was obtained from Sigma-Aldrich (Steinheim, Germany). Hexane (99.5 %), ethyl acetate (99 %) and dichloromethane (99.5 %) were purchased from Fluka (Steinheim, Germany). Magnesium sulphate was obtained from Sigma-Aldrich (Steinheim, Germany) and sodium chloride analytical grade was obtained from Merck KGaA (Darmstadt, Germany). For clean-up, 100 g of primary secondary amine (PSA) bonded with silica was purchased from Sulpeco (Bellefonte, USA). Methacryloxypropyltrimethoxysilane ($\gamma$-MPS)-coated magnetite, molecularly imprinted polymers (MIPs) and non-molecularly imprinted polymers (NIPs) were synthesized in our laboratory.[30,31] Carbon nanotubes (CNTs) were obtained readily synthesized from Mhlanga *et al.*[32] All reagents were used without any further purification. QuEChERS materials, Agilent SampliQ QuEChERS Kits were purchased from Agilent Technologies (Santa Clara, CA, USA).

An HPLC-fluorescence was used for the quantification of PAHs. HPLC system consisted of a Waters HPLC pump (Milford, Massachusetts) connected to a fluorescence detector. The pump's flow rate was set at 1 mL $min^{-1}$. The mobile phase used was acetonitrile/water (80/20, v/v). This was connected to RF-10AXL Shimadzu fluorescence detector (Kyoto, Japan) and clarity software purchased from Prodohradska (Prague, Czech). Excitation and emission wavelengths for HPLC-fluorescence were set as follows: Nap (280 nm and 490 nm), Phe (225 nm and 460 nm), Pyr (333 nm and 390 nm), Ace (280 nm and 490 nm) and Flu (290 nm and 320 nm). 100 $\mu$L syringes obtained from Supelco Analytical (Pennsylvania, USA) were used for HPLC manual injections in a 20 $\mu$L loop. The centrifuge used was an S-8 centrifuge obtained from Boeco (Hamburg, Germany). A 460 Elma ultrasonic bath (Elma, Germany) was used for removal of bubbles from mobile phase and for dissolving PAH standards.

### 2.2. Sampling Sites

Carp fish samples were obtained from local fishermen at Hartbeespoort Dam (25.7475°S, 27.8669°E) in Gauteng Province. Fish samples were kept in a cool box and transported to the laboratory where they were frozen until analysis. Hartbeespoort Dam was chosen because it receives water from Jukskei River that passes through major industrial and residential areas to the south of Johannesburg city. The biggest wastewater treatment plant in the city also pumps its treated water in this river upstream. Thus the river and in turn the dam are regarded as one of the most polluted in the country.[15]

### 2.3. Preparation of Stock and Calibration Solutions

1000 mg $L^{-1}$ stock solution of PAHs was prepared by dissolving 50 mg of PAHs in acetonitrile. The volume was diluted to the 50 mL mark with acetonitrile for HPLC-fluorescence analysis. A 10 mg $L^{-1}$ mixture stock solution was prepared from the 1000 mg $L^{-1}$ by withdrawing 100 $\mu$L from the 1000 mg $L^{-1}$ into a 10 mL volumetric flask, thereafter, the flask was filled to mark with acetonitrile. The calibration standards were then prepared from the mixture of PAHs in acetonitrile in the range of 0.01–0.1 mg $L^{-1}$ for HPLC-fluorescence analysis. The calibration curve gave a good level of linearity with a correlation coefficient ($R^2$) between 0.9585 and 1.000 (Table 1). The limit of detection of the PAHs in fish samples ranged from 0.2–1.1 $\mu$g $kg^{-1}$.

**Table 1** HPLC-fluorescence calibration curve.

| PAH | $R^2$ | Slope | Intercept | LOD/$\mu$g $kg^{-1}$ |
|---|---|---|---|---|
| Nap | 0.9585 | 35208 | 3972 | 0.2 |
| Ace | 0.9998 | 21062 | 3548.6 | 1.1 |
| Phen | 1.0000 | 7902 | 1843.3 | 1.1 |
| Flu | 1.0000 | 207219 | 131.9 | 0.2 |
| Pyr | 0.9954 | 3402 | 513.7 | 0.7 |

### 2.4. Sample Preparation and Optimization for the QuEChERS Technique

The carp fish samples were eviscerated and filleted. Fish muscles were homogenized using a mortar and stored in a foil wrap and kept frozen until analysis. The QuEChERS extraction method was done using the procedure reported by Ramalhosa *et al.*[33] In brief, a 2.5 g of fish sample was weighed in a 25 mL Teflon tube and spiked with 0.13 mg $L^{-1}$ of 10 mg $L^{-1}$ standard of the five PAHs. The spiked sample was mixed and allowed to stand for 30 min and then 10 mL of acetonitrile was added and shaken vigorously for 1 min. This was followed by the addition of 2 g of $MgSO_4$ and 0.5 g of NaCl salt into the tube, and the mixture was shaken vigorously for 1 min and then centrifuged. After centrifugation, 5.5 mL of sample was collected and 150 mg PSA and 2 g of $MgSO_4$ was added for clean-up. The sample was centrifuged for 5 min before filtering using a 0.45 $\mu$m PTFE and injected in the GC-FID for analysis. For optimization, parameters that affected extraction, such as centrifugation time (10–30 min), centrifugation speed (3400–6000 rpm), type of solvent (ethylacetate, acetone and acetonitrile), fish mass (0.5–2.5 g), amount of salt (1.0–2.5 g) and volume of solvent (6–10 mL) were investigated in that order and the experiments were done in triplicate. As a clean-up sorbent, the same procedure as above was followed but instead of PSA other sorbents were investigated: molecular imprinted polymers (MIP), non-imprinted polymers (NIP), $\gamma$-MPS magnetite (MAG) and carbon nanotubes (CNTs).

### 2.5. Soxhlet Extraction Procedure

Homogenized fish samples as described above were Soxhlet extracted using method previously reported (US EPA, 1996C). Fish samples (15 g) were weighed in triplicate and spiked with different concentrations of PAHs ranging from 0.5, 1.0 and 1.5 $\mu$g $g^{-1}$. Spiked fish sample were placed in a Soxhlet thimble and mixed with 15 g of $MgSO_4$. Fish samples were extracted using 200 mL of dichloromethane/acetone (1/1, v/v) ratio for 20 h at a temperature of 35°C. After extraction, the solvent was evaporated to 5 mL by a rotary evaporator and was made up to 10 mL with hexane and then further evaporated under nitrogen to 2 mL. Extract was passed through a homogenized column consisting of 3 g of silica and 2 g of $Na_2SO_4$ which had been previously dried. Dichloromethane/hexane (2/8, v/v) was used to elute the compounds from the column and solvent was evapo-

rated to dryness under a gentle steam of nitrogen. A volume of 3 mL of acetonitrile was then added and 20 $\mu$L of extract was injected into HPLC-fluorescence.

## 3. Results and Discussion

### 3.1. Optimization of the QuEChERS Method

The results obtained (Fig. 1a) when centrifugation time was varied while keeping all other parameters constant. Since the recoveries were almost independent of time (in the investigated time range), the least time was selected as the optimum. This was based on the economical motivation and 10 min was chosen as the optimal time for centrifuge. The extraction process is governed by a mass transfer which is time-dependent.[34] Extraction process in QuEChERS is generally regarded as fast. Ramalhosa *et al.*[33] studied recovery of PAHs from fish sample using ultrasonic bath by increasing extraction time from 3 to 20 min, and found 20 min to be optimum. Centrifuge time was also investigated by Keegan *et al.*[35] and 10 min was found to give optimum recovery. The optimum time of 10 min found in this study was therefore consistent with other previous studies.

From the investigation of centrifuge speeds (Fig. 1b), there was not much variation in recovery as the centrifuge speed was increased from 3400 to 5000 rpm. Centrifuging allows the solvent to be in contact with the sample, therefore making it to be more effective in dissolution of analyte.[36] The centrifuge speed can reduce the time needed for extraction.[37] Rodrigues *et al.*[38] applied centrifuge speed of 5000 rpm for the QuEChERS extraction of pesticides. Herrero *et al.*[39] and Lopes *et al.*[40] also used centrifuge speeds of 5000 rpm. This shows that 5000 rpm is the most commonly used. In this instance, as the speed was increased, most of the PAHs were recovered at 5000 rpm. Initially, the amount extracted increased with stirring speed as this enhanced the movement of the PAHs from the sample to the solvent. However, at too high stirring speed, the extraction of PAHs decreased because of generation of air bubbles. King *et al.*[41] varied the

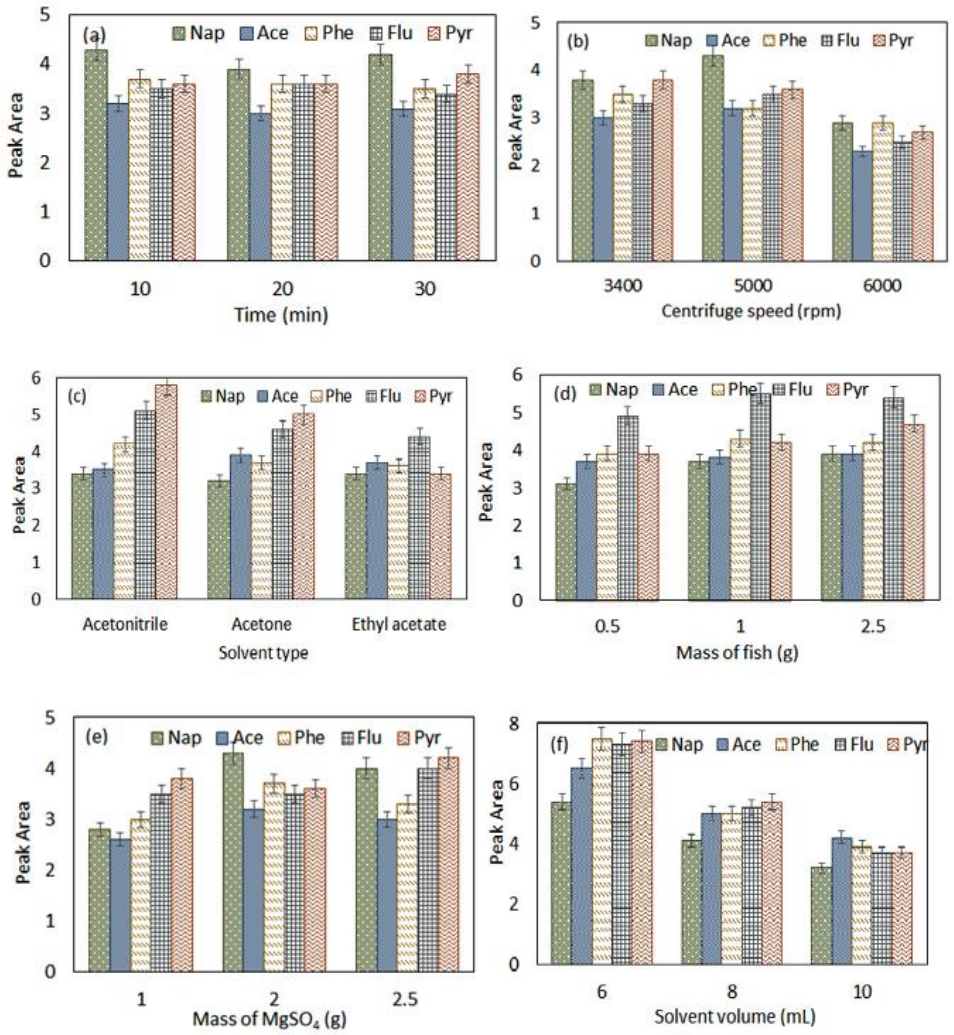



**Figure 1** Effect of (**a**) centrifuge time, (**b**) centrifuge speed, (**c**) solvent type, (**d**) mass of fish, (**e**) mass of salt, and (**f**) solvent volume. [Experimental conditions: (a) 5000 rpm, 8 mL acetonitrile, 2.5 g of fish, 2 g $MgSO_4$, 0.5 NaCl (b) 10 min, 8 mL acetonitrile, 2.5 g of fish, 2 g $MgSO_4$, 0.5 NaCl (c) 10 min, 8 mL of the solvent, 2.5 g of fish, 2 g $MgSO_4$, 0.5 NaCl (d) 10 min, 8 mL acetonitrile, 2 g $MgSO_4$, 0.5 NaCl (e) 10 min, 8 mL acetonitrile, 2.5 g of fish, 0.5 NaCl and (f) 10 min, 2.5 g of fish, 2 g $MgSO_4$, 0.5 NaCl].

stirring speed (0 to 1225 rpm) in their analysis of PAHs and also observed creation of air bubbles at over 800 rpm.

Acetonitrile and ethyl acetate have been widely used to extract polar to non-polar analytes[42] and were tested together with acetone (Fig. 1c). Solvent type is very important when the QuEChERS method is developed. Pyr, Flu and Phe were better extracted using acetonitrile. Those slight differences reflect the type of intermolecular interaction that takes place between the PAHs and extraction solvent. PAHs are non-polar with mostly hydrophobic interactions through pi bonds being involved. This may explain why acetonitrile, also with pi bonds and linear in geometry, gave slightly better extractions. The structure of the solvent should allow maximum interactions with the analytes, besides its polarity. Acetonitrile separates more easily from water than other polar solvents used (acetone and ethyl acetate) in the QuEChERS method in the presence of salts. This gives a good phase separation which prevents interaction of polar matrix.[43] Therefore, acetonitrile was chosen as the optimal solvent for extraction.

The results on the optimization of fish mass revealed that there was slight variation in the peak areas obtained (Fig. 1d). Overall, 1.0 and 2.5 g gave slightly higher peak areas than 0.5 g. Homem *et al.*[44] investigated the mass to solvent volume ratio and observed that a ratio lower than 0.17 g $mL^{-1}$ gave very low recoveries. In this study, solvent volume was kept at 10 mL and fish mass of 0.5, 1.0 and 2.5 g were tested. This gave mass to solvent ratios of 0.05, 0.1 and 0.25, respectively. In this study, 2.5 g was used as optimum fish mass as this mass gave a slightly higher peak area.

The results obtained when the mass of $MgSO_4$ was varied during the extraction showed that there was an increase in recovery of Nap, Ace and Phe with the use of 2 g of $MgSO_4$ (Fig. 1e). Increase in salt allows greater phase separation but high salt level can also affect the effectiveness of the extraction system.[45] The right combination of quantity of salt used in phase separation is important as it regulates the polarity of the mixture. $MgSO_4$ removes a lot of water and the reaction is exothermic which can improve the process of extraction.[23] Addition of salt increases the temperature of the system, lowers activation energy and also decreases the viscosity of the solvent thereby increasing solvent matrix interaction.[46] The result shows that the optimal mass of salt is 2 g as there is not much variation between the 2 g mass and the 2.5 g mass of salt.

A decrease in the amount extracted was observed with increase in volume of solvent (Fig. 1f). Decrease was more pronounced with 10 mL. However, it can be noted that from recovery, 6 and 8 mL gave high recoveries. Homem *et al.*[44] studied the effect of sample mass to solvent ratio on recovery. Optimum ratio obtained was 0.17. In this study, the volumes used gave sample mass to volume of 0.41, 0.31 and 0.25, respectively. Closest mass to solvent volume obtained by Homem *et al.*[44] was 0.25 which was equivalent to 10 mL. Satisfactory recovery was obtained for 10 mL volume which ranged from 95 to 104 % recovery as noted above, while for the 6 and 8 mL volume; recovery of Flu was 130 % while in the 6 mL volume recovery of Phe exceeded 120 %. Larger recoveries may be due to matrix effect.[39,44] Thus 10 mL solvent volume was taken as optimum.

### 3.2. Comparison of Different Sorbents

The structures of the different sorbents are shown in Fig. 2 and their recoveries in QuEChERS method are compared in Fig. 3. After synthesis, the MIP and NIP were washed with distilled water to remove the unreacted pre-polymerization reagents before use. γ-MPS-coated magnetite was washed with water followed by methanol. Washing solutions were analyzed to check for any impurities. The recovery of PAHs from different sorbents showed that there was not much differences (Fig. 3). The selectivities of the different sorbents was tested by extracting unspiked samples (blank) of carp fish samples. Chromatograms (not presented) of extracts from various sorbents showed that CNTs gave the least selectivity. γ-MPS and polymer sorbents (MIP and NIP) gave slightly cleaner chromatograms followed by PSA. It should be noted that the MIP used were not specific for PAHs, and therefore acted as ordinary sorbent like the NIP. In this case, PSA was still taken as the best sorbent since recovery and selectivity was not that different from other sorbents. Generally, PSA is recommended for clean-up of sugars, organic acids and polar pigments.

### 3.3. Comparison of Recoveries between QuEChERS and Soxhlet Extraction Methods

Figure 4 shows the recoveries obtained for the QuEChERS and Soxhlet extraction methods at optimized conditions. As spiking concentrations were increased, the peak areas increased in both methods and recoveries obtained were independent of the spiking concentration. However, at lower concentration, the recoveries were higher than 100 % for some analytes (Nap, Phe, Flu and Pyr) due to matrix effects. QuEChERS gave higher recovery for all the five PAHs than Soxhlet extraction. This was

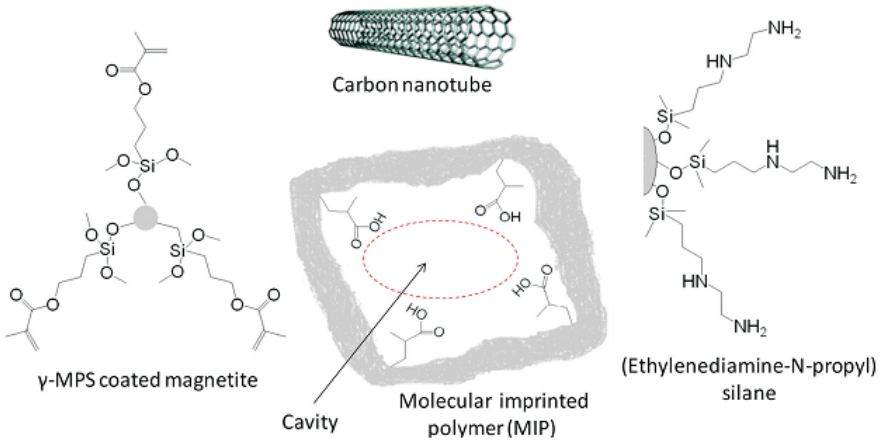



**Figure 2** Different sorbents used for the QuEChERS method.

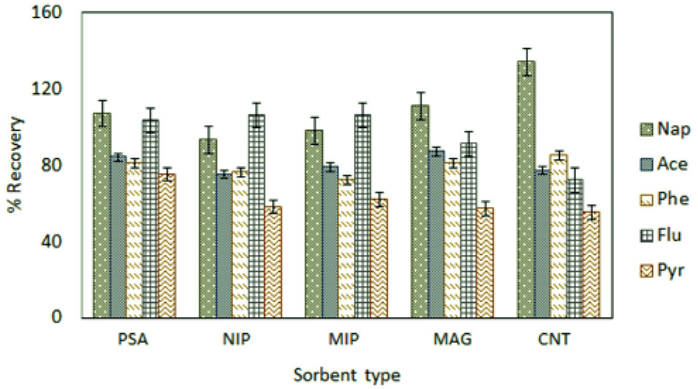



**Figure 3** Comparision of recoveries obtained for different sorbent in QuEChERS extraction method ($n = 3$). [Experimental conditions: 2.5 g of fish, 10 mL acetonitrile, 2 g $MgSO_4$, 0.5 g of NaCl and 5000 rpm].

expected as the latter has slow mass transfer and thus extraction takes hours compared to few minutes with QuEChERS, besides large amounts of solvents are consumed.

### 3.4. Application of QuEChERS Method and Comparison with Soxhlet Exaction Method

A typical chromatogram of an spiked fish sample obtained using HPLC-fluorescence is shown in Fig. 5. Table 2 shows the concentration levels of PAHs obtained in carp fish samples taken from Hartbeespoort Dam (HPB). Nap was not detected in all the samples by both methods. This might be due to variation in the possible sources of these compounds in the dam. Phe was detected in highest concentration in both methods followed by Ace, then Flu and Pyr. The results showed that there was no statistical difference between the Soxhlet extraction as compared to the QuEChERS method for the Ace and Flu ($t_{cal} < t_{table}$ (2.447)). However, significant difference was found between the two methods for Phe and Pyr (Phe and Pyr $t_{cal}$ values of 7.132 and 5.808, respectively were both $> t_{table}$ of 2.447 at 95 % confidence interval). The explanation for this difference in the methods for Phe and Pyr can be attributed to matrix effects in the samples especially for Sohxlet extraction which is less selective compared to QuEChERS method. A plot (not shown) of concentration of PAHs against fish length for Pyr and Ace from Hartbeespoort Dam gave positive correlations $R^2 = 0.919$ and $R^2 = 0.773$, respectively. For other PAHs in fish samples, there was no positive

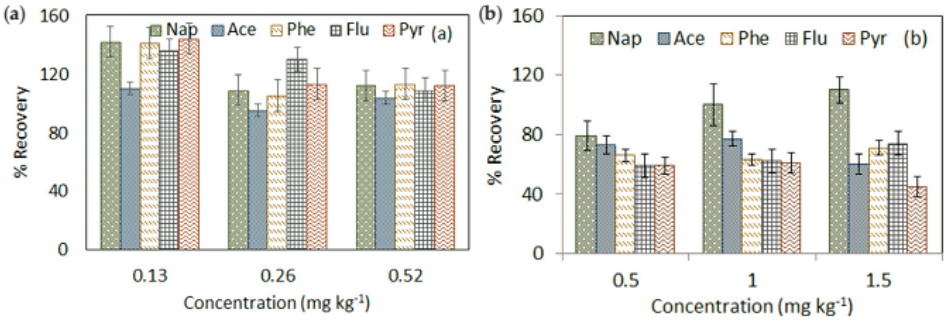



**Figure 4** Recoveries of PAHs by **(a)** QuEChERS and **(b)** Soxhlet extraction ($n = 3$). [Experimental conditions: 2.5 g of fish, 10 mL acetonitrile, 2 g $MgSO_4$, 0.5 g of NaCl and 5000 rpm].

**Table 2** Concentration obtained from fish samples from Hartbeespoort dam in Gauteng using the QuEChERS and Soxhlet extraction methods ($n = 3$).

| Sample site | Fish length /cm | Fish width /cm | PAHs concentration/$\mu$g kg$^{-1}$ | | | | |
|---|---|---|---|---|---|---|---|
| | | | Nap | Ace | Phe | Flu | Pyr |
| QuEChERS extraction method | | | | | | | |
| HPB 1 | 21 | 7.0 | nd | 37.7 (4.1) | 683.6 (0.9) | 0.9 (13.2) | 1.7 (3.9) |
| HPB 2 | 22.4 | 7.6 | nd | 40.3 (3.5) | 739.0 (0.5) | 4.7 (11.3) | 1.5 (8.0) |
| HPB 3 | 24.5 | 8.6 | nd | 38.1 (1.6) | 717.2 (4.9) | 3.7 (8.6) | 1.7 (5.3) |
| HPB 4 | 35.5 | 12.5 | nd | 50.3 (0.5) | 641.4 (1.2) | 6.1 (10.5) | 2.0 (2.2) |
| Soxhlet extraction method | | | | | | | |
| HPB 1 | 21 | 7.0 | nd | 37.8 (0.6) | 838.5 (1.0)) | 1.9 (2.2) | 5.2 (0.1) |
| HPB 2 | 22.4 | 7.6 | nd | 43.2 (2.3) | 890.0 (7.2) | 9.4 (0.2) | 4.5 (0.4) |
| HPB 3 | 24.5 | 8.6 | nd | 46.3 (0.4) | 908.5 (0.7) | 6.1 (0.1) | 6.2 (1.0) |
| HPB 4 | 35.5 | 12.5 | nd | 55.2 (2.4) | 902.6 (3.8) | 6.1 (1.1) | 7.8 (4.1) |

Note: nd = not detected, standard deviations are in brackets.

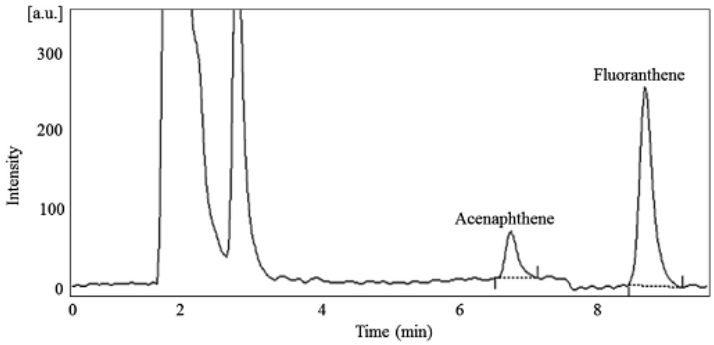



**Figure 5** A Chromatogram of an unspiked fish sample obtained from QuEChERS extraction method using HPLC-fluorescence.

correlation. These diffferences could be due to factors such as fish metabolism of the compounds, bioavailabilty of the compounds from the water which affects the their bioconcentration.

## 4. Conclusions

The results indicated that polymeric sorbents and γ-MPS-coated magnetite can serve as good alternative to PSA as they gave comparable recovery and selectivity for PAHs in fish. QuEChERs method was found to be very efficient in extraction PAHs in fish compared to Soxhlet extraction as it was faster and gave better recoveries. The concentration of PAHs in fish samples from Hartesbeesport Dam found using QuEChERS method was comparable to Soxhlet extraction method though for some PAHs, the latter gave slightly higher results. Results of PAH concentration in fish samples from the dam indicate that the dam is acting as a sink for pollution occurring upstream and is a cause of concern. Further monitoring of substituted PAHs and all 16 US EPA listed PAHs is recommended.

## Acknowledgements

This work was funded by the Water Research Commission (WRC) of South Africa, Project number K8-849.

## References

1 E. Morillo, A.S. Romero, C. Maqueda, L. Madrid, F. Ajmone-Marsan, H. Grcman, C.M. Davidson, A.S. Hursthouse and J. Villaverde, Soil pollution by PAHs in urban soils: a comparison of three European cities, *J. Environ. Monit.*, 2007, **9**, 1001–1008.

2 M. Nadal, M. Schuhmacher and J.L. Domingo, Levels of PAHs in soil and vegetation samples from Tarragona County, Spain, *Environ. Pollut.*, 2004, **132**, 1–11.

3 A. Schecter, L. Birnbaum, J.J. Ryan and J.D. Constable, Dioxins: an overview, *Environ. Res.*, 2006, **101**, 419–428.

4 S. Boonchan, M.L. Britz and G.A. Stanley, Surfactant-enhanced biodegradation of high molecular weight polycyclic aromatic hydrocarbons by *Stenotrophomonas maltophilia*, *Biotechnol. Bioeng.*, 1998, **59**, 482–494.

5 I.N. Nasr, N.H.A. EL-Enaen and T.A. Yosef, Study of some polycyclic aromatic hydrocarbons residues in fish at Sharkia Governorate markets in relation to public health, *Global Veterinaria*, 2012, **8**, 670–675.

6 J.S. Latimer and J. Zheng, The sources, transport and fate of PAHs in the marine environment, in *PAH: An Ecotoxicological Perspective* (P.E.T Douben, ed.), Wiley, Chichester, UK, 2003, pp. 9–33.

7 Y. Liang, M.F. Tse, L. Young and M.H. Wong, Distribution patterns of polycyclic aromatic hydrocarbons (PAHs) in the sediments and fish at Mai Po Marshes Nature Reserve, Hong Kong, *Water Res.*, 2007, **41**, 1303–1311.

8 M. Perugini, P. Visciano, A. Giammarino, M. Manera, W. Di Nardo and M. Amorena, Polycyclic aromatic hydrocarbons in marine organisms from the Adriatic Sea, Italy, *Chemosphere* 2007, **66**, 1904–1910.

9 L.R. Bordajandi, M. Dabrio, F. Ulberth and H. Emons, Optimisation of the GC-MS conditions for the determination of the 15 EU foodstuff priority polycyclic aromatic hydrocarbons, *J. Sep. Sci.*, 2008, **31**, 1769–1778.

10 E. Manoli and C. Samara, Polycyclic aromatic hydrocarbons in waste waters and sewage sludge: extraction and clean-up for HPLC analysis with fluorescence detection, *Chromatographia* 1996, **43** , 135–142.

11 K. Li, H. Li, L. Liu, Y. Hashi, T. Maedac and J. Lin, Solid-phase extraction with C30 bonded silica for analysis of polycyclic aromatic hydrocarbons in airborne particulate matters by gas chromatography-mass spectrometry, *J. Chromatogr. A* 2007, **1154**, 74–80.

12 R.E. Majors, New chromatography columns and accessories at the 2003 Pittsburg conference, Part II. *LC GC Europe*, 2003, **21**, 332–348.

13 K.D. Bartle, in *Food Contaminant, Sources and Surveillance* (C.S. Creaser and R. Purchase, eds.), Royal Society of Chemistry, Cambridge, UK, 1991.

14 A. Lazartigues, L. Wies, R. Baudot, M. Thomas, C. Feidt and C. Cren-Olivé, Multi residue method to quantify pesticides in fish muscle by QuEChERS-based extraction and LC-MS/MS, *Anal. Bioanal. Chem.*, 2011, **400**, 2185–2193.

15 P. Sibiya, L. Chimuka, E. Cukrowska and H. Tutu, Development and application of microwave assisted extraction (MAE) for the extraction of five polycyclic aromatic hydrocarbons in sediment samples in Johannesburg area, South Africa, *Environ. Monit. Assess.*, 2013, **185**, 5537–5550.

16 D.R. Banjoo and P.K. Nelson, Improved ultrasonic extraction procedure for the determination of polycyclic aromatic hydrocarbons in sediments, *J. Chromatogr. A* 2005, 1066, 9–18.

17 S.D. Haskins, J.M. Duval, D.G. Kelly, S.L. Lundgreen-Nielsen and R.D. Weir, Pressurized fluid extraction of polycyclic aromatic hydrocarbons using silanized extraction vessels, *Microchim. Acta*, 2012, **178**, 187–193.

18 T. Andersson, K.T.H. Hartonen and M.L. Riekkola, Pressurised hot water extraction and thermal desorption of polycyclic aromatic hydrocarbons from sediment with use of a novel extraction vessel, *Anal. Chim. Acta* 2002, **446**, 93–100.

19 N. Cardellicchio, S. Cavalli and P. Ragone, Supercritical fluid extraction of polycyclic aromatic hydrocarbons (PAHs) in marine sediments and GC-MS analysis, *Polycyclic Aromat. Compd.*, 1996, **9**, 365–372.

20 A. Sadowska-Rociek, M. Surma and E. Cieślik, Application of QuEChERS method for simultaneous determination of pesticide residues and PAHs in fresh herbs, *Bull. Environ. Contam. Toxicol.*, 2013, **90**, 508–513.

21 A. Albinet, S. Tomaz and F. Lestremau, A really quick easy cheap effective rugged and safe (QuEChERS) extraction procedure for the analysis of particle-bound PAHs in ambient air and emission samples, *Sci. Total Environ.*, 2013, **450-451**, 31–38.

22 M. Andrascikova, S. Hrouzkova and S.C. Cunha, Combination of QuEChERS and DLLME for GC-MS determination of pesticide residues in orange samples, *Food Addit. Contam.*, 2013, **30**, 286–297

23 M. Anastassiades, S.J. Lehotay, D. Stajnbaher and F.J. Schenck, Fast and easy multi residue method employing acetonitrile extraction/partitioning and "dispersive solid-phase extraction" for the determination of pesticide residues in produce, *J AOAC Int.*, 2003, **86**, 412–431.

24 C. Przybylski and C. Segard, Method for routine screening of pesticides and metabolites in meat based baby-food using extraction and gas chromatography-mass spectrometry, *J. Sep. Sci.*, 2009, **32**, 1858–1867.

25 A. Sadowska-Rociek, M. Surma and E. Cieślik, Comparison of different modifications on QuEChERS sample preparation method for PAHs determination in black, green, red and white tea, *Environ. Sci. Poll. Res.*, 2014, **21**, 1326–1338.

26 P. Sibiya, E. Cukrowska, J.Å. Jönsson and L. Chimuka, Development and application of solid phase extraction method for polycyclic aromatic hydrocarbons in water samples in Johannesburg area, South Africa, *S. Afr. J. Chem.*, 2012, **65**, 206–213.

27 S.K. Das, J. Routh and A.N. Roychoudhury, Sources and historic changes in polycyclic aromatic hydrocarbon input in a shallow lake, Zeekoevlei, South Africa, *Org Geochem.*, 2008, **39**, 1109–1112.

28 L. Quinn, R. Pieters, C. Nieuwoudt, A.R. Borgen, H. Kylin and H. Bouwman, Distribution profiles of selected organic pollutants in soils and sediments of industrial, residential and agricultural areas of South Africa, *J. Environ. Monit.*, 2009, **11**, 1647–1657.

29 C. Nieuwoudt, R. Pieters, L. Quinn, H. Kylin, A.R. Borgen and H. Bouwman, Polycyclic aromatic hydrocarbons (PAHs) in soil sediment from industrial, residential, and agricultural areas in central South Africa: an initial assessment, *Soil Sediment Contam.*, 2011, **20**, 188–204.

30 N.T. Tavengwa, E. Cukrowska and L. Chimuka, Preparation, characterization and application of $NaHCO_3$ leached bulk U(VI) imprinted polymers endowed with $\gamma$-MPS coated magnetite in contaminated water, *J. Hazard. Mater.*, 2014, **267**, 221–228.

31 B. Mhaka, E. Cukrowska, S.B.B. Tse, O. Ramström, K. Haupt, H. Tutu and L. Chimuka, Selective extraction of triazine herbicides from food samples based on a combination of a liquid membrane and molecularly imprinted polymers, *J. Chromatogr. A* 2009, **1216**, 6796–6801.

32 S.D. Mhlanga and N.J. Coville, Iron–cobalt catalysts synthesized by a reverse micelle impregnation method for controlled growth of carbon nanotubes, *Diamond Relat. Mater.*, 2008, **17**, 1489–1493.

33 M.J. Ramalhosa, P. Paiga, S. Morias, C. Delerue-Matos, M.B. Oliveira, Analysis of polycyclic aromatic hydrocarbons in fish: evaluation of a quick, easy, cheap, effective, rugged, and safe extraction method, *J. Sep. Sci.*, 2009, **32**, 3529–3538.

34 C. Basheer, R. Balasubramanian and H.K. Lee, Determination of organic micropollutants in rainwater using hollow fiber membrane/liquid-phase microextraction combined with gas chromatography-mass spectrometry, *J. Chromatogr. A* 2003, **1016**, 11–20.

35 J. Keegan, M.D. Whelan, S. Crooks, R. Sayers, A. Anastasio, C. Elliott, D. Brandon, A. Furey and R. O'Kennedy, Benzimidazole carbamate residues in milk: detection by surface plasmon resonance-biosensor, using a modified QuEChERS (Quick, Easy, Cheap, Effective, Rugged and Safe) method for extraction, *Anal. Chim. Acta* 2009, **654**, 111–119.

36 A. Kouzayha, M.A. Iskandarani, S. Mokh, A.R. Rabaa, H. Budzinski and F. Jaber, Optimization of a solid-phase extraction method using centrifugation for the determination of 16 polycyclic aromatic hydrocarbons in water, *J. Agric. Food. Chem.*, 2011, **59**, 7592–7600.

37 D. Bai, J. Li, S.B. Chen and B.H. Chen, A novel cloud-point extraction process for preconcentrating selected polycyclic aromatic hydrocarbons in aqueous solution, *Environ. Sci. Technol.*, 2001, **35**, 3936–3940.

38 S.A. Rodrigues, S.S. Caldas, M.H.S. Kurz, L.D Cabrera, F.A. Duarte, R. Zanella and E.G. Primel, Comparison of matrix solid-phase dispersion and modified QuEChERS methods for extraction of pesticide residues from onion, *Anal. Methods*, 2012, **4**, 1820–1824.

39 M.S. Herrero, P.C. García, P.J.C. Pérez, V. Homem, J.A. Silva, C. Cunha, A. Alves and L. Santos, New analytical method for the determination of musks in personal care products by Quick, Easy, Cheap, Effective, Rugged, and Safe extraction followed by GC-MS, *J. Sep. Sci.*, 2013, **36**, 2176–2184.

40 R.P. Lopes, R.C. Reyes, R. Romero-Gonzalez, A.G. Frenich and J.L. Vidal, Development and validation of a multiclass method for the determination of veterinary drug residues in chicken by ultra-high performance liquid chromatography-tandem mass spectrometry, *Talanta* 2012, **89**, 201–208.

41 S. King, J.S. Meyer and A.R.J. Andrews, Polycylic aromatic hydrocarbons in soil using hollow fiber membrane solvent microextraction, *J. Chromatogr. A* 2002, **982**, 201–208.

42 R. Carabias-Martinez, E. Rodriguez-Gonzalo, P. Revilla-Ruiz and J. Hernandez-Mendez, Pressurized liquid extraction in the analysis of food and biological samples, *J. Chromatogr. A* 2005, **1089**, 1–17.

43 C. Diez, W.A. Traag, P. Zommer, P. Marinero and J. Atienza, Comparison of an acetonitrile extraction/partitioning and dispersive solid-phase extraction method with classical multi-residue methods for the extraction of herbicide residues in barley samples, *J. Chromatogr. A* 2006, **1131**, 11–23.

44 V. Homem, S.J. Avelino, C. Cunha, A. Alves and L. Santos, New analytical method for the determination of musks in personal care products by Quick, Easy, Cheap, Effective, Rugged, and Safe extraction followed by GC–MS, *J. Sep. Sci.*, 2013, **36**, 2176–2184.

45 E. Coelho, C. Ferreira and C.M.M. Almeida, Analysis of polynuclear aromatic hydrocarbons by SPME-GC-FID in environmental and tap waters, *J. Braz. Chem. Soc.*, 2008, **19**, 1084–1097.

46 B.E. Richter, B.A. Jones, J.L. Ezzell and N.L. Porter, Accelerated solvent extraction: a technique for sample preparation, *Anal. Chem.*, 1996, **68**, 1033–1039.